Design, construction, and performance of heated concrete pavements system

by

Hesham Abdualla

A dissertation submitted to the graduate faculty

in partial fulfillment of the requirements for the degree of

DOCTOR OF PHILOSOPHY

Major: Civil Engineering (Materials)

Program of Study Committee:
Halil Ceylan, Co-major Professor
Kasthurirangan Gopalakrishnan, Co-major Professor
Sunghwan Kim
Peter C. Taylor
Kristen S. Cetin
Mani Mina
Bora Cetin

The student author, whose presentation of the scholarship herein was approved by the program of study committee, is solely responsible for the content of this dissertation. The Graduate College will ensure this dissertation is globally accessible and will not permit alterations after a degree is conferred.

Iowa State University

Ames, Iowa

2018

DEDICATION

This dissertation is dedicated to my parents for their endless love, to my wife, and to my precious son, Yousif, and my beautiful daughters Noora and Danya.

TABLE OF CONTENTS

Page

LIST OF FIGURES

Page

LIST OF TABLES

ACKNOWLEDGMENTS

First and foremost, I thank God for making all things possible. I would like to express my deepest appreciation to my major advisors, Dr. Halil Ceylan and Dr. Kasthurirangan Gopalakrishnan for their guidance, encouragement, and support throughout this research study. Without their guidance and support, this dissertation would not have been possible. My sincere thanks also go to Dr. Sunghwan Kim for his invaluable guidance. I am very thankful for his scientific advice, knowledge, and suggestions that continuously improved my knowledge and understanding.

In addition to my major advisors, I would also like to thank my committee members, Dr. Kristen S. Cetin, Dr. Peter C. Taylor, Dr. Mani Mina, and Dr. Bora Cetin, for their insightful comments, motivation, and encouragement. I want to thank Mr. Robert Frank Steffes, the lab manager in the Portland Cement Concrete Research Laboratory for his endless help and Mr. Gary Mitchell, American Concrete Pavement Association for his significant assistance and guidance. This research was supported by the Federal Aviation Administration (FAA) Air Transportation Center of Excellence (COE) for PEGASAS and the support provided by FAA and ISU is greatly appreciated.

My mother and father are the source of happiness in my life and I would like to express my deepest love to them for their continuous prayers and support that helped me get through my years of study. I would also like to thank my brothers and sisters for their support and encouragement.

Last, but definitely not least, I wanted to express my love to my beloved wife for providing me her full support and making my life amazing in my journey throughout my Ph.D. study. I owe her more than words can express.

ABSTRACT

Ice and snow accumulation on airport paved surfaces has the potential to cause fatal accidents and monetary loss due to associated flight delays and cancellations. Traditional de-icing methods involving the application of chemicals or salt, and deployment of large machines can create negative environmental and structural impact on airport infrastructure systems. Such methods are also considered to be both labor-intensive and safety hazards, especially in congested areas such as aprons.

In recent years, hydronic and/or electrically conductive concrete (ECON) heated pavement systems (HPS) have been receiving attention for mitigating problems associated with the presence of ice/snow on roadways and paved areas of airfields. In this study, the system requirements of electrically-conductive concrete (ECON) heated pavement systems were identified for their potential with respect to achieving cost-effective performance. A prototype small-scale ECON heated concrete slab was designed, constructed, and tested using an optimized ECON mixture recently developed at Iowa State University (ISU), to obtain the efficiency and performance results. This prototype ECON slab provided the lowest energy consumption and lowest energy cost among the electrically-heated pavement systems developed so far. The two-layer approach utilized in design and construction of the prototype ECON slab is cost-effective in terms of construction cost, energy consumption, and operational cost savings. Given the promising results from the ECON slab research studies, both the airport owner and the FAA have demonstrated interest in providing assistance and support in taking this technology developed in-house and implementing it full-scale on-site at the DSM airport, representing the first full-scale ECON-based HPS conducted and tested at a U.S. airport. Two ECON slabs were designed and constructed in 2016 at the General

Aviation (GA) apron at the Des Moines International Airport (DSM), Iowa. Systematic design components were identified and construction procedures were developed and implemented for ECON-based HPS. Using sensor data collection, the performance of the remotely-operated ECON slabs was evaluated under real weather conditions at DSM during the 2016-2017 winter season, with results demonstrating that ECON-based HPS offer promising deicing and anti-icing capacities for providing uniform heat distribution and preventing snow and ice accumulation on the entire area of application under various winter weather conditions.

Going forward, there is an imperative need to investigate and/or develop new technologies to best automate and accelerate the construction of large-scale heated pavements at airports. This study attempted to partially fulfill that need by conducting a detailed review of advanced pavement construction techniques and practices and evaluating their efficacy and applicability to construction of HPS at airports. System requirements of ECON and hydronic HPS were identified and laboratory experimental investigations were carried out to study their efficiency and performance results, leading to the development of a design procedure for large-scale HPS at airports. Advanced construction techniques and workflows for precast concrete (PC), two-lift paving, and concrete overlays for heated pavements were demonstrated using 3D visualizations to provide design and construction guidance for large-scale heated airport pavements. A 3-D finite element (FE) model was developed for ECON which can be used as a cost-effective evaluation tool for examining the effects of various design parameters on the time-dependent heating performance of ECON HPS design optimization.

CHAPTER 1. INTRODUCTION

1.1 Background

In colder regions, snow and ice on pavement surfaces are among the major concerns that may cause infrastructure deterioration, damage to concrete pavement, and negative environmental impact through the use of traditional deicing methods (Xi and Olsgard 2000) that include spraying chemicals on the pavement surface and employing large snow removal machines such as snow plows and snow broom vehicles. There are several drawbacks to these traditional methods, including ineffectiveness in removing snow at low temperatures, negative environmental impact because of possible contamination of nearby water bodies, and increased labor costs. These methods are also challenging to implement in congested and smaller areas such as sidewalks, aprons, and taxiways at airports because they could be hazardous to airport ground crews as well as to aircraft.

Heated pavement systems (HPS) offer alternative options for melting ice and snow and can be classified into two general categories, hydronic heated-pavement systems (HHPS) and electrically-heated pavement systems (EHPS). HHPS melt ice and snow by circulating heated fluid through pipes embedded inside pavement structures; the cooled fluid circulates back through a heat source that reheats the fluid during each cycle. There are different types of heat sources, including geothermal water, boilers, and heat exchangers. Geothermal water is considered to be efficient in locations with good geothermal potential (FAA 2011). EHPS melt ice and snow using either resistive cables embedded in concrete or electrically-conductive concrete (ECON). The use of resistive cables embedded inside concrete structures has been applied to deicing of snow and ice in Oregon, Texas, and Pennsylvania, and the performance of electrical cable was sometimes found inadequate due to the high power

density required (Zenewitz 1977) and damage to electrical cables or associated sensing elements for triggering the system (Joerger and Martinez 2006).

In recent years, ECON-based HPS have been receiving attention for use in mitigating problems associated with the presence of ice/snow on roadways and paved areas of airfields. ECON works by applying a voltage to electrodes embedded in the ECON layer to deliver power to conductive materials and thereby melt ice and snow. The effectiveness of the use of various conductive materials such as steel fiber, carbon fiber, etc., added to conventional concrete to produce ECON with sufficient electrical conductivity (i.e., low electrical resistivity), and other favorable engineering properties has been thoroughly investigated (Gopalakrishnan et al. 2015).

1.2 Objective

The primary objectives of this research are:

- To identify requirements related to material selection, design, construction, and operational performance for an electrically conductive concrete (ECON) heated pavement system (HPS).
- To develop a 3-D finite element (FE) modeling approach as an alternative method for evaluating ECON HPS time-dependent heating performance and thereby achieve design optimization in a timely manner; and
- To demonstrate the world's first full-scale field implementation of ECON HPS in a real airport environment.

The overall goal of this study is to advance the state-of-the-art knowledge concerning design, construction, and performance of heated pavement systems. Such well-designed, well-constructed, and well-performing heated pavement systems prevent ice and snow

accumulation on paved surfaces with the potential to dramatically enhance the safety, sustainability, and durability of the transportation infrastructure systems.

1.3 Dissertation Organization

This dissertation written in the alternative journal paper format is organized as follows: Chapter 1 presents general background, research objectives and approach, and dissertation organization.

Chapter 2 provides a state-of-the-art review of heated-pavement systems, including hydronic heated-pavement systems (HHPS) and electrically-conductive concrete (ECON) heated-pavement systems (HPS) along with their advanced construction techniques, highlighting their potential for heated pavement construction. Advanced construction techniques considered in this study include use of precast concrete (PC), two-lift paving, and concrete overlays. Advantages and limitation of these techniques are reviewed and discussed to identify the feasibility of utilizing these techniques in large-scale HPS construction.

Chapter 3 presents the first journal article: ***System Requirements for Electrically Conductive Concrete Heated Pavements*** that discusses the system requirements for ECON HPS related to material selection, design, and construction to achieve cost-effective performance. Design flow was developed for large-scale ECON HPS applications for optimizing ECON parameters such as electrode spacing, power, voltage, etc.

Chapter 4 presents the second journal article: ***A 3-D Finite Element Model for Simulating the Heat Performance of Electrically Conductive Concrete Heated Pavements*** that describes a feasibility study on development of a 3-D finite element (FE) modeling approach for use as an alternative method for evaluating ECON HPS time-dependent heating performance and thereby achieve design optimization in a timely manner. It describes a 3-D

FE model for ECON slab that was developed by examining decoupling of thermal-electrical analysis (Joule heating) using COMSOL Multiphysics software and validated though comparison with experimental test results. Sensitivity of various ECON HPS design variables with respect to heat generation and distribution performance is also described.

Chapter 5 presents the third journal article: ***Design and Construction of The World's First Full-Scale Electrically Conductive Concrete Heated Airport Pavement System at A US Airport*** that demonstrates the 2016 design, construction, and performance of the world's first full-scale ECON-based HPS at the Des Moines International Airport (DSM) in Iowa. Installation plans and instrumentation methods for electrodes and sensors were identified. ECON HPS power density and energy consumption were calculated from data produced from electric current and voltage sensors during deicing and ant-icing scenarios.

Chapter 6 presents the fourth journal article: ***Development of Construction Techniques for Heated Pavements*** that focuses on developing a conceptual design framework and provide construction guidance for electrically conductive concrete (ECON) and hydronic heated pavement system (HHPS) using precast concrete (PC), concrete overlay, and two-lift paving (2LCP) to expedite construction work during large-scale construction of heated pavements and provide different construction techniques

Chapter 7 summarizes the research work accomplished in this dissertation. It also describes the contributions of this study and makes recommendations for future research.

CHAPTER 2. LITERATURE REVIEW

This chapter attempts to present a comprehensive literature review on recent heated pavement systems and advanced pavement construction techniques. HPS can be classified into two general categories, HHPS and EHPS. Advanced pavement construction techniques include precast concrete (PC), two-lift concrete paving (2LCP), and concrete overlay. In addition, each paper will have its own literature review relevant to the paper's focus.

2.1 Review on Heated Pavement Systems

2.1.1 Hydronic Heated Pavement System (HHPS)

Hydronic heating systems melt ice and snow by circulating heated fluid through pipes embedded inside pavement structures. The cooled fluid runs through a heat source which reheats the fluid each cycle. There are different types of heat sources: geothermal waters, boiler, and heat exchangers. Geothermal water is considered to be efficient in locations with good geothermal potential (Lund 2005). The disadvantages of hydronic systems include construction difficulties, high installation costs, and challenges associated with repair, if fluid leakage occurs.

HHPS has been implemented in the Klamath Falls Bridge, located in Oregon in 1948 (Lund 2005). The fluid was heated using geothermal well through a heat exchanger to warm the bridge deck surfaces to melt ice and snow and to enhance the skid resistance and, thereby, eliminate car accidents. Recently, HHPS using geothermal well as a heat source was constructed in the aprons at the Greater Binghamton Airport, located in Binghamton (See Figure 2-1) and the total area of the project was a 3,200 ft^2 (297 m^2) with construction cost of $ 1,600,000 (Brill 2016). The Gardermoen International Airport implemented HHPS using Aquifer Thermal Energy Storage (ATES) that was able to heats and cools the aircraft parking

with a total area of 7,450 ft^2 (700 m^2) (Barbagallo 2013). The system was also supported by an electric and oil fired and boiler to help increasing the design load of 248 W/m^2 since the ATES was not capable of meeting the deign load.

Figure 2-1 HHPS using geothermal source (Brill 2016)

The components of HHPS include heat transfer fluid, piping, fluid heater, pumps, and controls as shown in Figure 2-2 (ASHRAE 2015). HHPS melts ice and snow by circulating heated fluid through pipes embedded inside concrete structures. The cooled fluid runs through a heat source that reheats the fluid for each cycle. A common practice is the use of propylene glycol as a heat transfer fluid due to its moderate cost, high specific heat, and low viscosity. Pipes can be made of metal, plastic, or rubber. The drawback of using steel pipes is their susceptibility to rusting, so, the use of steel embedded in pavement is not a common practice. An alternative to steel pipe is plastic pipes such as polyethylene (PE) or cross-linked polyethylene (PEX) because it has resistance to corrosion and lower material cost.

Polyethylene (PE) and cross-linked polyethylene (PEX) withstand fluid temperatures up to 60ºC and 93ºC, respectively.

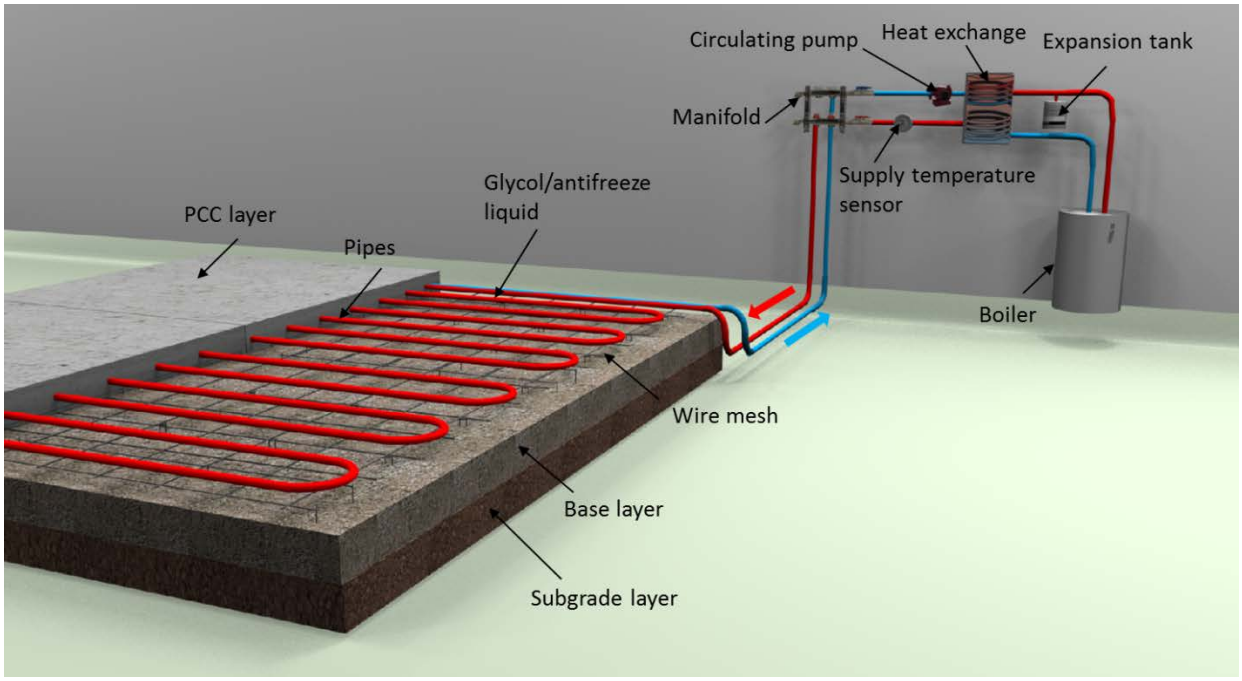

Figure 2-2 Detail of HHPS

The different types of fluid heaters include geothermal hot water, underground thermal energy storage (UTES), boilers, and heat exchangers (FAA 2011). The fluid heater can be selected based on availability at the project site. Geothermal energy is considered to be efficient in locations with good geothermal potential (Joerger and Martinez 2006). The efficiency of HHPS in melting ice and snow significantly depends on different factors (Ceylan et al. 2014), including fluid temperature, pavement conductivity, pipe depth, and pipe spacing. The thermal conductivity of Portland cement concrete (PCC) is higher than for Hot-Mix Asphalt (HMA), so PCC has potential to conduct more heat.

A hydronic slab's pipes can be arranged in different patterns – serpentine or slinky, for example – to provide uniform heat on the hydronic slab surface to prevent ice and snow

accumulation. The serpentine pattern (Figure 2-3) is commonly used in melting snow and ice on paved surfaces (FAA 2011). In the serpentine pattern, straight pipes are placed on equal centers and connected to a manifold using U-shaped pipes. The slinky pattern is placed in a circular shape with each circle overlapping the other one. A hydronic heated system was constructed into a 44.5 m long and a 17.7 m wide bridge deck in Amarillo, Texas and a serpentine pipe pattern was selected (Minsk 1999). The geothermal well was used as the energy source to heat the fluid, resulting in a reduction in operation cost.

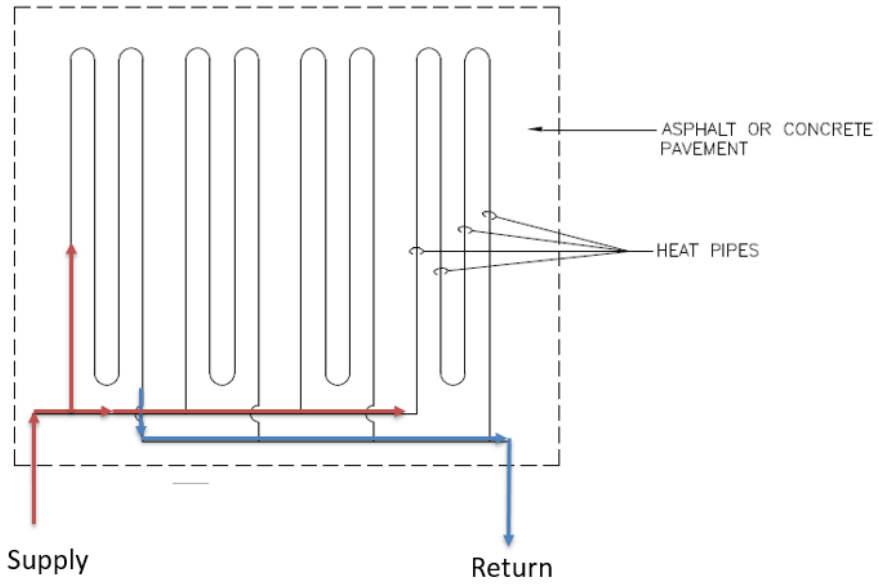

Figure 2-3 Hydronic pipes pattern (FAA 2011)

The pipe pattern can be designed using industrial software such as LoopCAD 2016 (LoopCAD 2016). LoopCAD can generate circuit layout drawings and zones for the project site and perform detailed hydronic calculations such as energy density based on ASHRAE methods (See Figure 2-4). LoopCAD software has the flexibility to adjust the pipe layout drawings, and loop lengths are generated by the program.

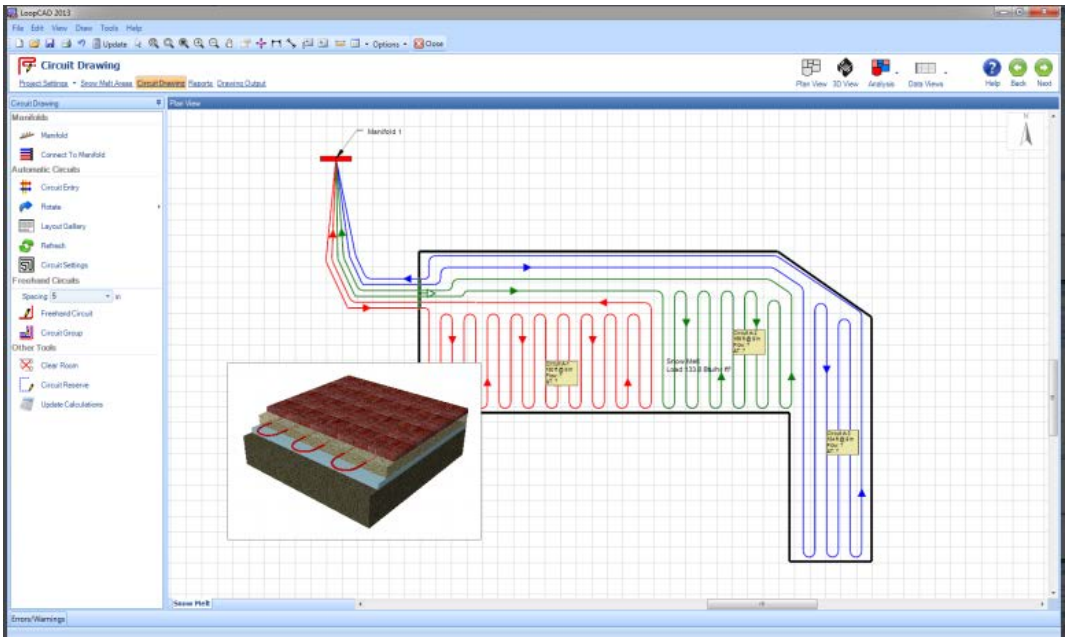

Figure 2-4 Snowmelt design LoopCAD software (LoopCAD 2016)

2.1.2 Electrically Heated Pavement System (EHPS)

EHPS melts ice and snow by using either resistive cables embedded in concrete or ECON. Recent research studies (Tuan 2008 and Heymsfield et al. 2013) have demonstrated that ECON can enable sufficient electrical conduction to facilitate the prevention of ice and snow formation when connected to a power source. These research studies serve as benchmarks for carrying out further investigations to design and develop the most effective ECON for heated airport pavement systems. EHPS reported in literature up to date are compared in

Table 2-1. Carbon fiber grille (Lai et al., 2014) was embedded inside concrete to generate heat by supplying electric power. The carbon fiber grille made of steel mesh and carbon fiber heating wires was placed at 2-in. below the concrete pavement surface. The size of each concrete slab was 15-ft. × 15-ft. × 16-in. Thermometer sensors were placed along the concrete at various depths. The study reported that the pavement was heated for 2 hours by

supplying 350 w/m^2 of power density to melt 1-in. thick of snow by increasing the concrete surface temperature from -1.2^{o}C to 3.4^{o}C.

The ECON HPS is considered as an alternative option to traditional methods because it has potential to melt ice and snow in a stipulated time frame and to overcome the drawbacks of using traditional de-icing methods (Gopalakrishnan et al. 2015 and Abdualla et al. 2016). The earliest patent on the topic of ECON was issued in 1965 (Barnard 1965). Since then a number of ECON recipes (i.e., mix proportions, combinations of different conductive materials, etc.) and applications have evolved (Freeman and Hymers 1979; Xie et al. 1996; Zaleski et al. 2005; Arnott et al. 2005; Tuan et al. 2010; Ramme et al. 2012).

ECON mixture was developed by using steel and carbon fibers as an additive to reduce the electrical resistivity and slab tests were constructed with the developed ECON mixture that provides promising results in melting ice and snow (Tuan 2008). The Nebraska department of roads selected a potential bridge site to demonstrate the ECON HPS for the Roca Spur Bridge. The bridge deck consisted of 52 slabs; each slab size was 4-ft. × 12-ft. × 4-in. and had two electrodes and a temperature sensor embedded in the 4-in. ECON layer. The average power of the Roca Spur Bridge system was 500 w/m2 and its unit cost was about $ 250 per snowstorm (Tuan 2004).

Table 2-1 Comparisons of electrically heated pavement systems reported

Deicing systems	Surface Temperature before heating (ºC)	Surface Temperature after heating (ºC)	Snow melting time (h)	Power density (W/m^2)	Snow thickness (in)
Carbon fiber grille (Lai et al. 2014)	-1.2 °C	3.4 °C	2 h	350 W/m^2	27mm (1in)
Conductive concrete mixing with steel fibers and carbon particles (Tuan 1998, 2004)	-1.1°C (30°F)	15.6 °C (60°F)	30 min	516 W/m^2 (48 W/ft^2)	NA
	NA	9 °C	3 days	500 W/m^2 (46 W/ft^2)	6mm (0.24in)
Carbon fiber tape heating panel (Yang et al. 2012)	-11.2 °C (12 °F)	0 °C (32 °F)	9.3 h	127 W/m^2	15mm (0.6 in)

The electrical resistivity of concrete is significantly influenced by the porosity, relative humidity and the resistivity of the pore water containing dissolved salts (which in turn is influenced by the concrete age, origin, and type of cement) (Simon and Vass 2012). Note that, depending on the context, both electrical resistivity and conductivity have been used interchangeably in the literature to describe the electrical properties of cement paste, mortar and concrete systems. Concrete is a multi-component, micro-porous construction material typically comprised of cement, coarse and fine aggregates, and water. Conventional or normal concrete is not electrically conductive and is primarily comprised of three phases (Spragg et al. 2013): (1) a vapor phase (pore filled with air) with about 10^{11} Ω-cm of electrical resistivity (i.e., extremely low conductivity); (2) a solid phase (aggregate and cementitious solids) with about 10^{17} Ω-cm of electrical resistivity; and (3) a fluid phase (pore filled with liquid solution including water) with about 5 to 100 Ω-cm of electrical resistivity. Since the fluid phase in concrete has relatively higher conductivity compared to that of vapor and solid phases, the conductivity measurements of concrete is higher (or resistivity is lower) when the specimen is wet or saturated with liquid solution as opposed to measurements from

unsaturated specimens. Note that several factors have been identified to have influence on the electrical conductivity measurements in cementitious systems. For instance, Spragg et al. (Spragg et al. 2013) reported that specimen geometry, temperature of the specimen during the test (related to the mobility of the ionic species in the pore solution), sample storage and conditioning (sealed versus saturated) are all key factors that should be considered in standardizing tests for measuring electrical resistivity/conductivity of cement-based materials.

Cement-based materials conduct electricity electrolytically through the motion of ions in pore solution of a fluid phase and electronically through the continuous contacting motion of free electrons of conductive materials in a solid phase (Yehia 2000). Concrete is considered as a good electrical insulator in dry condition. The electrical resistivity of air dried normal concrete ranges from 600 to 1,000 kΩ-cm (Whittington et al. 1981) and oven dried normal concrete has an electrical resistivity of about 10^8 kΩ-cm (Ramme et al. 2012). However, the electrical resistivity of moist concrete is about 10 kΩ-cm and is therefore classified as a semiconductor (Ramme et al. 2012). Conductive materials with extremely high conductivity values (i.e., electrical resistivity values less than 0.1 Ω-cm) can be used to replace aggregate materials in normal concrete to achieve conductive concrete. Reported literature suggests that conductive materials incorporated into concrete can broadly be categorized as: (1) powders (substituting for fine aggregate in part) – carbon, graphite; (2) fibers (substituting for fine aggregate in part) – carbon fiber (CF), steel fiber (SF), steel shaving (SS), carbon nano-fiber (CNF); and (3) solid particles (substituting for coarse aggregate in part) – steel slag and marconite. Most of the studies reported in the literature tried to experiment with various conductive materials individually or in combination, their

dosage rates, and their impact on ECON mechanical properties in an effort to identify the optimized conductive material compositions and mix designs to achieve well performing ECON.

None of the reported studies indicate the need for special aggregate gradation requirements to achieve well-performing ECON. There is no special reference to strict requirements on aggregate type and size for achieving conductive concrete. Most of the studies reviewed in this paper investigated limestone mixes. Few studies experimented with the idea of either partially or fully replacing limestone aggregate with Blast Furnace Slag (BFS) along with smaller amounts of graphite powder, but were not successful in achieving desired conductive properties (Heymsfield et al. 2013, Ramme et al. 2012). One study (Dehdezi and Dawson 2011) revealed that quartzite has greater thermal conductivity than regular aggregates such as limestone and gravel and therefore has great potential for enhancing the pavement energy harvesting properties. So far, quartzite has not been investigated in electrically conductive concrete.

Cost-effectiveness is also an important ECON mix design consideration to implement ECON for heated pavement systems. However, very few studies have evaluated the cost-effectiveness of ECON based HPS in depth by employing economic analysis methods such as benefit-cost analysis (BCA). Yang et al. (2011) presented simple cost comparison results of the currently available ECON based heated pavement systems with radiant snowmelt systems such as electrical and hydronic heating systems. The reported installation costs ranged from \$48/m^2 to \$205/m^2 for ECON based heated pavement systems and are about twice expensive than radiant snowmelt systems (\$23/m^2 to \$161/m^2). However, the unit energy costs of ECON based heated pavement system operations were reported to range from

$0.033/[m^2-cm] to $0.075/[m^2-cm] compared to about $0.368/[m^2-cm] in operating other snowmelt systems. Although these ballpark cost data comparisons are not enough to establish the cost-effectiveness of ECON based heated pavement system, they do demonstrate the potential of ECON for pavement deicing applications if reduction in installation costs could be achieved using innovative means, including the use of cost-effective conductive material systems and economical ECON mix design optimization.

2.1.3 Snow Melting Heat Flux Requirement

The minimum design requirement of a heated pavement system is that it must be capable of keeping a surface condition of "now worse than wet" and maintaining a surface temperature above the freezing point before and during the snow accumulation (FAA 2011). The heating requirement for snow melting depends on the rate of snowfall, air temperature, relative humidity, and wind speed. The steady-state energy balance equation for required heat flux (q_o) in (W/m^2) is presented below:

$$q_o = q_s + q_m + A_r(q_h + q_e) \quad (1)$$

where, q_s, q_m, A_r, q_h, q_e are sensible heat flux (W/m^2), latent heat flux (W/m^2), snow-free area ratio, convective and radiative heat flux from a snow-free surface (W/m^2), and heat flux of evaporation (W/m^2), respectively. The detailed equation definition and parameters are available in the ASHRAE 2015 HVAC handbook (ASHRAE 2015) and the FAA advisory Circular AC 150/5370-17 (FAA 2011). The heat flux q_o, equation (1), does not account for the back and edge heat losses that increase the total heat slab output (q_o), that can vary from 4 to 20% depending on factors such as pavement construction, operating temperature, ground temperature, or back exposure (Viega 2005).

The heat requirement for a snow-melting installation are based on classification systems I, II or III. Class I (minimum): residential walks or driveways, class II (moderate) commercial sidewalks and driveways, and class III (maximum) toll plazas of highways and bridges; aprons and loading areas of airports; hospital emergency entrances. These classifications are correlated to snow-free area A_r values. Class I has a snow-free area ratio of 0 and the surface is allowed to be covered with sufficient thickness of snow before beginning to melt the snow. Class II has a snow-free area ratio of 0.5 and the surface must be kept clear of snow accumulation, while a wet surface is acceptable. Class III has a snow-free area ratio of 1 and the surface must melt snow quickly while it is falling, and the surface must remain dry.

The FAA AC No. 150/5370-17 provides guidance on the minimum performance requirements for the design, construction, inspection, and maintenance of heated airport pavements (ASHRAE 2015). For airport pavement deicing applications, conductive concrete is recommended to be installed as a thin concrete overlay, formulated to satisfy Item P-501 (Portland Cement Concrete Pavement) specifications.

2.2 Review on Advanced Pavement Construction Techniques

This section summarizes a state-of-the-art review of advanced construction techniques, highlighting their potential for heated pavement construction. Advanced construction techniques considered in this study include PC, two-lift paving, and concrete overlays. Advantages and limitation of these techniques are reviewed and discussed to identify the feasibility of utilizing these techniques for large-scale HPS construction.

2.2.1 Precast Concrete (PC)

PC has demonstrated satisfactory performance in bridges, pavements, buildings, and airfield construction. It provides high strength, low permeability, and low cracking potential;

these features are consequences of preparing the panels at off-site where quality control can be more effectively implemented. The use of PC technique instead of cast-in-place for construction of pavements expedites the construction process by eliminating the need for concrete strength-gaining time from the construction procedure (Bly et al. 2013; Merritt et al. 2004; Priddy 2013). PC expedites rehabilitation of airfield pavements where the construction work is faster or can be done overnight because PC already has gained its strength and cured at the plant (off-site), so no time is needed for PC to attain its strength after finishing the reconstruction work. Since flight operations must be resumed in the shortest time frame possible, often with only 4 to 6 hours available to complete repairs, the PC technique is a good choice for minimization of the downtime of airport pavement facilities (Bly et al. 2013).

The PC technique was used to rehabilitate a taxiway at LaGuardia airport, New York during September of 2002. The selection of PC as a rehabilitation option over asphalt concrete or PCC was due to the fact that the asphalt concrete requires frequent rehabilitation because of the highly concentered and repetitive aircraft movements and reduce the construction downtime (Chen et al. 2003). This study was initiated to investigate and evaluate various PC techniques and the feasibility of placing the PC within a 36-hours closed period. The feasibility parameters investigated included the ability to place the PC on a milled or newly paved, the bedding materials for the PC slab size, the transportation of the PC slabs from the production to the job sites, the weight of the PC slab, and the ability to accommodate taxiway lighting (Chen et al. 2003). The PC was designed to accommodate the joining of the electrical conduit that was embedded in some PC panels and the electrical conduit slots were filled with a rapid-setting, finely-graded concrete mix. Prior to the

placement of PC, the existing asphalt concrete was milled to eliminate the surface distresses and bedding materials were utilized to provide a uniform base for the PC. The panel size of PC was 16 in. (406.4 mm) thick × 12.5 ft. (3.8 m) wide × 25 ft. (7.6 m) long.

While the sensitivity of PCC to weather conditions does not permit cast-in-place concrete paving under all weather conditions, different weather conditions, such as extremely cold or hot temperatures would not prevent the construction work if PC was used (Merritt et al. 2004). Table 2-2 presents the differences between PC and cast-in-place Portland cement concrete pavement (Chang et al. 2004) highlighting their relative advantages and disadvantages.

Table 2-2 Comparison between PC and cast-in-place (FAA 2007)

Rigid Pavement Alternative	Advantages	Disadvantages
Cast-in-place	• High final strength • Contractor/Work Crews have experience with material • Workability of material • Specifications, testing procedures and design are proven • Low cost in comparison with other rigid pavement alternatives	• Length of construction time. • Length curing time • If concrete does not meet specifications in the field then it may have to be removed
Precast concrete	• Rapid placement of panels • Panels are cast in controlled conditions in pre-cast yard • Panels are already at loading strength when placed	• High cost • Placing and moving panels may be difficult • Sizes of panels are generally smaller than if cast in place • Trucking panels to site • Requires precise fine grading • Edges of panels are easily damaged

2.2.1.2 Precast Concrete Experience in the United States

Little has been done or documented with respect to PC construction in airfield pavements. Highway PC construction in the US began over 50 to 80 years ago, but it did not appear to be a cost-effective technique at that time because of lack of technical information that resulted in an increased installation labor requirement. The process of installing PC can be time-consuming and require heavy equipment (Priddy et al. 2013), and while many US highway agencies did not implement PC technology for a long time, over the last 10 years several US highway agencies have been implementing the technology (Tayabji et al. 2013).

The implementation of PC systems may include both proprietary and non-proprietary systems. Figure 2-5a and Figure 2-5b shows the variation of intermittent repair technique with dowel bars positioned in existing concrete pavement. The Strategic Highway Research Program 2 (SHRP2) project R05 provided a guideline for design and construction of different PC applications and developed a guideline for project selection, design, fabrication, installation, and rehabilitation of PC systems (Tayabji et al. 2013). PC can be used to repair distressed areas of an existing pavement that represent either a small area of localized distress or an extended long-distance distress in the pavement.

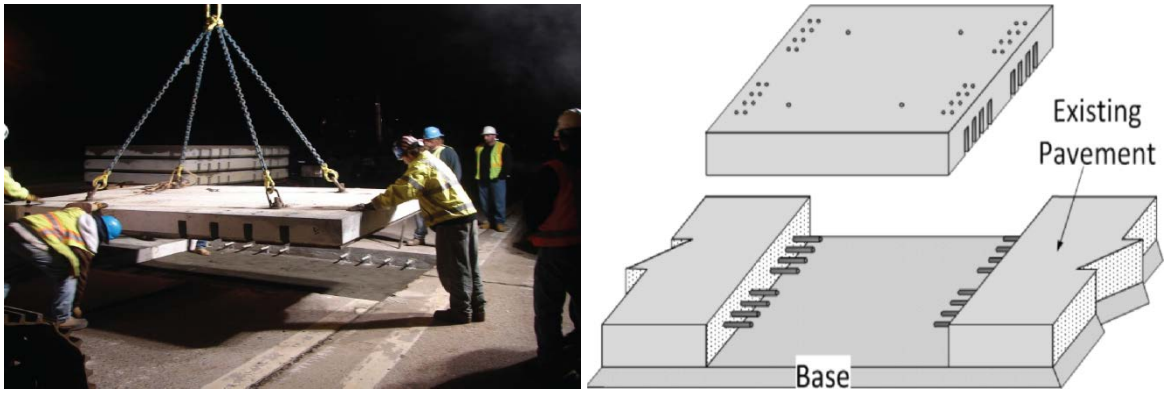

(a) **(b)**

Figure 2-5 Intermittent repair application for existing concrete pavement

Because of increases in implementation of the PC, several agencies have participated in developing specifications and guidelines for such systems. The American Association of State Highway and Transportation Officials (AASHTO) established a Technology Implementation Group (TIG) during 2006 that developed a specification for fabrication and construction of PC and guidelines for the design of PC systems (Tayabji et al. 2009).

The application of PC technology can be classified into intermittent repair and continuous application (Tayabji et al. 2009). Full-depth repair (FDRs) and full-panel replacement are two types of repair categorized as intermittent repairs. Continuous application, unlike intermittent repair of concrete pavement, uses full-scale project reconstruction or putting an overlay on existing pavements; this can apply to either Portland and asphalt cement concrete pavements. Three different types of PC can be defined as continuous systems; (1) jointed precast concrete pavement (JPrCP) systems, (2) precast prestressed concrete pavement (PPCP) systems, and (3) incrementally connected precast concrete pavements (ICPCP) systems (Tayabji et al. 2009 and Tayabji 2010).

Various PC types have been assessed in comparison to conventional concrete pavement systems; these include joint plain concrete pavement (JPCP) and joint reinforced concrete pavement (JRCP) in terms of design concepts, field installation procedures, advantages, limitations, and costs (Chang et al. 2004). The PC types evaluated include Super-slab, Full-depth repair, Stitch-in-time, and Uretek methods (Chang et al. 2004). The Super-slab system designed by the Fort Miller Co. is intended for use in rapid construction work such as highways, ramps, taxiways, and in heavy traffic areas. Furthermore, it can be used to reduce user cost and to shorten the duration of construction operation. Precast panels of super-slab can be used either for intermittent repairs or continuous paving. The length of

each panel can range up to 25 feet, and width can range from a minimum of 4 feet to a maximum of 12 feet. Precast pavement panels have dowel bars and tie bars on two sides and slots on the other sides. Dowel bars are used to transfer loads to adjacent panels and to connect precast panels. A precast panel has two grout ports, one for bedding the grout ports and the second to fill the dowel slots. Bedding grout ports are used to fill voids between the panels and the graded bedding base. A high-strength grout material is poured through the bedding grout port to provide good interlock with adjacent slabs.

The Super-slab system was selected for installation in the Tappan Zee Bridge toll plaza in New York. The reasons for using Super-slab was that the construction work could be conducted during night-time hours and allow opening of lanes during morning rush hours, avoiding excessively high user costs. The project sponsor was satisfied with the construction results, including the appearance and the quality of the precast panels. The capital cost of this project was about $\$26/ft^2$ including fabrication, delivery, and installation that, while higher than that of a conventional concrete pavement, used PC to dramatically reduce user costs resulting from traffic delay caused by pavement rehabilitation operations.

Full Depth Repairs (FDR), also known as the Michigan method, can be used only for intermittent paving, not in continuous paving. The panel size is typically 6ft ×12ft (1.8m × 3.6m), and each panel contains three dowel bars in each wheel path with the dowels embedded in the PC at the transverse joints. The FDR does not require curing after the placement of PC since it is prepared and cured off-site.

The Uretek method uses small drilled holes to allow the polymer resin to lift the panels and fill the underside voids between the panels and the graded bedding base. This method can be used for repairing differential settlements and void conditions underneath

concrete or asphalt pavements in both highways and airports. Instead of using dowels as in the Super-slab system, the Uretek method utilizes a ‘stich-in-time’ system, a procedure that places a composite-reinforced resin blade (fiberglass tie) to transfer load into an adjacent panel. Once the blade is inserted, the remaining space in the slot is filled with high-density polymer resin. The advantage of the stich-in-time method is that it is less expensive than the procedure of inserting dowels. Other PC types (Bly et al. 2013) recently applied in airfield applications include “Soviet-style” slabs and “US Air Force Methods”.

2.2.2 Two-Lift Concrete Paving

Two-lift concrete paving (2LCP) has become a common construction practice in Europe where the lower lift can be optimized to enable the use of locally available or recycled materials, while the top lift is optimized for long life and functionality (Figure 2-6). 2LCP involves the placement of two wet-on-wet layers of concrete or bonding wet to dry layers of concrete where the bottom layer is relatively thicker and the top layers is relatively thinner (Cable 2004). The benefits of 2LCP includes using recycled aggregate that leads to cost reduction and production of more sustainable pavements; this method also provides a high-quality and durable surface, improves skid resistance, and reduces noise (Cable 2004). These benefits could compensate for the required use of two slipform pavers needed for each layer, and the extra labor and trucking costs associated with them. The use of 2LCP is currently under investigation by several agencies in the United States.

Figure 2-6 Two-lift construction of concrete pavement in progress (Hu et al. 2014)

2LCP is not a new concept and has been around almost as long as concrete paving itself (Cable 2004). 2LCP was conceptually developed and first constructed in the United States, but it later became more common in Europe (Cable 2004 and Cable and Frentress 2004). In the early 1950s, the common practice of 2LCP included placement of a mesh layer between the bottom layer and top layer of concrete, but recently in the United States a single homogenous layer of concrete – the same material – has typically been used, along with reducing the pavement slab joint length, thereby reducing the application of 2LCP (Cable 2004). However, 2LCP has been implemented in the United States since 1970 in Iowa, Florida, and Michigan and since the 1930s in European countries, including Austria, Belgium, Germany, and the Netherlands (Cable and Frentress 2004).

2.2.2.1 The United States and Europe' Experience with Two-Lift Concrete Paving

The first use of 2LCP was in 1891 in Bellefontaine, Ohio and the method was patented in 1906 in Chicago, IL (Cable 2004 and Cable and Frentress 2004). 2LCP was implemented in the United States with a top-layer concrete thickness in the range of 1.6-4

inch and a bottom layer concrete thickness range of 6-11.8 inch (based on a survey from 1976 to 2012) (Jensen and Hu 2013). 2LCP was constructed in Lyon County, Iowa to demonstrate the feasibility of using recycled aggregate at the bottom lift while the top lift was made with high quality aggregates. In 1978, Florida constructed a test section of two-lift pavement to investigate the performance of pavement with two different flexural strengths in which the top lift had higher flexural strength than the bottom lift due to the use of low-quality or recycled materials for the bottom lift. The pavement constructed in those projects – both in Iowa and Florida – has been reported as being in good conditions (Cable 2004). Because of availability of local low-quality aggregate in Kansas, a 2LCP approach was adopted using the local aggregate at the bottom lift and imported high-quality aggregate for the top lift to provide longevity and functionality. In Michigan, since pavement surface noise was an issue, two-lift pavements were built with high-quality aggregates in the top lift, the exposed surface, to reduce noise. Application of two-lift paving will help agencies in reducing paving costs and environmental impact of pavements.

In Europe, 2LCP was implemented in different countries where, according to a survey from 1989 to 2008, the top-layer thickness of concrete was in the range of 1.6-5.5 in., and the bottom layer thickness of concrete was in the range of 6-10 in. (Jensen and Hu 2013). 2LCP was used in Germany to reduce noise, increase friction, and achieve a smooth profile by building the top lift of pavements with high-quality aggregate that was also resistant to freeze-thaw effects (Cable and Frentress 2004). 2LCP was used at the Munich airport, with a bottom lift thickness of 9.5 in. and a top lift thickness of 5.5 in. Locally-available aggregates were used in the bottom lift and high quality aggregates were used in the top lift. Germany has one of the largest companies – Wirgeten GmbH - that manufactures slipform pavers

capable of paving with a width between 16.4 feet and 50 feet and a depth of up to 17 in. (Cable 2004). The Austrian government enforced regulations on any upcoming new construction of highway to utilize site materials such as recycled aggregates in concrete mixture; as a result, 2LCP was used to fulfill the new regulations (Cable and Frentress 2004). For example, a deteriorated Freeway A1 pavement – a connecting road between Vienna and Salzburg – was torn up and its materials were recycled to be used for building new pavement. The recycled aggregate was used for the 8.5inch-thick bottom lift since the bottom lift is not as sensitive as the 1.6 inch-thick top lift that contained high-quality aggregate to reduce noise and increase friction.

2.2.2.2 Construction of Two-Lift Concrete Paving

There are no guidance or standards available to specify minimum requirements (strength, durability, etc.) for the characteristics of bottom concrete lift nor are there guidelines for how to achieve durability, safety, and noise reduction on the top lift (Hu et al. 2014).

2LCP requires additional paving machines, mixing plants, belt placers, extra trucks, and labor for the second paver, as shown in Figure 2-7 (Hu et al. 2014). Since two types of concrete are used in two-lift construction, inspection of incoming concrete loads is required to identify the different concrete mixtures for each layer. 2LCP was used in I-70 highway construction in Saline County, Kansas in 2008. Figure 2-7a depicts the construction work showing a two-lift paving-equipment train that includes a spreader with a belt placer, a slipform paver, a burlap drag, and the curing/texturing equipment. The belt placer and slipform paver for the bottom lift is shown in Figure 2-7b. The bottom lift was placed with the spreader and the first slipform paver, and the bottom lift concrete mixture was stiffened by adding viscosity-modifying admixtures to inhibit deformation of the bottom lift during

placement of the top lift (Figure 2-7c). In addition, a grid was placed under the concrete discharge spreader of the top lift to mitigate the deformation of the bottom lift while placing the concrete for the top lift. Dowel baskets were placed prior to paving and tie bars were inserted in front of the bottom lift paver. Figure 2-7d illustrates the paving procedures of the top lift using the second belt spreader and slipform paver.

(a) (b)

(c) (d)

Figure 2-7 Two-lift construction of concrete pavement in progress: (a) two-lift paving equipment train, (b) bottom lift belt placer/spreader and paver, (c) demonstration of the concrete stiffness of the bottom lift, and (d) top lift belt placer/spreader and paver (Hu et al. 2014 and Gerhardt 2013)

The recommended time for placing the top lift of concrete is between 30-60 minutes after the placement of the bottom lift concrete to mitigate combining the two concrete mixtures and to help obtaining a sufficient bond in the wet-on-wet procedure (Cable 2004). Additional equipment demand such as slipform paver, belt placer, bath plant, extra labor, and land for placing the equipment has increased the cost of two-lift paving to about twice that of single-lift paving (Gerhardt 2013). This cost could be reduced by using low-quality or recycled materials at the bottom lift and by utilizing only one slipform to cast both lifts. In an attempt to reduce the construction cost of two-lift paving, GOMACO – an American company – and Wirtgen – a German company – have developed a slipform paver to facilitate the two lift-paving using one slipform paver for both lifts.

2.2.3 Concrete Overlays for Highway Application

Concrete overlay systems have been proposed as cost-effective maintenance and rehabilitation solutions for a wide range of combinations of existing pavement types, conditions, desired service lives, and anticipated traffic loading. Although they in the past have been referred to as ultrathin whitetopping, conventional whitetopping, bonded overlays, unbonded overlays, etc., they have more recently been classified into two broad types (Figure 2-8): the bonded resurfacing family and the unbonded resurfacing family (Mallick and El-Korchi 2013 and Torres et al. 2012). Concrete overlays are discussed in detail in the national concrete pavement technology center (NCPC) – guide to concrete overlays solution 2007 – and ACI 325.13R-06 concrete overlays for pavement rehabilitation (ACI 2006).

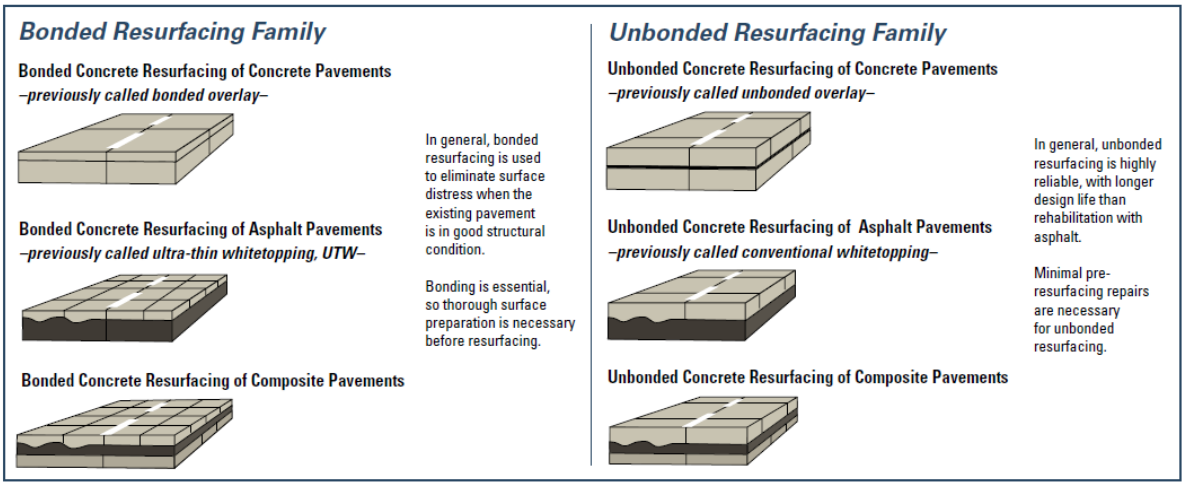

Figure 2-8 Two families of concrete overlay system (Harrington et al. 2007)

2.2.3.1 Unbonded Resurfacing Family

Unbonded resurfacing has been used to restore structural capacity of existing pavements that are in poor or deteriorated condition. Due to the isolated layer, unbonded resurfacing and existing pavement act independently of one another to mitigate reflective cracking. Since unbonded resurfacing is structurally isolated from the existing pavement, dowel bars should be used to transfer load when the thickness of the pavement is greater than 8 in. (20.3 cm) and undergoes heavy loads.

2.2.3.1.1 Unbonded Concrete Resurfacing of Concrete Pavements

In the past, unbonded resurfacing of concrete pavements was called unbonded overlay. The recommended thickness of unbonded resurfacing of concrete pavement is in the range of 4-11 in. (10.2-27.9 cm) depending on the anticipated traffic load and condition of the existing pavement. Unbonded resurfacing of concrete pavements has been successfully implemented with good-to-excellent performance in many states, including California and Iowa. The crucial parameters that affect the performance of unbonded concrete resurfacing

are separator layer design, resurfacing thickness, joint spacing, and load transfer, as well as the condition of the subgrade that may pose failure to the surface, shoulder, and clearance.

Design

The design thickness of unbonded concrete resurfacing placed on existing concrete pavement may be calculated using a design procedure similar to that for designing a new concrete pavement on a rigid base while taking into consideration the separated layer. The design procedures for highway roads include the AASHTO 1993 design guide or the Portland Cement Association (PCA, 1984) design guideline (Mallick and El-Korchi 2013). The FAA advisory circular (AC) 150/5320-6F provides guidance on the design and evaluation of pavements used by aircraft at civil airports (FAA 2016). The joints of unbonded resurfacing may be matched or mismatched with the existing concrete pavement because some states enforce matching the joints of the unbonded resurfacing while others deliberately mismatch the joints. The reason for mismatching joints of unbonded resurfacing with existing pavement – according to previous specifications – is to increase the efficiency of load transfer (Mallick and El-Korchi 2013). The load transfer performance has been recognized as better than a new concrete pavement because of the support provided by the underlying pavement. Dowels are recommended when unbonded resurfacing must support high volumes of traffic. In general, if the unbonded resurfacing thickness exceeds 8 in or more, dowels should be used. Short joint spacings are recommended to mitigate the effect of curling stresses. Joint spacing is typically 6-15 ft depending on the unbonded resurfacing thickness.

Since unbonded resurfacing relies on the absence of bonding between the resurfacing and the existing pavement, the design of the separator layer can have a dramatic effect on pavement performance. The separator layer prevents reflective cracking and isolates the

concrete resurfacing from the existing pavement so that both layers move individually. A fine-grade asphalt mixture has been recommended as a separator layer and this provides excellent results when compared to others such as polyethylene sheeting, liquid asphalt, and chip seal; these are not recommended due to poor performance [Mallick and El-Korchi 2013 and ACI 2006). The thickness of the separator layer is typically 1-1.5 in. depending on the existing pavement condition. The separator layer also does not enhance the pavement's structural capacity. The drainage condition of the existing pavement also has a significant effect on the separator layer performance, increasing the risk of stripping in the separator layer. The separator layer has the potential to cause early-age shrinkage in unbonded resurfacing if the weather temperature exceeds 120^{o}F (48.9^{o}C), so proper curing should be used to reduce the surface temperature before placing concrete resurfacing.

Construction

The construction procedure for unbonded concrete resurfacing of concrete pavement is similar to that of placing, spreading, consolidating, and finishing conventional concrete. The construction of unbonded resurfacing may entail constructing a new shoulder due to the fact that the grade elevation might increase, typically in the range of 10-12 in. (25-30 cm) (Mallick and El-Korchi 2013), so if a shoulder is needed, a tied shoulder should be used to widen the unbonded resurfacing pavement. The benefits of a tied shoulder are to reduce edge stresses and longitudinal cracking. The depth of transverse and longitudinal saw-cuts is typically between one-fourth and one-third of the resurfacing concrete thickness.

2.2.3.1.2 Unbonded Concrete Resurfacing of Asphalt Pavements

Unbonded concrete resurfacing of asphalt pavements has been used in different states as a rehabilitation and maintenance solution providing good to excellent performance. In the past, unbonded concrete resurfacing of asphalt pavements was called conventional

whitetopping. Unbonded resurfacing has the potential to increase the life of pavements that exhibit extensive deterioration, include rutting, shoving, potholes, and pumping (Figure 2-9). While distresses asphalt pavement areas do not have to be repaired before placing concrete resurfacing, milling may be required if the existing asphalt has extensive deterioration.

The crucial factor affecting the performance of concrete resurfacing of existing asphalt or composite pavement is uniformity of the base support that can contribute to enhanced pavement performance. Although this resurfacing type does not rely on bonding, some partial bonding between the resurfacing and existing asphalt pavement can contribute to better pavement performance.

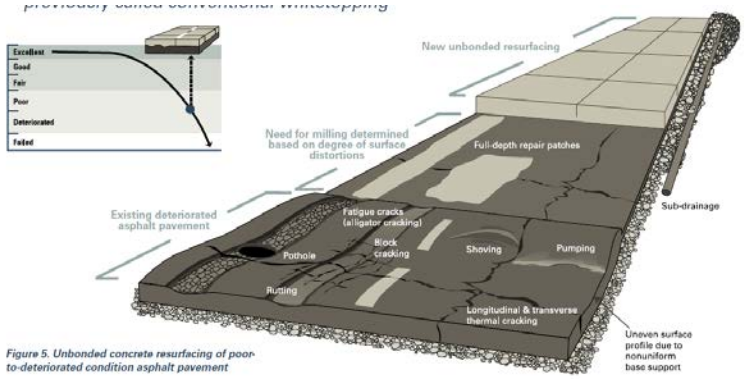

Figure 2-9 Unbonded concrete resurfacing of asphalt pavement (Harrington et al. 2007)

Design

The thickness of unbonded resurfacing of asphalt pavement is typically 4-11 in. (10.2-27.9 cm) depending on desired life, anticipated traffic loading, and the condition of the existing pavement. The thickness of unbonded resurfacing can be designed using conventional concrete pavement procedures such as those given in the AASHTO design guide 1993 and the ACPA StresstPave program. Doweling of joints is recommended if the unbonded pavement resurfacing undergoes high volume traffic. Joint spacing may be estimated – based on extensive experience – in feet as twice the slab thickness in inches.

Short joints are recommended to reduce curling and warping stresses due to high k-values. There is discrepancy regarding whether dowel bars should be used or not. In previous experiences reported by different agencies, unbonded resurfacing without dowel bars was used and its performance was reported satisfactory (Mallick and El-Korchi 2013). On the other hand, other agencies reported highway faulting problems attributed to the absence of dowels in unbonded resurfacing (Mallick and El-Korchi 2013). To accelerate early-age strength gains of concrete pavement to significantly reduce the downtime of the traffic lane, accelerating admixtures should be used to achieve early opening and reduce road user cost.

Construction

Before placing unbonded concrete resurfacing of asphalt pavements, the existing pavement should be smooth, free of extensive rutting and surface distortion (See Figure 2-10). High surface asphalt temperature also has the potential to cause early-age shrinkage in unbonded resurfacing if the weather temperature exceeds 120^{o}F (48.9^{o}C), so proper curing should be used to reduce the surface temperature before placing unbonded concrete resurfacing. The construction procedure of unbonded concrete resurfacing of asphalt pavement is similar to placing, spreading, consolidating, and finishing conventional concrete. The depth of transverse and longitudinal saw-cut is typically between one-fourth and one-third of the resurfacing concrete thickness.

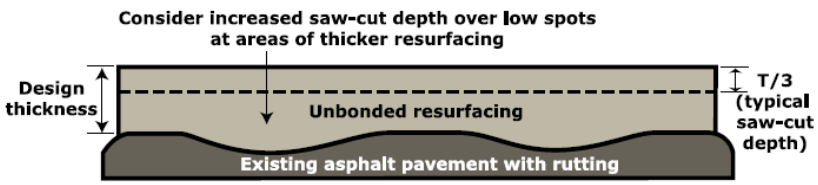

Figure 2-10 Asphalt rut depth when determining saw-cut depth (Harrington et al. 2007)

2.2.3.2 Bonded Concrete Resurfacing Family

Bonded concrete resurfacing, in contrast to unbonded concrete resurfacing, can be used when the existing pavement is in good or better structural condition, perhaps with some surface distress. Bonded resurfacing can be used to extend the life of existing pavements by eliminating structural and functional deficiencies such as rutting, pothole problems, surface friction, noise, ride quality, etc.

Bonded concrete resurfacing has been successfully used in existing concrete pavements. When bonded resurfacing is placed on concrete pavements – joint plain concrete pavement (JPCP) – joints should match with the underlying pavement to prevent reflective cracking and to behave as a monolithic pavement. Moreover, the aggregate properties of the bonded surfacing should be compatible with those of the underlying pavement to mitigate shear stress. When a bonded resurfacing is to be placed on asphalt concrete, it is important to ensure that the pavement surface is uniform and free of surface distortion to provide a sufficient bond.

2.2.3.2.1 Bonded Concrete Resurfacing of Concrete Pavements

In the past, bonded resurfacing of concrete pavements was called bonded overlay. The recommended thickness of bonded concrete resurfacing of concrete pavement is in the range of 2-5 in (5.1-12.7 cm) and it can be selected based on desired life, anticipated traffic loading, and the condition of existing pavement.

Design

The design concept of bonded resurfacing is based on the assumption that the bonded resurfacing and the existing pavement behave monotonically to reduce stresses and deflections. If the bonded resurfacing and existing pavements are not adequately bonded,

chances are that an early age cracking will occur due to the increase of curling and loading stresses in the concrete resurfacing.

Before applying bonded concrete resurfacing of concrete pavements, the existing concrete pavements should be in good or better structural condition with some surface distress as shown in Figure 2-11, so an evaluation of existing pavement is significantly important in determining the feasibility of applying bonded concrete resurfacing as the best candidate for a rehabilitation solution. The evaluation of existing concrete pavements includes falling weight deflection (FWD), visual inspection, and coring of the existing pavement. The design thickness of bonded resurfacing can be calculated using AASHTO Pavement Design Guide (AASHTO 1993) or the Portland Cement Association (PCA 1984) design guideline (Mallick and El-Korchi 2013). The required thickness of bonded resurfacing - using the AASHTO approach – is the difference between the structural capacity of a new concrete pavement and the effective thickness of the existing pavement. The joints of bonded resurfacing of concrete pavements should be matched with existing pavements to eliminate reflective cracking and behave as a monolithic pavement. Since the thickness of bonded resurfacing is thin, while dowels may not be used, the dowels in the existing pavement can transfer the loads to the adjacent slabs.

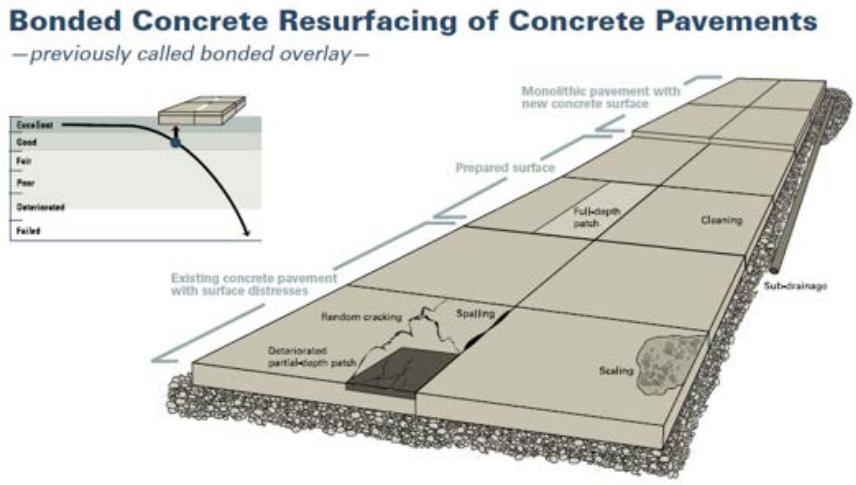

Figure 2-11 Bonded concrete resurfacing of good condition concrete pavement (Harrington et al. 2007)

Construction

The concrete mixture of bonded resurfacing should be compatible with the existing concrete pavement. This recommends using rapid strength materials to quickly gain strength as well as considering the effect of thermal expansion, contraction, and shrinkage to minimize stresses at the bonding layer. A slump value in the range of 2-3 in. (5.1-7.6 cm) is suggested to provide sufficient bonding grout. Fibers added to the bonded resurfacing mixture reduce plastic shrinkage cracking and improve toughness and post-cracking behavior. The aggregate coefficient of thermal expansion of the resurfacing concrete should be comparable to that of the existing concrete to reduce thermal stresses at the bond interface. To ensure sufficient bond between bonded resurfacing and existing concrete pavement, an assortment of approaches to surface preparation may be implemented, including shot-blasting, milling, and sandblasting. The most common practice for surface preparation is to use shot-blasting followed with air blasting, then placing the resurfacing concrete. A bonding agent is not recommended for use as a bonding materials because a bonding agent may cause

debonding between the layers if it dries before placing the resurfacing concrete (Delatte 2014). After paving the resurfacing concrete, the recommended sawing time is in the range of 4-12 hours as long as the concrete pavement gains its strength to prevent spalling or raveling at joints (Mallick and El-Korchi 2013 and Delatte 2014). The suggested saw-cut joint depth is half the overlays thickness, although others have recommended a saw-cut extending through the entire depth of the overlay.

2.2.3.2.2 Bonded Concrete Resurfacing of Asphalt Pavements

Bonded concrete resurfacing has been previously known as ultra-thin whitetopping. The recommended thickness of bonded concrete resurfacing of asphalt pavements is in the range of 2-5 in. (5.1-12.7 cm) depending on desired life, anticipated traffic loading, and the condition of the existing pavement. Good performance of bonded resurfacing of asphalt pavement has been successfully implemented in many states. The existing asphalt pavement should be structurally in good to fair condition, and asphalt pavements with severe surface distress such as rutting, shoving, or alligator cracking may be milled to provide better bonding (Delatte 2014). A proper evaluation of asphalt pavement is significantly important to ensure the bond quality between the resurfacing concrete and the asphalt pavement and to help in evaluating the design thickness of the resurfacing concrete. The evaluation of asphalt pavement can be performed using visual inspection, core samples for testing, and a falling weight reflectometer (FWD).

Design

The design thickness of bonded concrete resurfacing of asphalt pavements can be calculated using design procedures of the American Concrete Pavement Association (ACPA 2006). The joint spacing for bonded resurfacing of asphalt pavements ranges from 3-8 ft (0.9-2.4 m) and – as a rule of thumb – the joint spacing in feet is typically 1-2 times pavement

thickness in inches, and the resurfacing concrete is saw-cut into squares. Use of the recommended joint spacing helps in reducing the stresses due to curling and warping. Joints should be located in such a way as to avoid the wheel path, or otherwise aggregate interlock may be unable to withstand and transfer heavy truck loads (Delatte 2014) and there would be no need for sealing the joints. The depth of the saw-cut for longitudinal joints and transvers joints should be one-third and one-fourth of the resurfacing concrete thickness, respectively.

Construction

Before placing the bonded concrete resurfacing of asphalt, the distresses in the existing pavement should be removed. Milling can be used to repair the surface of the existing pavement from significant surface distortions and to enhance the bond between two layers. Either fixed form or slipform paving can be used to place the bonded concrete once the existing surface has been prepared, and the choice depends on the size of the project (Mallick and El-Korchi 2013).

2.2.3.3 Concrete Overlays and ECON Requirements

Table 2 and table 3 summarize the characteristics of bonded and unbonded concrete overlays and also compare them against ECON requirements. The ECON thickness is recommended to be in the range of 2-4 in., similar to the thickness of bonded concrete overlays. ECON using a bonded concrete overlay will meet the requirements for the bonded overlay thickness. The ECON mixture includes conductive materials and other admixtures to reduce the electrical resistivity from that of bonded or unbonded concrete mixture as shown in Table 2-2 and Table 2-3. Embedding of dowel bars and tie bars in the ECON layer is not recommended.

2.2.4 Concrete Overlays for Airfield Application

The use of concrete overlays for airfield pavement have been classified – based on the recent FAA advisory circular AC 150/5320-6F (FAA 2016) - into four broad types: PCC overlay of existing flexible or rigid pavement, and hot mix asphalt overlay of existing flexible or rigid pavement (FAA 2016). PCC overlay of existing flexible or rigid pavement will be summarized in term of its design and construction. HMA overlay of existing flexible or rigid pavement is not the focus of this report. The design and construction of the concrete overlays are discussed in detail in the FAA advisory circular (AC) – airport pavement overlays and reconstruction – AC No: 150/5320-6F (FAA 2016).

2.2.4.1 Concrete Overlays of an Existing Rigid Pavement

Existing pavement characteristics are very important design inputs in the design of concrete overlays (FAA 2016). Load transfer capabilities of the existing pavement would greatly influence the load-bearing capacity of the concrete overlay for both bonded and unbonded concrete overlay; however, bonded overlays are influenced to a greater degree by the underlying pavement condition compared to their unbonded counterparts.

Table 2-3 Summary of bonded concrete overlays and ECON requirements

Items	Bonded concrete overlay options			ECON requirements
	On asphalt pavements	On concrete pavements	On composite pavements	ECON
Old name	Ultra-thin whitetopping	Bonded overlays	Not Applicable	ECC
Thickness	2-6 in	2-6 in.	2-6 in.	2-4 in.
Mixture design				
Fiber	Optional	Optional	Optional	Carbon fiber
Aggregate property (CTE)	Similar or lower than the existing pavement	Similar or lower than the existing pavement	Similar or lower than the existing pavement	Similar or lower than the existing pavement
Accelerated mixtures	Optional	Optional	Optional	Optional
Joints				
Max. joint spacing (ft)	1.5 times thickness (in)	Match existing cracks and joints and cut intermediate joints	1.5 times thickness (in)	Flexible
Transverse joint spacing	3-8 ft	Match existing joints	3-8 ft	Flexible
Longitudinal joint spacing	3-8 ft	Match existing joints	3-8 ft	Flexible
Transverse joint saw-cut depth	T/3	Full depth plus 0.50	T/3	Flexible
Longitudinal joint saw-cut depth	T/3	T/2 (at least) or (Full depth plus 0.50)	T/3	Flexible
Joint pattern	Square	Joints must match with existing pavement (to reduce curling stresses, smaller overlay panels might be used)	Square	Flexible
Transverse dowel bars	No	No	No	Prefer not to have dowel or tie bars
Longitudinal tie bars	No	No	No	Prefer not to have dowel or tie bars
Separator layer - HMA	No	No	No	No
Joint sealing	Contraction and construction joints should be filled with hot-poured joint sealant (backer rod is not recommended)	Yes, hot-poured joint sealant	Contraction and construction joints should be filled with hot-poured joint sealant (backer rod is not recommended)	Flexible

Table 2-4 Summary of unbonded concrete overlays and ECON requirements

Items	Unbonded concrete overlay option			ECON requirements
	On asphalt pavements	On concrete pavements	On composite pavements	ECON
Old name	Conventional whitetopping	Unbonded overlay	Not Applicable	
Thickness	4-11 in.	4-11 in.	4-11 in.	2-4 in.
Mixture design				
Fiber	Optional	Optional	Optional	Carbon fiber
Aggregate property (CTE)	Similar or lower than the existing pavement	Similar or lower than the existing pavement	Similar or lower than the existing pavement	Similar or lower than the existing pavement
Accelerated mixtures	Optional	Optional	Optional	Optional
Joints				
Max. joint spacing (ft)	T < 6 in. - spacing 2 times T (in.) T ≥ 6 in. - spacing 2 times T (in.) T > 7 in. - spacing 15 ft	T < 5 in. - spacing 6 x 6 ft T 5-7 in. - spacing 2 times T (in.) T > 7 in. - spacing 15 ft	T < 6 in. - spacing 2 times T (in.) T ≥ 6 in. - spacing 2 times T (in.) T > 7 in. - spacing 15 ft	3-6 ft
Transverse joint saw-cut depth	T/4 min - T/3 max	T/4 min - T/3 max	T/4 min - T/3 max	Flexible
Longitudinal joint saw-cut depth	T/3	T/3	T/3	Flexible
Joint pattern	Square	It is not critical to mismatch overlay joints to the underlying joints. Mismatch joints enhance the benefit of load transfer	Square	Flexible
Transverse dowel bars	Yes, when T ≥7 in	Yes, when T ≥7 in	Yes, when T ≥7 in	Prefer not to have dowel or tie bars
Longitudinal tie bars	Yes, when T ≥6 in	Yes, when T ≥6 in	Yes, when T ≥6 in	Prefer not to have dowel or tie bars
Separator layer - HMA	No	Typically 1 in. asphalt or geotextile fabric	No	Not Applicable
Joint sealing	Yes, hot-poured joint sealant	Yes, hot-poured joint sealant	Yes, hot-poured joint sealant	Flexible

Cores and historical records could be used to characterize the existing condition of the pavement. In addition, overall current condition of the existing pavement should be evaluated in order to select proper concrete overlay system (bonded or unbonded) and the type, location, and extent of any preoverlay repairs needed.

2.2.4.1 Concrete Overlays of an Existing Rigid Pavement

Existing pavement characteristics are very important design inputs in the design of concrete overlays (FAA 2016). Load transfer capabilities of the existing pavement would greatly influence the load-bearing capacity of the concrete overlay for both bonded and unbonded concrete overlay; however, bonded overlays are influenced to a greater degree by the underlying pavement condition compared to their unbonded counterparts. Cores and historical records could be used to characterize the existing condition of the pavement. In addition, overall current condition of the existing pavement should be evaluated in order to select proper concrete overlay system (bonded or unbonded) and the type, location, and extent of any preoverlay repairs needed.

There are many factors that need to be considered during the concrete overlay design process. As a first step, the scope of the planned project and its intended structural performance requirements need to be taken into consideration. Expected design life affects the thickness design, the amount of repairs needed and in turn, total cost of the project. Understanding the current condition of the pavement structure, the projected traffic levels, and available pavement material options are other design inputs. There are two types of concrete overlays that can be placed on existing rigid pavement: fully unbonded or bonded concrete overlays.

2.2.4.1.1 Fully Unbonded Concrete Overlay of an Existing Rigid Pavement

There are not many design procedures and programs available to conduct concrete overlay design. The thickness of a fully unbonded overlay can be calculated by using the FAA's FAARFIELD software. The minimum thickness for a fully unbonded concrete overlay is 6 in. (150 mm). A thick hot-mix layer or fabric bondbreaker must be placed on the existing pavement to prevent bonding between two layers.

2.2.4.1.2 Bonded Concrete Overlays of an Existing Rigid Pavement

Bonded concrete overlay can be used only when the existing rigid pavement is in good to excellent condition. The FAARFIELD software can be used to design the thickness of the bonded overlay. The thickness of a bonded concrete overlay is calculated by subtracting the thickness of the existing pavement from the total thickness of the required slab as computed by FAARFIELD. The bonded concrete overlay and the existing concrete should behave as a monolithic slab and the bonded overlays can be designed as a new pavement. To ensure bonding between the existing concrete and a concrete overlay, the surface of the existing pavement should be thoroughly cleaned and a bonding agent may be required to enhance the bonding between two layers. The design of bonded concrete overlays for federal funded project requires FAA approval. Joints in bonded overlays should be located within 0.5 inch (13 mm) of joints in the existing base pavement.

2.2.4.2 Concrete Overlay of an Existing Flexible Pavement

The design of a concrete overlay on an existing flexible pavement is essentially the same as designing a new rigid pavement. The existing asphalt pavement should be evaluated before placing a concrete overlay. The FAARFIELD software can be used to design the thickness of the bonded overlay and a frictionless interface can be assumed between the

concrete overlay and the existing flexible surface. The minimum allowable thickness for a concrete overlay of an existing flexible pavement is 6 inches (150 mm).

2.2.4.3 Concrete Overlay Implementation at an Airport

Concrete overlay was implemented at the Spirit of St. Louis airport in Chesterfield, Missouri on December 1994 (Mowris 1995). This airport is one of the largest GA airports and was opened in 1964. The existing asphalt pavement at the airport site was deteriorated due to the increase in the aircraft sizes and weights and a feasibility study for rehabilitation showed that concrete overlay was a cost-effective approach to extend the pavement life. The FAA provided funds for the project through a pilot program with the Missouri Highway Transportation Department (MHTD) (Mowris 1995). The thickness of the concrete overlay varied from 3.5 in. to 10.0 in. due to a wide range of aircraft sizes and weights. The thickness of the overlay subjected to aircraft loads up to 120,000 pound was 10 in. while the thickness of the overlay for aircraft loads up to 12,500 pound was 3.5 in. A comprehensive study was carried out to evaluate the subgrade, base and the existing asphalt pavement to ensure that the concrete overlay will provide desirable performance. The performance of the concrete overlays were evaluated after 20 years since its completion and it showed good performance with regular maintenance.

2.2.4 Summary: Advantages and Limitations of Advanced Construction Techniques for Heated Pavement Applications

Table 2-5 summarizes advantages and limitation of use of advanced construction techniques for heated pavement applications in comparison to use of cast-in-place in HPS construction (Chang et al. 2004; Tayabji et al. 2013; Hu et al. 2014; Harrington et al. 2007)

Table 2-5 Advantages and limitations of use of advanced construction techniques for heated pavement applications

	Advantages	Limitations
Precast concrete	• Better concrete quality • Better curing conditions – at fabrication plant • Minimal weather-dependency of concrete placement • Reduced delay prior to opening to traffic – no on-site curing of concrete • A mature, but still evolving technology	• Expensive • Still relatively new • Difficult to achieve smooth surface
Two-lift paving	• Economic paving sections can be achieved • Many choices available for surface texture • Improved sustainability by recycling	• Not a time-efficient process • Not sufficient data to support long-term performance • Majority of the contractors in the United States have perceived concerns on two-lift concrete paving • Fewer contractors in the United States have completed two-lift paving project • Extra permits and land space needed for additional equipment
Concrete overlay	• Can be designed to achieve a service life in the range of 15 to over 40 years • Can be constructed rapidly and with effective construction traffic management • Can be applied to a wide variety of existing pavements exhibiting a wide range of performance issues • Cost effective	• Lack of consideration of the structural contribution of the interlayer and its interaction with the overlay and the existing pavement in terms of friction or bonding • Overestimation of the existing pavement effective thickness when the existing slab is relatively thick • Not sufficient data to support long-term performance • Lack of consideration of curling and joint spacing in the concrete overlay

CHAPTER 3. SYSTEM REQUIREMENTS FOR ELECTRICALLY CONDUCTIVE CONCRETE HEATED PAVEMENTS

A journal paper submitted and accepted for publication in *Transportation Research Board (TRR), Journal of the to The Transportation Research Board*

Hesham Abdualla[1], Halil Ceylan[2], Sunghwan Kim[3], Kasthurirangan Gopalakrishnan[4], Peter C. Taylor[5], and Yelda Turkan[6]

3.1 Abstract

Ice and snow on airport pavements can contribute to flight cancellations and delays. Traditional deicing methods that involve chemical or salt application can cause environmental or structural damage to airport infrastructure. Electric heated pavements, in which electric heating energy is transferred to the pavement via embedded insulated conductors or conductive materials to maintain surface temperatures above freezing, have gained attention as a promising technology for mitigating snow and ice accumulation. The objective of the study was to identify the requirements of an electrically conductive concrete (ECON) heated pavement system to achieve cost-effective performance. A small-scale prototype ECON heated slab was designed and constructed with the optimized ECON mixture recently developed at Iowa State University and then tested to determine its performance and efficiency. The energy consumption and energy cost of the prototype ECON slab were found to be the lowest of the electric heated pavement systems developed to

[1] Graduate Research Assistance, Department of Civil, Construction and Environmental Engineering (CCEE), Iowa State University, Ames, IA. E-mail: abdualla@iastate.edu
[2] Professor, CCEE, Iowa State University, Ames, IA. E-mail: hceylan@iastate.edu
[3] Research Scientist, Institute for Transportation, Ames, IA. E-mail: sunghwan@iastate.edu
[4] Research Associate Professor, CCEE, Ames, IA. E-mail: rangan@iastate.edu
[5] Director, National Concrete Pavement Technology Center, Ames, IA. E-mail: ptaylor@iastate.edu
[6] Assistant Professor, CCEE, Iowa State University, Ames, IA. E-mail: yturkan@iastate.edu

date. The cost-effective two-layer design also can be implemented for large-scale ECON-based heated pavements by using a precast concrete technique, concrete overlay, and two-lift paving. From the prototype ECON slab results, a design flow chart and three-dimensional visualizations were developed to discuss the design and construction procedures for real, large-scale applications.

3.2 Introduction

In cold regions, ice and snow are classified as major concerns on pavement surfaces. Traditional deicing methods—which include spraying chemicals on the pavement surface and using large machines such as plows and broom vehicles to remove snow—have some drawbacks; for example, they can deteriorate infrastructure, damage concrete pavement, and adversely affect the environment (1). They may be ineffective at low temperatures, may contaminate nearby water bodies, and may require labor hours that translate to increased costs. These methods also are challenging to implement in congested and small areas, such as sidewalks and airport aprons and taxiways, where airport ground crews and aircraft may be in danger.

A heated pavement system (HPS) that uses hydronic heating, resistive cables, and electrically conductive paving materials is recommended as an alternative for melting ice and snow. Hydronic heating melt ice and snow by circulating heated fluid through pipes embedded in pavement. The cooled fluid runs through a heat source (geothermal water, a boiler, or a heat exchanger) that reheats the fluid each cycle. Geothermal water is considered to be an efficient heat source in locations with good geothermal potential (2). The disadvantages of hydronic systems include construction difficulties, high installation costs, and challenges associated with repair in the event of fluid leakage. Resistive cables have

been embedded in concrete structures for deicing snow and ice in Oregon, Texas, and Pennsylvania. Performance was unacceptable because of the high power density required for operation and damage to the electrical cables or associated sensing elements that trigger the system (3, 4).

Even though the concept of electrically conductive concrete (ECON) is not new for nonstructural applications such as heating (deicing), sensing, monitoring, and electromagnetic interference shielding, the investigation of this concept for application to heating airport pavements has been limited (5). Furthermore, little guidance and detailed information exist on the design, construction, and performance of ECON-based HPSs. For example, key issues to be clarified for real scale applications include heating element requirements, detailed design and construction procedures, and energy requirements during operations. Because the ECON-based HPS is an emerging technology, its system requirements must be addressed to ensure its efficacy, quality, and performance.

3.3 Objective and Scope

The objective of this study was to identify the requirements for an ECON-based HPS related to material selection, design, construction, and operational performance. A prototype ECON slab was constructed and tested to evaluate efficiency and performance. Results from the prototype slab evaluation were incorporated into the design of a real, large-scale ECON slab constructed with a precast concrete technique. Design flow and three-dimensional (3-D) renderings were developed to clarify the design and construction procedures for large-scale HPS applications.

3.4 ECON Heated Slab Prototype

3.4.1 Construction Materials

The main components of the ECON HPS include conductive materials (heating elements) for ECON, electrodes, insulation layers, a power supply, and temperature sensors. An ECON-based HPS works by applying an electric current through electrodes embedded in a conductive concrete layer. Because it has lower electrical resistivity than normal concrete, ECON behaves like a conductor of electricity.

The ability of an ECON HPS to melt snow and ice depends on the electrical resistivity (i.e., the reciprocal of electrical conductivity) of conductive materials; the value required for deicing applications should be less than 1,000 Ω-cm (5, 6). The electrical resistivity of conventional concrete varies according to whether it was air dried, oven dried, or not dried at all. The electrical resistivity values of air-dried conventional concrete range from 600 to 1,000 kΩ-cm; oven-dried values are about 108 kΩ-cm. When not dry, conventional concrete is considered to be a semiconductor, the resistivity value of which is about 10 kΩ-cm (5).

Previous studies have investigated the addition of conductive materials to conventional concrete as heating elements (5–16). Such materials typically include steel fibers, graphite powder, and carbon particles, and they are incorporated into concrete in proportions from 1% to 20% by volume; reported electrical resistivity values range from 400 to 2.4 × 105 Ω-cm.

Researchers at Iowa State University (ISU) recently developed a new ECON mix that includes carbon fiber–based materials (17, 18). The mix contains 6-mm-long carbon fibers, 0.75% by volume of the total concrete mix, and uses methylcellulose as an agent to disperse the carbon fiber particles evenly and improve electrical conductivity as a result. All

components and proportions are listed in Table 3-1. The electrical resistivity value of the ISU ECON mix was in the range of 50 Ω-cm at room temperature (i.e., 20°C ambient temperature), consistent with electrical conductivity magnitudes reported in previous studies (6, 9, 10–16). The 28-day compressive strength of the developed ECON mix was 40 MPa, which translates to a 28-day flexural strength value of 4.0 to 5.0 MPa with various strength conversion equations included in the American Concrete Pavement Association's online strength converter tool (19). These strength properties meet the minimum strength requirements mentioned in the FAA specification (20). Results imply that the developed ECON has better electrical properties than ones reported in the literature, with adequate mechanical properties.

Table 3-1 ISU ECON mix proportion

Components		**Type**	**Content**
Basic	Coarse aggregate	Limestone	1,010 kg/m^3
	Fine aggregate	River sand	634 kg/m^3
	Fly ash	Class F	72 kg/m^3
	Cement	Holcim Type I/II	289 kg/m^3
	Water	Tap water	162.5 kg/m^3
Admixtures	Methylcellulose	Dispersive agent	1.4 kg/m^3
	Air entraining agent (AEA)	MasterAir AE 90	324 ml/ m^3
	High range water reducer (HRWR)	MasterGlenium 7500	2.5 kg/m^3
	Carbon fiber 6-mm	Synthetic Carbon fiber	0.75 (% Vol.)

Note: Aggregate contents presented are in saturated surface dry condition (SSD)

Table 3-2 summarizes the electrode types reported in the literature in the use of ECON for ice and snow melting purposes. The electrode types reported in the literature in the context of ECON's usage for ice- and snow-melting purposes include steel (9), perforated steel (12), perforated stainless steel (14, 21), and galvanized iron (22). Most metallic materials identified as electrodes could provide sufficient electric current flow results

because the electrical conductivity of ECON is higher than that of any metal. However, one important lesson learned from previous studies is that a good bond between the electrodes and the conductive concrete is essential to ensure sufficient heating performance. Embedded steel plates did not provide desirable heating performance because of smooth bonding between the conductive concrete and the electrodes (12). Conductive adhesive was suggested to achieve sufficient bonding but reportedly is not cost-effective (13). Perforated steel and perforated stainless steel plates with gaps larger than the maximum aggregate size are recommended to ensure that conductive concrete can be bonded with the electrode (12, 14, 21). For the prototype ECON heated slab in this study, perforated galvanized steel with a gap size larger than the maximum aggregate size was selected as an electrode for its advantages. Perforated stainless steel performs similarly but is not cost-effective.

Table 3-2 Summary of electrode materials and shapes reported in literature

Material type	**Shape**	**Result reported**	**Reference**
Steel	Circular bar	Ineffective bonding and affected by corrosion	(*9*)
Perforated steel	Angle plate	Effective bonding	(*12*)
Perforated stainless steel	Plate	Effective bonding and resisted corrosion	(*14*,*21*)
Galvanized iron	Not reported	Effective bonding and resisted corrosion	(*22*)

As a cost-effective solution, a thin layer of thermal insulation could be applied to minimize heat loss and reduce the total heat required to melt ice and snow. The percentage of back and edge heat loss can be defined as follows: 0% heat loss if below and edges are insulated, 4% heat loss if only below is insulated, 10% heat loss if perimeter and edge are isolated, and 20% heat loss if no insulation is used (23). The materials reportedly in use for the insulation layer include the epoxy coating and mortar [the sawdust mortar consisting of equal parts of cement, sand, and sawdust (24)] and extruded polystyrene insulation board

(25). However, epoxy coating and mortar did not provide good thermal insulation and is not recommended. The results report that the use of extruded polystyrene foam board as thermal insulation was sufficient to prevent heat loss and thus minimize cost of energy consumption. Therefore, for the prototype ECON heated slab in this study, extruded polystyrene foam board insulation was used to prevent heat loss.

The resistivity of conductive concrete decreases with increasing voltage, regardless of whether alternating current (AC) or direct current (DC) is used, but is lower with AC than with DC (22). When used to power ECON, AC takes different paths, is better distributed through the slab, and consequently provides even heat (12). However, when used for the same purpose, DC takes one path and can create localized hot spots (12). A photovoltaic system has been investigated as an alternative energy source but could not provide enough power to melt snow and ice through ECON material (9).

3.4.2 Electrical Circuit Model

The electrical circuit model for the ECON HPS is illustrated in Figure 3-1. The heating element (conductive material) equivalent circuit is represented by a set of resistors R (which model the material resistivity) and capacitors C (which insulate between the conductive materials). A distributed model is selected to represent the evenly spread conductive material under the snow and ice. The circuit to the conductive material is fed by an AC power supply to generate the heat to melt snow and ice. A temperature sensor (Temp_Sensor in Figure 3-1) could be used in the control circuit to monitor the surface temperature of the pavement to control the voltage.

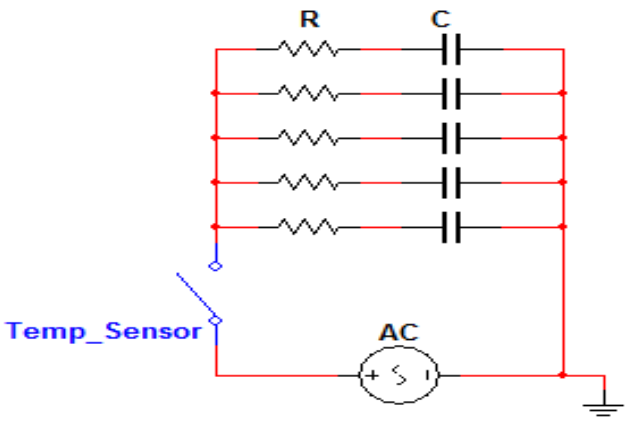

Figure 3-1 Electrical circuit model for ECON heated pavement system

Figure 3-2 illustrates the voltage changes applied to ECON through embedded electrodes during the snow- and ice-melting process. After the electric power is turned on, voltage increases over a period Ta to a time t_1, when the temperature reaches a previously set temperature. The sensor then triggers the control circuit to make the voltage rate constant to hold the temperature constant. During this period T_b, the surface heats evenly and melts the snow and ice. When period T_b elapses at time t_2, the sensor triggers the control unit to turn off the power. During the period T_c that follows, the charges gained by the capacitors start discharging, and the snow and ice melt completely with heat from the temperature drop, without any electric power source.

3.4.3 ECON Heated Slab Design

To identify any construction and operation issues, a prototype ECON slab (122 cm long × 86 cm wide × 10 cm thick) was designed for construction at the ISU Portland Cement Concrete Pavement and Materials Research Laboratory (Figure 3-3). The two-layer 10-cm-thick slab comprised a 5-cm ECON top layer and a 5-cm bottom layer of conventional concrete.

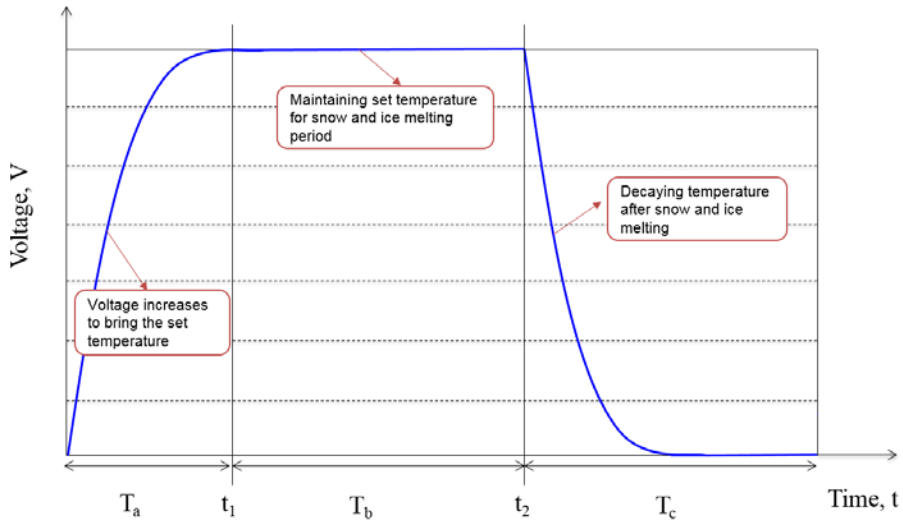

Note: T_a: time period to reach set voltage and temperature
t_1: time when the temperature reaches targeted temperature
T_b: time period to maintain set temperature to allow heating to be equally spread into snow and ice melting by providing constant voltage rate
t_2: time when the sensor triggers the control circuit to turn the power off
T_c: time period after which the snow and ice is expected to completely melt

Figure 3-2 Voltage changes in snow and ice melting process

The purpose of a thin ECON layer was to lower the cost and to heat the surface as much as required to melt snow and ice. The concept of implementing two layers of concrete is not new and is a sustainable construction technique for the placement of concrete (e.g., concrete overlay and two-lift concrete paving). Two perforated galvanized steel angles (3.175 cm long × 3.175 cm wide × 0.32 cm thick) were embedded 65 cm apart in the ECON layer. Each hole in the perforated galvanized steel is larger than the maximum aggregate size to ensure that the conductive concrete can be bonded with the electrode. The electrodes were connected to an AC supply to power the conductive concrete. Temperature sensors were installed in both the ECON and the conventional concrete layers. Layers of insulation (2.5 cm thick) were placed at the edges and bottom of the slab to minimize heat loss.

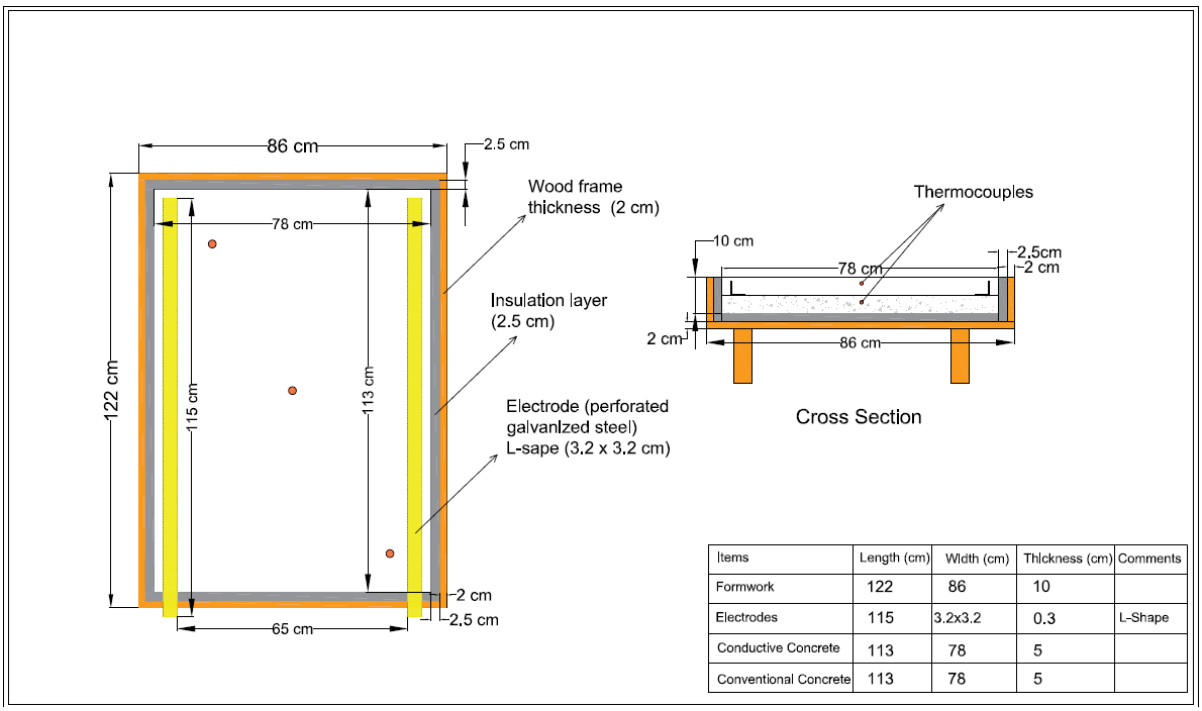

Items	Length (cm)	Width (cm)	Thickness (cm)	Comments
Formwork	122	86	10	
Electrodes	115	3.2x3.2	0.3	L-Shape
Conductive Concrete	113	78	5	
Conventional Concrete	113	78	5	

Figure 3-3 Detailed design of the prototype ECON heated slab

3.4.4 ECON Heated Slab Construction

Construction of the prototype ECON heated slab at the ISU Portland Cement Concrete Pavement and Materials Research Laboratory is demonstrated in Figure 3-4. Layers of 2.5-cm-thick extruded polystyrene foam were placed in the slab formwork before paving to insulate against heat loss (Figure 3-4a). The ECON slab was constructed in two stages.

First, a 5-cm-thick layer of conventional concrete was placed into the slab formwork, and the top surface was screened and then grooved to provide an effective bond with the ECON layer (Figure 3-4b, c, and d). Two angle-shaped perforated electrodes were placed on top of the conventional concrete layer (Figure 3-4c).

Second, a 5-cm-thick layer of ECON was placed on top of the conventional concrete (Figure 3-4e). The ECON used in this study is a mixture recently developed at ISU that contains 0.75% 6-mm-long carbon fiber by volume and provides about 50 Ω-cm of electrical

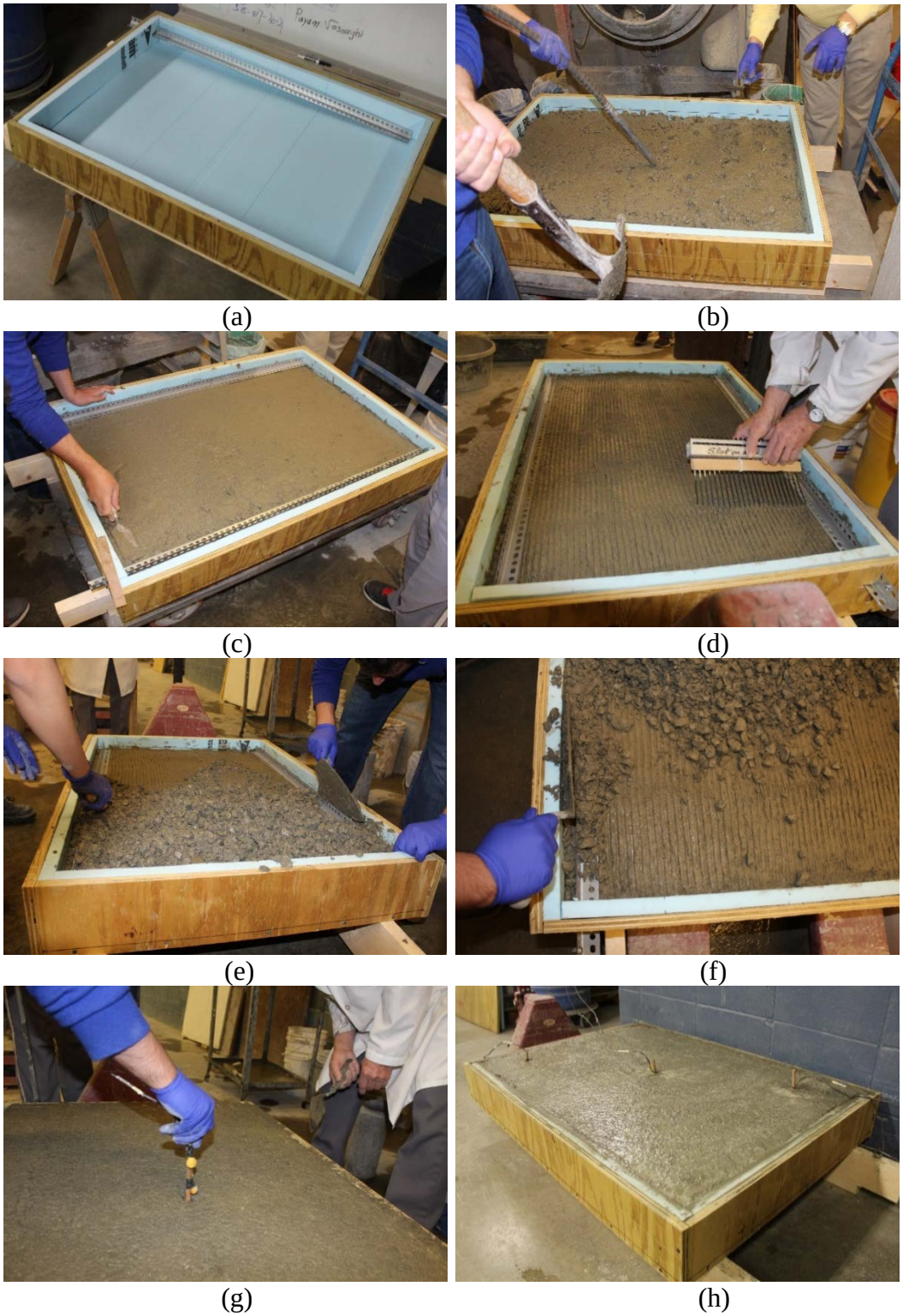

(a) (b)

(c) (d)

(e) (f)

(g) (h)

Figure 3-4 Construction of the prototype ECON heated slab

resistivity with about 40 MPa of 28-day compressive strength. During ECON placement, attention was paid to ensure good bonding between the ECON and the perforated electrodes (Figure 3-4f). Temperature sensors were installed in both the ECON and the conventional concrete layers (Figure 3-4g). The total construction cost for producing the final prototype ECON heated slab is estimated to be $130 (Figure 3-4h). The total construction cost depends highly on the heating element and the potential for it to provide the desired heat radiation for melting snow at an efficient rate of energy consumption.

3.4.5 Snow-Melting Performance

After the ECON slab was constructed, a series of experimental tests was conducted to evaluate slab performance in melting 2.5 cm of snow from its surface. An AC power supply (80 V and 11 A) was used to provide electricity via electrodes to the ECON slab. The ambient temperature was −1°C, and the wind speed was 10 mph. The snow-melting process of the ECON slab after 2.5 cm of snow was placed on its 1-m2 surface is illustrated in Figure 3-5. More than one-half of the snow was melted after 25 min of slab operation (Figure 3-5b) and most of the snow was completely melted after 35 min (Figure 3-5d). An energy density of 880 W/m^2 was reported (by multiplying 80 V by 11 A for 1 m^2 of ECON slab surface). Energy density is correlated with snow-melting time; as energy density increases, melting time decreases.

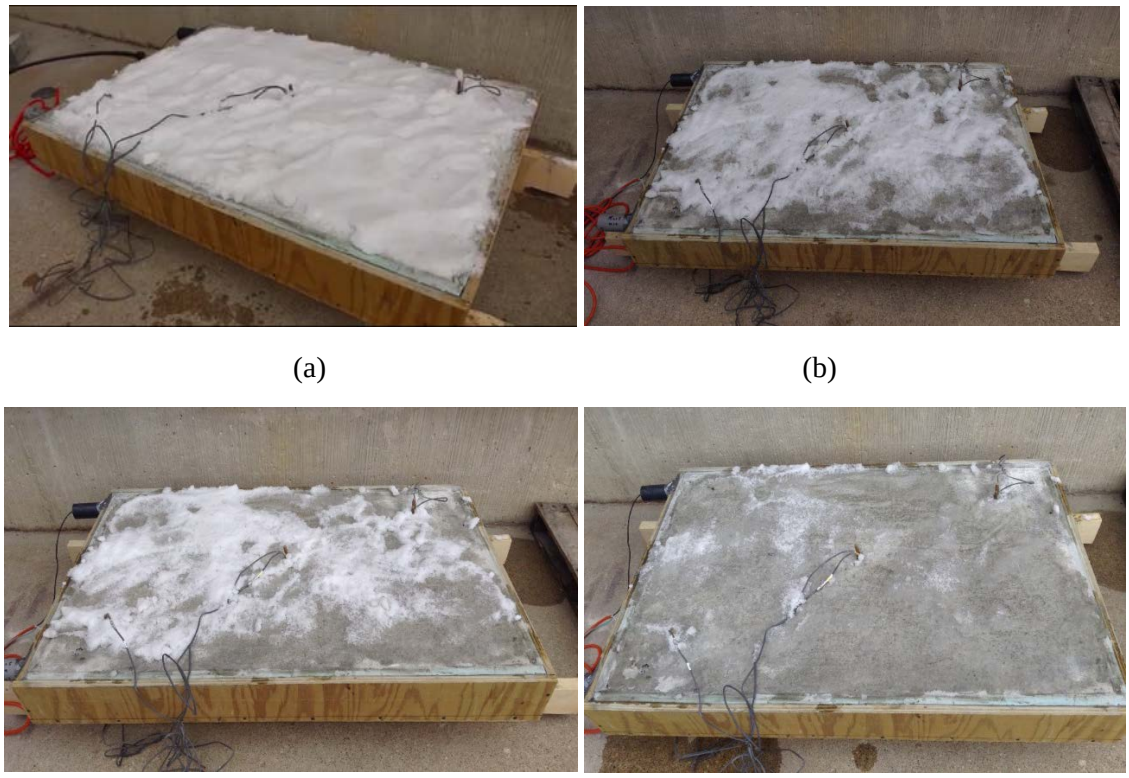

(a) (b)

(c) (d)

Figure 3-5 Snow melting performance test on prototype ECON slab: (a) placement of 2.5 cm snow on the heated slab, (b) after 25 minutes, (c) after 30 minutes, (d) after 35 minutes

Figure 3-6 is a snapshot of heat distribution taken with an infrared thermographic camera about 30 min of operation of the ECON heating slab. The infrared heat map demonstrates that the ECON slab can generate enough heat to melt snow and ice simultaneously on the entire slab surface. Slightly different heating zones are observed on the surface because the nonhomogeneous ECON structure consists of cementitious materials, fibers, aggregate, moisture, and pores.

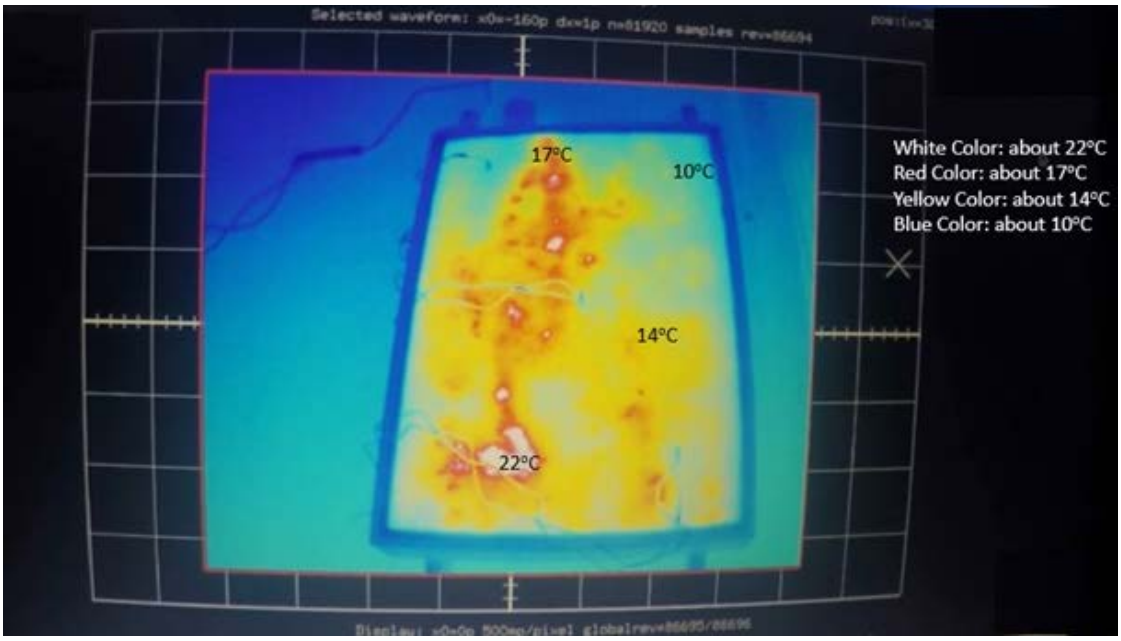

Figure 3-6 Infrared thermographic image snapshot of ECON in operation

The energy consumption and energy cost of the ECON slab to melt 2.5-cm-thick snow were estimated and compared with those of electric HPSs previously developed and reported in the literature (Table 3-3). For one-to-one comparison, energy consumption was calculated from the energy density (in W/m^2) and melting time (in hours) by using information directly from the literature. Energy cost was estimated by multiplying energy consumption (in $kW\text{-}h/m^2$) by \$0.12/kW-h (i.e., the average electricity cost assumed from average 2015 costs).

Compared with electric HPSs developed and reported in the literature, the prototype ECON slab developed in this study consumes the least energy (0.54 kW-h/m2) and has the lowest energy cost ($\$0.065/m^2$) (Table 3-3). In other previously developed HPSs, estimated energy consumption ranged from 0.70 to 2.28 kW-h/m2, and estimated energy costs ranged from $\$0.084/m^2$ to $\$0.274/m^2$ (14, 25, 26). The better operational performance of the ECON

heating slab in this study is attributed to higher conductivity in the newly developed ECON mixture, which allows the entire surface to heat uniformly and melt snow and ice quickly.

Table 3-3 Energy consumption and cost comparisons of electrically heated pavement systems

Deicing System	Ambient Temp. (ºC)	Melting Time (min.)	Snow Thickness (mm)	Energy Consumption[1] (kW-h/m^2)	Energy Cost[2] (¢/m^2)	Ref.
Conductive concrete steel fiber and steel shaving	2	300	50	2.28	27.4	(*26*)
Carbon fiber tape heating panel	-11	558	15	1.14	13.6	(*25*)
Carbon fiber grille	-1	120	27	0.70	8.4	(*14*)
ISU ECON Slab	-1	35	25	0.54	6.5	NR[3]

Note: [1] an energy consumption of each system was calculated for comparison purpose, [2] average electricity cost assumed ¢12/kw-h based on average cost of 2015; [3] NR stands for not required

3.4.6 Large-Scale ECON HPS Design

Conceptual designs for real, large-scale ECON HPS construction projects were developed with 3-D artist rendition and visualization schematics to provide a clear understanding of its construction and operation. Figure 3-7 illustrates ECON HPS construction with the precast concrete technique. Precast concrete has exhibited high performance for bridges, pavements, buildings, and airfield pavements. It provides high strength and low permeability with few cracks—features that result from fabricating the

panels off site, where quality can be controlled. The incentive to use precast concrete in pavement applications has increased because construction can be much more rapid than cast-in-place construction, which requires a long curing time to attain strength before opening to traffic (27–29).

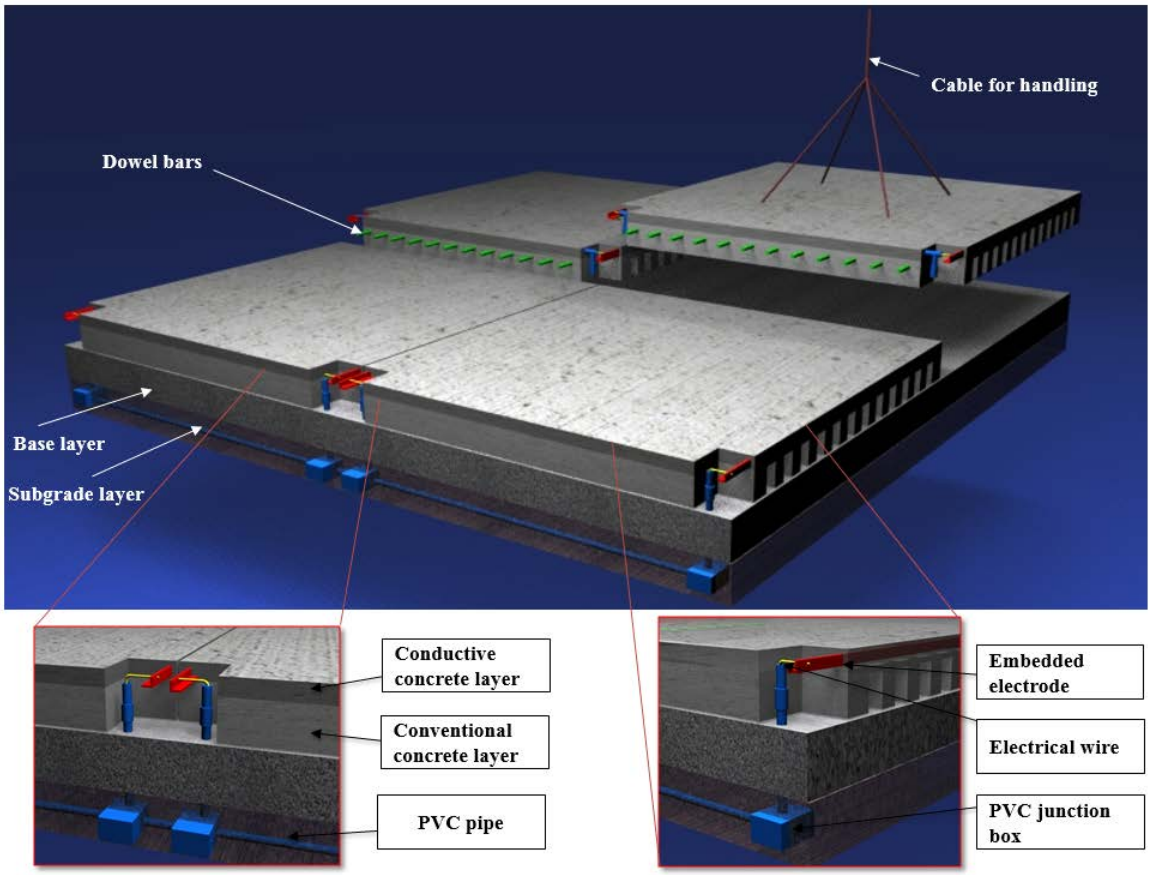

Figure 3-7 3D artist rendition and visualization schematics for construction of ECON heated pavement system utilizing precast concrete technique

A thin ECON slab can be precast with a conventional concrete slab to construct a large-scale ECON heated slab by using a construction procedure similar to that followed for the prototype ECON slab (Figure 3-7). If needed, a thin ECON slab can be precast and placed on a newly constructed (or an existing) conventional concrete slab. Each ECON panel contains two electrodes in the edges to provide the electricity that will be converted to heat during ECON operation. The polyvinyl chloride conduit and junction box, designed to house

and protect the electrical wire and temperature sensors, can be embedded in the subgrade layer. Renderings of the ECON HPS in operation are presented in Figure 3-8.

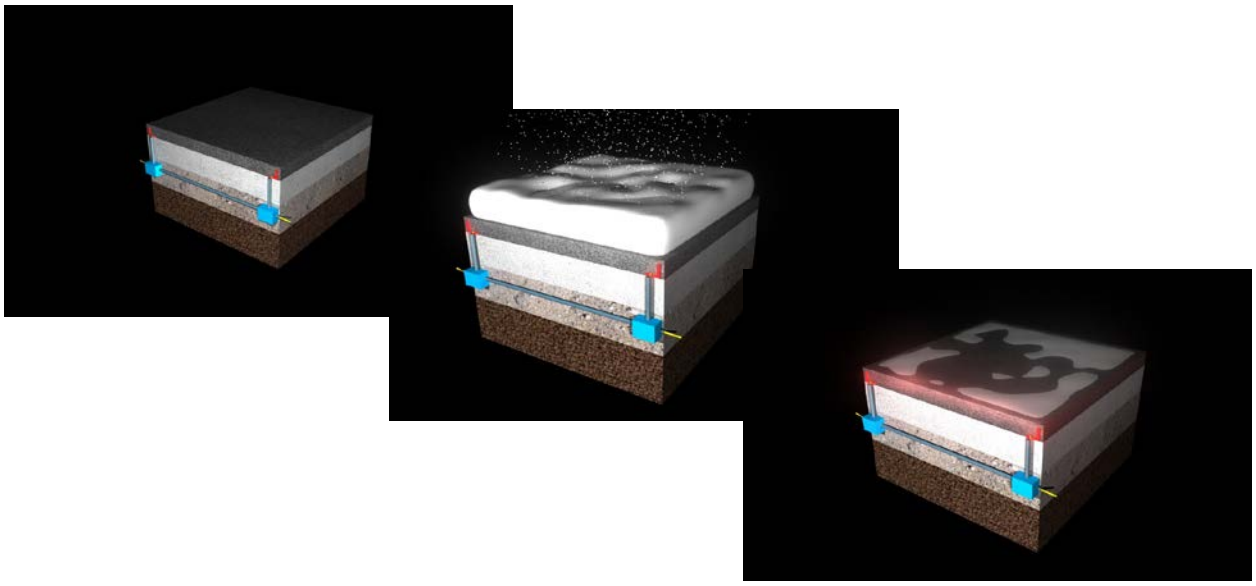

Figure 3-8 3D artist rendition and visualization schematics of ECON HPS in operation

The design flow chart for a large-scale ECON heated slab is presented in Figure 3-9. The first step involves determining the design criteria, which include snow- and ice-melting time, amount of snow and ice to be melted, and the associated power density requirement. Design parameters to be determined include slab dimensions [i.e., length (*L*), width (*W*), and thickness (*T*)], the distance between electrodes (*Ls*), electrical resistance (*R*), and electric voltage (*V*).

The slab dimensions should be selected with consideration of actual concrete design and construction practices. The slab surface area (*A*) is the product of length *L* and width *W*. The distance between electrodes *Ls* can be calculated by subtracting the distance between the slab edge and the embedded electrode (*d*) from the slab length L. Electrical resistance *R* can be calculated by multiplying Ls by the resistivity (ρ) of ECON material and dividing the

product by the cross section parallel to the electrodes (A_c). By selecting the electric voltage V, the electric current (I) and the power density (P_d) can be calculated with other design parameter values previously selected. If the calculated P_d value does not meet the power density requirement, then the selected design parameter values should be revised to meet the power density requirement and additional design criteria.

To better understand this design procedure, an example is presented. The design criteria for snow- and ice-melting performance in this example are similar to those of the prototype ECON heating slab discussed previously. For the small-scale prototype ECON heating slab (1.22 m long × 0.86 m wide × 0.1 m thick), 880 W/m^2 of P_d is required to melt 2.5 cm of snow in 35 min. The dimensions of the large-scale ECON heated slab are 4.6 m long × 4.6 m wide × 35.5 cm thick, which is close to that of concrete slabs used in airport pavement construction. This large-scale slab consists of two layers: a 10-cm-thick ECON top layer and a 25.5-cm-thick bottom layer of conventional concrete.

According to the flow chart in Figure 9, the other design parameters (including L_s, R, and V) can be selected. If 40 cm is selected for d for two electrodes (i.e., 20 cm for each electrode), then Ls is calculated as 4.2 m. By using 50 Ω-cm for ρ (from ECON materials used in the prototype ECON slab), L_s equal to 4.2 m, and an A_c of 0.46 m2 (4.6-m-wide × 0.1-m-thick ECON layer), the R can be calculated as 4.6 Ω. If 300 V is selected for V, then I and P_d are calculated as 65 A and 920 W/m^2, respectively, for the large-scale ECON heated slab. The calculated P_d value of 920 W/m^2 is higher than the 880 W/m^2 required to melt 2.5 cm of snow in 35 min.

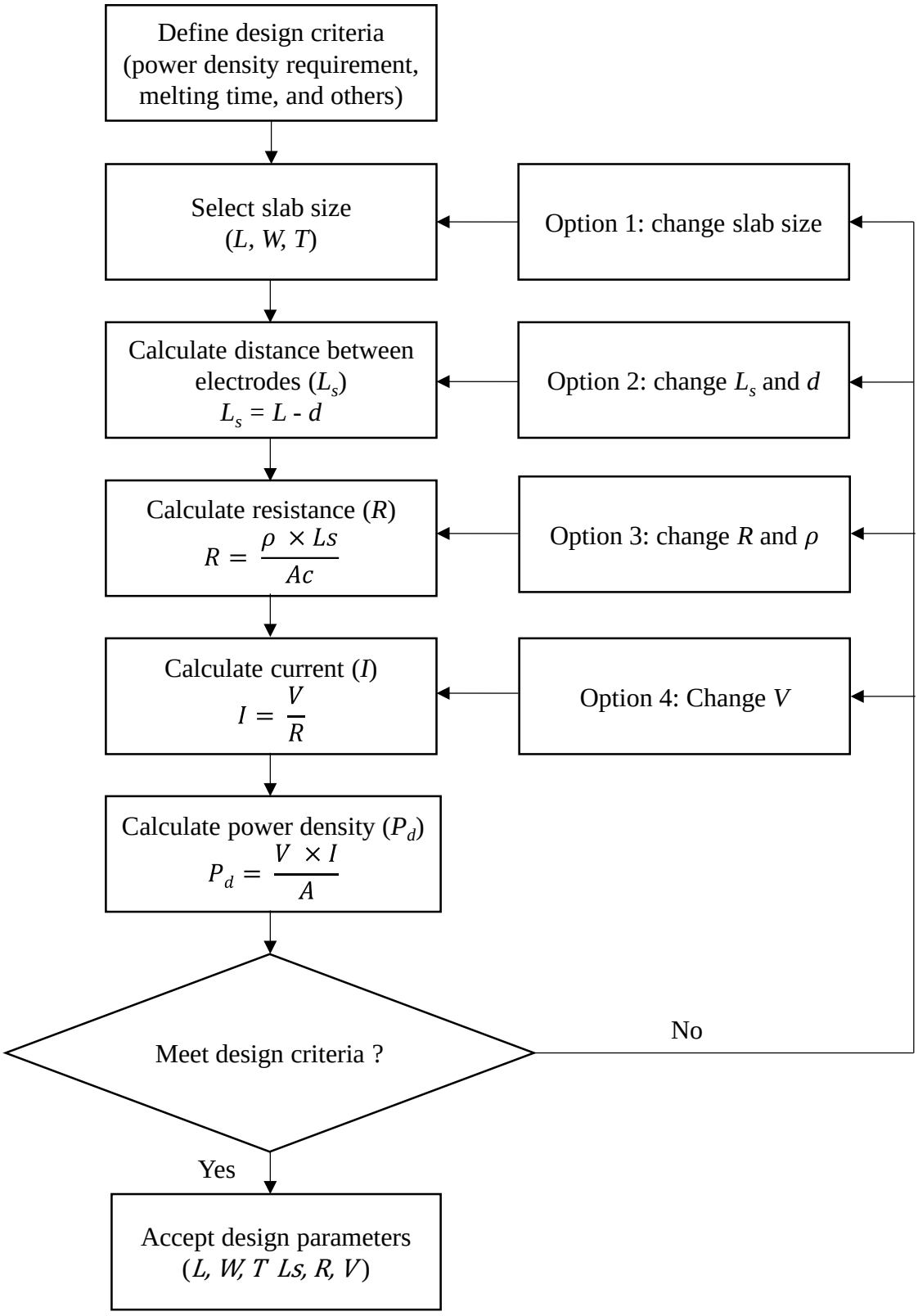

Figure 3-9 Design flow for a large-scale ECON heated slab

It implies that accepting the design parameters determined in this example will melt snow more quickly than the selected design criteria (i.e., 35 min). Of course, the design parameters determined in this example can be revised if additional design criteria are required for each design parameter.

3.5 Conclusions

The goal of this study was to identify material, design, construction, and operational requirements for the cost-effective performance of an ECON HPS. A prototype ECON heated slab was designed and constructed with the use of a new ECON mixture recently developed at ISU. To aid the design and construction procedures for real, large-scale HPS applications, design flow and 3-D renderings were developed from the results of the performance evaluation of the prototype ECON heated slab. The major conclusions are as follows:

- The energy consumption and energy cost of the prototype ECON heating slab were the lowest of the electric HPSs developed and reported in the literature to date (14, 25, 26). Such excellent operational performance is attributed to the recently developed ECON mixture that provides higher conductivity (about 50 Ω-cm of electrical resistivity) to even surface heating to melt snow and ice quickly.
- The prototype ECON heating slab comprises a thin ECON top layer on a conventional concrete bottom layer. This cost-effective two-layer approach can be implemented for a large-scale ECON HPS by using a precast concrete technique, concrete overlay, and two lift paving.
- The design parameters to be determined for the large-scale ECON HPS include slab dimensions, distance between electrodes, electrical resistance, and electric voltage.

The design flow developed in this study can be used to determine these parameters for given design criteria.

- Key construction materials required for a well-performing ECON HPS are low-resistivity (i.e., high-conductivity) ECON materials, electrodes that bond well with ECON, and cost-effective thermal insulation.
- ECON should be heated with AC, which enables electrons to take different paths into the conductive materials to distribute heat evenly in the slab.

3.6 Acknowledgments

This paper was prepared from a study conducted at Iowa State University under FAA Air Transportation Center of Excellence Cooperative Agreement 12-C-GA-ISU for the Partnership to Enhance General Aviation Safety, Accessibility and Sustainability. The authors thank current FAA Technical Monitor Benjamin J. Mahaffay and former FAA Technical Monitors Jeffrey Gagnon, Charles A. Ishee, and Donald Barbagallo for invaluable guidance during this study. The authors also thank Gary L. Mitchell at the American Concrete Pavement Association for valuable discussions and comments on concrete pavement construction.

References

1. Xi, Y., and P. J. Olsgard. *Effect of De-Icing Agents (Magnesium Chloride and Sodium Chloride) on Corrosion of Truck Components.* CDOT-DTDR-2000-10. Colorado Department of Transportation, Denver, 2000.

2. *Airside Use of Heated Pavement Systems.* AC 150/5370-17. Federal Aviation Administration, U.S. Department of Transportation, 2011.

3. Zenewitz, J. A. *Survey of Alternatives to the Use of Chlorides for Highway Deicing.* FHWA-RD-77-52. Federal Highway Administration, U.S. Department of Transportation, 1977.

4. Joerger, M. D., and F. C. Martinez. Electrical Heating of I-84 in Land Canyon, Oregon. FHWA-OR-RD06-17. Oregon Department of Transportation, Salem, 2006.

5. Gopalakrishnan, K., H. Ceylan, S. Kim, S. Yang, and H. Abdualla. Electrically Conductive Mortar Characterization for Self-Heating Airfield Concrete Pavement Mix Design. *International Journal of Pavement Research and Technology,* Vol. 8, Issue 5, 2015, pp. 315–324.

6. Yehia, S., C. Y. Tuan, D. Ferdon, and B. Chen. Conductive Concrete Overlay for Bridge Deck Deicing: Mixture Proportioning, Optimization, and Properties. *ACI Materials Journal,* Vol. 97, Issue 2, 2000, pp. 172–181.

7. Xie, P., P. Gu, Y. Fun, and J. J. Beaudoin. *Low Electrical Resistance, High Mechanical Strength; Electromagnetic Shields.* US5447564 A. U.S. Patent and Trademark Office, Alexandria, Va., Jan. 19, 1965. https://www.google.com/patents/US3166518. Accessed June 27, 2015.

8. Derwin, D., P. Booth, P. Zaleski, W. Marsey, and W. Flood, Jr. *Snowfree® Heated Pavement System to Eliminate Icy Runways.* SAE Technical Paper 2003-01-2145. SAE International, Warrendale, Pa., 2003.

9. Heymsfield, E., A. B. Osweiler, R. P. Selvam, and M. Kuss. *Feasibility of Anti-Icing Airfield Pavements Using Conductive Concrete and Renewable Solar Energy.* DOT/FAA/TC-13/8. U.S. Department of Transportation, Federal Aviation Administration, April 2013.

10. Tuan, C. Y. *Implementation of Conductive Concrete for Deicing (Roca Bridge).* SPR-PL-1(04) P565. University of Nebraska, Lincoln, 2008.

11. Tuan, C. Y., L. Nguyen, and B. Chen. *Conductive Concrete for Heating and Electrical Safety.* Patent no. WO2010059169 A1, European Patent Office, Munich, Germany, 2010. https://www.google.com/patents/WO2010059169A1. Accessed June 27, 2015.

12. Tuan, C. Y. Electrical Resistance Heating of Conductive Concrete Containing Steel Fibers and Shavings. *ACI Materials Journal,* Vol. 101, No. 1, 2004, pp. 65–71.

13. Xie, P., and J. J. Beaudoin. Electrically Conductive Concrete and Its Application in Deicing. In *Advances in Concrete Technology: Proceedings of the 2nd CANMET/ACI International Symposium* (V. M. Malhhotra, ed.). American Concrete Institute, Farmington Hills, Mich., 1995, pp. 399–418.

14. Zuofu, H., L. Zhuoqiu, and W. Jianjum. Electrical Conductivity of the Carbon Fiber Conductive Concrete. *Journal of Wuhan University of Technology–Materials Science Edition,* Vol. 22, No. 2, 2007, pp. 346–349.

15. Wu, T., R. Huang, M. Chi, and T. Weng. A Study on Electrical and Thermal Properties of Conductive Concrete. *Computers and Concrete,* Vol. 12, No. 3, 2013, pp. 337–349.
16. Tuan, C. Y. *Conductive Concrete for Bridge Deck Deicing and Anti- Icing.* SPR-PL-1(037) P512. University of Nebraska, Lincoln, 2004.

17. Ceylan, H. FAA PEGASAS COE Project 1: Heated Airport Pavements. Presented at FAA PEGASAS COE 3nd Annual Meeting, Purdue University, West Lafayette, Ind., May 27 and 28, 2015.

18. Sassani, A., H. Ceylan, S. Kim, and K. Gopalakrishnan. Optimization of Electrically Conductive Concrete (ECC) Mix Design for Self-Heating Pavement Systems. Presented at 2015 Mid Continent Transportation Research Symposium, Ames, Iowa, Aug. 19 and 20, 2015.

19. *Strength Converter* (online tool). American Concrete Pavement Association, Rosemont, Ill. http://apps.acpa.org/applibrary/StrengthConverter. Accessed Oct. 25, 2015.

20. *Standards for Specifying Construction of Airports.* AC 150/5370-10G. Federal Aviation Administration, U.S. Department of Transportation, 2014.

21. Chen, W., and P. Gao. Performance of Electrically Conductive Concrete with Layered Stainless Steel Fibers. In *Proceedings of Sustainable Construction Materials 2012* (S. Wu, L. Mo, B. Huang, and B. F. Bowers, eds.). American Society of Civil Engineers, Reston, Va., 2012, pp. 164–172.

22. Tian, X., and H. Hu. Test and Study on Electrical Property of Conductive Concrete. *Procedia Earth and Planetary Science,* Vol. 5, 2012, pp. 83–87.

23. *S-no-Ice® Snow Melting System: Installation Manual.* Viega, Wichita, Kans., 2005. http://www.viega.us/xbcr/en-us/Viega_S-no-ice_Snow_Melting_System.pdf. Accessed July 15, 2015.

24. Yehia, S. A., and C. Y. Tuan. Conductive Concrete Overlay for Bridge Deck Deicing. *ACI Materials Journal,* Vol. 96, No. 3, 1999, pp. 382–390.

25. Yang, Z., T. Yang, G. Song, and M. Singla. *Experimental Study on an Electrical Deicing Technology Utilizing Carbon Fiber Tape.* INE/AUTC12.26. Alaska University Transportation Center, Fairbanks, 2012.

26. Tuan, C. Y., and S. A. Yehia. Airfield Pavement Deicing with Conductive Concrete Overlay. Presented at 2002 Federal Aviation Administration Technology Transfer Conference, Atlantic City, N.J., May 5–7, 2002.

27. Merritt, D. K., B. F. McCullough, N. H. Burns, and R. O. Rasmussen. *Construction of the California Precast Concrete Pavement: Demonstration Project.* FHWA-IF-06-010. Federal Highway Administration, U.S. Department of Transportation, 2004.

28. Priddy, L. P., P. G. Bly, and G. W. Flintsch. Review of Precast Portland Cement Concrete Panel Technologies for Use in Expedient Portland Cement Concrete Airfield Pavement Repairs. Presented at 92nd Annual Meeting of the Transportation Research Board, Washington, D.C., 2013.

29. Bly, P. G., L. P. Priddy, C. J. Jackson, and Q. S. Mason. *Evaluation of Precast Panels for Airfield Pavement Repair Phase I: System Optimization and Test Section Construction.* ERDC/GSL TR 13-24. U.S. Army Engineer Research and Development Center, Vicksburg, Miss., 2013.

CHAPTER 4. A 3-D FINITE ELEMENT MODEL FOR SIMULATING THE HEAT PERFORMANCE OF ELECTRICALLY CONDUCTIVE CONCRETE HEATED PAVEMENTS

A journal paper submitted to The *Journal of Cold Regions Engineering - ASCE*

Hesham Abdualla[1], Kasthurirangan Gopalakrishnan[2], Halil Ceylan[3], Sunghwan Kim[4], Mani Mina[5], Peter C. Taylor[6], Kristen S. Cetin[7]

4.1 Abstract

Electrically conductive concrete (ECON) heated pavement system (HPS) is a promising snow and ice removal technology for airports with the advantages of enhanced safety for ground crew servicing the aircraft, reduced dependency on deicing salts, and minimal use of snow removal equipment. Current ECON HPS design practices do not fully consider the time-dependent variables in relation to the achievement of sufficient temperature ranges (i.e., above the freezing point) to melt snow and ice, and consequently cannot evaluate the heat generation and distribution performance of the ECON HPS designed. To incorporate time-dependent heating performance evaluation into ECON HPS design, a 3-D finite element

[1] Graduate Research Assistance, Department of Civil, Construction and Environmental Engineering (CCEE), Iowa State University, Ames, IA. E-mail: abdualla@iastate.edu
[2] Research Associate Professor, CCEE, Ames, IA. E-mail: rangan@iastate.edu
[3] Professor, CCEE, Iowa State University, Ames, IA. E-mail: hceylan@iastate.edu
[4] Research Scientist, Institute for Transportation, Ames, IA. E-mail: sunghwan@iastate.edu
[5] Associate Professor, Department of Electrical and Computer Engineering, Iowa State University, Ames, IA. Email: mmina@iastate.edu
[6] Director, National Concrete Pavement Technology Center, Ames, IA. E-mail: ptaylor@iastate.edu
[7] Assistant Professor, CCEE, Iowa State University, Ames, IA. E-mail: kcetin@iastate.edu

(FE) modeling approach was developed as a new alternative approach. A 3-D FE model of an ECON slab (122 cm long × 86 cm wide × 10 cm thick) built at Ames, Iowa was developed and validated in comparison to the laboratory experimental test results. By using the developed 3-D FE modeling approach, a sensitivity analysis of various design variables on heat generation and distribution performance was conducted for a typical large-scale airport pavement ECON slab (4.6 m long × 4.6 m wide × 19 cm thick). The results demonstrate that the developed 3-D FE modeling approach can be utilized as a cost-effective evaluation tool to examine effects of various design parameters on the time-dependent ECON heating performance for ECON HPS design optimization.

4.2 Introduction

Ice and snow accumulations on paved surfaces in airports have the potential to cause flight delays and/or cancellations, pavement deterioration, and safety concerns. It has recently been reported that an aircraft skidded off the runway because of the presence of ice and snow on the runway at Chicago's Midway airport and at Detroit Metropolitan airport, leading to a fatality and serious injuries (BBC 2006 and CNN 2016). Traditional deicing methods, including spraying large amounts of chemical deicing agent on paved surfaces and deploying plows and brooms, are costly, labor-intensive, and cause corrosion to vehicles (Xi and Olsgard 2000). In recent years, electrically conductive concrete (ECON)-based heated pavement systems (HPS) are receiving attention for mitigating problems associated with the presence of ice/snow on roadways and paved areas of airfields. ECON works by applying a voltage across electrodes embedded in the ECON layer. The ECON layer acts as a resistor, generating heat that heats up the concrete, then subsequently melts the ice and snow covering the concrete (Sassani et al. 2015). An electrical circuit model was developed to illustrate the

ECON HPS, which consisted of resistors and capacitors. The resistors and capacitors were the conductive materials and non-conductive materials (insulation between conductive materials) respectively (Abdualla et al. 2016). The effectiveness of the use of various conductive materials such as steel fiber, carbon fiber, etc. added to conventional concrete to produce ECON with sufficient electrical conductivity (i.e., low electrical resistivity) and engineering properties has been thoroughly investigated (Gopalakrishnan et al. 2015). Existing heated pavement technologies include hydronic heating and resistive cable heating; these have disadvantages such as leakage from hydronic pipes (Lund 2005) and resistive cable damage embedded in pavements due to cracking of pavements (Zenewitz 1977; Joerger and Martinez 2006).

ECON-based HPS has the potential to enhance the safety and working conditions of the ground staff at airport gates, to reduce dependency on deicing salts, and to minimize the use of snow removal equipment. ECON has been developed and tested by Abdualla et al. (2016) to demonstrate the feasibility of melting ice and snow as a practical and cost-effective solution in comparison to others. ECON system requirements for large-scale HPS construction have also been identified, along with a newly-developed methodology for designing and optimizing ECON parameters to achieve sufficient heating based on the required energy (Abdualla et al. 2016).

To design ECON HPS, the energy required to achieve satisfactory heating performance needed to melt ice and snow should be determined based on local weather conditions including rate of the snow, ambient temperature, and wind speed to the location of study. After identifying the energy required, ECON parameters including electrode spacing, voltage, slab dimensions, and electrical resistivity can be designed and determined. The

required energy can be calculated using steady-state energy balance equations by taking into consideration the expected rate of snowfall, the air temperature, the relative humidity, the wind speed, and the slab dimensions (ASHRAE 2015 and FAA 2011). However, these equations do not consider time-dependent variables associated with the ECON HPS capability to achieve temperature ranges (i.e., above freezing point) sufficient to melt snow and ice and the thermal mass of the materials. Consequently, existing design equations cannot be effectively used to evaluate the heat generation and distribution performance of most ECON HPS designs.

Evaluation of ECON HPS heat generation and distribution performance during the design stage will help determine more realistic and optimized values for many ECON HPS design variables. Experimental tests can be utilized for measuring these changes, but they have significant costs and time investment associated with them in testing various design options for ECON HPS design optimization. Alternative simulation-based approaches are needed to evaluate the thermal characteristics of ECON HPS in a more cost-effective manner.

4.3 Objective and Scope

The primary objective of this study was to develop a 3-D finite element (FE) modeling approach as an alternative method for evaluating ECON HPS time-dependent heating performance and thereby achieve design optimization in a timely manner. The 3-D FE model for ECON slab was developed by examining the decoupling of thermal-electrical analysis (Joule heating) (Sridharan et al. 2011) using COMSOL Multiphysics software (COMSOL 2012) and validated though comparison with experimental test results. By employing the developed 3-D FE modeling approach, the sensitivity of various ECON HPS

design variables to heat generation and distribution performance was identified. This could be useful for providing guidance on design optimization.

4.4 Theoretical Considerations: Joule Heating

The ECON HPS operates by applying voltage through embedded electrodes in a conductive concrete layer. As the conductive concrete acts as a resistor, it generates heat energy through Joule heating, which can be numerically evaluated using coupled electrical field and heat transfer equations.

A transient heat conduction model was employed to predict variation of the temperature as a function of time and position in an ECON slab. The three dimensional mathematical model for transient heat conduction in solids (Cengel 2013) is given by Equation 1:

$$\rho C_p \frac{\partial T}{\partial t} - \nabla \cdot (k \nabla T) = Q \quad (1)$$

where, ρ is the density in (kg/m^3), Cp is the heat capacity in (J/(kg.K)), T is the temperature in (^{O}C), t is time in (s), ∇ is the Laplace operator, k is the thermal conductivity in (W/(m·K)), and Q is the rate of heat generation in (W/m^3).

The required electrical current in the ECON layer is generated by applying an electrical potential to electrodes embedded within the ECON layer. The three-dimensional mathematical model for the electric field in a solid (Tungjitkusolmun et al. 2000) is:

$$\boldsymbol{E} = -\nabla V \quad (2)$$

where, V is the electrical potential in (V) and ∇ is the gradient operator.

Joule heating describes the rate of electrical energy dissipated by electrical current flowing through a conductor and is correlated with the amount of electrical energy converted into heat (Ogasawara et al. 2010), as described in Equation 3:

$$Q = \boldsymbol{J} \cdot \boldsymbol{E} = (\sigma \cdot \boldsymbol{E}) \cdot \boldsymbol{E} \quad (3)$$

where, J is the electrical current density in (A/m^2), σ is the electrical conductivity in (S/m), and E is the electrical field in (V/m). The value of the electrical conductivity is (σ), which depends on the material temperature.

4.5 Development of 3-D FE Model for ECON Slab

A description of FE model and subsequent analysis of the heat generation and distribution in an ECON slab using decoupling thermal-electrical interfaces in COMSOL is presented in the following sections.

4.5.1 Description of ECON Slab and Geometry Modeling

A prototype ECON slab (122 cm long × 86 cm wide × 10 cm thick) was constructed at Ames, IA (Abdualla et al. 2016) for experimental investigations. The 10-cm-thick layer consisted of a 5-cm ECON top layer and a 5-cm conventional concrete bottom layer. Two perforated galvanized steel angles were embedded in the ECON layer. These angles were connected to an AC power supply to enable generation of heat. Temperature sensors were installed in both concrete layers. Insulation layers of 2.5-cm-thick extruded polystyrene foam with an R-value of 1.32 $C \cdot m^2/W$ were placed at the edges and the bottom of the slab to reduce heat loss. The ECON slab was tested in a controlled laboratory testing environment, and temperature was recorded for a total time duration of 9,000 seconds (2.5 hours).

COMSOL Multiphysics (release 5.1) was used to develop a 3-D FE model of the ECON slab. The FE model illustrated in Fig. 1 was developed to numerically simulate the heat generation response and distribution under the application of electric potential from an AC power supply. The dimensions of the modeled ECON slab mirrored those of the prototype tested at ISU - 122 cm long x 86 cm wide x 10 cm thick. Electrodes were also

modeled in the 3-D FE model (See Figure 4-1) to be considered as boundaries for electric potential values used to generate current flow through the ECON layer.

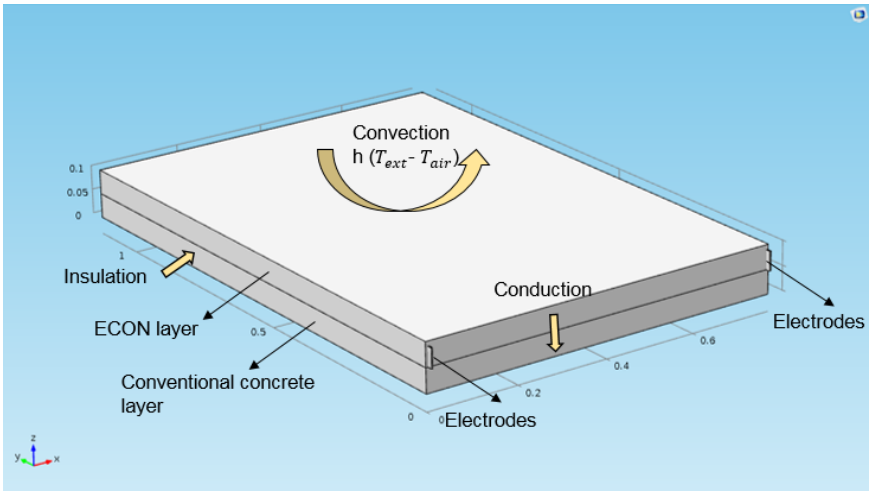

Figure 4-1 FE model of ISU ECON slab and boundary conditions

4.5.2 Assumptions and Boundary Conditions

Since multi-physics interfaces – thermal-electrical coupling – were used to analyze the modeled ECON slab, boundary conditions (see Figure 4-1) were assigned for each interface to simulate ECON slab heat generation and distribution as a function of time. The ECON slab, composed of conventional concrete and ECON, was treated as homogenous and isotropic. The various heat transfer mechanisms that could possibly effect thermal performance include conduction, convection, and short and longwave radiation. In the 3-D FE analysis, only conduction and convection were considered. The effect of radiation heat flux was neglected since the temperature difference between the ECON surface temperature and the ambient temperature were considered negligible during snowfall (ASHRAE 2015 and Zhao et al. 2011).

For the transient heat transfer physics, a boundary condition was set up by utilizing the energy balance at a solid surface (Cengel 2003), where the convection heat flux equals the conduction heat flux at the ECON slab surface (Equation 4).

$$\boldsymbol{n} \cdot (k\nabla T) = h_c(T_{sur} - T_{air}) \quad (4)$$

where **n** is the normal vector to the surface, k is the thermal conductivity, T_{sur} is the pavement surface temperature in (^{O}C), T_{air} is the ambient temperature in (^{O}C), and h_c is the heat transfer coefficient in (W/m^{2}.^{O}C)).

The convection heat transfer coefficient, h_c, was calculated based on ASHRAE handbook (ASHRAE 2015) by assuming an average wind speed of 16 km/h that was obtained during the experimental test. The pavement surface temperature was -1^{o}C at the beginning of the experimental tests conducted on the ISU ECON slab, and the ambient temperature was equal to -1 ^{o}C, so this value was introduced into the COMSOL environment as an initial value. It was assumed that the ECON slab edges and the bottom were insulated since insulation boards had been placed at these locations.

The electrical ground and electrical potential boundaries were selected as 0 V and 80 V, respectively, at each electrode. These represent the power supply voltages assigned to the ECON slab during the experimental test to create heat generation in the electrically conductive concrete layer. Electrodes were embedded in the electrically conductive layer and their material properties were defined in the COMSOL environment to represent the actual electrode material and the galvanized steel used in constructing the ECON slab.

4.5.3 Description of Material Modeling

The slab modeled in this study is comprised of ECON and conventional concrete. The electrical resistivity of ECON is very small in comparison to that of conventional concrete that has resistivity values higher than 1,000 kΩ·cm (Gopalakrishnan et al. 2015). An ECON

HPS with lower resistivity (i.e., higher conductivity) can reduce energy demands needed to melt snow and ice and improve cost-effectiveness.

There is an inverse relationship between the electrical resistivity and temperature that follows the Arrhenius equation (Chang 2013). The electrical resistivity can be calculated using first and second Ohm's law (Wu 2013) as follows:

$$R = \frac{V}{I}, \rho = \frac{R \times A}{L} \quad (5)$$

where, ρ is electrical resistivity (i.e., reciprocal of electrical conductivity), R is the electrical resistance, A is the cross-sectional area parallel to the electrodes, L is the electrode spacing, V is voltage, and I is electrical current.

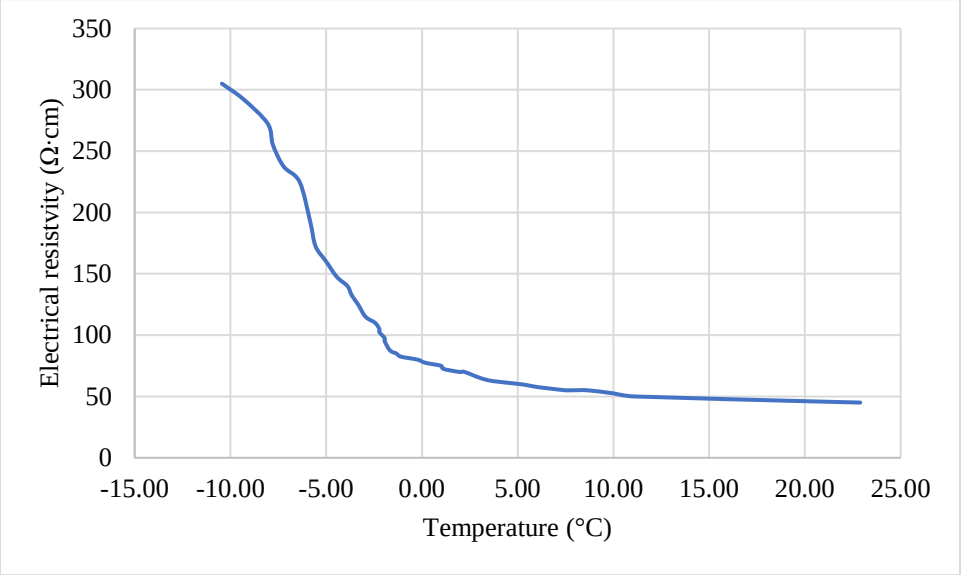

Figure 4-2 Correlation between ECON electrical resistivity and temperature

The material properties used in the FE model were obtained from experimental laboratory tests conducted in this study, from the COMSOL library, and from a previous study (Tuan 2004). The material property inputs include electrical resistivity, density, heat capacity, and thermal conductivity for conventional concrete, electrodes, and ECON (see

Table 4-1). The material properties for conventional concrete and galvanized steel electrodes were obtained from the COMSOL material library. An experimental test was executed to identify the electrical resistivity values of ECON under various temperature conditions (Figure 4-2). Figure 4-2 shows that the electrical resistivity value decreases as the temperature increases. However, the electrical resistivity values of ECON are only slightly differed in the range -1 to 15 ^{o}C which are heated pavement operation ranges to melt snow and ice. Based on these experimental test results, a constant electrical resistivity value of 70 Ω·cm for ECON was used at -1 ^{o}C ambient temperature as a constant value in the FE model.

Table 4-1 Material properties used in FE Simulations

Material	Density (kg/m^3)	Thermal conductivity (W/m·K)	Heat Capacity (J/kg·K)	Electrical Resistivity (Ω·cm)
Conventional Concrete	2300	1.4	880	5.4×10^5
Steel AISI 4340 (electrodes)	7850	44	475	1.7×10^{-9}
ECON	2500	4.2	480	70

4.5.4 Description of Mesh Generation

After defining the geometry features and other required variables including boundary conditions and material properties, the element type and FE mesh were defined. A tetrahedral element type was used to discretize the ECON slab into smaller elements. The tetrahedral element has four points and six edges with two degrees of freedoms with respect to temperature and electrical potential. The convergence of the FE model was evaluated using different mesh sizes with a number of linear and quadratic tetrahedral elements ranging from 15,125 to 201,253. The quadratic tetrahedral elements showed that the results tend to better match the experimental results as mesh size decreases. The results of FE differed very little

when the number of element was greater than 60,000. Therefore, quadratic tetrahedral elements at this mesh size were selected and used for meshing the 3-D FE model.

The electrical potential was applied through electrodes and the temperature at each node was calculated. The embedded electrodes and their surrounding areas were more finely meshed (See Figure 4-3) to enhance the interaction between the electrodes and the surrounding areas so that the results could be more precisely estimated.

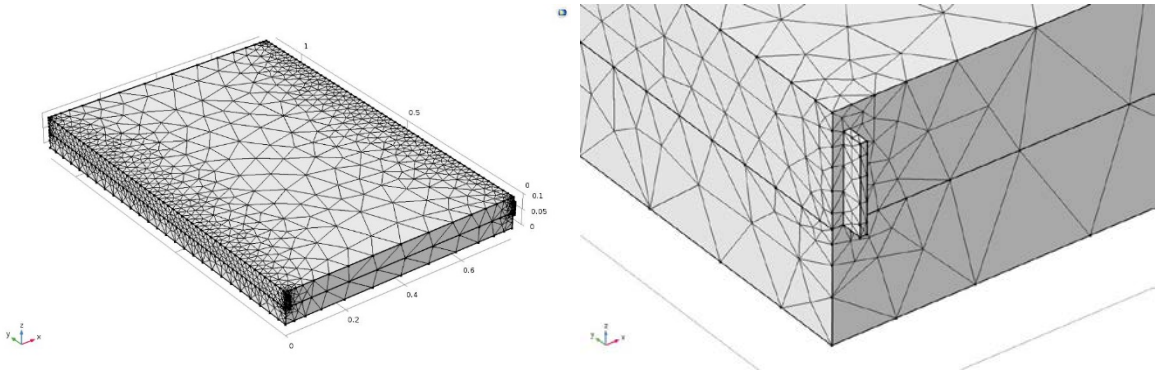

(a) **(b)**

Figure 4-3 ECON mesh distribution: (a) 3-D mesh of ECON slab (b) zoomed of the meshed construction region around the electrode and ECON slab

4.6 Results and Discussions

A FE analysis of joule heating was conducted using an electrical potential of 80 V to power the ECON layer. The temperature distribution of the ECON slab was numerically calculated over the interval from 0 to 150 minutes at time divisions of 8 minutes.

Temperature values on the 3-D FE modeled ECON slab surface are presented in Figure 4-4*a* at 8 minutes, Figure 4-4*c* at 100 minutes, and Figure 4-4*e* at 150 minutes. The heat initially tends to accumulate in the central part of the ECON surface and then is distributed across the entire surface area. The highest temperature predicted by the FE analysis was observed in the middle area of the ECON surface and the temperature near the electrodes was about 2 to 5 ^{o}C less compared to that of the middle area. This could be

attributed to the electrodes radiating electrical energy that got converted into heat (energy); the middle areas thus heated first and become hotter.

Temperature distributions inside the 3-D FE modeled ECON slab are presented in Figure 4-4*b* at 8 minutes, Figure 4-4*d* at 100 minutes, and Figure 4-4*f* at 150 minutes. Because of the low electrical resistivity (i.e., high electrical conductivity) of the ECON layer, heat was initially induced in the ECON layer due to its lower resistivity, then transferred through conduction into the adjacent conventional concrete layer. This behavior could be explained as follows: the electrical energy passing into the ECON layer is converted into heat through resistive losses and the heat is then transferred to the other layer through thermal conduction by the collision of the molecular particles (Cengel 2003).

The temperature of the center of the 3-D FE modeled ECON slab surface was 2.2 ^{o}C at 500 seconds (See Figure 4-4*a*). The temperatures in the middle depths of the ECON and conventional layers were about 2.4 ^{o}C and -0.5 ^{o}C, respectively, at 8 minutes (See Figure 4-4*b*).

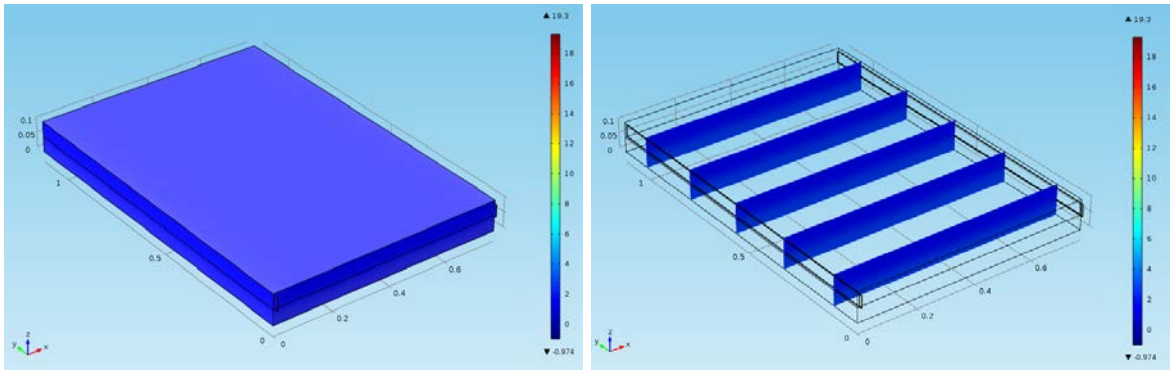

(a) (b)

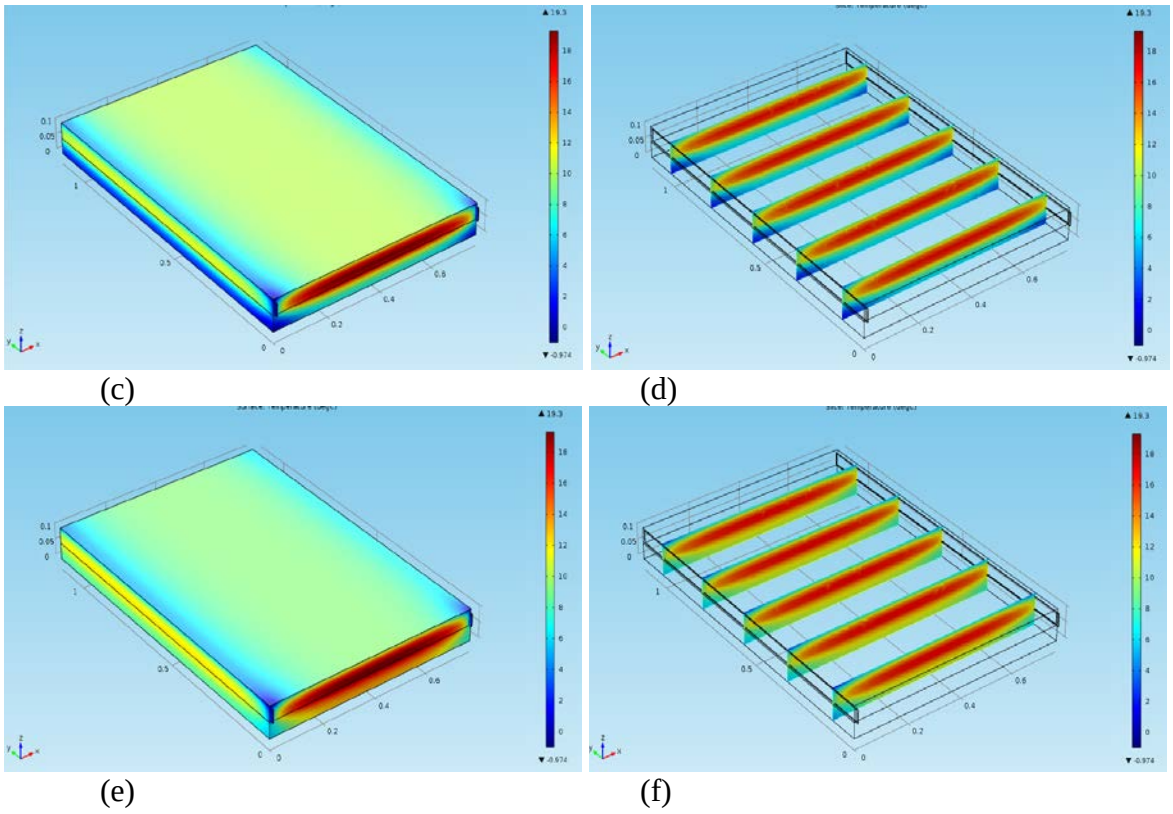

(c) (d)

(e) (f)

Figure 4-4 Changes in temperature Vs time in the 3-D FE modeled ECON slab: (a) the surface temperature at 8 minutes, (b) the inside temperature at 8 minutes, (c) the surface temperature at 100 minutes, (d) the inside temperature at 100 minutes, (e) the surface at 150 minutes, and (f) the inside temperature at 150 minutes

The temperature of the center of the ECON slab surface was 13.4 ^{o}C at 100 minutes (See Figure 4-4*c*) and the temperature at the middle depth of the ECON layer was 15.3 ^{o}C at 100 minutes (See Figure 4-4*d*). The reason for this difference was that the ECON slab surface was exposed to the environment and the convection heat transfer was considered on the top surface of the ECON slab.

The temperatures at the middle depth of the ECON and the conventional layers were about 16.4 ^{o}C and 17.4 ^{o}C, respectively, at 150 minutes (See Figure 4-4*e* and Figure 4-4*f*), showing that the temperatures inside the two layers were close to one another at 150 minutes. This result indicates that thermal stresses will not be an issue due to the small temperature differences between the ECON and the conventional layers. The temperature inside the

conventional concrete increased with time due to its thermal mass to absorb and store heat as well as the effect of the insulation layer that prevents heat loss.

The temperature changes at the center of the ISU ECON slab during its operation were measured (See Figure 4-5*a*) and compared to those obtained from the 3D-FE model. As seen in Figure 4-5*b*, this comparison acknowledged the validity of the results obtained from the FE analysis. The FE model tended to slightly overestimate the predicted temperature in comparison to the experimental data. The reason for this difference could be that only convection effects were considered in the FE model, but not those due to other sources of heat loss such as radiation.

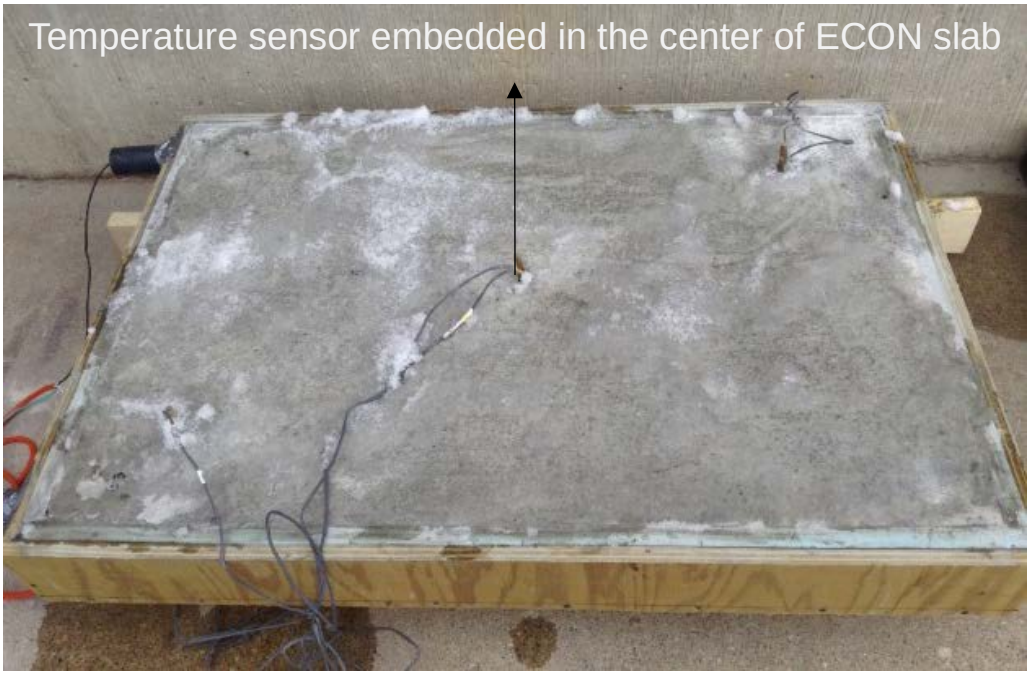

(a)

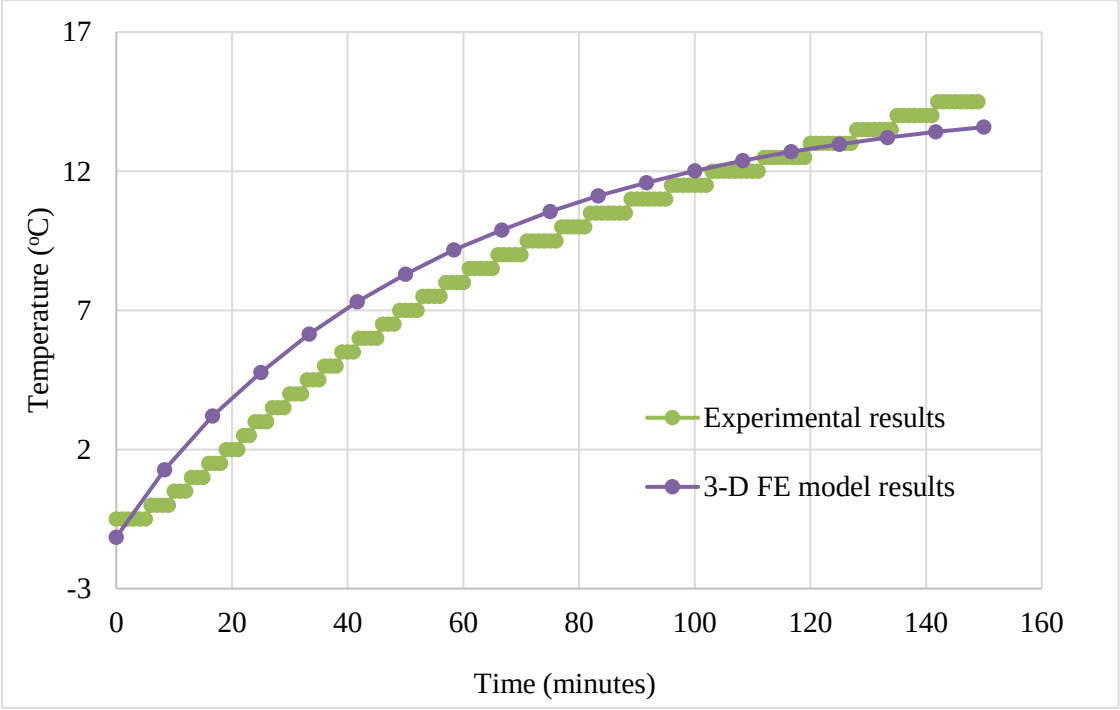

(b)

Figure 4-5 3D-FE model validation: (a) ISU ECON slab with embedded temperature sensor, and (b) comparison of temperature changes between experimental measurements and FE simulation results (R^2= 0.80)

4.7 Sensitivity Analysis of the Developed 3-D FE Model

The design variables for ECON HPS include ECON electrical resistivity, electrode spacing, voltage, and ambient temperature. To evaluate the effect of these design variables on the heating performance of ECON HPS, sensitivity of these variables to temperature changes to the center surface of slab was identified using the developed ECON 3-D FE model.

The geometry of ECON slab, 4.6 m long × 4.6 m wide × 19 cm thick, was selected to represent one of the real large-scale airport pavements. The thickness of the model is made up of two layers: a 7.6-cm ECON top layer and an 11.4-cm bottom layer of conventional concrete. Table 2 lists the base case values for each variable of the ECON layer. In the one-at-a-time (OAT) sensitivity analysis, value for one of these variables was changed while the other variables were kept constant. The material properties of conventional concrete used as

base case values (i.e., constant values) in the sensitivity analysis were obtained from Table 4-2.

Table 4-2 Base case variables and values of the ECON layer for sensitivity analysis

Variables	Values
Electrode spacing	1.5 m
Electrical resistivity	50 Ω·cm
Voltage	220 V
Width of ECON slab	4.6 m
Ambient temperature	-10 ^{o}C

4.7.1 Effect of Electrical Resistivity on Heating Performance

To better understand the effect of electrical resistivity, the temperature changes with time were investigated by alternating the electrical resistivity from 50 to 300 Ω·cm. Figure 4-6 shows that increasing the electrical resistivity value of ECON layer - while fixing the other variables - the temperature considerably increases within 150 minutes of time duration investigated. When the electrical resistivity value was 50 Ω·cm, the surface temperature increased from -10 ^{o}C to above-freezing point (i.e., about 1 ^{o}C to 2 ^{o}C) in about 10 minutes. When the electrical resistivity values were 100 Ω·cm and 200 Ω·cm, the surface temperature increased from -10 ^{o}C to above-freezing point in about 25 minutes and over 66 minutes, respectively. However, an electrical resistivity of 300 Ω·cm was not sufficient enough to increase surface temperature to above-freezing point within 150 minutes of time duration investigated.

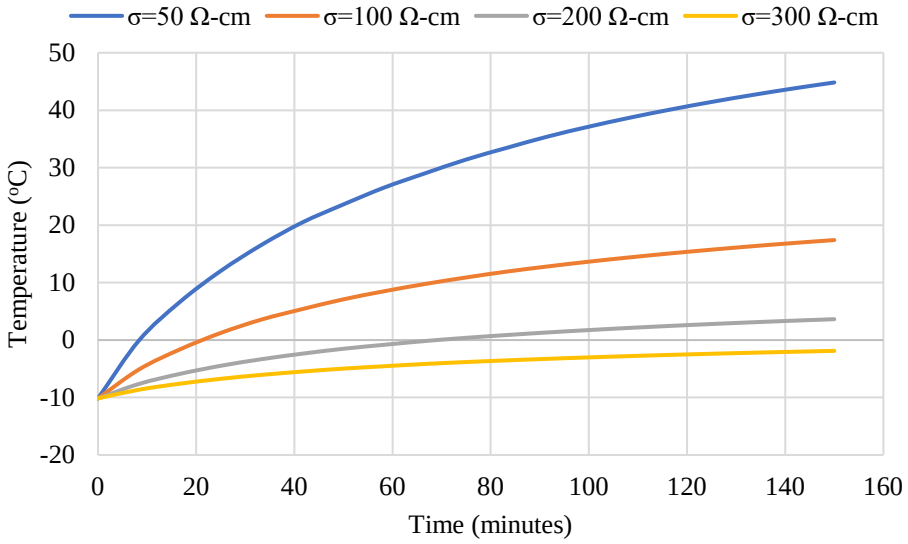

Figure 4-6 Changes in ECON temperature time for different electrical resistivity values

4.7.2 Effect of Electrode Spacing on Heating Performance

The design of electrode spacing is one of the challenging tasks in achieving an efficient ECON system. To investigate the effect of electrode spacing on ECON slab heating performance, the changes in ECON temperature with time were investigated by choosing three electrode spacing design options which are 1.5 m for 4-electrode installation, 2.3 m for 3-electrode installation, and 4.6 m for 2-electrode installation on a given ECON slab dimension (i.e., 4.6 m long × 4.6 m wide).

As the electrode spacing increases, the time to achieve temperature above freezing point on ECON surface dramatically increases (See Figure 4-7). When 1.5 m and 2.3 m electrode spacing design options were selected, the surface temperature increased from -10 ^{o}C to above-freezing point within 30 minutes which is expected to prevent snow and ice accumulation after operating ECON pavement system. However, the 4.6 m electrode spacing design option could not increase surface temperature to above-freezing point within the 150-minutes interval.

The obtained results are in agreement with Ohm's law – the relation between electrical resistance and electrode spacing – as electrode spacing increases, the resistance increases. From these findings, it would be recommended that the electrode spacing in ECON slab needs to be optimized by taking into consideration all factors such as electrical resistivity, ambient temperature, power supply, etc., for a large-scale project since building and testing a large-scale ECON slab is not an efficient way to design electrode spacing. In that case, the 3-D FE model is considered to be a useful and powerful tool.

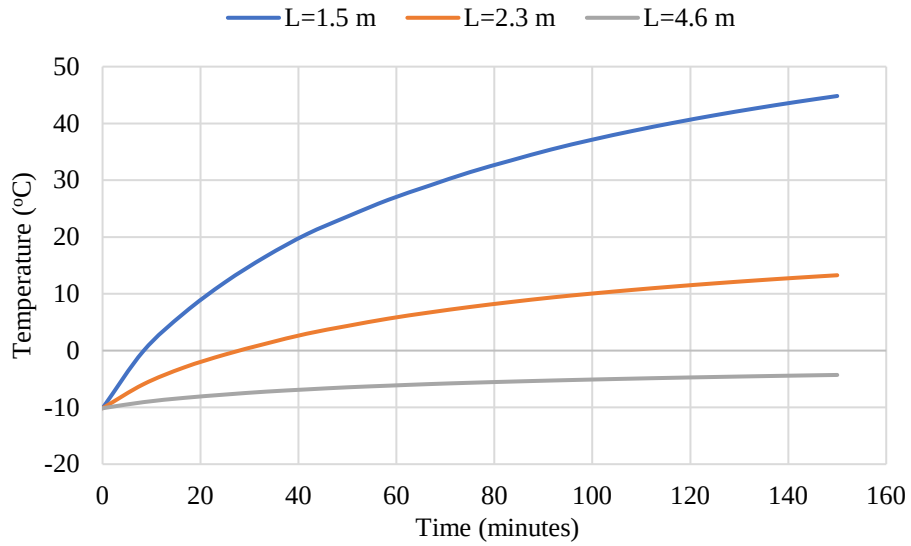

Figure 4-7 Changes in ECON temperature with time for different electrode spacing values

4.7.3 Effect of Voltage on Heating Performance

Voltage and power density are important parameters to be determined for maintaining low-cost operation of the ECON system. Figure 4-8 shows ECON slab temperature changes with time for different voltage values ranging from 60 to 220 V. When the applied voltage increased from 120 to 220 V, the time to reach temperature above freezing point decreased from 42 minutes to 9 minutes. These results are in agreement with the experimental results reported in a previous study wherein a set of voltage values were applied during the

experiment test and a noticeable increase in the temperature was observed (Wu 2013). However, voltage values of 60 V and 80 V could not increase the surface temperature above freezing point within the 150-minutes intervals.

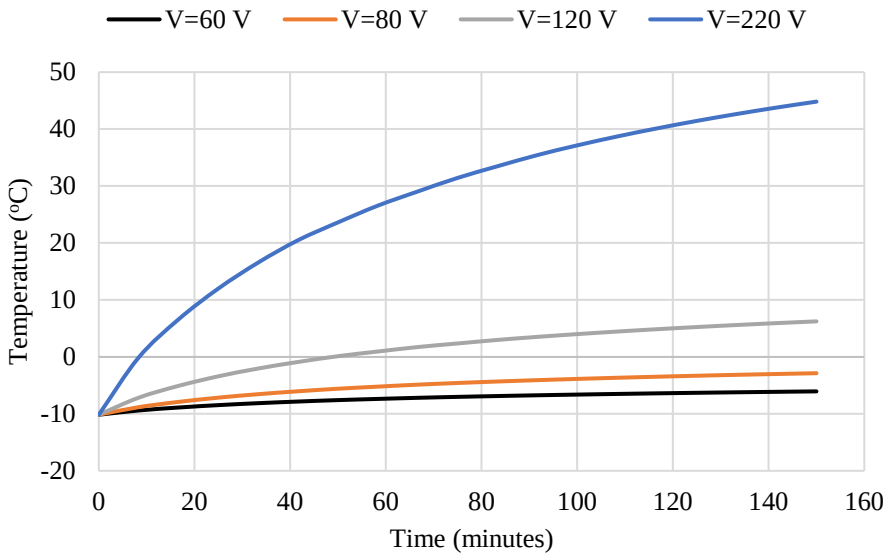

Figure 4-8 Changes in ECON temperature with time for different voltage values

4.7.4 Effect of Ambient Temperature on Heating Performance

Ambient temperature has been used to determine the required energy for HPS operation using the steady-state energy balance equations which do not consider time-dependent heating performance. The effect of ambient temperature on ECON slab heating performance was investigated by alternating three ambient temperature values (-5, -15, -25 ^{o}C) which can represent temperature conditions in a wide range of geographical locations in the US in which ECON might be used.

Figure 4-9 displays the changes in ECON slab temperature with time for different ambient temperature conditions. The time required to increase the temperature from -5 ^{o}C, -15 ^{o}C, and -25 ^{o}C to above-freezing point was about 5, 16, and 32 minutes, respectively. The

results indicate that the ECON HPS could be employed in most geographical locations within the US by achieving temperatures above freezing point immediately after its operation.

Based on temperature sensor or weather forecast data, the ECON system could be turned on about 30 minutes before the expected snow falling time in some geographical locations (or seasonal times) with ambient temperature below -25 ^{o}C. In such cases, snow and ice will melt more quickly when they hit the ECON HPS surface. Such an operation strategy can reduce snow and ice accumulations and consequently reduce electrical power demands and run the system more efficiently.

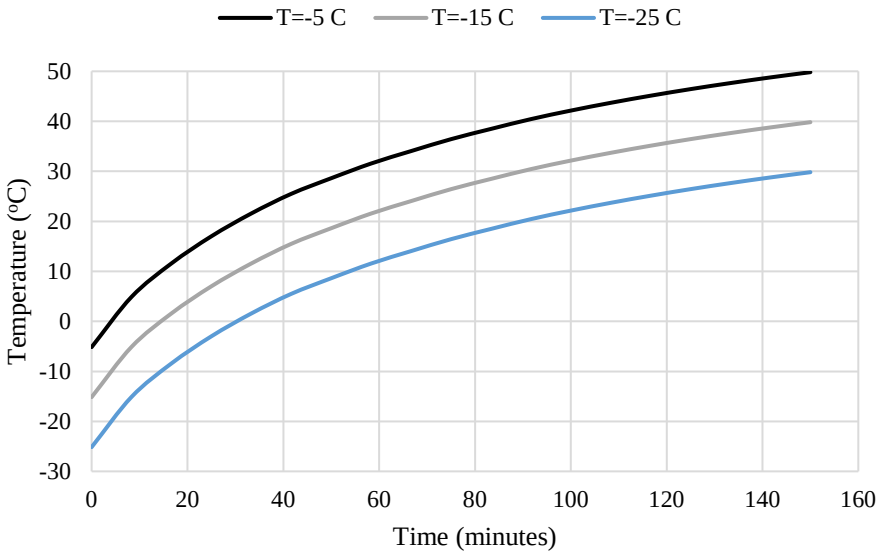

Figure 4-9 Changes in ECON temperature with time for different ambient temperatures

4.8 Conclusions

The primary goal of this study was to develop a 3-D FE model for evaluating the effects of various design parameters on time-dependent ECON heating performance for ECON HPS design optimization. A 3-D FE model was developed based on an ECON slab (122 cm long × 86 cm wide × 10 cm thick) built at ISU. To validate the 3-D FE model, changes in ECON temperature from the 3-D FE model simulations were compared with the

temperature change measurements obtained from the center of ISU ECON slab during its operation. By employing the developed 3-D FE modeling approach, a sensitivity analysis was conducted on various design variables with respect to ECON heat generation and distribution performance. For the sensitivity analysis, realistic, large-scale airport pavement ECON slab dimensions (4.6 m long × 4.6 m wide × 19 cm thick) were used. The major conclusions of this study are as follows:

- The developed 3-D FE model for ECON can predict heat generation and distribution changes over operational time. It can be utilized as a cost-effective evaluation tool for examining the effects of various design parameters on the time-dependent heating performance of ECON HPS design optimization.
- Given the assumed boundary conditions, the model shows that, initially, during the ECON operation the temperature is highest at the central area of ECON surface and is then distributed across the entire slab.
- The temperature inside the conventional concrete layer increases with time because the insulation layer and the slab boundaries reduce heat losses. This temperature comes closer to the temperature inside the ECON layer within 9,000 seconds of time after beginning ECON operation. These results indicate that thermal stresses between surfaces will not be an issue because there was minor temperature differences between the ECON and conventional layers.
- The ECON electrical resistivity is one of the most influential parameters governing the heating performance. As the electrical resistivity value increases, the time to achieve temperature above freezing point on ECON surface increases. The 3-D FE model results indicate that electrical resistivity ranges of about 50 to 200 Ω·cm can

provide sufficient heat for the realistic ECON slab (4.6 m long × 4.6 m wide × 19 cm thick) dimensions representing one of the real, large-scale airport pavement slabs.

- As the electrode spacing increases, the time to achieve temperature above freezing point on ECON surface dramatically increases. Based on the 3-D FE model results, it is recommended to design electrode spacing such that more than two electrodes could be accommodated in an ECON slab to ensure that the ECON surface temperature will be above-freezing.
- The voltage values and the ambient temperature can also affect the time to achieve above-freezing point temperature on ECON surface. As voltage values increase, the ECON surface temperature reaches above-freezing point temperature more quickly.
- Thirty minutes or less are required to increase from ambient temperature ranges (-5, -15, -25 ^{o}C) to above-freezing temperatures. Considering that the ambient temperature ranges selected for the study are representative of temperature conditions in a wide range of geographical locations in the US, ECON HPS could be employed in most geographical locations in the US and be able to achieve above-freezing point temperatures in these locations.

4.9 Acknowledgements

This paper was prepared from a study conducted at Iowa State University under the Federal Aviation Administration (FAA) Air Transportation Center of Excellence Cooperative Agreement 12-C-GA-ISU for the Partnership to Enhance General Aviation Safety, Accessibility and Sustainability (PEGASAS). The authors would like to thank the current project Technical Monitor, Mr. Benjamin J. Mahaffay, and the former project Technical Monitors, Mr. Jeffrey S. Gagnon (interim), Mr. Donald Barbagallo, and Dr. Charles A. Ishee

for their invaluable guidance on this study. The authors also would like to thank the PEGASAS Industry Advisory Board members for their valuable support and feedback. Although the FAA has sponsored this project, it neither endorses nor rejects the findings of this research. The presentation of this information is in the interest of invoking comments by the technical community on the results and conclusions of the research.

References

Abdualla, H., Ceylan, H., Kim, S., Gopalakrishnan, K., Taylor, P. C., and Turkan, Y. (2016). "System requirements for electrically conductive concrete heated pavements." *Transportation Research Record: Journal of the Transportation Research Board, No 2569*, Transportation Research Board of the National Academies, Washington, D.C., pp. 70-79.

ASHRAE (2015). *ASHRAE Handbook - HVAC Applications American Society of Heating, Chapter 51 – Snow Melting and Freeze Protection.* American Society of Heating, Refrigeration and Air-Conditioning Engineer, Inc., Atlanta, GA, pp. 51.1 – 51.20.

BBC news (2006). *"Boy Killed after Plane Skids Off Runway."* http://www.cnn.com/2005/US/12/08/chicago.airplane/. Accessed July 23, 2016.

CNN news (2016). *"Snowy weather caused damage in parts of the country."* http://www.cnn.com/2016/12/11/us/winter-weather-storm/. Accessed December 27, 2016.

Cengel, Y. A. (2003). *Heat and Mass Transfer: A Practical Approach*. McGraw-Hill, New York.

Chang, C., Song, G., Gao, D., and Mo, Y. L. (2013). "Temperature and mixing effects on electrical resistivity of carbon fiber enhanced concrete." *Smart Material Structural*, Vol. 22, No. 3, p. 035021.

COMSOL Multiphysics User's Guide, Stockholm, Sweden. 2012, pp. 707-755.

FAA. (2011). *Airside use of heated pavement systems*, FAA Advisory Circular (AC) No: 150/5370-17. FAA, U.S. Department of Transportation, Washington, D.C.

Gopalakrishnan, K., Ceylan, H., Kim, S., Yang, S., and Abdualla, H. (2015). "Electrically conductive mortar characterization for self-heating airfield concrete pavement mix design." *International Journal of Pavement Research and Technology* 8, No. 5, pp. 315-324.

Joerger, M. D., and Martinez, F. C. (2006). *Electrical Heating of I-84 in Land Canyon, Oregon*, Publication FHWA-OR-RD06-17. Oregon Department of Transportation, Salem, OR.

Lund, J. W. (2005). *Pavement Snow Melting*. Geo-Heat Center, Oregon Institute of Technology, Klamath Falls, OR.

Ogasawara, T., Hirano, Y., and Yoshimura, A. (2010). "Coupled thermal–electrical analysis for carbon fiber/epoxy composites exposed to simulated lightning current." *Composites Part A: Applied Science and Manufacturing*, Vol. 41, No. 8, pp. 973-981.

Sassani, A., Ceylan, H., Kim, S., and Gopalakrishnan, K. (2015). "Optimization of electrically conductive concrete (ECC) mix design for self-heating pavement systems." Presented at the *2015 Mid Continent Transportation Research Symposium*, Ames, IA.

Sridharan, S., Zhu, J., Hu, G., and Xuan, X. (2011). "Joule heating effects on electroosmotic flow in insulator-based dielectrophoresis." *Electrophoresis*, Vol. 32, No. 17, pp. 2274-2281.

Tuan, C. Y. (2004). *Conductive Concrete for Bridge Deck Deicing and Anti-icing*, Final Report for Project No. SPR-PL-1(037) P512, Department of Civil Engineering, University of Nebraska-Lincoln, NE.

Tungjitkusolmun, S., Woo, E. J., Cao, H., Tsai, J. Z., Vorperian, V. R., and Webster, J. G. (2000). "Thermal—electrical finite element modelling for radio frequency cardiac ablation: effects of changes in myocardial properties." *Medical and Biological Engineering and Computing*, Vol. 38, No. 5, pp. 562-568.

Wu, T., Huang, R., Chi, M., and Weng, T. (2013). "A study on electrical and thermal properties of conductive concrete." *Computers and Concrete*, Vol 12, No. 3, pp. 337-349.

Xi, Y., and Olsgard, P. J. (2000). *Effect of De-Icing Agents (Magnesium Chloride and Sodium Chloride) on Corrosion of Truck Components*, Final Report for Report No. CDOT-DTD-R-2000-10. Colorado Department of Transportation, Denver, CO.

Zenewitz, J. A. (1977). *Survey of Alternatives to the Use of Chlorides for Highway Deicing.* Publication FHWA-RD-77-52. Federal Highway Administration, U.S. Department of Transportation.

Zhao, H., Wu, Z., Wang, S., Zheng, J., and Che, G. (2011). "Concrete pavement deicing with carbon fiber heating wires." *Cold Regions Science and Technology*, Vol *65, No.* 3, pp. 413-420.

CHAPTER 5. DESIGN AND CONSTRUCTION OF THE WORLD'S FIRST FULL-SCALE ELECTRICALLY CONDUCTIVE CONCRETE HEATED AIRPORT PAVEMENT SYSTEM AT A US AIRPORT

A journal paper submitted and accepted for publication in *Transportation Research Board (TRR), Journal of the to The Transportation Research Board*

Hesham Abdualla[1], Halil Ceylan[2], Sunghwan Kim[3], Mani Mina[4], Kristen S. Cetin[5], Peter C. Taylor[6], Kasthurirangan Gopalakrishnan[7],Bora Cetin[8],Shuo Yang[9], Akash Vidyadharan[10]

5.1 Abstract

Airport agencies spend millions of dollars to remove ice and snow from airport pavement surfaces to achieve accessible, safe, and sustainable operations during the winter. Electrically conductive concrete (ECON) based heated pavement system (HPS) has gained attention as a promising alternative technology for preventing snow and ice accumulation by maintaining pavement surface temperatures above the freezing point. The objective of this study was to demonstrate the first full-scale ECON-based HPS at a U.S. airport. Two ECON slabs were designed and constructed in the General Aviation (GA) apron at the Des Moines

[1] Graduate Research Assistance, Department of Civil, Construction and Environmental Engineering (CCEE), Iowa State University, Ames, IA. E-mail: abdualla@iastate.edu
[2] Professor, CCEE, Iowa State University, Ames, IA. E-mail: hceylan@iastate.edu
[3] Research Scientist, Institute for Transportation, Ames, IA. E-mail: sunghwan@iastate.edu
[4] Associate Professor, Department of Electrical and Computer Engineering, Iowa State University, Ames, IA. Email: mmina@iastate.edu
[5] Assistant Professor, CCEE, Iowa State University, Ames, IA. E-mail: kcetin@iastate.edu
[6] Director, National Concrete Pavement Technology Center, Ames, IA. E-mail: ptaylor@iastate.edu
[7] Research Associate Professor, CCEE, Ames, IA. E-mail: rangan@iastate.edu
[8] Assistant Professor, CCEE, Iowa State University, Ames, IA. E-mail: bcetin@iastate.edu
[9] Graduate Research Assistance, CCEE, Iowa State University, Ames, IA. E-mail: shuoy@iastate.edu
[10] Graduate Research Assistance, CCEE, Iowa State University, Ames, IA. E-mail: akashv@iastate.edu

International Airport (DSM), Iowa in 2016. Systematic design components were identified and construction procedures were developed and implemented for ECON-based HPS. Using collected sensor data, the performance of the constructed and remotely-operated ECON slabs was evaluated under real weather conditions at DSM in the 2016-2017 winter season. The results demonstrate that ECON-based HPS have promising deicing and anti-icing capacities promising to provide uniform heat distribution and prevent snow and ice accumulations on the entire area of application under various winter weather conditions, including extreme cold weather (i.e., arctic blasts).

5.2 Introduction

Airport agencies spend millions of dollars per year to remove ice and snow from airport pavement surfaces to achieve accessible, safe, and sustainable operations during the winter season. The presence of ice or snow on such surfaces has the potential to cause flight delays impacting travel throughout the U.S. and worldwide, and may contribute to airplane incidents and accidents (1, 2). Using snow removal equipment (SRE) such as brooms and plows to remove snow/ice from congested areas is a challenging task and could also lead to accidents (3). The use of sand/chemical mixtures has the potential to cause foreign object damage (FOD) to aircraft engines, cause corrosion to the overall airplane structure, and lead to environmental issues including possible contamination of groundwater and nearby bodies of water (4).

In recent years, new alternative approaches are receiving increased attention for mitigating problems associated with the presence of ice/snow on the paved areas of airfields and roadways, including engineering surfaces through application of nanotechnology for repelling water/ice (5) and heated pavement systems (HPS) (6). Developed technologies for

HPS include hydronic heating (7), resistive cables embedded inside concrete structures (8), and electrically conductive concrete (ECON) (9-11).

Electrically conductive concrete (ECON)-based HPS have gained attention as a promising alternative technology for preventing snow and ice accumulation by maintaining pavement surface temperatures above the freezing point. The advantages of such methods include environmental friendliness, extended life and durability of concrete pavements, and, most importantly, melting ice and snow in a short period of time (9). ECON, by virtue of its lower electrical resistivity compared to that of conventional Portland cement concrete (PCC), behaves like an electrical conductor. As electric current flows through the conductive material network inside ECON, its resistance results in conversion of electrical energy into thermal energy (heat).

A previous study on ECON HPS implementation for transportation systems was focused only on bridge deck winter maintenance (12). However, the use of steel fibers as the conductive material for ECON HPS in that study cannot be used for airport pavement applications since steel fiber has potential to corrode, creating foreign objective debris (FOD), and damaging aircraft tires. In addition, in the previous study, the electrode configuration and installation approach isolated each pair of electrodes, requiring supplemental construction procedures, which result in additional cost and time penalties. Recently, an ECON HPS system design using a newly developed ECON mix design recipe for airport pavement application (9, 13) has been developed and evaluated by an Iowa State University (ISU) research team, using a prototype ECON heated slab. Even though there has been no guidance with respect to ECON HPS construction practices reported at actual airports, it is imperative to investigate full-scale implementation of HPS through field

demonstrations in real airport environments. The outcome of such research will result in a thorough and practical understanding of heated concrete pavement system operations at actual airport sites.

5.3 Objective and Scope

The objective of this study was to demonstrate field implementation of ECON HPS in real airport environments. Two ECON test slabs were constructed in 2016 in the northern General Aviation (GA) apron of Des Moines International Airport (DSM) located in Iowa. To construct these slabs, the best design approach under the given airport conditions was first identified; then, accordingly, systematic construction details (electrode installation, slab instrumentation, power supply, controlling unit, etc.) were planned and executed. Following construction, the slabs were constantly monitored using an automated data acquisition system. The gathered data were analyzed and the performance of the ECON slabs was thoroughly evaluated for a range of winter weather conditions characteristics of cold climate zones (ASHRAE Climate Zone 5, 6 and 7) (14), including different snow precipitation rates, ice formation conditions, and arctic-blast weather. The rest of the paper is organized in sections as follows: full-scale ECON HPS demonstration overview, system design, description of materials, instrumentation plan and installation methods, construction and instrumentation, DSM ECON heated pavement performance evaluation, and conclusions and recommendations.

5.4 Full-Scale ECON HPS Demonstration Overview

5.4.1 Construction Site Descriptions

The location for the ECON HPS field demonstration was in the north GA apron reconstruction area at the DSM in Iowa (See Figure 5-1). The selected location was close to the main power supply located in Building 69, approximately 15 ft. from the ECON slabs. As

part of a GA apron reconstruction project (construction project contractor: Foth Infrastructure and Environment, LCC, located in Johnston, Iowa), two slabs were utilized for the ECON HSP implementation and demonstration conducted by ISU researchers. Each slab was 15 ft. long × 12.5 ft. wide ×7.5 in. thick.

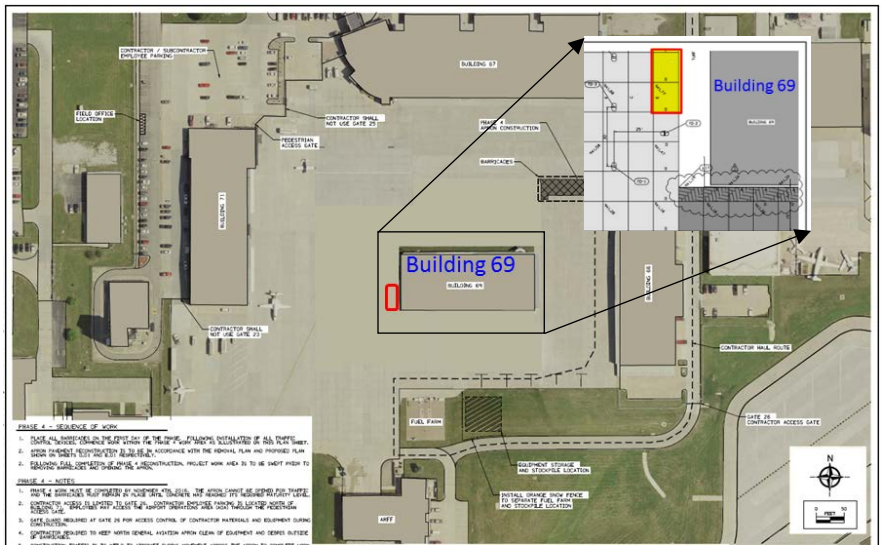

Figure 5-1 ECON HPS construction location at DSM

5.4.2 Key Components of Full-Scale ECON HPS Demonstration

The overall components of the ECON HPS for large-scale construction are illustrated in Figure 5-2. These include ECON as a conductive paving material (heating element), electrodes, temperature sensors, power supply, control unit, and PVC conduits and junction boxes. ECON for melting ice and snow on the surface can be placed in a thin concrete layer on top of a thicker PCC layer in the HPS structure to save on construction costs while providing adequate pavement structural capacity. The construction of the ECON layer should be isolated from embedded pavement light and cabling (15). For activation and deactivation of the ECON system under certain conditions, temperature sensors installed in the ECON layer are used to sense predetermined setpoint temperatures for turning the system ‘on’ and

'off' should be defined (14, 15). The value of these temperatures is dependent HPS control may also be operated using an external thermostat and/or a snow detector as alternative options if the temperature sensor fails due to wear and tear resulting from long-term operation (14). Using the current control strategy, the HPS should be deactivated when the ambient temperature reaches a range of 35 to 41°F (14). The performance of an ECON system can be monitored using sensors and a data acquisition system to estimate energy density and energy consumption.

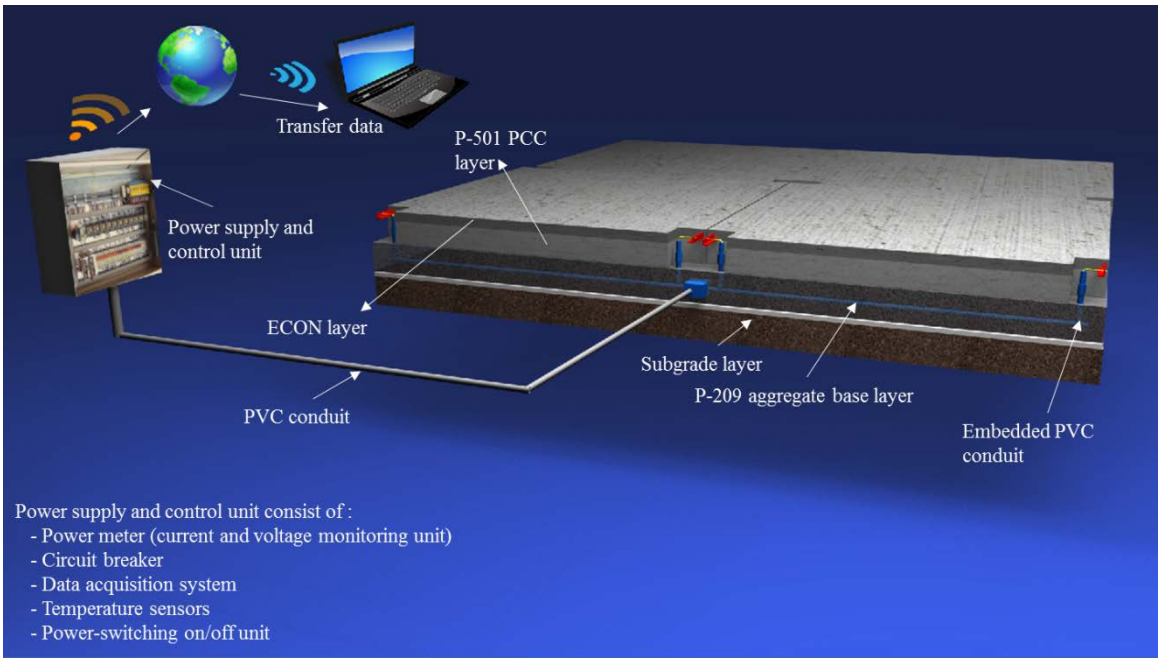

Figure 5-2 3D visualization schematic of ECON HPS

5.5 System Design

ECON HPS system design is a procedure for determining HPS geometric features (slab dimension, layer thickness, etc.) and electrode configuration consistent with given airport environments (i.e., winter weather conditions, estimated power density, electric power supply capacities available) to ensure adequate heating and structural performance during service life.

5.5.1 Design of ECON HPS Structures

To provide a clear understanding of ECON HPS construction, Figure 5-3 illustrates the overall 3-D design plan visualization and the structural layer. Each slab is 15 ft. long × 12.5 ft. wide ×7.5 in. thick and each has six electrodes. The designed ECON HPS structure consists of a two-layer 7.5-in-thick combined layer comprised of a 3.5 in. ECON top layer and a 4 in. P-501 PCC bottom layer, an 8 in. thick P-209 aggregate base course, and subgrade (Figure 5-3a). The purpose of only a thin ECON layer was to lower overall construction costs and to heat the surface as much as required to melt snow and ice without having to also heat addition concrete above the ECON layer. The concept of implementing two layers of concrete placed over another is not new and has been successfully used as a sustainable construction technique for placement of concrete such as with concrete overlay or two-lift concrete paving (16).

To provide electric power to the ECON layer, six angle-shaped perforated electrodes (1.5 in. long × 1.5 in. wide × 1/8 in. thick) per slab were embedded 3 ft. apart in the ECON layer (Figure 5-3b). Sensor systems were designed for measuring temperature and strain changes in the HPS during operation. An electric power sensor systems was also designed to monitor and measure power, voltage, and current to evaluate the power density and efficiency of the ECON HPS.

5.5.2 Design of Electrode Configuration

The electrode spacing of 3 ft. was determined based on the ECON material properties, ECON thickness, slab size, and the required amount of electric power. The electrode spacing was designed using a design flow (9) that met the design criteria, including the amount of snow/ice to be melted and the associated power density requirements.

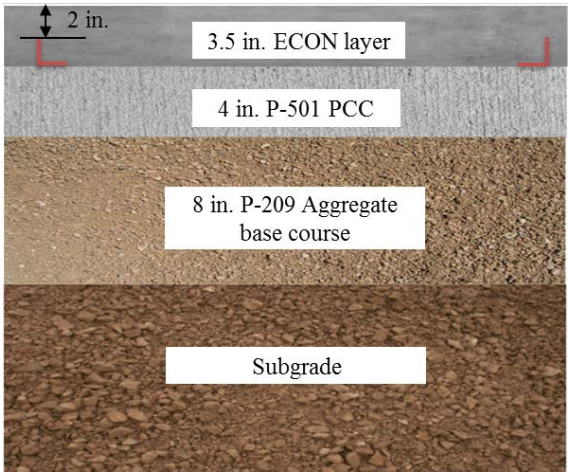

(a)

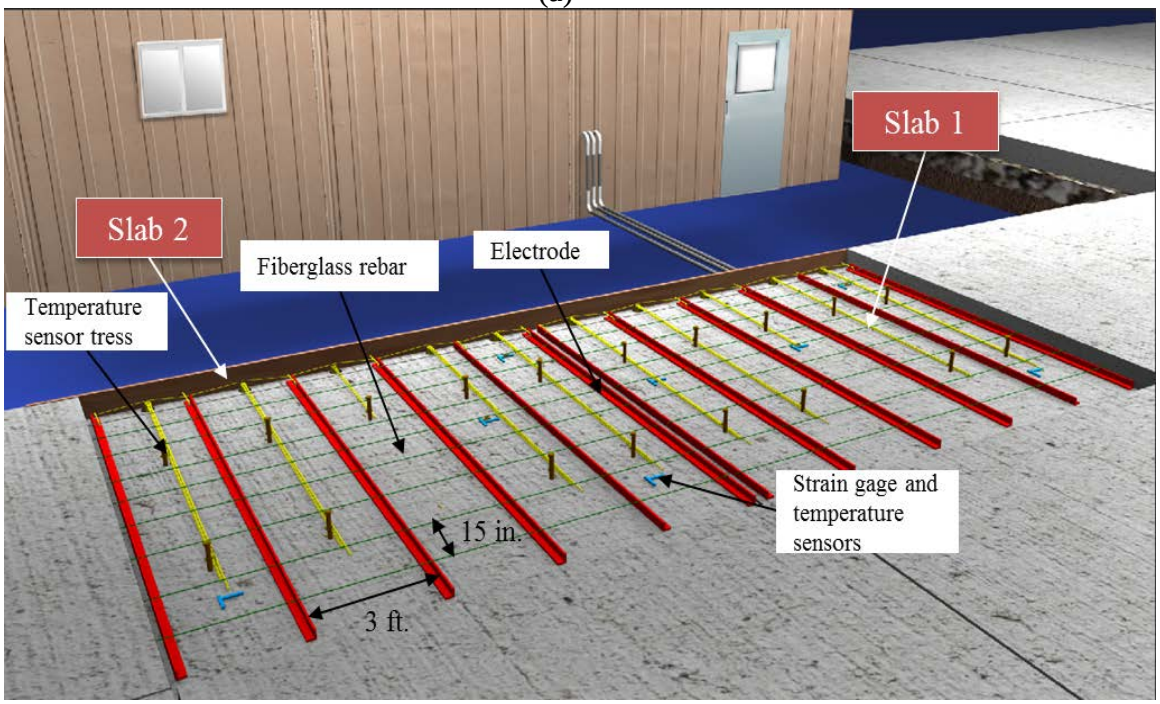

(b)

Figure 5-3 ECON HPS design plan visualization: (a) ECON HPS layer structure, and (b) 3D installation plan for ECON HPS

The power density requirement (design load) can either be experimentally obtained or estimated using the steady-state energy balance equation for required pavement heat output that considers expected rate of snowfall, air temperature, relative humidity, wind speed, and dimensions as well as pavement material characteristics (14, 15). A finite-element (FE)

method can also be used as a tool for estimation of the required power density and the snow/ice melting time for ECON HPS (17).

5.6 Description of Materials

5.6.1 ECON/P-501 PCC Mix Design

The mix design of ECON was developed and tested by researchers at ISU through a sequence of more than 40 trial mixes in the laboratory to attain a balance between workability, mechanical properties, and electrical conductivity (13). The final ECON mix design for field implementation is described in Table 5-1. The mix properties and materials were checked and tested for conformance to Federal Aviation Administration (FAA) advisory circular (AC) P-501 (18). The 28-day electrical resistivity value of ECON mix was about 307 Ω-in. at 73 ^{o}F ambient room temperature. The 28-day compressive strength and flexural strength of ECON mix were approximately 5,319 and 1,111 psi, respectively. The mix contained 1.0 % carbon fibers by volume of the total concrete mix; 70% of carbon fiber was a 0.23-in.-long and 30% of was a 0.12-in.-long, and used methylcellulose as an agent to evenly disperse the carbon fiber particles and thereby improve electrical conductivity. Derex corrosion inhibitor (DCI) is a liquid admixture meeting the requirement of ASTM C1582 that can both enhance the conductivity of the ECON mixture and mitigate the corrosive action of chlorides on reinforcing steel. The mix design for the P-501 PCC (bottom layer) was provided by the construction project contractor (i.e., Foth Infrastructure and Environment, LLC) in charge of the design of the reconstruction of the north GA apron at the DSM airport.

Table 5-1 ECON mix components and proportions for field implementation

Components		Type	Content
Basic	Coarse aggregate	3/4 in. concrete stone	1,001.0 lb./yd^3
	Intermediate aggregate	3/8 in. chips	499.0 lb./yd^3
	Fine aggregate	Concrete sand	1,134.0 lb./yd^3
	Cement	Holcim type I/II	800.0 lb./yd^3
	Water	Tap water	337.0 lb./yd^3
Admixtures	Methylcellulose	Fiber dispersive agent	1.6 lb./yd^3
	DCI admixture	30% calcium nitrite solution, corrosion inhibitor and conductivity improving agent	42.0 lb./yd^3
	Carbon fiber 0.23-in.	Synthetic carbon fiber	1.0 (% Vol.)

Note: Aggregate contents presented are in saturated surface dry condition (SSD)

5.6.2 Electrodes

While electrodes made from metallic materials are capable of enhancing electric current flow into an ECON layer since their conductivity is higher than that of ECON (9), the electrode material should have high resistance to corrosion so that electrodes will not degrade or crack, reducing efficiency and effectiveness. Angle-shaped perforated stainless steel 316L had 13 gaps (3/8-in-diameter) to allow ECON particles to interlock with the electrodes and to provide superior corrosion resistance (9, 19). The electrodes should be sufficiently bonded with the ECON to provide sufficient heat performance. The detailed properties for the 316L are included in ASTM A240 and ASTM A666. A nylon rod was selected to anchor the electrodes both because of its resistance to corrosion and its insulating properties that will prevent current leakage into the ground. The nylon-threaded rod and nut size was 4 in. × 3/8 in. diameter.

5.6.3 Sensors and Data Acquisition System

A set of sensors, both wired and wireless, was used to monitor temperature, moisture, strain, voltage, and electric current changes in HPS during operations. Before being selected as field instruments for the ECON slabs in DSM, these sensors had been evaluated using results from previous field studies to fulfill the needs of reliable long-term monitoring (20,

21). The wired sensors installed in DSM ECON HPS included Arduino based temperature (± 2%), Geokon strain gages (± 0.5%), Sensirion relative humidity sensors (± 3%), and Decagon electrical conductivity sensors (± 10%). The data acquisition system combined a Campbell Scientific CR6 data logger with a Campbell Scientific AM16/32 multiplexer.

A wireless-based sensing system can provide advantages of being less time-consuming and less labor-intensive than a wired-sensor system (20, 21). In this study, Monnit wireless sensors were used, including industrial and coin cell temperature (± 1%), humidity (± 3%), voltage (± 3%), and current (± 2%) sensors. Each Monnit wireless sensor consisted of a sensing unit (usually a probe), a cable, a transmission head, and an antenna, with measurements first taken by the probe, then sent to the sensor head that would process and then transmit the data wirelessly through the equipped external antenna. It should be noted that power for these wireless sensors was provided by batteries inside the transmission head that could be replaced when power runs low. A gateway was also used to capture data emitted from the collection of wireless sensors and upload them to pre-subscribed web-based software for real-time monitoring.

5.6.4 Remote Monitoring and Control System

The ECON HPS in DSM was equipped with surveillance cameras to monitor the ECON slabs, a control system to automatically turn the system on/off based on a setpoint temperature, and a remote access system for collecting sensor measurements and manually operating the ECON HPS using an off-site smart phone or computer.

Two on-site surveillance HD cameras were installed to provide reliable weather information from the slab site, to monitor the ECON slabs, and to capture the melting process activity during snow events. These cameras provided night vision, were

weatherproof, and continually stored video footage and other images using cloud-based storage.

Arduino board microcontrollers was used to control the ECON HPS through the universal serial bus (USB) communication interfaces provided by the on-site laptop by sending a signal in a code based on a set temperature. The code, developed using Arduino 1.6.13 software, based on C programming, was used to control the measuring interval and to convert data readings into the desired format and units through the serial USB connection to the laptop. Once programmed, the Arduinos ran this code in a continuous loop as long as power was available. The arduinos were programmed to send data every 5 minutes and to provide multiple options for operation of the ECON system. The options were as follows: “on” - turn the ECON HPS on, “off” - turn the ECON HPS, and “auto” - turn the ECON HPS off when the temperature on the control sensor pin falls below a given threshold. The logic-based breaker switches, used to control the power of the ECON HPS, were connected to the Arduino board microcontrollers and the on-site laptop.

The remote access system used Splashtop software to provide access to all data collected through the airport Wi-Fi from an off-site system from which it could be controlled and monitored as needed. The operation of the ECON system could be chosen as either automated or manual using a remote access system through a smart phone or computer. Splashtop software was used to remotely access an on-site laptop where all data was collected.

5.6.5 Other Materials

Fiberglass rebar installed in the ECON HPS (See Figure 5-3b) is highly corrosion resistant and coated with coarse quartz sand to provide bond adhesion to concrete. Fiberglass rebar is also electrically and thermally non-conductive and has a high tensile stress. ¼ in.

diameter fiberglass rebar rods were continuously placed perpendicular on top of the electrodes and secured using nylon cable ties to prevent potential cracking due to environmental load effects. PVC conduit was used to house and secure wires for all sensor and electrode systems. A laptop computer was located on-site to control ECON HPS operation and to collect and store data from the data acquisition system.

5.7 Instrumentation Plan and Installation Methods

Following material selection for the ECON HPS construction, the instrumentation plan and installation methods for electrodes, sensors, data acquisition system, and power supply system integrated with a remote-monitoring control system were developed based on extensive design and field construction experience on the part of the research team. Figure 5-4 depicts the installation methods and procedures used for electrodes and sensors, and Figure 5-4 shows the power supply panel integrated with the remote-monitoring control system.

(a) (b)

(c)

(d)

(e)

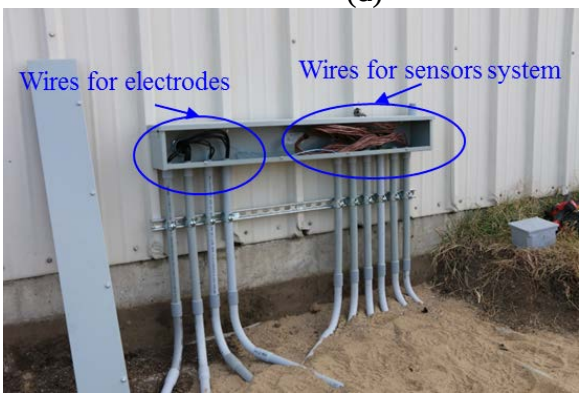

(f)

Figure 5-4 Electrode and sensor installations: (a) electrode with anchor, (b) electrodes installation, (c) electrode with electrical wire connection, (d) temperature sensor tree installation, (e) strain gages installation, and (f) PVC conduit and junction box

5.7.1 Electrodes Instrumentation Plan and Installation Methods

A nylon rod 4 in-long and with a 3/8-in-diameter was used to anchor and fix the electrodes to prevent movement during the placement of the ECON layer, as shown in Figure 5-4a. The electrodes can be anchored to the existing pavement using an electric drill to drill holes to fix the electrodes to (Figure 5-4b). After fixing the electrode, electrical wire should be connected to the electrodes using gauge-ring wire connectors to provide power to the ECON layer for generation of heat (Figure 5-4c).

Figure 5-5 Power supply panel integrated with remote monitoring control system

5.7.2 Sensors Instrumentation Plan and Installation Methods

Sensor locations were selected based on comprehensive plans, ensuring that critical locations in terms of temperature, strain, moisture, humidity, and electrical conductivity measurements were covered. Sensors were installed after electrode placement by first marking their locations on a temperature sensor tree, then mounting the temperature sensors, after which the temperature sensor tree was inserted into the drilled hole. A ¼ in. stainless steel rod was used for the temperature sensor tree; it was covered with plastic tubing to eliminate its effect on electric current during ECON operation. Figure 5-4b shows the installation of the temperature sensor tree with a clip used to anchor the wires of the temperature sensors.

Strain gages were fixed using plastic chairs and steel plates at the surface of the PCC layer. These plastic chairs held strain gages during ECON placement. An electric drill was

used to anchor the strain gages that were then placed in a perpendicular orientation to capture the strain measurements in different directions (Figure 5-4e).

After the installation of sensor and electrode systems, the wires for sensor and electrode systems were sorted and placed in PVC conduits connected to a junction box to prevent the wires from potential damage during construction. To prevent interruption or noise in the sensor data, the electrical wires of the electrodes were placed into separate conduits to prevent interference between sensor signals (Figure 5-4f).

5.7.3 Integration of Power Supply System and Remote Monitoring Control System

A single-phase power panel (120/240V, 200A power supply) was available in Building 69 near the ECON slabs. It was integrated with the electric sensors, data logger system, and laptop computer to support remote control and operation of the ECON slabs (See Figure 5-5). The power supply had six contactors connected to the electrodes through electrical wires, with each contactor connected to two electrodes. The contactors can receive remote signals to turn the system on and off based on temperature measurements from Arduino-based temperature sensors. Current and voltage sensors were installed to monitor and measure power density and consumption for the two ECON slabs, and a 60-Amp circuit breaker was used to control the current in each ECON slab. The data acquisition logger, connected to a laptop to remotely access and download data, records all data from sensors. The electric current and voltage data can be accessed through a web-based system, as described in previous sections.

5.8 Construction and Instrumentation

Figure 5-6 illustrates the construction process of the ECON HPS at DSM. Fixed-form paving was used with a form set on one side of the graded base for the entire 7.5-in thickness. A 4-in-thick layer (bottom layer) of P-501 PCC was placed on a prepared 8-in-thick layer of

P-209 aggregate based course (Figure 5-6a). Hand screed and hand-operated vibrators were used to strike the bottom layer off at the desired elevation and consolidate it. The surface of the bottom layer was screeded using brooms to create a rough surface to enhance the bonding with the ECON layer (Figure 5-6b). Six angel-shaped perforated electrodes per slab were placed on top of the PCC layer (Figure 5-6c), then sensors were placed in different locations (Figure 5-6d) and fiberglass rebar rods were continuously placed perpendicular on the electrodes (Figure 5-6e). Prior to placing the ECON layer, the surface of the bottom layer and the electrodes were thoroughly cleaned using an air-blower, brooms, and a pressure washer (Figure 5-6f).

A vibrating screed (Figure 5-6g), normally used for thin concrete pavements, was chosen to pave the two ECON layers, since the area of the ECON slabs was small. A 3.5 in. thick ECON layer was paved on top of a 4 in. thick P-501 PCC layer on November 03, 2016 (Figure 5-6h). The vibrating screed was attached with a vibrating motor to help consolidate and smooth the ECON layer. Caution was taken during the placement of the ECON layer to prevent any damage to the electrode and sensor systems. The ECON electric power supply system was tested to check wiring connections to the electrodes before placing the ECON layer.

A white-pigmented concrete compound was applied to the surface as a curing compound to avoid plastic and drying shrinkage and thermal stress cracking. A saw-cutting device was used to construct joints for control of cracking and to allow expansion and contraction due to temperature and moisture changes. The joints were cleaned and sealed using backer rod material and joint sealant. The bottom layer (4-in. PCC layer) was saw-cut at the joint so that both layers behave as monolithic pavement structures.

(a)

(b)

(c)

(d)

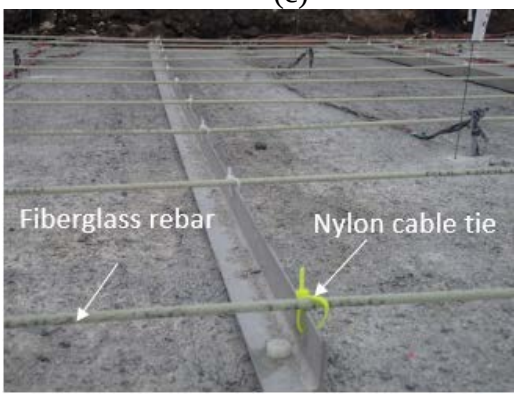

(e)

(f)

(g)

(h)

Figure 5-6 ECON HPS construction procedures at DSM: (a) P-501 PCC placement, (b) screed PCC surface, (c) electrode installation, (d) sensors installation, (e) fiberglass and nylon cable tie installation, (f) ECON surface cleaning, (g) vibrating screed, and (h) ECON placement

5.9 DSM ECON Heated Pavement Performance Evaluation

To evaluate the performance of the constructed ECON slabs in DSM under winter weather conditions, the ISU team operated the ECON HPS and collected data from December 2016 to February 2017.

Figure 5-7 illustrates the excellent ECON HPS performance results. The performance of the ECON HPS was very successful and capable of preventing snow accumulation on the ECON surface even while the apron all around the test slabs was covered with 1.2 in of snow in December 10, 2016 (Figure 5-7a and Figure 5-7b). Figure 5-7c shows the performance of the traditional snow removal method, viz., blows and brooms vehicles to remove snow, in comparison to the ECON HPS, that provides a safe environment and a reliable system, while mitigating the adverse effects of using traditional snow removal method. To provide evidence of the temperature uniformity of the ECON surface, an infrared (IR) thermographic camera was used to capture the heat distribution during the operation (Figure 5-7d), and this IR heat map demonstrates that the ECON slab could generate sufficient heat for preventing snow accumulation over the entire slab surface.

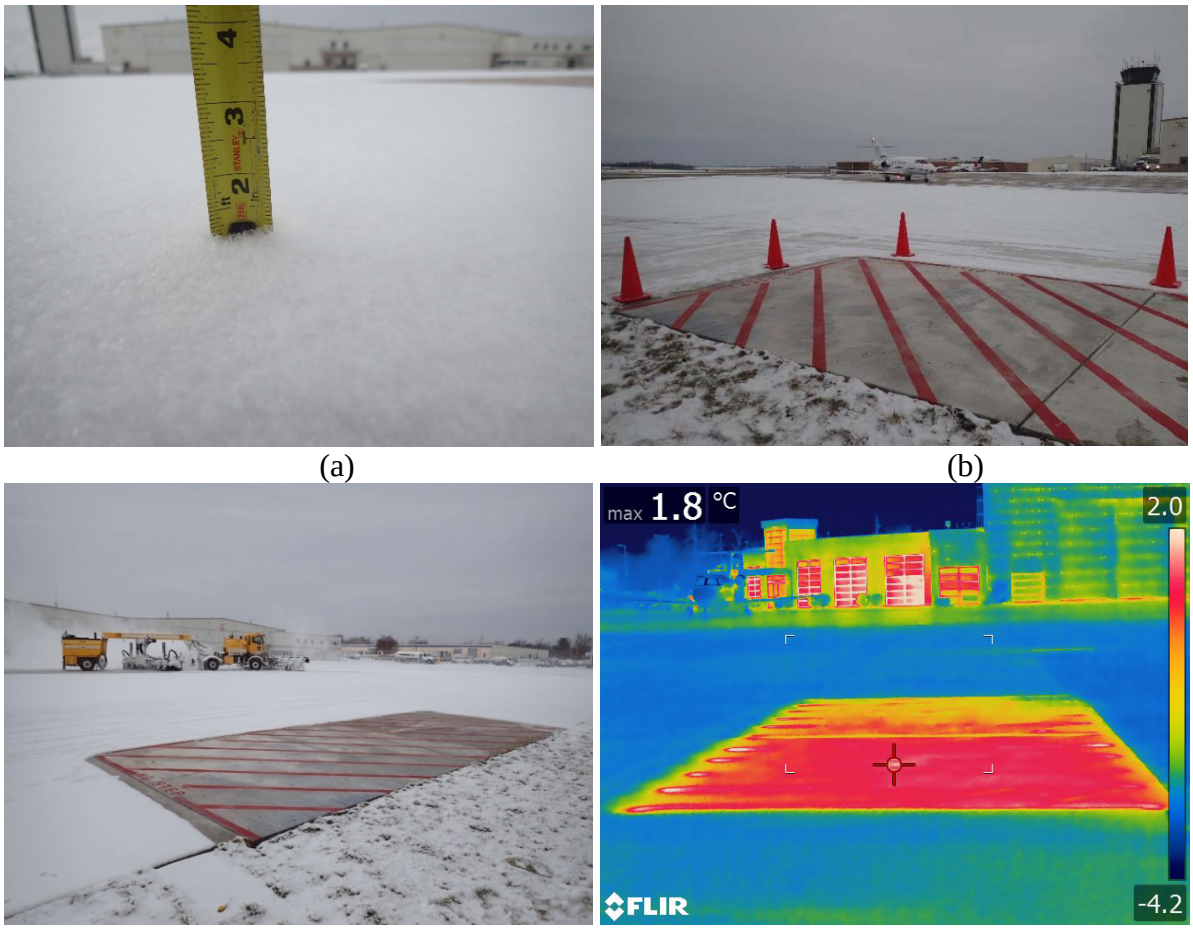

Figure 5-7 ECON HPS performance results: (a) a 1.2-in. thickness of snow accumulation at DSM in December 10, 2016, (b) ECON performance results in December 10, 2016, (c) ECON performance verse traditional method, (d) infrared thermographic image of the ECON slabs

Table 5-2 summarizes the constructed ECON slab operation performance results under various winter weather conditions during 2016-2017, ranging from light to severe snow storms and including arctic blast weather conditions that continued for two days (December 18 to 19 in 2016) (22). Two scenarios – anti-icing and deicing cases– were executed to examine the ECON HPS operation under different weather conditions. The anti-icing case refers to preheating the ECON slabs before snowfall, while the deicing case refers to heating the ECON slabs during/or after the snowfall. The wireless electric sensors installed measure electric current changes during ECON HPS operations while applying a 210 V

voltage. The average electric current measurements during ECON HPS operations were used to estimate the average power density and the energy consumption values listed in Table 5-2.

Table 5-2 Summary of ECON performance

Date	Condition	Average Air Temp. (^{o}F)	Wind Speed (mph)	Total Snow Thickness (in)	Average Power Density (W/ft^2)	Operation Time Minutes (hrs.)	Energy Consumption (kW-h/ft^2)
Dec. 10, 2016	Anti-icing	25	8	1.2	38	420 (7)	0.27
Dec. 18-19, 2016	Deicing	-11	16	1	39	1,286 (21.4)	0.84
Jan. 25, 2017	Deicing	14	14	0.5	38	90 (1.5)	0.06
Feb. 08, 2017	Deicing	14	13	1.5	35	210 (3.5)	0.12
Feb. 24, 2017	Deicing	22	17	0.8	37	150 (2.5)	0.09
Mar. 13, 2017	Deicing	21	13	1.3	33	120 (2)	0.07

Note: The anti-icing case is defined as preventing ice or snow accumulation on paved surface by preheating the ECON surface prior to snowfall or ice and the deicing case is defined as melting ice or snow following ice or snow accumulation on a paved surface.

The ECON performance results of December 10, 2016 demonstrate how ECON HSP works under anti-icing conditions. The ECON HPS was preheated to prevent ice and snow accumulation on ECON slabs before snowfall, then turned on at 5:40 am (i.e., about 3-hours before the snowfall event) based on a weather forecast reporting that snowfall was expected to begin at 7:40 am. The actual snowfall occurred from 9:00 am to 12:40 pm (i.e., about 4-hour snowfall event), thus the ECON HPS operational time was from 5:40 am to 12:40 pm (i.e., about a 7-hour operation), sufficient to prevent snow accumulation on the ECON surface. The energy consumption for this operation was 0.22 kWh/ft^2, while the average air temperature, relative humidity, and wind speed were 23 ^{o}F, 74%, and 8 mph respectively.

The ECON performance results of December 18 to 19, 2016 demonstrate how ECON HSP worked under arctic blast weather conditions. The ECON HPS was turned on after snow and ice had accumulated on ECON slabs, and outdoor ambient temperatures were very low

(i.e., an average of -11°F). The melting process took longer in comparison to other events (Table 5-2), although eventually snow and ice were melted. The energy consumption for this operation was 0.59 kWh/ft^2.

As seen for other dates of operation, under deicing conditions existing from January 25, 2017 to March 13, 2017, the ECON HPS appeared to be operating effectively under these weather conditions. The lowest energy consumption was 0.05 kWh/ft^2 to melt 0.5 in. of snow accumulation, while the highest energy consumption was 0.10 kWh/ft^2 to melt 1.5 in. of snow accumulation on the ECON slabs. The energy consumption varied due to the impact of the snowfall time, air temperature, operation time, and wind speed.

5.10 Conclusions and Recommendations

The goal of this study was to demonstrate system design, construction, and performance of an ECON HPS, the first such facility built at a U.S. airport. A full-scale implementation of two ECON slabs was designed and constructed at Des Moines International Airport (DSM), Iowa in 2016. Sensor instrumentations and a control unit were incorporated into the design of the ECON HPS to monitor the performance and support remote operation of the system. The ECON's power density, energy consumption, and performance during deicing and anti-icing were summarized and evaluated based on actual data obtained from the set of sensors implemented. The following summarize the results discussed in this work:

- Two ECON test slabs were constructed in the northern General Aviation (GA) apron of Des Moines International Airport (DSM), Iowa in 2016 as the first full-scale electrically conductive concrete heated airport pavement system in a US airport (or in the world to the best of the authors' knowledge and belief). The constructed ECON

HPS demonstrated deicing and ant-icing capacities for providing uniform heat distribution and preventing snow and ice accumulations on the entire area of application under various winter weather conditions, including extremely cold weather (i.e., arctic blast).

- The energy consumption of the ECON HSP for a deicing application ranged from 0.05 kW-h/ft^2 to 0.10 kW-h/ft^2 required to melt 0.5 to 1.5 in. of snow/ice accumulations under various winter weather conditions, except the arctic blast event that required 0.59 kW-h/ft^2 to melt 1 in. of snow/ice accumulations. The energy consumption of the ECON HSP for the anti-icing application was estimated at 0.22 kW-h/ft^2 for preventing snow and ice accumulations for 7 hrs.
- The ECON HSP in DSM was constructed using a two-lift approach that placed a thin ECON layer (top layer) on a P-501 PCC layer (bottom layer). This approach can be effective not only to save in construction costs instead of constructing a single thick ECON layer, but also to facilitate the electrode installation and electrical wire connections.
- The surface of the P-501 PCC layer (bottom layer) was screeded to create a rough surface to provide satisfactory bonding between the two layers.
- Perforated stainless steel was used for the electrodes because of its high corrosion resistance, and so that electrodes will not be reduced in efficiency; the use of stainless steel also eliminated cracking potential that would be possible with steel or galvanized steel.

- Electrodes should be placed at least 1to 2 inches below the ECON surface so as not to interfere with a paver's vibrator, pan, and augur when slipform paving is used during large-scale construction.

5.11 Acknowledgements

This paper was prepared from a study conducted at Iowa State University under the Federal Aviation Administration (FAA) Air Transportation Center of Excellence Cooperative Agreement 12-C-GA-ISU for the Partnership to Enhance General Aviation Safety, Accessibility and Sustainability (PEGASAS). The authors would like to thank the current project Technical Monitor, Mr. Benjamin J. Mahaffay, and the former project Technical Monitors, Mr. Jeffrey S. Gagnon (interim), Mr. Donald Barbagallo, and Dr. Charles A. Ishee, for their invaluable guidance on this study. The authors also thank Gary L. Mitchell at the American Concrete Pavement Association, and Mr. Gordon Smith and Mr. Dan King in ICPA for valuable discussions and comments on concrete pavement construction. The authors also would like to thank the PEGASAS Industry Advisory Board members for their valuable support. The authors also would like to thank Mr. Bryan Belt, Mr. Mark Duffy, Mr.William Konkol at the Des Moines International Airport (DSM), and Mr. Adam Wilhelm and Mr. Andrew Gettler, Foth infrastructure and environmental, LLC, Mr. Dan Hutton of Kingston Services, LLC, for their full support during construction. Special thanks are expressed to Zoltek, the Candlemakers Store (TCS), and WR Grace & Co for providing carbon fiber, methyl cellulose, and corrosion inhibitor admixture, respectively. The authors would like to express their sincere gratitude to Mr. Robert F. Steffes, ISU CCEE PCC Lab Manager, for his significant assistance with the lab and field investigations. Although the FAA has sponsored this project, it neither endorses nor rejects the findings of this

research. The presentation of this information is in the interest of invoking comments by the technical community with respect to the results and conclusions of the research.

References

1. McCartney, S. The Case for Heated Runways, *Wall Street Journal*, February 2014. http://www.wsj.com/news/article_email/SB10001424052702304914204579392883809689994-lMyQjAxMTA0MDIwMDEyNDAyWj. Accessed July 2017.

2. *Airport Winter Safety and Operation.* Advisory Circular 150/5200-30C. Federal Aviation Administration, U.S. Department of Transportation, 2008.

3. Hatch, C., S. Hartley, O. Roberto, and A. Alcala. *National Transportation Safety Board Aviation Accident Factual Repor*t, National Transportation Safety Board, December 2015. https://app.ntsb.gov/pdfgenerator/ReportGeneratorFile.ashx?EventID=20151224X81125&AKey=1&RType=Factual&IType=LA. Accessed July 2017.

4. Xi, Y., and P. J. Olsgard. *Effect of De-Icing Agents (Magnesium Chloride and Sodium Chloride) on Corrosion of Truck Components.* Final Report for Report No. CDOT-DTD-R-2000-10. Colorado Department of Transportation, Denver, CO, 2000.

5. Arabzadeh, A., H. Ceylan, S. Kim, K. Gopalakrishnan, and A. Sassani. Superhydrophobic Coatings on Asphalt Concrete Surfaces. *Transportation Research Record: Journal of the Transportation Research Board*, No. 2551, 2016, pp. 10-17. https://doi.org/10.3141/2551-02.

6. Ceylan, H., K. Gopalakrishnan, S. Kim, and W. Cord. Heated Transportation Infrastructure Systems: Existing and Emerging Technologies. *Proc., 12th International Symposium on Concrete Roads*, Prague, Czech Republic, September 2014. http://lib.dr.iastate.edu/ccee_conf/23.

7. Hoppe, E. J. Evaluation of Virginia's First Heated Bridge. *Transportation Research Record: Journal of the Transportation Research Board*, No. 1741, 2001, pp. 119-206. https://doi.org/10.3141/1741-28.

8. Joerger, M. D., and F. C. Martinez. *Electrical Heating of I-84 in Land Canyon, Oregon.* Report No. FHWA-OR-RD06-17. Oregon Department of Transportation, Salem, 2006.

9. Abdualla, H., H. Ceylan, S. Kim, K. Gopalakrishnan, P. C. Taylor and Y. Turkan. System Requirements for Electrically Conductive Concrete Heated Pavements. *Transportation Research Record: Journal of the Transportation Research Board*, No. 2569, 2016, pp. 70-79. https://doi.org/10.3141/2569-08.

10. Gopalakrishnan, K., H. Ceylan, S. Kim, S. Yang, and H. Abdualla. Electrically Conductive Mortar Characterization for Self-Heating Airfield Concrete Pavement Mix Design. *International Journal of Pavement Research and Technology*, Vol. 8, No. 5, 2015, pp. 315-324.

11. Gomis, J., O. Galao, V. Gomis, E. Zornoza, and P. Garcés. Self-Heating and Deicing Conductive Cement. Experimental study and modeling. *Construction and Building Materials*, Vol. 75, 2015, pp. 442–449. https://doi.org/10.1016/j.conbuildmat.2014.11.042.

12. Tuan, C. Y. *Implementation of Conductive Concrete for Deicing (Roca Bridge).* Final Report for Project No. SPR-PL-1(04) P565. University of Nebraska-Lincoln, NE, 2008.

13. Sassani, A., H. Ceylan, S. Kim, K. Gopalakrishnan, A. Arabzadeh, and P. C. Taylor. Influence of Mix Design Variables on Engineering Properties of Carbon Fiber-Modified Electrically Conductive Concrete. *Construction and Building Materials*, Vol. 152, 2017, pp. 168-181.

14. ASHRAE. *ASHRAE Handbook - HVAC Applications American Society of Heating, Chapter 51 – Snow Melting and Freeze Protection.* American Society of Heating, Refrigeration and Air-Conditioning Engineer, Inc., Atlanta, GA, 2015, pp. 51.1-51.20.

15. *Airside Use of Heated Pavement Systems.* Advisory Circular 150/5370-17. Federal Aviation Administration, U.S. Department of Transportation, 2011.

16. Gillen, S. L., A. S. Brand, J. R. Roesler, and W. R. Vavrik. Sustainable Long-Lift Composite Concrete Pavement for Illinois Tollway. *Proc., International Conference on Long-Lift Concrete Pavements*, Seattle, Washington, September, 2012, pp. 18-21.

17. Abdualla, H., K. Gopalakrishnan, H. Ceylan, S. Kim, M. Mina, P. C. Taylor, and K. S. Cetin. Development of A Finite Element Model for Electrically Conductive Concrete Heated Pavements. Presented at 96th Annual Meeting of the Transportation Research Board, Washington, D.C., January 8-12, 2017.

18. *Standards for Specifying Construction of Airports.* Advisory Circular 150/5370-10G. Federal Aviation Administration, U.S. Department of Transportation, 2014.

19. Hilbert, L. R., D. Bagge-Ravn, J. Kold, and L. Gram. Influence of Surface Roughness of Stainless Steel on Microbial Adhesion and Corrosion Resistance. *International Biodeterioration and Biodegradation*, No. 52, 2003, pp. 175-185. https://doi.org/10.1016/S0964-8305(03)00104-5.

20. Ceylan, H., K. Gopalakrishnan, S., Kim, P. C. Taylor, M. Prokudin, and A. F. Buss. Highway infrastructure health monitoring using micro-electromechanical sensors and

systems (MEMS). *Journal of Civil Engineering and Management*, Vol. 19, Issue sup1, 2013, pp. S188-S201.
http://dx.doi.org/10.3846/13923730.2013.801894.

21. Yang, S., H. Ceylan, K. Gopalakrishnan, and S. Kim. Smart Airport Pavement Instrumentation and Health Monitoring. Presented at 2014 FAA Worldwide Airport Technology Transfer Conference, Galloway, NJ, 2014.

22. Bitter Cold Arctic Air Sets Dozens of Record Lows in the Midwest and Plains, *Weather Underground*, December 19, 2016. https://www.wunderground.com/news/back-to-back-arctic-cold-blasts-midwest-east-december-2016. Accessed July 2017.

CHAPTER 6. DEVELOPMENT OF CONSTRUCTION TECHNIQUES FOR HEATED PAVEMENTS

A journal paper to be submitted to The *Journal of Cold Regions Engineering - ASCE*

Hesham Abdualla[1], Halil Ceylan[2], Sunghwan Kim[3], Peter C. Taylor[4], Kristen Cetin[5], Kasthurirangan Gopalakrishnan[6]

6.1 Abstract

Ice and snow accumulations on paved surfaces at airports have potential for causing flight delays and/or cancellations, pavement deterioration, and safety concerns. The use of deicing chemical agents and/or deployment of snow removal equipment (SRE) to remove snow/ice has potential for causing foreign object damage (FOD) to aircraft engines or corrosion to overall airplane structure, potentially leading to undesirable environmental issues, and is also typically costly and time-consuming. In recent years, heated-pavement systems (HPS), categorized as hydronic heated-pavement systems (HHPS) and electrically-conductive concrete (ECON) based heated-pavement systems (HPS) represent alternative options for melting ice and snow on paved surfaces. The objective of this study was to develop systematic design and construction guidance for ECON based HPS and HHPS using two-lift concrete paving (2LCP), concrete overlay, and precast concrete (PC) to expedite construction work during large-scale construction of heated pavements. The outcome of this study will help contractors and transportation agencies envision the constructability of

[1] Graduate Research Student, Iowa State University; email: abdualla@iastate.edu
[2] Professor, Iowa State University; Phone: 515-294-8051; Fax: 515-294-8216; email:hceylan@iastate.edu
[3] Research Scientist, Iowa State University; email: sunghwan@iastate.edu
[4] Director, National Concrete Pavement Technology Center; email: ptaylor@iastate.edu
[5] Assistant Professor; Iowa State University; email: kcetin@iastate.edu
[6] Assistant Professor; Iowa State University; email: rangan@iastate.edu

different components, including heating elements, electrodes configurations, and material selections, in HHPS and ECON based HPS.

6.2 Background

Ice and snow accumulation on paved surfaces has potential for reducing pavement surface skid resistance and thereby cause hazardous conditions that may lead to aircraft incidents and accidents (McCartney 2014; FAA 2008). The use of deicing chemical agents or deployment of snow removal equipment (SRE) to remove snow/ice has potential for causing foreign object damage (FOD) to aircraft engines and corrosion to overall airplane structure, leading to undesirable environmental issues (Xi and Patricia 2000), and is also typically costly and time-consuming (Anand et al. 2016).

Heated pavement systems (HPS) represent alternative options for melting ice and snow and can be classified into two general categories, hydronic heated-pavement systems (HHPS) and electrically-heated pavement systems (EHPS). HHPS melt ice and snow by circulating heated fluid through pipes embedded inside pavement structures, with the cooled fluid circulated back through a heat source that reheats the fluid during each cycle. There are different types of heat sources, including geothermal water, boilers, and heat exchangers. Geothermal water is considered to be efficient in locations with good geothermal potential (FAA 2011). EHPS melt ice and snow using resistive cables embedded in regular concrete or electrically-conductive concrete (ECON). The use of resistive cables embedded inside concrete structures has been applied to deicing of snow and ice in Oregon, Texas, and Pennsylvania; in those applications the performance of electrical cable was sometimes found inadequate due to the high power density required (Zenewitz 1977) and damage to electrical cables or associated sensing elements for triggering the system (Joerger and Martinez 2006).

PC has demonstrated satisfactory performance in bridges, pavements, buildings, and airfield construction. It provides high strength, low permeability, and low cracking potential, features that are consequences of preparing the panels off-site where quality control can be more effectively implemented. Using a PC technique instead of cast-in-place for construction of pavements can expedite the construction process by eliminating the need for concrete strength-gaining time as for on-site construction procedures (Merritt et al. 2004; Priddly et al. 2013). PC technology enables rapid repair of pavement facilities and can be beneficially applied in situations where extended road closures could increase road congestion and result in increased lost work time, fuel consumption, and user-delay costs (Kohler at al. 2004). A study has shown that estimated daily user-delay costs for a four-lane divided facility carrying 50,000 vehicles per day can be as high as $383,000 per day for 24-hour lane closure, compared to only $1,800 per day for nighttime-only lane closure (Priddly et al. 2013).

Little has been done or documented with respect to PC construction in airfield pavements. The PC technique was used to rehabilitate a taxiway at LaGuardia airport, New York during September 2002. The selection of PC as a rehabilitation option over asphalt concrete or Portland cement concrete (PCC) was due to the fact that the asphalt concrete requires frequent rehabilitation if under the influence of highly concentered and repetitive aircraft movements; the PC approach also reduces the construction downtime (Chen et al. 2003).

Two-lift concrete paving (2LCP) in which a lower lift can be optimized to enable the use of locally available or recycled materials, while a top lift is optimized for long life and functionality, has become a common construction practice in Europe. 2LCP involves either sequential placement of two wet-on-wet layers of concrete or bonding wet to dry layers of

concrete, where the bottom layer is thicker than the top layer (Cable, 2004). The benefits of 2LCP may include using recycled aggregate to achieve cost reduction and production of more sustainable pavements; this method can also provide a high-quality and durable surface, improve skid resistance, and reduce road noise (Cable, 2004) and these benefits could compensate for the extra labor and trucking costs associated with the requirement for two slip-form pavers. The use of 2LCP is currently under investigation by several agencies in the United States.

Concrete overlay systems have been proposed as cost-effective maintenance and rehabilitation solutions for a wide range of combinations of existing pavement types, conditions, desired service lives, and anticipated traffic loading. Although in the past these approaches have been referred to as ultrathin whitetopping, conventional whitetopping, bonded overlays, unbonded overlays, etc., they have more recently been classified into two broad types: the bonded resurfacing family and the unbonded resurfacing family (Harrington et al. 2007 and ASHRAE 2015). Concrete overlays are discussed in detail in the national concrete pavement technology center (NCPC) – guide to concrete overlays solution 2007 – and ACI 325.13R-06 concrete overlays for pavement rehabilitation (ACI 2006).

Concrete overlays for airfield pavement have been classified – based on the recent FAA advisory circular AC 150/5320-6F (FAA 2016) - into four broad types: PCC overlay of existing flexible or rigid pavement, and hot mix asphalt overlay of existing flexible or rigid pavement [26]. The design and construction of concrete overlays are discussed in detail in the FAA advisory circular (AC) – Airport Pavement Overlays and Reconstruction – AC No: 150/5320-6F (FAA 2016).

Design and construction procedures for HPS using advanced technologies such as PC, concrete overlays, and 2LCP have not previously been investigated. An important benefit of different advanced construction techniques for HPS is that they provide alternative options for constructing HPS in new or existing pavements and can accelerate construction procedures. For example, construction of a HPS as an overlay not requiring demolition of existing good-condition pavement has great potential as a cost-effective approach.

6.3 Objectives

The objective of this research is to develop construction guidance for large-scale ECON based HPS and HHPS using 2LCP, concrete overlay, and PC technologies to promote good construction practices. To this end, systematic design and 3-D visualization of construction procedures have been developed to support envisioning the constructability of ECON based HPS and HHPS using different construction technologies. The reminder of the paper is organized into sections as follows: overall conceptual design of ECON HPS and HHPS, ECON HPS and HHPS using 2LCP, concrete overlay, and PC, and conclusions.

6.4 Overall Conceptual Design of ECON HPS

Figure 6-1 depicts a conceptual design for ECON HPS using 3-D visualization, illustrating the main components that include conductive paving materials (heating elements), electrodes, a power supply, a control unit, and temperature sensors (Abdualla et al., 2016). The Iowa State University (ISU) research team has developed an ECON mixture with desirable electrical and mechanical properties for airfield pavement ant-icing and deicing applications (Abdualla et al., 2016 and Sassani et al., 2017). Electrodes carry electrical current into the ECON, within which heat is generated through resistive heating. This particular electrode configuration and installation approach for large-scale ECON HPS

has been investigated and developed to provide sufficient heat performance and cost-effective solutions (Abdualla et al., 2017). The ECON HPS could be operated using either a 120V or a 210V power source, based on system design parameters such as electrode spacing and ECON materials properties. The selection of electrode spacing can be achieved using a design flow (Abdualla et al., 2016) that meet the design criteria, including the amount of snow/ ice to be melted and the associated power density requirement. The power density can be experimentally obtained or calculated using a steady-state energy balance equation for required pavement heat output (ASHRAE, 2015). A sensor system (i.e., temperature sensors) could be integrated into the ECON HPS to trigger system operation, including activation, deactivation, and maintenance of snow and ice-free surfaces based on a selected temperature.

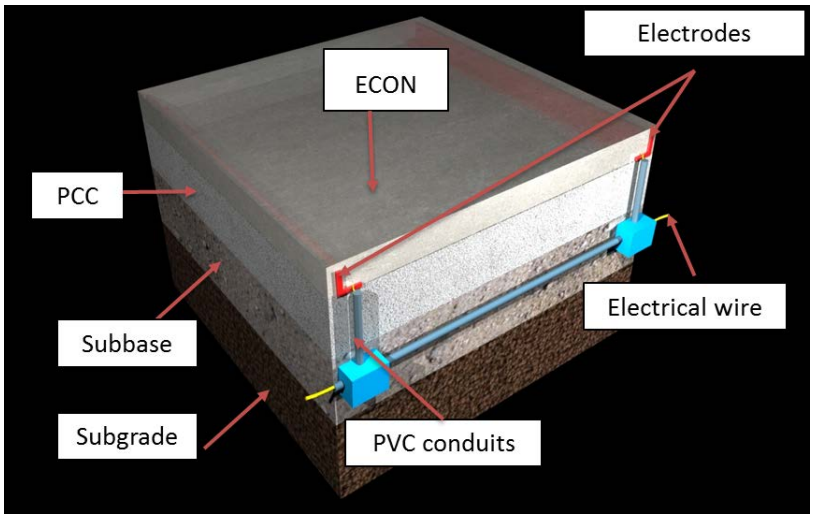

Figure 6-1 Conceptual design of ECON HPS

6.5 Overall Conceptual Design of HHPS

HHPS are typically closed-loop systems as shown in Figure 6-2 in which the fluid releases heat into the pavement, then returns to a heat source to be sent back through the pipes (Barbagallo 2013). The fluid can be heated by one of several different types of fluid

heaters, including geothermal hot water, underground thermal energy storage (UTES), boilers, and heat exchangers (FAA 2011), with the selection based on availability at the project site. Geothermal water would be considered efficient in locations with good geothermal potential (Joerger and Martinez 2006). Geothermally-heated hydronic systems often incorporate heat pumps to obtain greater heating capacity, because in many places ambient ground temperatures are not high enough to melt the snow (Minsk 1999). The efficiency of HHPS in melting ice and snow depends significantly on various factors, including fluid temperature, pavement conductivity, pipe depth, and pipe spacing (Ceylan et al. 2014). The components of HHPS include heat transfer fluid, piping, a fluid heater, pumps, and controls (ASHRAE 2015). While pipes can be made of metal, plastic, or rubber, a drawback of steel pipes is their susceptibility to rusting, so the use of steel embedded in pavement is not a common practice. An attractive alternative to steel pipe is plastic pipe made of polyethylene (PE) or cross-linked polyethylene (PEX) because it is corrosion-resistant and offers lower material cost. Polyethylene (PE) and cross-linked polyethylene (PEX) can withstand fluid temperatures up to 140^{o}F and 200^{o}F, respectively (ASHRAE 2015). Propylene glycol is commonly used as a heat transfer fluid because of its moderate cost, high specific heat, and low viscosity.

Figure 6-3 shows the construction steps required for constructing the ECON using 2LCP. The major difference between the construction of ECON using 2LCP and typical 2LCP is that the ECON using 2LCP is constructed in two layers, wet-on-dry, to facilitate electrode installation and wire connections for the electrode system.

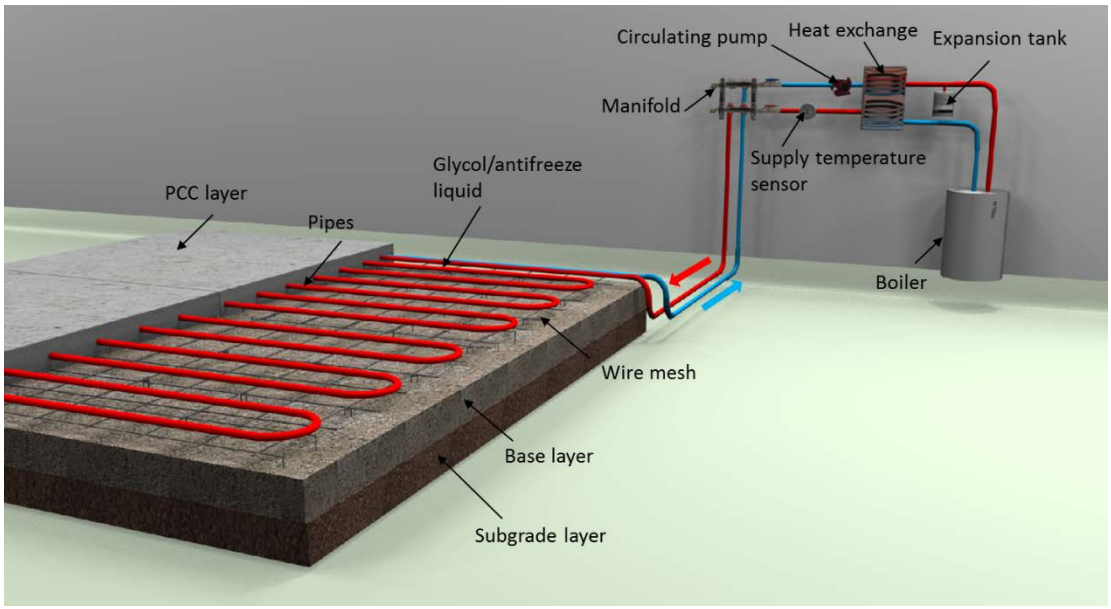

Figure 6-2 Schematic of HHPS

6.6 ECON HPS Using 2LCP

Step 1: Prepare the Base Layer, Place Dowel Baskets, and PVC Conduits. Prepare and compact the base layer, install dowel baskets, and install PVC conduits to accommodate the electrode system wires (Figure 6-4). The PVC conduit should be placed at the bottom of the base layer and on top of the subgrade layer to protect the PVC conduit from being damaged or displaced during placement of the PCC layer.

Step 2: Place PCC Layer. Place the PCC layer (bottom layer) using slip-form paving (See Figure 6-5). The surface of the PCC layer should be screeded with brooms to create a rough surface for enhancing bonding with the ECON layer. Extra attention should be given during concrete paving to protect the PVC conduit embedded in the base layer, and since the PVC conduit must not interfere with the slip-form paver's vibrators, pan, and auger, its location and spacing should be chosen so as not to interfere with the vibrators and thereby avoid PVC damage.

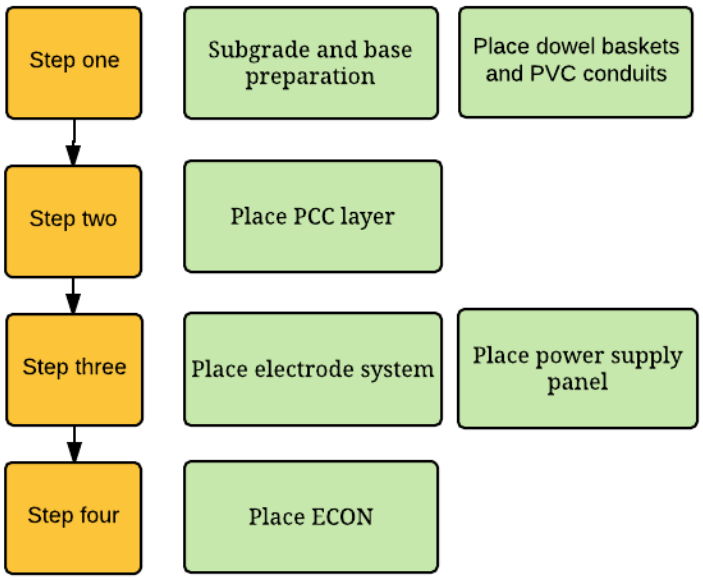

Figure 6-3 Work sequence of ECON HPS using 2LCP

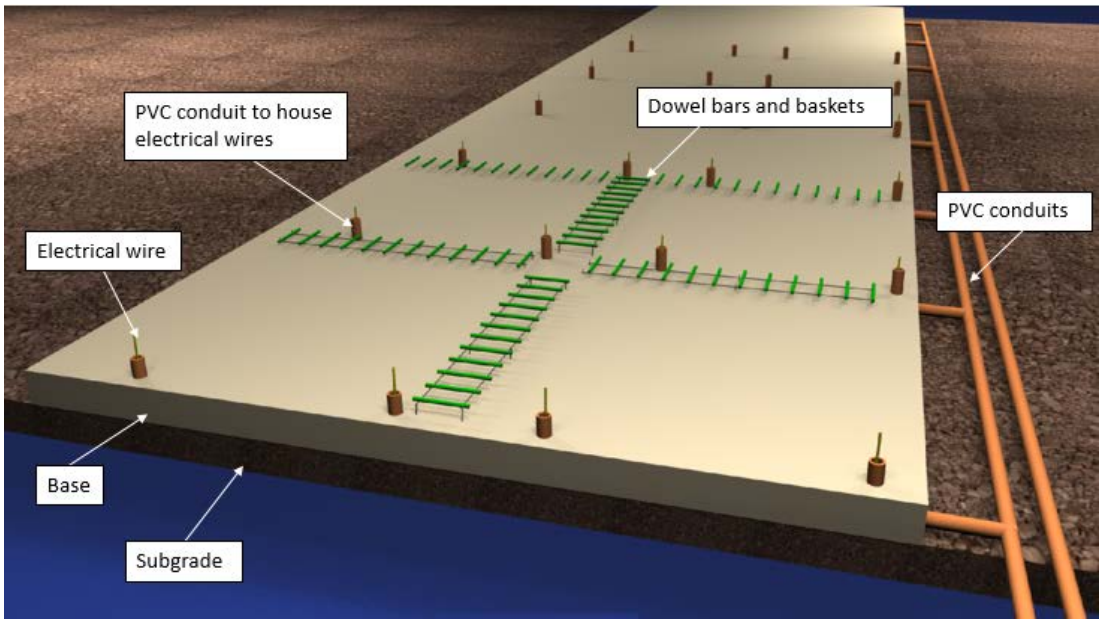

Figure 6-4 Prepare base and place dowel baskets and PVC conduits

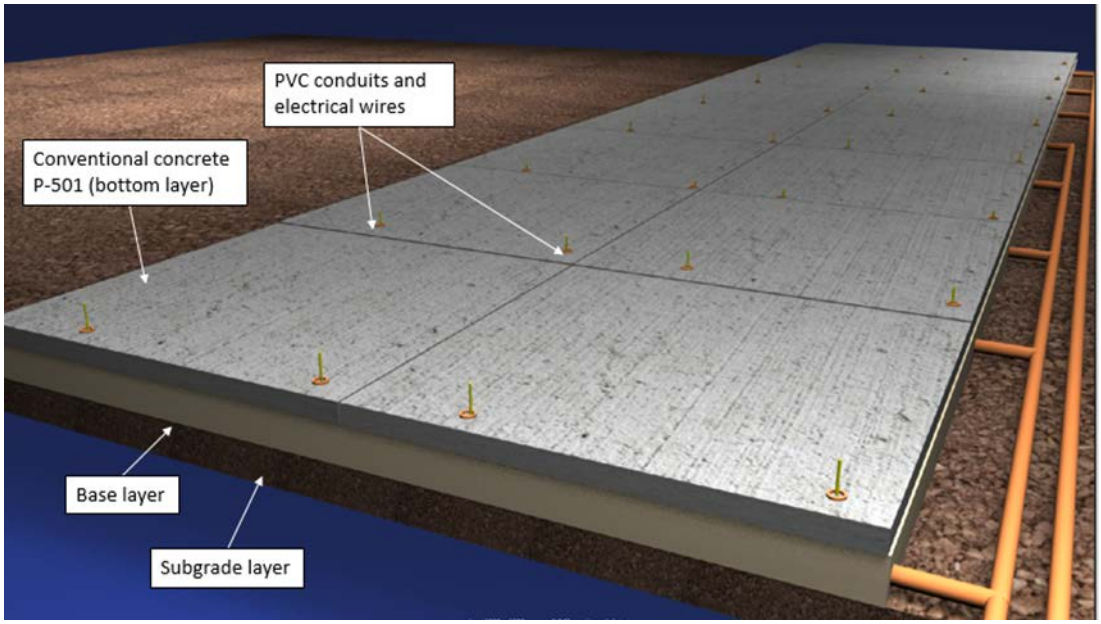

Figure 6-5 Place PCC layer

Step 3: Place Electrode System and Power Supply. After placing the PCC, electrodes should be placed and fixed using nylon rods, and electrical wire connections then made for the electrode system (See Figure 6-6). The recommended time for placing the electrodes on top of the PCC layer is when the PCC layer has gained sufficient strength to support them. Since this issue may pose challenges for a "wet-on-wet" process in 2LCP, it is recommended that only a "wet-on-dry" method be considered as the 2LCP method for ECON HPS construction. Note that a "wet-on-dry" choice implies that the first lift should have been cured for 24 hours prior to placing the next lift. This will require "wet" curing. A wax-based curing compound cannot be used because it could act as a bond breaker between the concrete lifts. Saw-cut joints will be needed in the slab to prevent shrinkage cracking, and the top layer should also be saw-cut at precisely the same locations as those in the bottom layer. A power supply system can be specified based on an energy density sufficient to heat the ECON surface enough to prevent ice and snow accumulation.

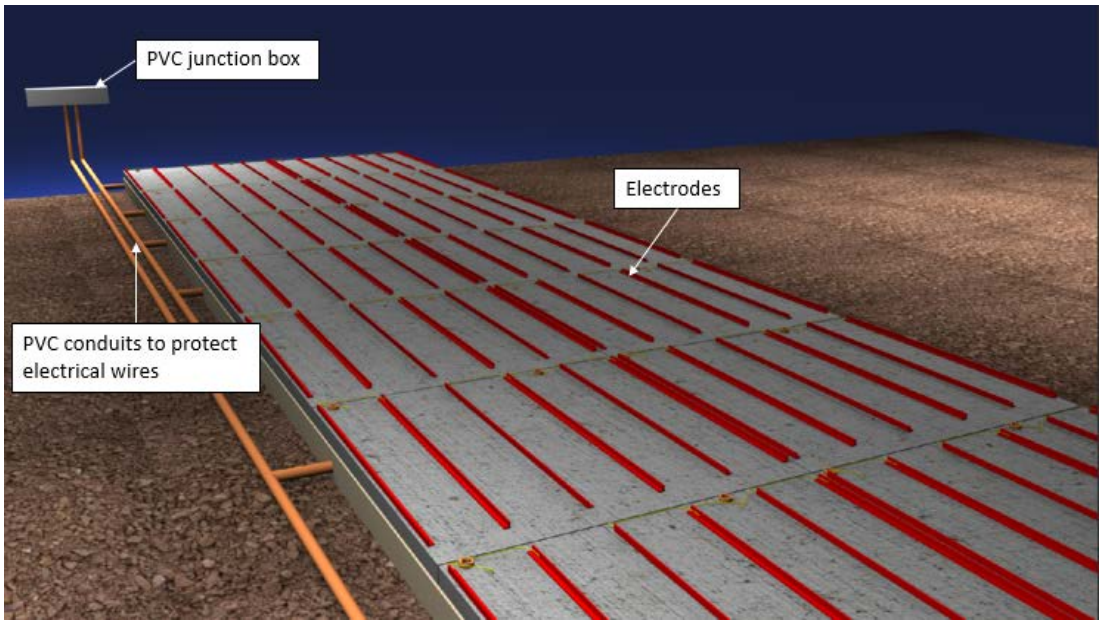

Figure 6-6 Place electrodes

Step 4: Place ECON Layer. The ECON layer can be placed as the top layer with the second paver forming the final pavement profile of the ECON HPS (See Figure 6-7). Prior to placing the ECON layer, electrodes should be cleaned using an air-blower, brooms, and a pressure washer to ensure sufficient bonding between electrodes and the ECON layer. Electrodes placement should not cause slipform paving clearance problems and should not interfere with the vibrators, auger, or pan. Electrodes should be located within 2-in of the ECON surface to provide clearance for slipform paving (See Figure 6-8a and Figure 6-8b). The vibrators are generally positioned no more than 4-in. below the finished pavement surface (Kohn et al., 2003). The vibrator spacing should be different from the electrode spacing to prevent damage or interference with the electrodes.

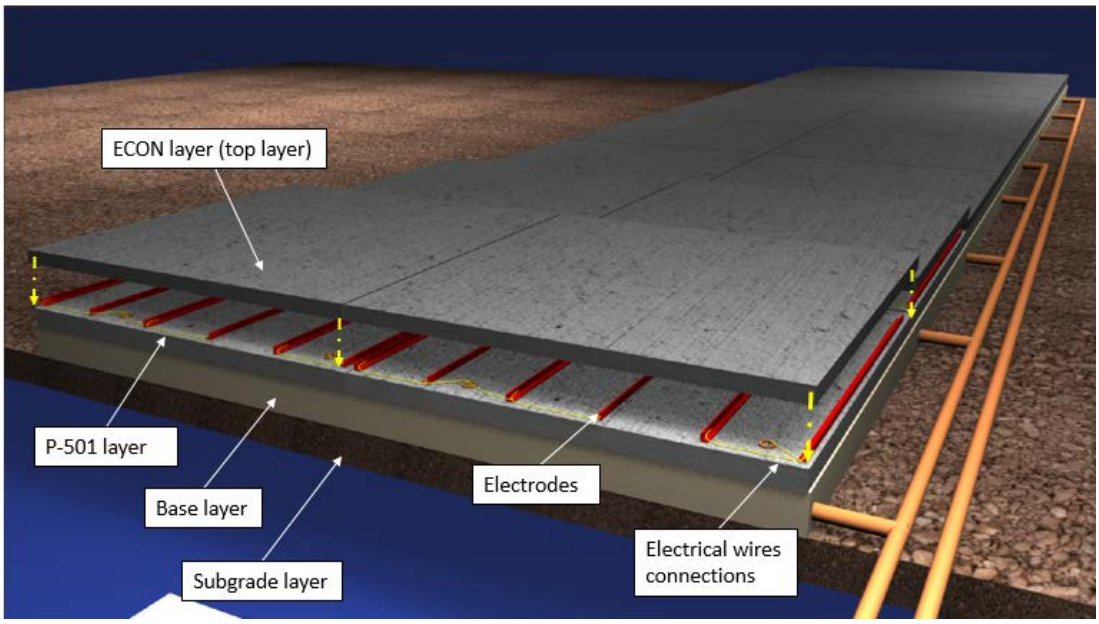

Figure 6-7 Place ECON layer

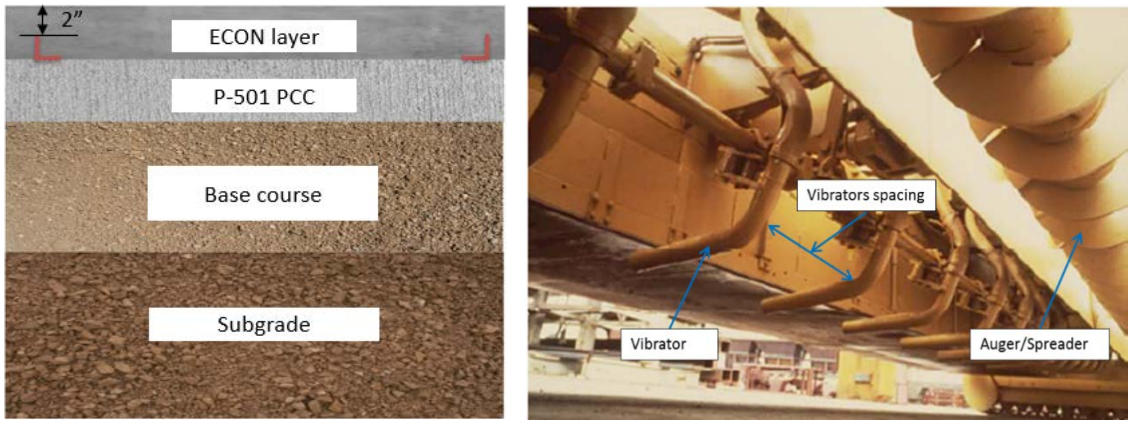

(a) **(b)**

Figure 6-8 Paving considerations: (a) ECON cross section and (b) Slip-form paver

6.7 ECON HPS Using Concrete Overlay

Figure 6-9 shows the construction steps required for constructing ECON HPS using concrete overlay. Concrete overlay systems can be classified into a bonded resurfacing family and an unbonded resurfacing family. The construction sequence of the ECON HPS using either type of concrete overlay system may be similar, except that for an unbonded concrete overlay a separate interlay should be placed on the existing concrete pavement to

mitigate the reflective cracking potential. The construction sequence of the ECON HPS using concrete overlay involves the following four major steps:

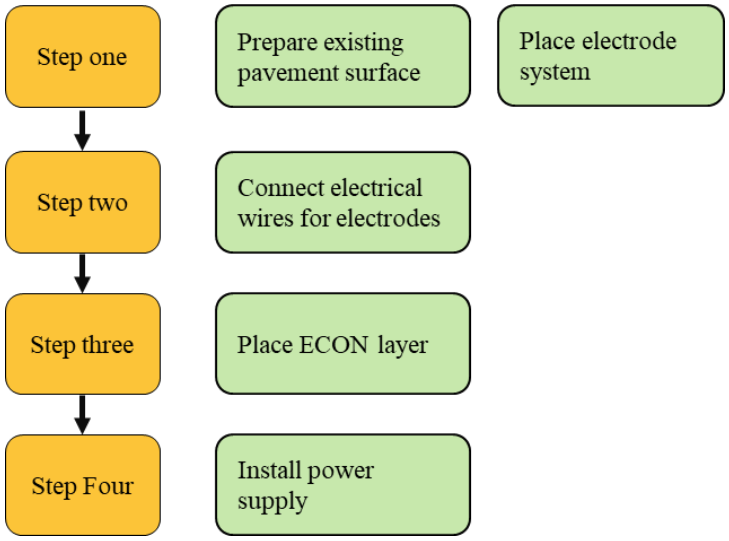

Figure 6-9 Work sequence of ECON HPS using concrete overlay

Step 1: Prepare Existing Pavements and Place the Electrodes System. Place and secure the electrodes on the existing concrete; wire connections can be made later (See Figure 6-10). Perforated stainless steel 316-L is recommended for electrode materials because of its high corrosion resistance. The existing surface may require pre-resurfacing repairs to meet the required elevation. Threaded nylon rods and nuts can be used to fix electrode positions on the conventional concrete surface to prevent electrode movement during pouring of the ECON layer, as shown in Figure 6-10a and Figure 6-10b. Nylon materials are used to avoid corrosion and electrical current leakage to the ground as well as to prevent interaction with the electrical field. The electrodes can be anchored on the existing pavement using a drilling machine to drill holes to fix the electrode positions (See Figure 6-10c and 6-10d).

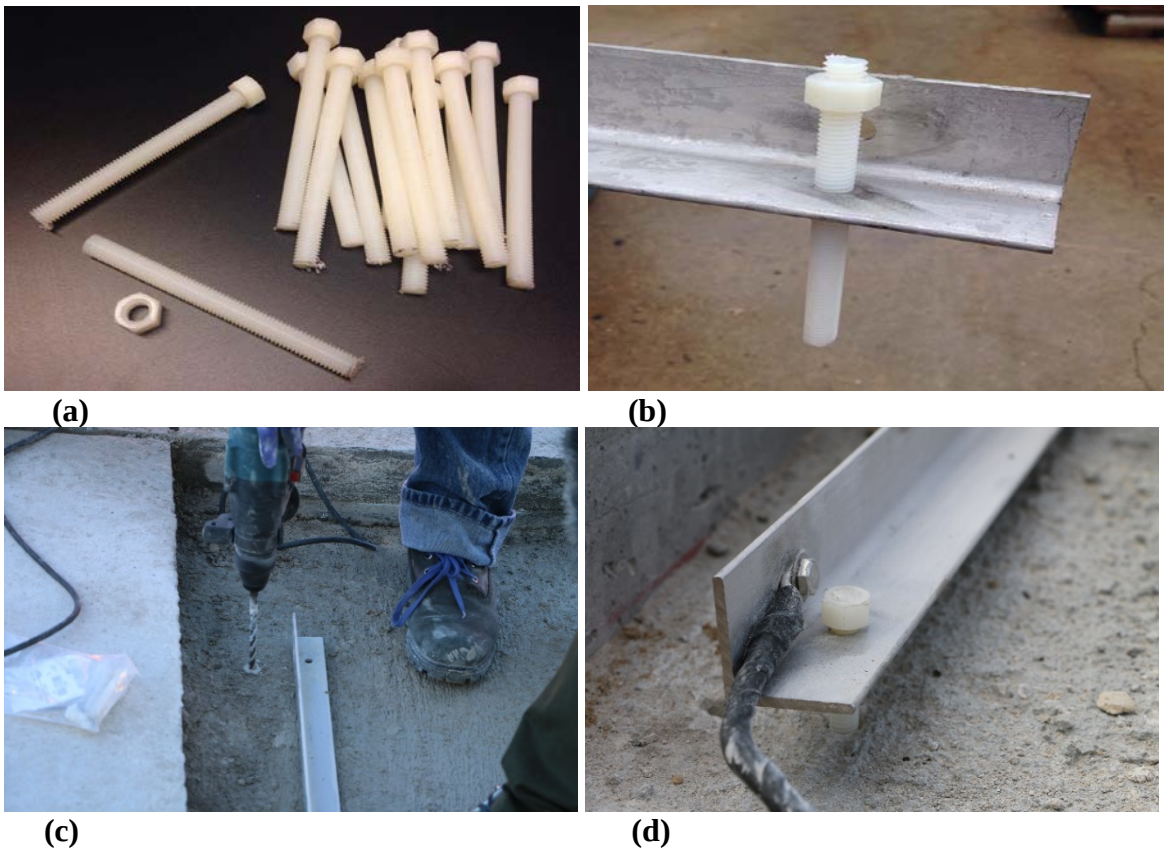

Figure 6-10 Fixing electrodes on existing pavement: (a) nylon rods and nuts, (b) electrode with nylon rod, (c) drill hole to fix electrode, and (d) placement of electrode

Figure 6-11 shows the electrode installation layout on an existing pavement. Electrodes should be placed within each individual slab so that they will not cross the pavement joints, and installing the electrodes at the designed spacing ensures the performance of the ECON HPS and the required energy density. A minimum of 2 in. clearance above the top of the electrodes is recommended to prevent any cracking along the electrode lengths.

To speed up the installation of electrodes on existing pavement, electrodes for a given slab can be assembled together (See Figure 6-12) and then placed and secured using nylon threaded rods and nuts. The fiberglass rebar is intended to support and assemble the electrodes so that all electrodes can be simultaneously placed and then secured. Fiberglass

rebar for assembling and supporting the multiple-electrode assemblies can be placed across pre-drilled holes in the electrodes. Electrodes connected with fiberglass rebar may be pre-assembled and shipped to the project site to expedite construction procedures.

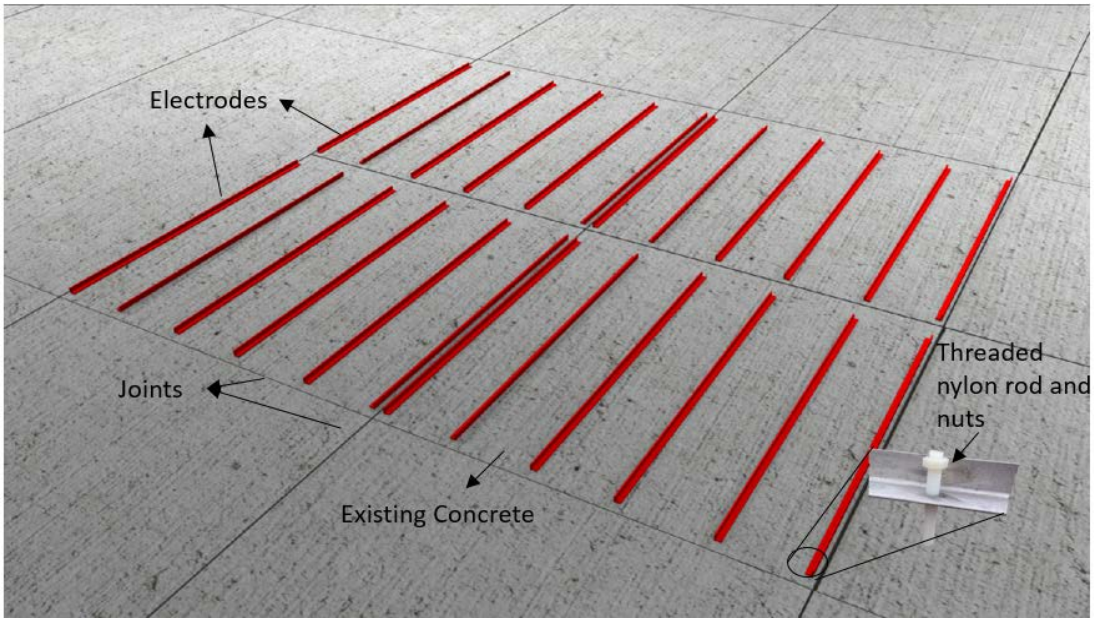

Figure 6-11 Electrodes installation on existing pavement

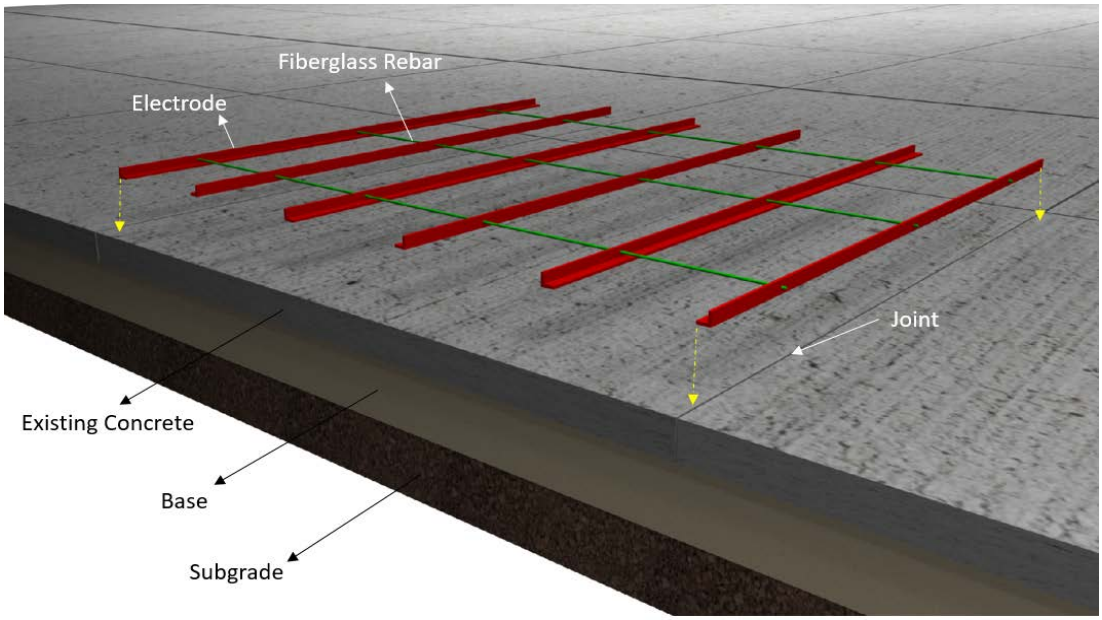

Figure 6-12 Electrodes assembly installation on existing pavement

Step 2: Connect Electrical Wires for Electrodes Systems. Electrical wires may be placed either right on the existing concrete surface or by forming a trench in which to place the wires (See Figure 6-13). These wires should pass under the joints to protect them (See Figure 6-14) from damage because of concrete expansion or contraction at the saw-cut joints of the ECON layer.

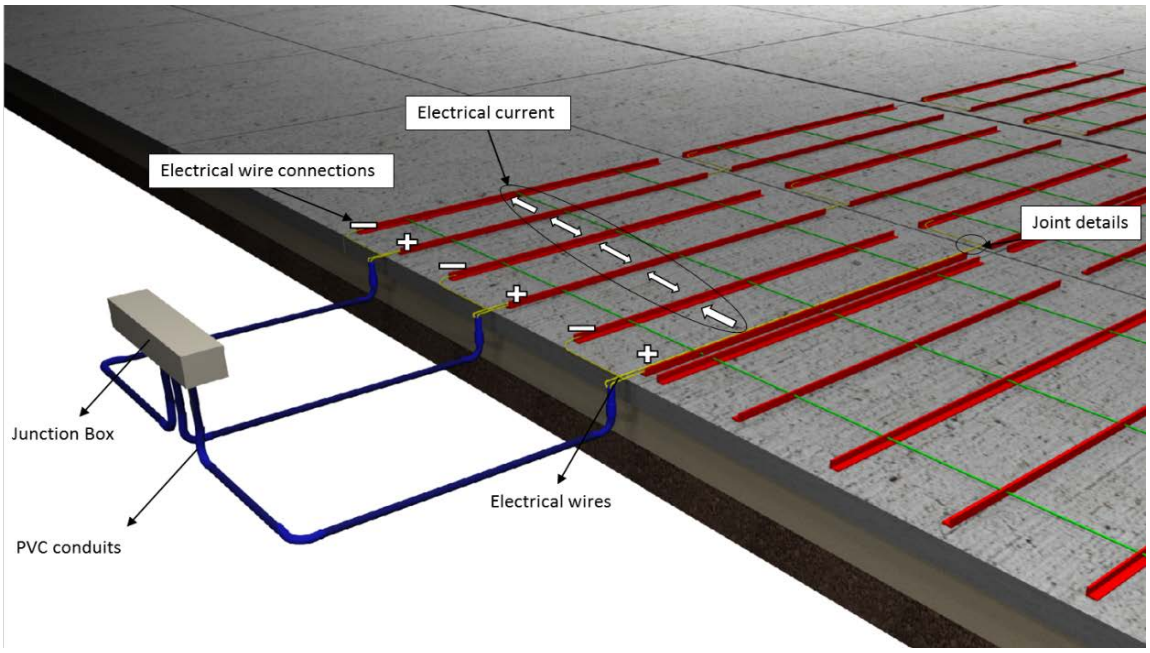

Figure 6-13 Electrical wire connections for the electrode system

Step 3: Place the ECON Layer. The ECON layer can be placed after placing, securing electrodes, and connecting the electrode wires. Concrete overlays are constructed using conventional equipment and procedures (Harrington and Fick 2014). Figure 6-15 shows the recommended placement of concrete overlay for large areas such as parking (Harrington and Riley 2012) that could be similarly applied for airfield concrete pavement. These types of placements are known as block placement (See Figure 6-15a) and strip placement (See Figure 6-15b).

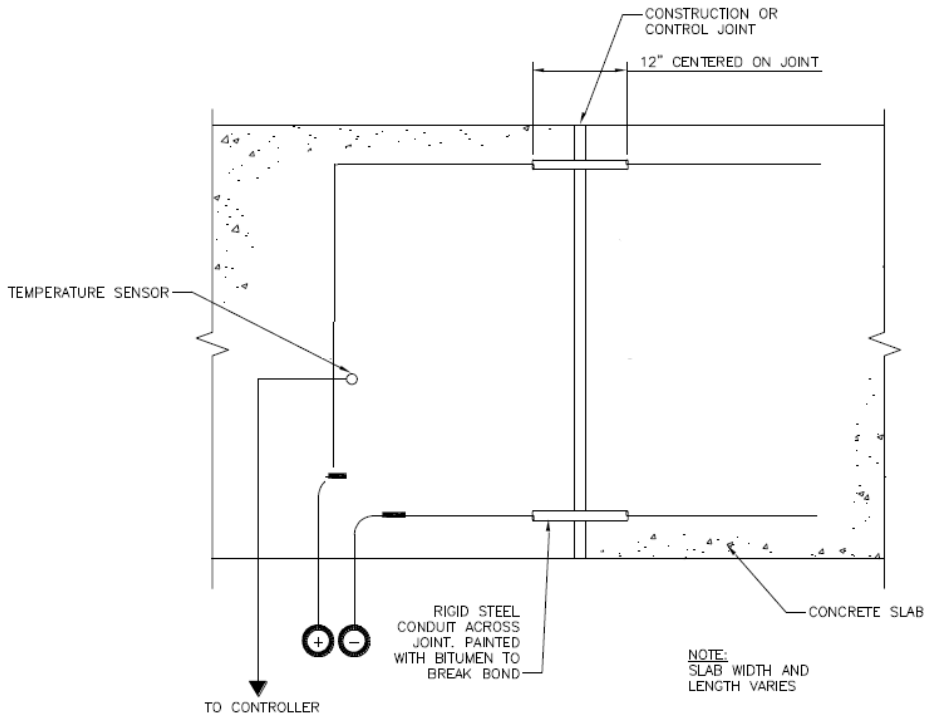

Figure 6-14 Electrical wire details at joints (ASHRAE 2015)

Block placement may be used to expedite the paving procedure and to reduce the formwork for large areas. Laser screeds are one of the options to be used for block placement. This method, a common practice for parking lots, may also be used in airfield pavements since they also have large areas. Strip placement, in comparison to block placement, is considered a very highly-productive paving method in which a slipform paver can be used for the strip placement at pre-designed widths.

Consideration and Recommendation Before Placing the ECON Layer:

- Electrodes should be located 2 in. below the ECON surface to provide clearance for slipform paving (See Figure 6-8a)
    - Electrodes should not interfere with the vibrators and auger (See Figure 6-8b)

- Electrodes should be cleaned prior to placing the ECON layer using an air-blower, brooms, and a pressure washer to ensure sufficient bond between electrodes and the ECON layer
- Ensure that the electrode elevations are equal
- Electrodes should be placed and fixed to prevent any electrode movement while placing the ECON layer
- Electrode system connections should be tested to ensure that the power supply is properly providing power to the ECON HPS
- Visual inspection of electrode system connections is also recommended

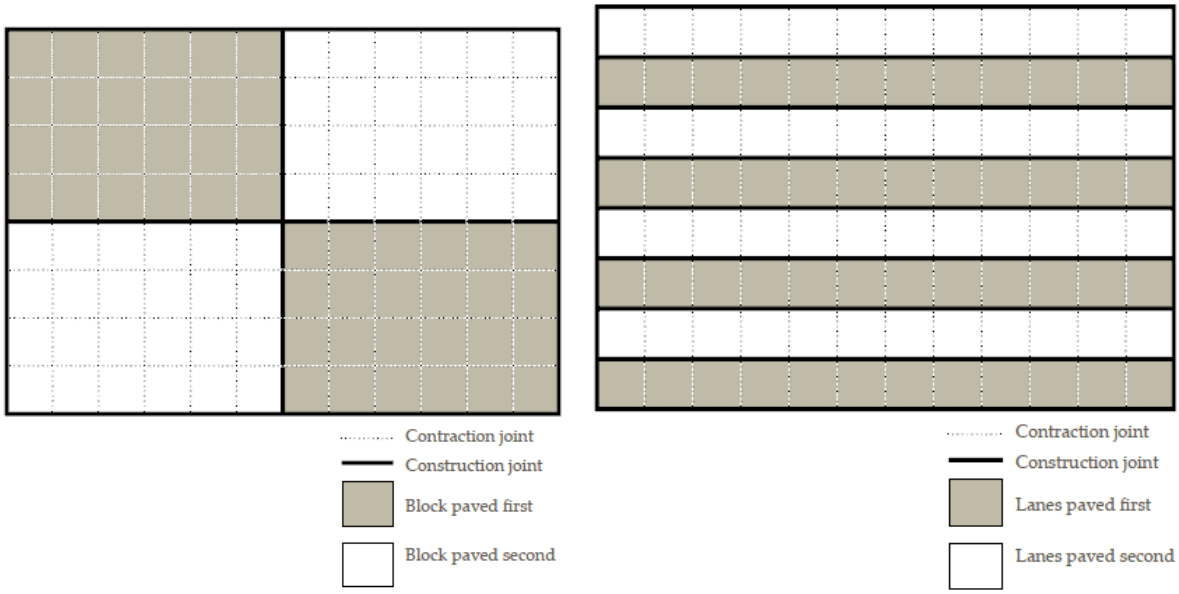

(a) Block placement (b) Strip placement

Figure 6-15 Placement of the ECON layer: (a) block placement and (b) strip placement (Harrington and Riley 2012)

An ECON layer may be placed as either a bonded or an unbonded layer depending on existing pavement conditions. The main difference between unbonded and bonded overlays is an HMA layer or Geotextile fiber placed on the existing layer to break the bond between two layers

Figure 6-16 shows the cross-section of the ECON slab using a bonded overlay. For highway applications, bonded concrete overlays (top layer) are generally 2-5 in. thick (Harrington and Fick 2014) with recommended joint spacing of the bonded concrete overlay in the range of 3-8 ft. to reduce curling and warping stresses (Harrington and Fick 2014). For airfield applications, the thickness of bonded concrete overlays and joint spacing should be designed according to FAA AC150/5320-6F (FAA 2016).

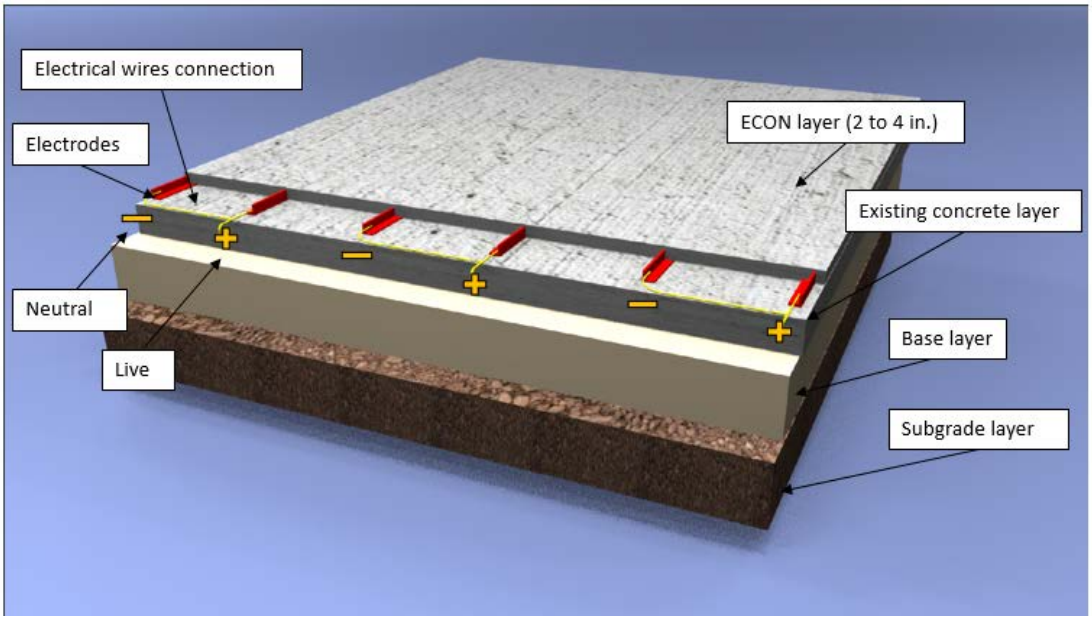

Figure 6-16 ECON layer for bonded concrete overlay

Figure 6-17 shows the cross section of an ECON slab utilizing unbonded overlay techniques. For highway applications, an unbonded concrete overlay is generally between 4 and 11 in. thick and the typical recommended joint spacing is between 6 and 15ft., depending on the thickness of the overlay (Harrington and Fick 2014). For airfield applications, the minimum thickness of unbonded concrete overlay is 6 in. thick (FAA 2016). If the unbonded overly thickness is greater than 4 in., the top layer may be divided into two layers; the top layer is the ECON layer and the bottom layer is regular concrete, as can be seen in Figure 6-17.

The recommended ECON layer (top layer) thickness is in the range of 2 to 4 in. The electrode number and spacing can be designed according to the energy density required to meet the required heating performance, i.e., it should be capable of maintaining the temperature of the ECON surface above the freezing point. The electrodes are installed and fixed on a prepared surface, and the ECON layer (top layer) can be placed on any existing surface such as concrete, asphalt, or composite.

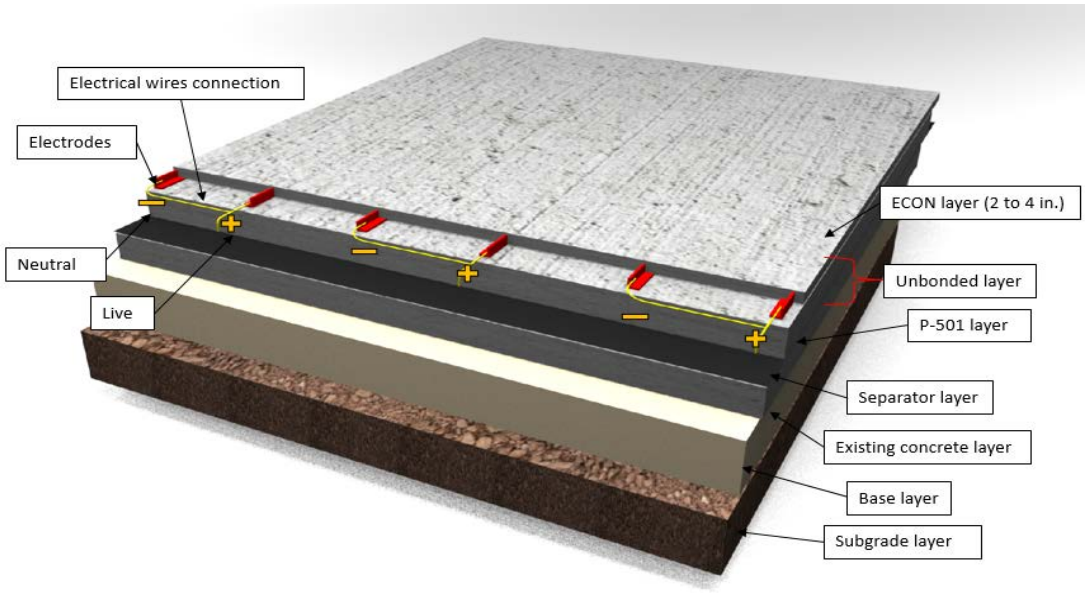

Figure 6-17 ECON layer for unbonded concrete overlay

Step 4: Install Power Supply and Control System. The power supply and the control system should be placed near the PVC junction box where both electrical and sensor wires can go through a junction box and then connect to the power supply and the control system (See Figure 6-18). The control system is comprised of a data acquisition unit for collecting temperature sensors, a laptop, and operator interface units. The control system is designed to turn the system on/off either manually or automatically based on programing for temperature values provided. The power supply is comprised of contactors, circuit breakers, and electrical sensors. The contactors can remotely receive a signal for turning the system on or off based

on temperature sensor readings. The circuit breaker is designed to monitor the electrical current usage and to not allow drawing more than the designed value. The circuit breaker will turn the system off if current values exceed the designed values.

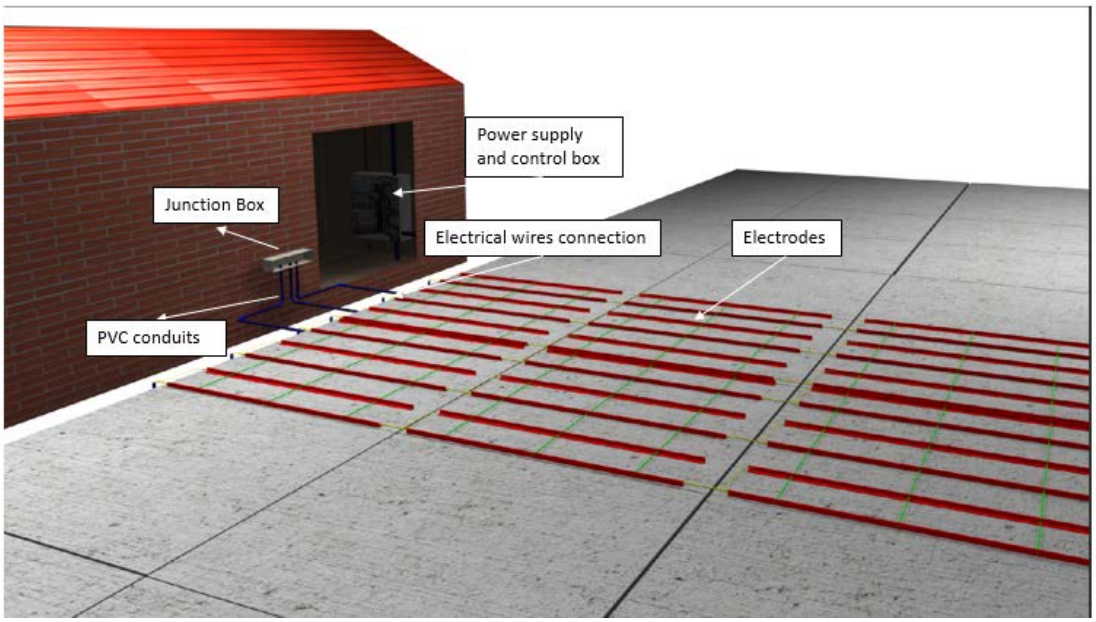

Figure 6-18 ECON HPS using concrete overlay

6.8 ECON HPS Using PC

The work sequence required for constructing ECON HPS using PC is presented in Figure 6-19. The major difference between the construction of ECON HPS using PC and that of a typical PC installation is that ECON HPS using PC requires electrodes embedded in the ECON layer to allow current to pass through the ECON layer and thereby release heat that warms the paved surfaces and melts ice and snow. The construction sequence for ECON HPS using PC involves the following four major steps:

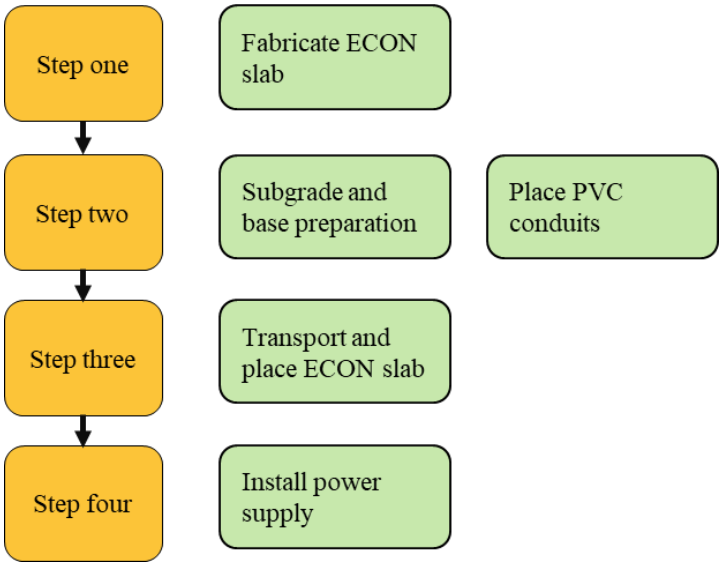

Figure 6-19 Work sequence of ECON HPS using PC

Step1: Fabricate ECON Slab off-site. The ECON slab can be fabricated using off-site construction as shown in Figure 6-20a and 6-20b. The total thickness of the ECON slab can be divided into two layers; the top layer is the ECON layer and the bottom layer is the PCC layer. The PCC layer can be placed after positioning dowel bars and providing slots for load transfer to adjacent slabs. Electrodes should be anchored to the bottom layer using nylon anchor rods. The precast ECON slabs can be cured and tested before their transfer to a construction site. Each ECON slab contains two electrodes located at its edges to provide electrical connectability. The number of electrodes and their spacing can be determined and designed to provide sufficient heat generation to prevent snow and ice accumulation based on the required energy density for each specific project site. Finally, to enhance the bond between the two layers, the ECON layer can be placed after anchoring and securing the electrodes while the bottom layer is still wet. The ECON layer is generally 2 to 4 in. in thickness to reduce ECON slab construction costs and to primarily heat only the top ECON surface.

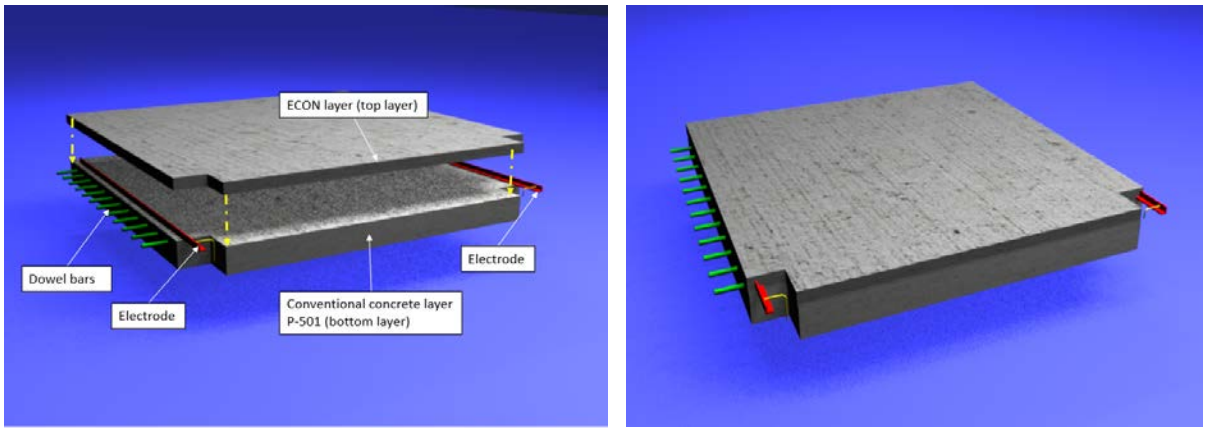

(a) (b)

Figure 6-20 3D Visualization of ECON heated slab fabrication using PC

Step2: Prepare the Base Layer and Install PVC Conduits. Prepare and compact the subgrade and base layers to meet the required density, and install PVC conduits and junction box to accommodate the electrical wires for the electrode system (See Figure 6-21). The installation of PVC conduits can be accomplished after preparing the base layer. Trenching should be provided for installation of PVC conduits whose positions should align with electrodes so that wires can be connected to the electrodes for providing electrical energy. An alternative option for installing the PVC would be that the PVC could be placed at the bottom of the base layer while sitting on top of the subgrade layer; this option is used for in-pavement lighting conduit.

Step 3: Place the ECON Slabs. Transfer the precast ECON slabs into the construction site and place them on the prepared base layers (See Figure 6-22a). The ECON slab has dowel bars and slots like those in a traditional precast panel to transfer mechanical loads. The ECON slab includes two electrodes embedded in ECON layer to provide connections to electrical wires after placing the ECON slab, and the exposed electrodes at the edges (See Figure 6-22b) of the ECON slabs should be placed above the PVC conduits so that such

electrical connections can be made. The wires should not cross the joints because of potential damage to them.

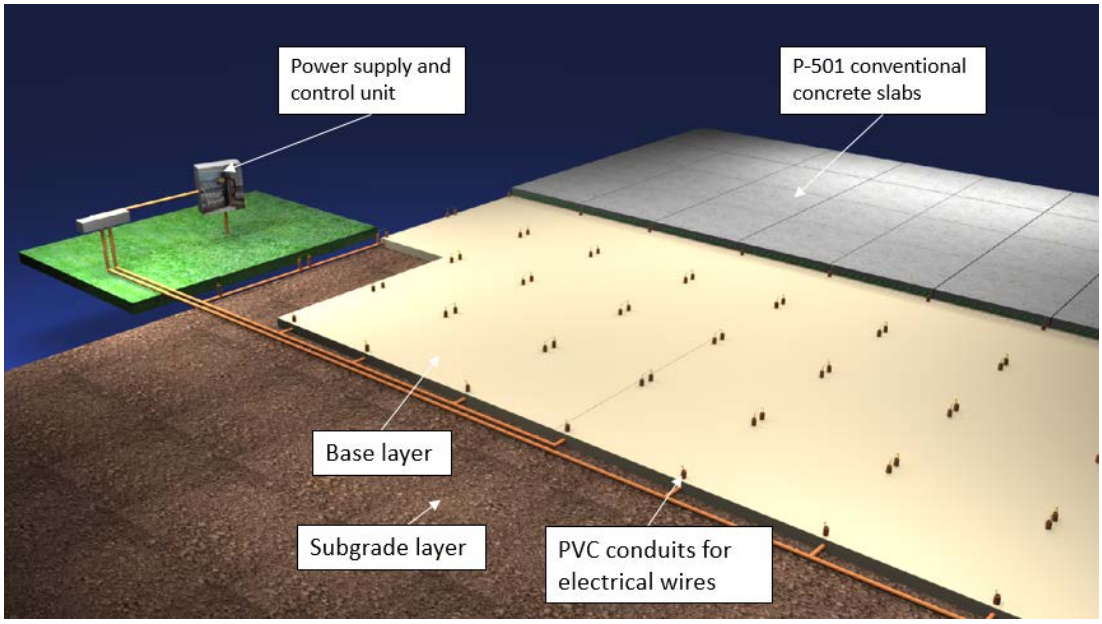

Figure 6-21 Preparing the base layer and installing PVC conduits and junction box

Step 4: Install Power Supply. Install the power supply and the control unit. The power supply system can be specified based on the designed energy density sufficient to heat the ECON surface to prevent ice and snow accumulation. The ECON system can be operated under from a 120V or 240V power source based on the designed electrode spacing and ECON material properties such as electrical resistivity. All electrical wires should be connected to the electrode system and tested before filling voids above the exposed electrodes (See Figure 6-22c), after which the voids can be filled with conductive patching concrete. The voids of the dowel slots may be filled with grout as in traditional precast panels. The grout can be pumped through a dowel grout port and a bedding grout port (Chang et al. 2004).

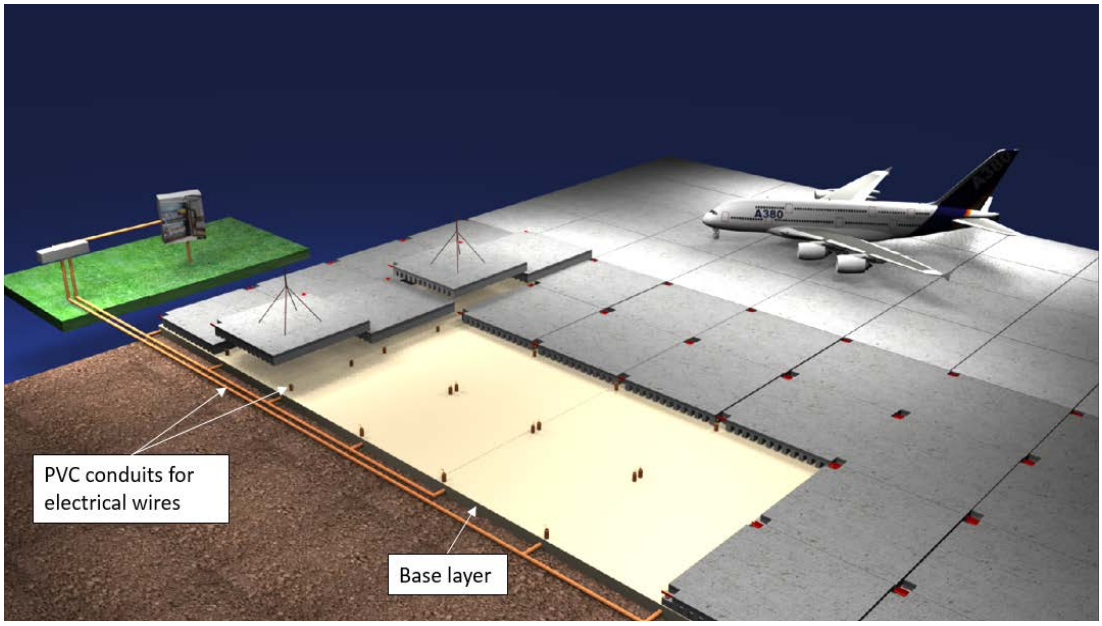
PVC conduits for electrical wires
Base layer

(a)

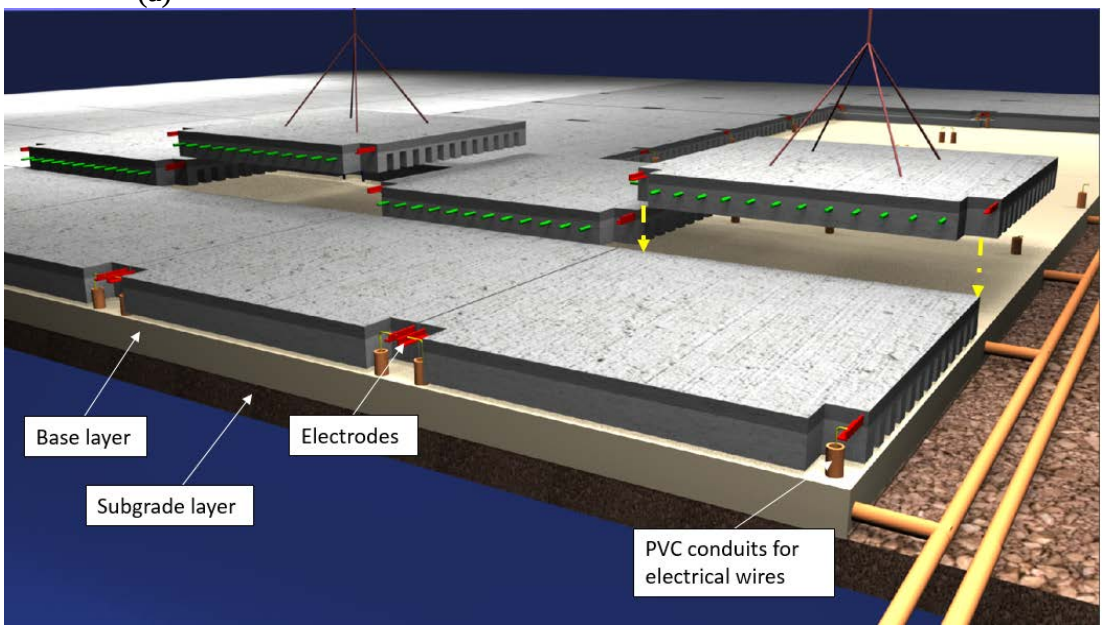
Base layer
Subgrade layer
Electrodes
PVC conduits for electrical wires

(b)

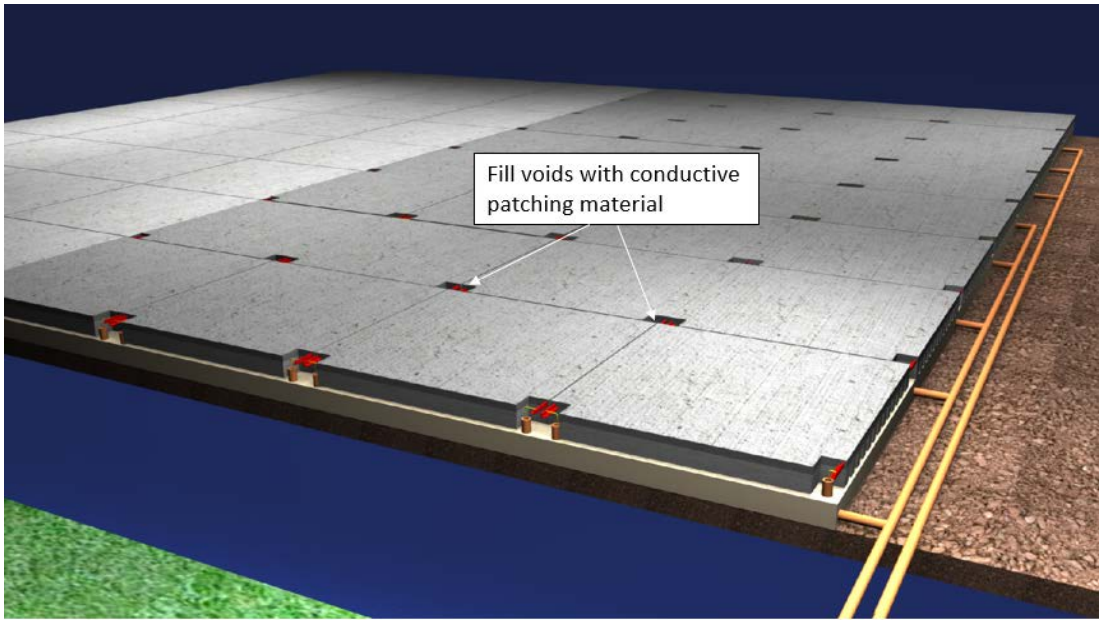

(c)

Figure 6-22 ECON construction sequence using PC: (a) place ECON slab, (b) connect electrical wires to the electrode systems, (c) fill voids with conductive patching materials

6.9 HHPS Using 2LCP

Figure 6-23 depicts the construction steps required for constructing a HHPS using 2LCP. The major difference between the construction of a HHPS using 2LCP and one with typical 2LCP is that the HHPS using 2LCP involves the placement of embedded pipes into the PCC pavement through which hot fluids are circulated and thereby release heat to warm the paved surfaces and melt ice and snow. The construction sequence for a HHPS using 2LCP involves the following three major steps.

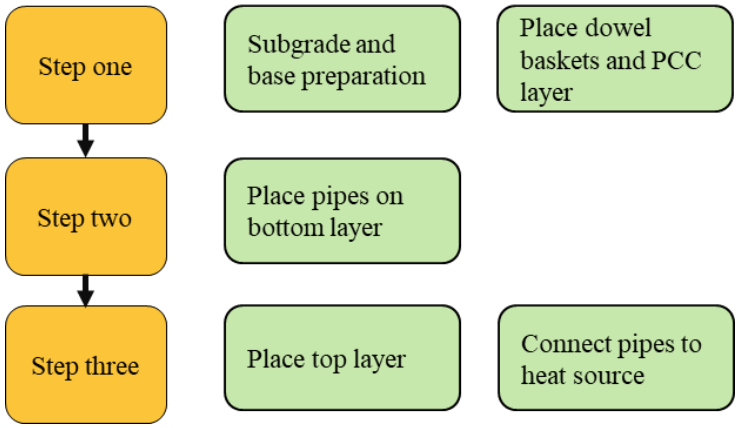

Figure 6-23 Work sequence of HHPS using 2LCP

Step 1: Prepare the Base Layer, Install Dowel Baskets, and Place the PCC layer. This step involves several tasks, including preparing and compacting the base layer, then installing dowel baskets, and finally placing PCC layer (bottom layer) on the prepared bases (See Figure 6-24). Instead of using a two-lift paving approach, the pipes could be placed on the prepared base layer before concrete paving if the designed pavement thickness is not too thick (i.e., less than 11 in. thick). In such a case, a wire mesh and plastic chairs could be utilized for positioning the pipes on the prepared base layer to prevent movement while pouring the concrete.

Step 2: Place Pipes on PCC layer (Bottom Layer). Define the pipe pattern and spacing and the location of the manifold. Pipe could be placed on top of the P-501 (bottom layer) and anchored using clip (Figure 6-25a). The pipe pattern and spacing are based on the energy density required for melting ice and snow at the specific project site. To prevent them from being damaged, the pipes should not interfere with the saw-cuts at the joints. The joint options recommended for protecting the pipes across the joints are presented in Figure 6-25b (FAA 2011 and ASHRAE 2015). The pipes should be inspected using air testing to identify any cracks or leakages before pouring the concrete.

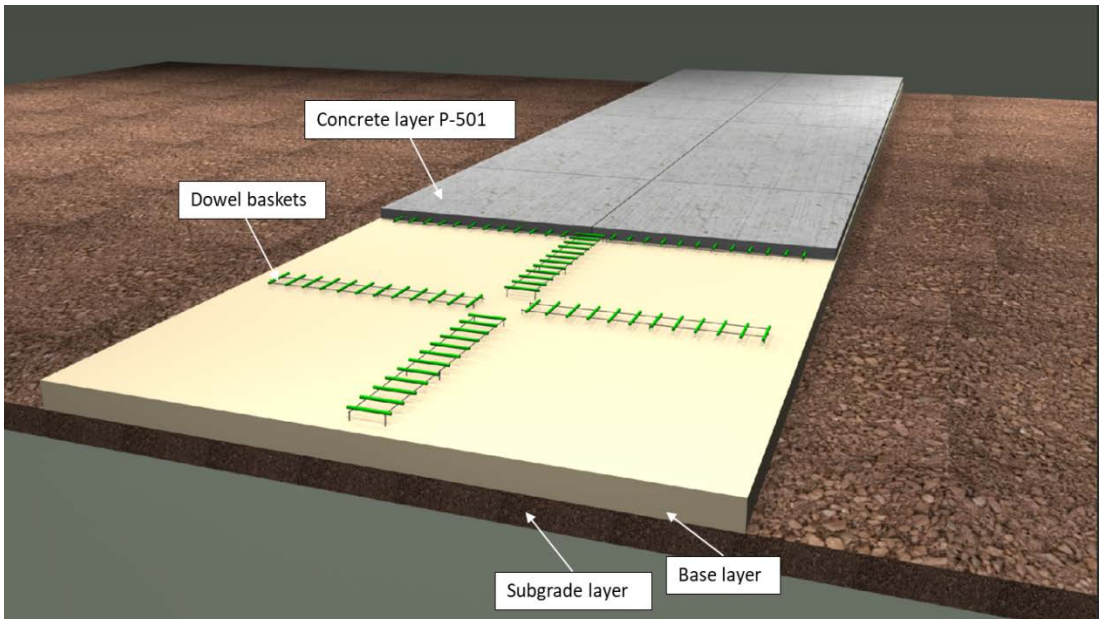

Figure 6-24 the base layer preparation for HHPS

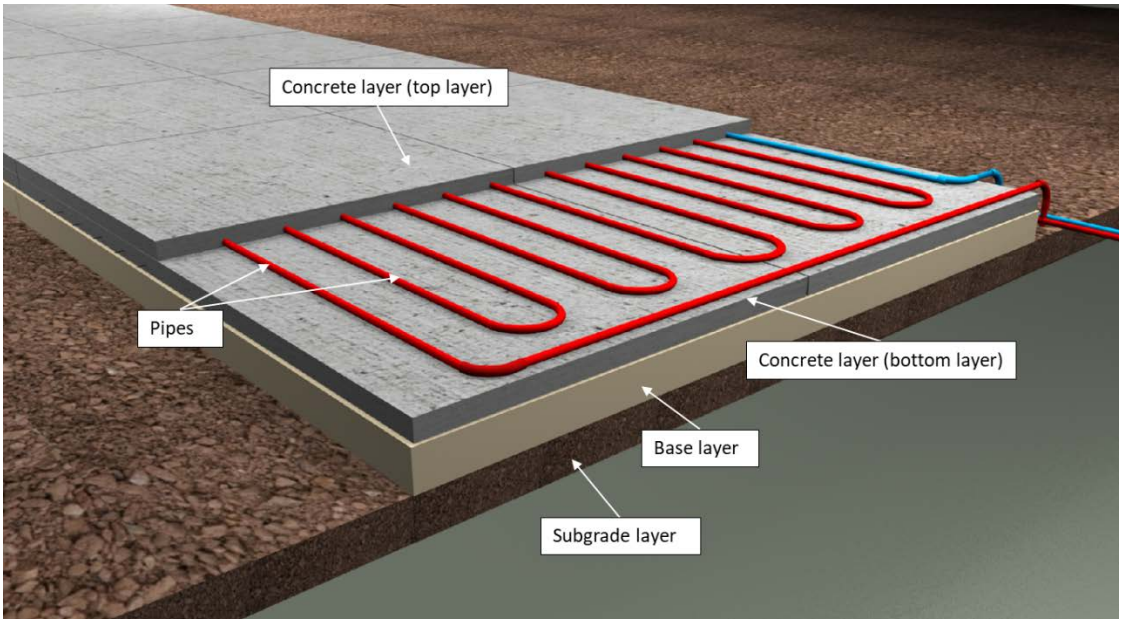

(a)

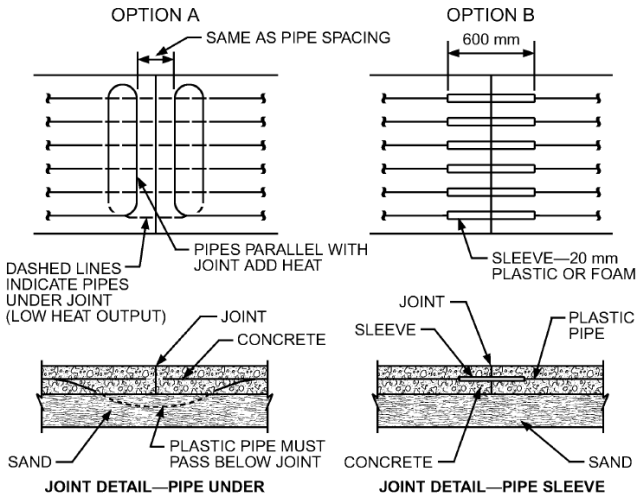

(b)

Figure 6-25 HHPS using 2LCP: (a) place pipes and top layer (concrete layer) and (b) pipe details for concrete construction (ASHRAE 2015)

Step 3: Place PCC Layer (Top Layer). Place the PCC layer and connect pipes to a heat source. The PCC can be placed after ensuring that the pipes will not cause slipform paving clearance problems. Pipes should be located 2 in. below the concrete surface to provide appropriate clearance for a slipform paver's vibrators and auger (See Figure 6-26a and 6-26b). The fluid circulated in the closed-loop pipe can be heated using geothermal energy, as shown in Figure 6-27. A geothermal energy system costing1.6 million dollars was installed at the greater Binghamton airport to heat an area of 260 m^2 (Ziegler 2013), and while this seems quite expensive, the resulting reduction in operational costs of using geothermal energy makes such a system cost-effective.

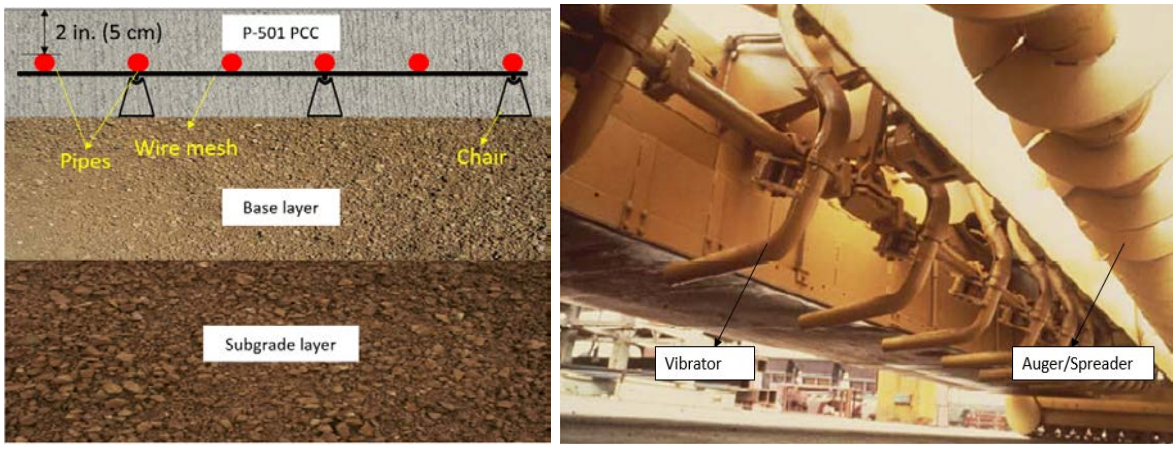

(a) (b)

Figure 6-26 Paving considerations: (a) cross section of HHPS and (b) slipform paver

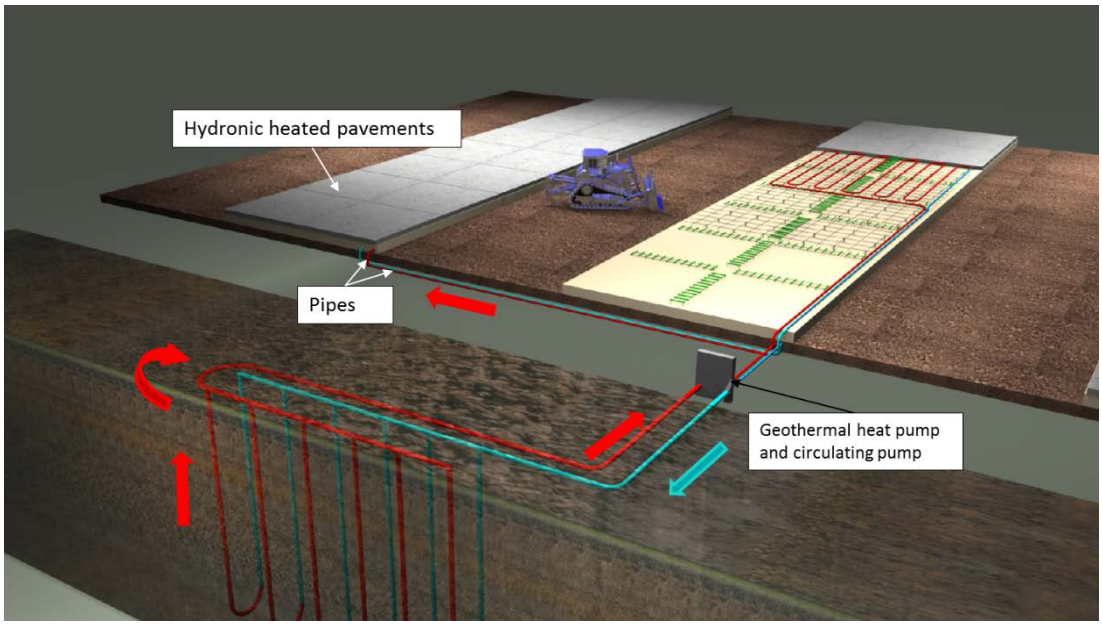

Figure 6-27 HHPS using 2LCP with geothermal wells as heat source

6.10 HHPS Using Concrete Overlays

The construction sequence of HHPS using concrete overlay shown in Figure 6-28 involves the following two major steps:

Step 1: Prepare Existing Pavements and Place Pipes. Prepare the existing pavement, place pipes on existing pavement, and identify manifold locations. The preparation for existing

pavement depends on its condition, and if necessary the existing surface may be milled to meet the required elevation.

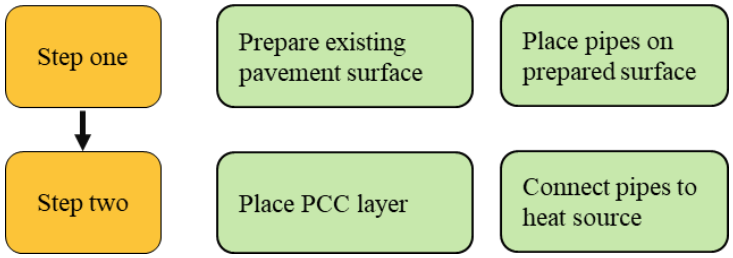

Figure 6-28 Work sequence of HHPS using concrete overlay

Pipes are installed on existing pavement and either anchored using clips or tied to wire mesh to prevent their movement while pouring concrete (See Figure 6-29). Choice of pipe pattern and spacing, size, and lengths are based on the required energy density for the specific project location. To prevent damaging them, the pipes should not interfere with the saw-cuts at the joints. The recommended joint options for passing the pipes through the joints are shown in Figure 6-25b (ASHRAE 2015). The number of manifolds required depends on the project size and total length of pipe. Insulation layers such as extruded polystyrene (XPS) boards can be placed on the existing pavement before placing pipes to reduce the heat loss. The pipes should be air-tested for cracks or leakage before placing the concrete.

Step 2: Place PCC Layer. Place the concrete layer and connect pipes to the heat source. Concrete can be placed after ensuring that the pipes will not cause slipform paving-clearance problems. Pipes should be located at least 2 in (5 cm) below the concrete surface to provide clearance for slipform paver vibrators and augers (See Figure 6-26a and 6-26b). After identifying and connecting the manifolds to the pipes, the manifold should be connected to the heat source. The fluid circulated in the closed-loop pipes can be heated using geothermal energy as shown in Figure 6-30, and can be operated automatically using the control system to turn the system on/off based on a set temperature value and readings from embedded

temperature sensors in the concrete. To provide satisfactory operation the hydronic-heated system should be warmed up for some time before snow and ice have accumulated on the pavement surface (ASHRAE 2015).

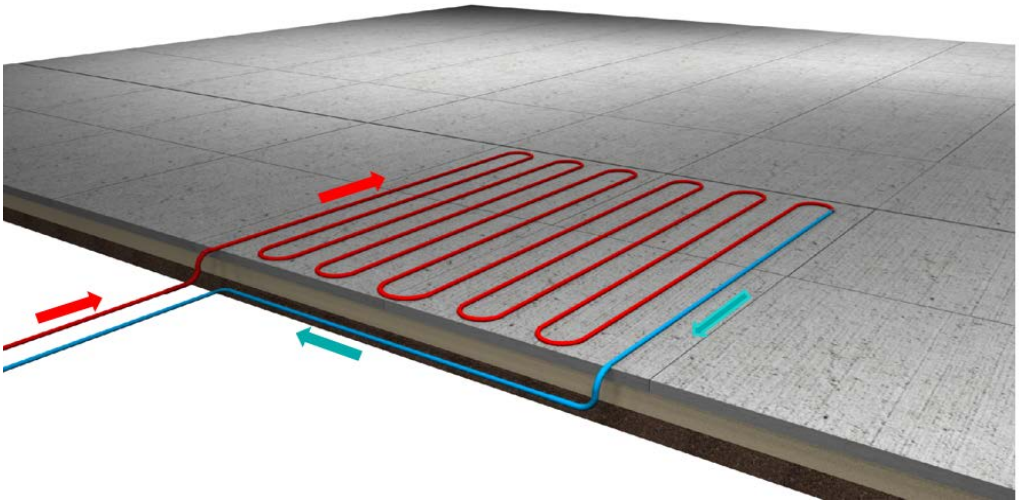

Figure 6-29 HHPS using concrete overlay

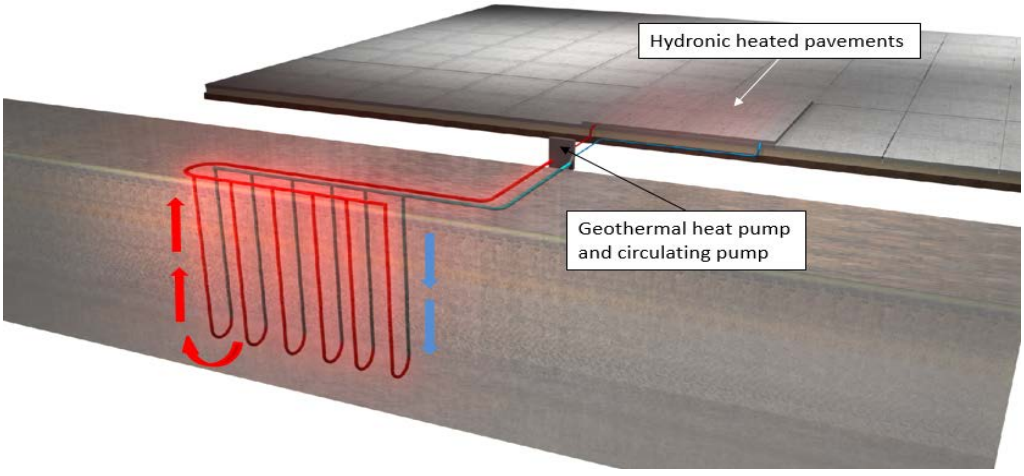

Figure 6-30 HHPS using concrete overlays with geothermal wells as heat source

HHPS can be installed using either bonded or unbonded concrete overlay techniques, and cross-sections of HHPS using bonded and unbonded concrete overlays are shown in

Figure 6-31a and Figure 6-31b. In HHPS using bonded concrete overlay techniques, pipes are installed and anchored using wire ties on a prepared existing surface (See Figure 6-31a). In HHPS using unbonded concrete overlay techniques, pipes are placed and anchored on separator layers if the top layer thickness is small (See Figure 6-31b).

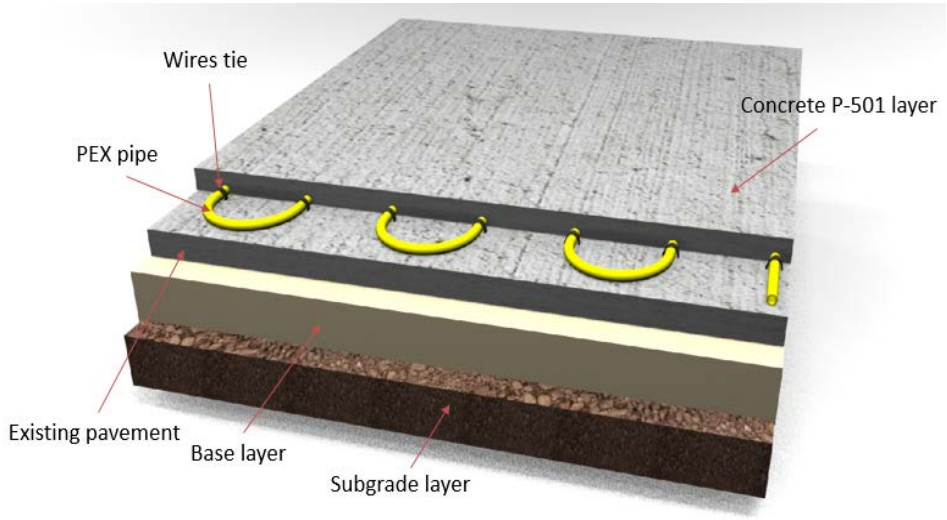

(a)

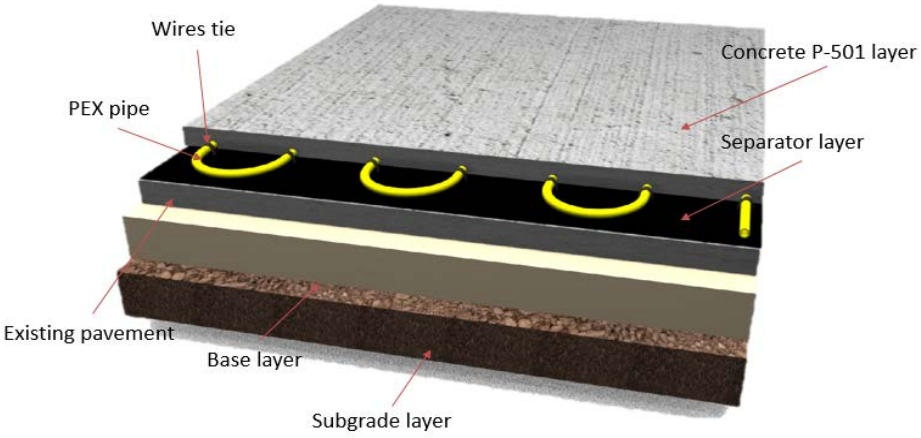

(b)

Figure 6-31 HHPS cross section (a) using bonded concrete overlay, (b) using unbonded concrete overlay

6.11 HHPS Using PC

Figure 6-32 depicts the construction steps required for constructing a HHPS using PC. The major difference between the construction of HHPS using PC and typical PC installation is that a HHPS using PC requires installation allowing hot fluids to run through the pipes and thereby release heat to warm paved surfaces and melt ice and snow. The construction sequence for a HHPS using PC involves the following three major steps:

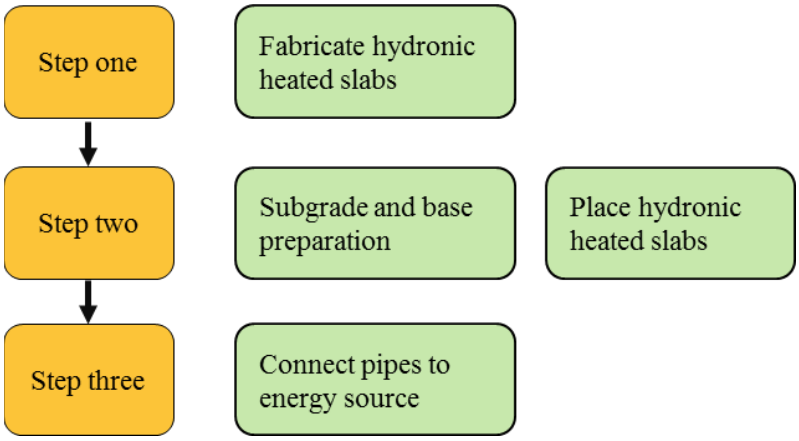

Figure 6-32 Work sequence of HHPS using PC

Step1: Fabricate Hydronic Heated Slab Off-Site. A hydronic heated slab can be fabricated off-site using PC (Figure 6-33) with formwork designed to facilitate placement of the pipes, the wire mesh, the dowel bars, and the slots (Figure 6-33a and Figure 6-33b). The formwork has open areas to permit inlet and outlet pipes to be connected to other hydronic slabs. The pipe is placed on top of wire mesh to elevate it closer to the surface and hold it there while the concrete is poured. A minimum of 2 in. of concrete cover extending above the top of the pipe is typically required (ASHRAE 2015). The pipe pattern can be designed for a particular job site to provide sufficient heat for melting ice and snow. After securing the pipe, concrete is poured into the formwork and is then screeded and cured before transferring the completed structure to a construction site (Figure 6-33c and Figure 6-33d).

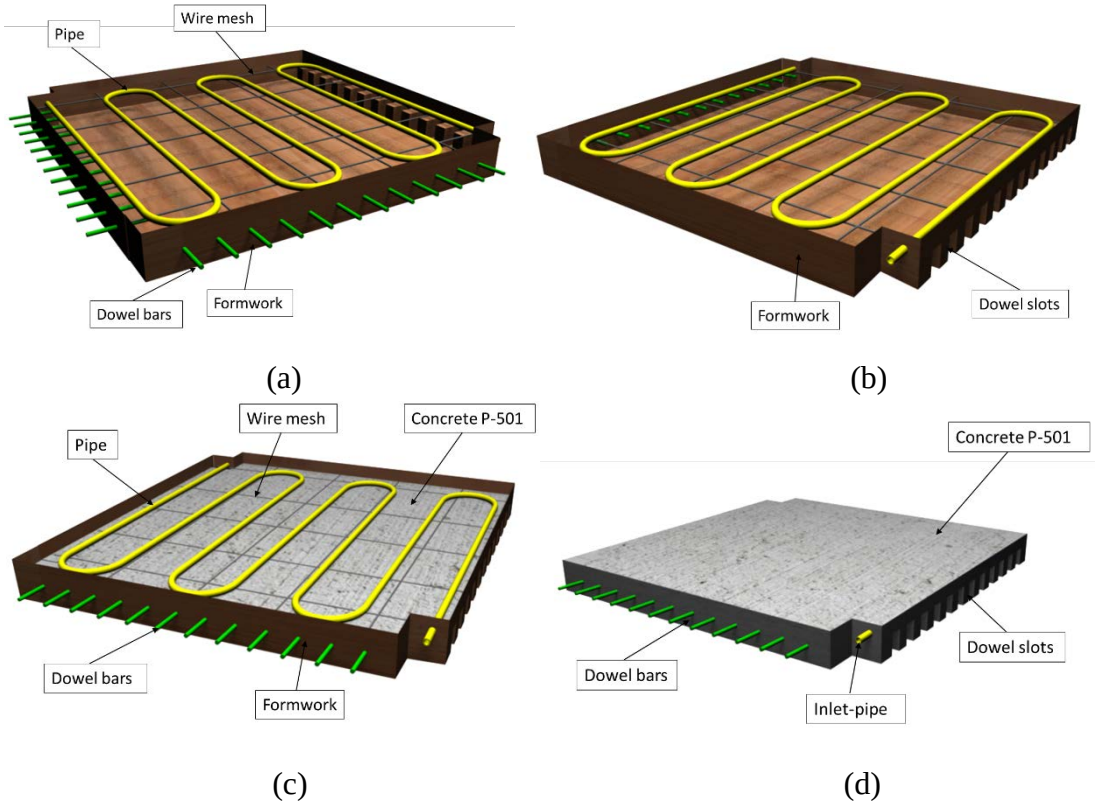

Figure 6-33 Hydronic heated slab fabrication using PC

Step2: Prepare the Base Layer and Place Hydronic Heated Slabs. Prepare and compact both subgrade and base layers to satisfy density requirements and identify manifold locations to define pipe circuit length and pattern, with the pipe pattern and pipe spacing adjusted based on the project site, geometry, size, required energy, and locations. Like a traditional PC structure, the slab has dowel bars and slots to provide load transfer, and it can be transported and placed into position at the project site. The pipes can be interconnected at the joints after placing the hydronic slabs, filling the dowel slot voids, and ensuring that the desired panel elevation is achieved. Figure 6-34a and Figure 6-34b show the pipe pattern and the connections between hydronic-heated slabs, respectively.

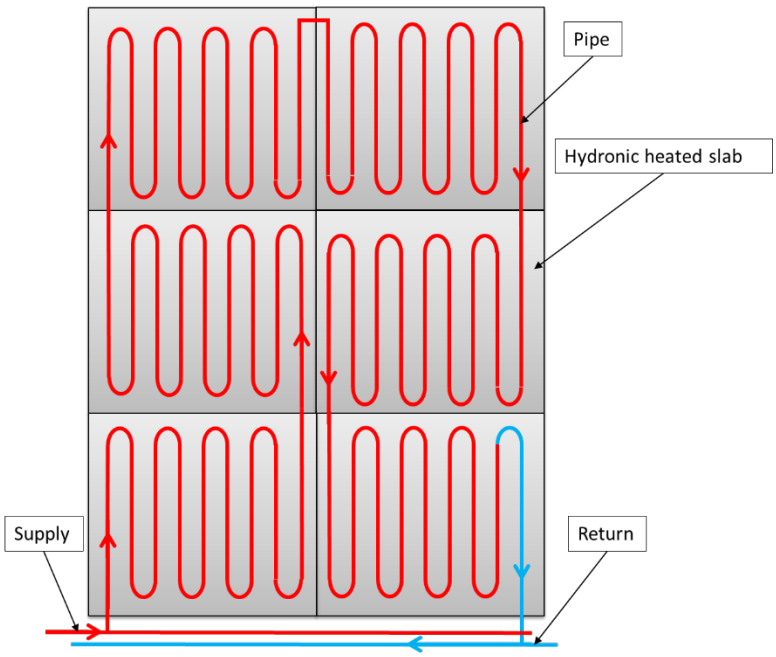

(a)

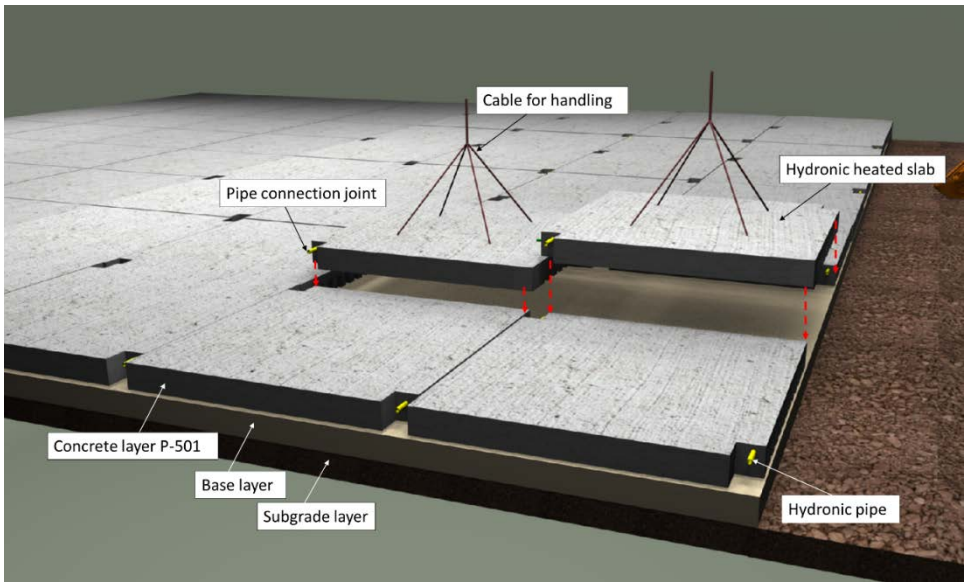

(b)

Figure 6-34 Hydronic heated slabs assembly

Step3: Connect Pipes to Energy Source. After identifying and connecting the manifold to the pipes, it should be connected to the heat source to permit fluid to circulate in the embedded pipe through a heat source (Figure 6-35). A HHPS can be operated automatically using a control system to turn the system on and off based on set temperature value that can

be measured by temperature sensors embedded in the concrete. To provide satisfactory operation the HHPS should be warmed up before snow and ice accumulates on the surface (ASHRAE 2015).

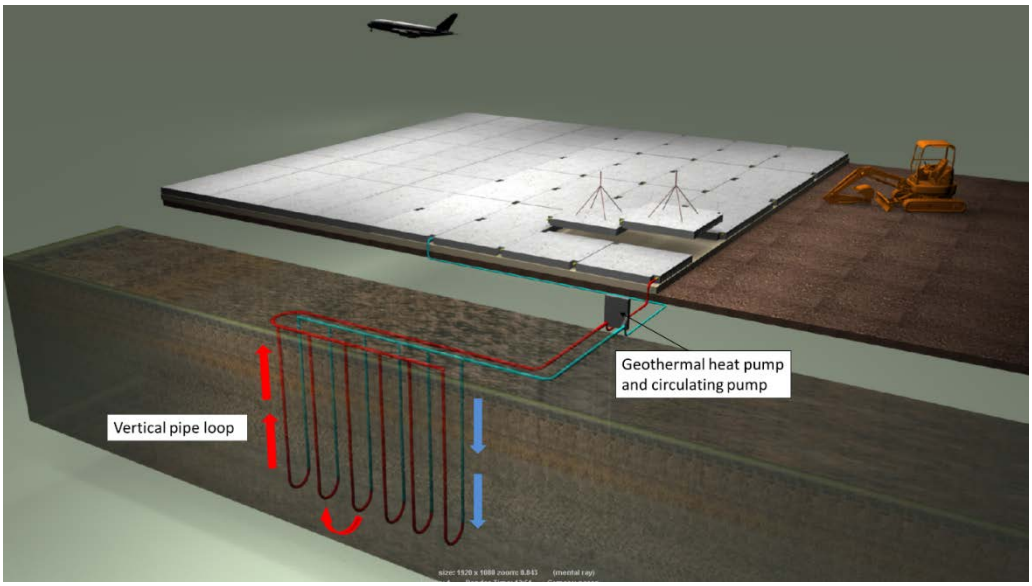

Figure 6-35 HHPS with geothermal wells as heat source

6.12 Conclusions

The goal of this study was to develop a conceptual design framework and provide construction guidance for electrically conductive concrete (ECON) and hydronic heated pavement system (HHPS) using precast concrete (PC), concrete overlay, and two-lift paving (2LCP). The results of this work can be enumerated as follows:

- Construction considerations and 3D visualization workflows for HPS were developed through the use of different construction techniques to develop more robust construction schemes and well-performing heated airport pavements
- HPS using PC is a viable option for accelerating construction procedures, reducing labor costs, and minimizing traffic disruption. In addition, the heat distribution of the

pavement surface is enhanced because the HPS panels are fabricated offsite where quality can be better controlled

- HPS using two-lift paving has potential for expediting the construction work of HPS for new construction through the use of a slipform paver. The mixture of the bottom lift could be used to mitigate the heat loss by using lightweight aggregates
- HPS using concrete overlays has the benefit of facilitating the HPS's components such as electrodes or pipes easily in comparison to other construction techniques. It is also suitable for construction of existing pavements and is considered a cost-effective solution
- Design details such as joint interfaces and material selection was provided to ensure that good construction practices using advanced construction techniques were followed

References

Abdualla, H., Ceylan, H., Kim, S., Mina, M., Gopalakrishnan, K., Sassani, A., Taylor, C.P., Cetin C.K. (2017). "Configuration of Electrodes for Electrically Conductive Concrete Heated Pavement". *Proc. ASCE International Conference on Highway Pavements and Airfield Technology*, Philadelphia, Pennsylvania, August 27-30, 2017.

Abdualla, H., Ceylan, H., Kim, S., Gopalakrishnan, K., Taylor C.P., Turkan, Y. (2016). "System Requirements for Electrically Conductive Concrete Heated Pavements". *Transportation Research Record: Journal of the Transportation Research Board*, No. 2569, pp. 70-79.

ACI Committee 325, (2006). "Concrete Overlays for Pavement Rehabilitation," American Concrete Institute Publication ACI 325.13R-06. Farmington Hills, MI, 2006.

Anand, P., Ceylan, H., Pyrialakou, D. V., Gkritza, K., Gopalakrishnan, K., Kim, S., and Taylor, P. C. (2016). "Economic assessment of heated pavements for the Minneapoli-St. Paul international airport," *the Proceedings of ASCE ICDT* 2016, 28-139.

American Society of Heating, Refrigerating and Air-Conditioning Engineers (ASHRAE.) (2015). *ASHRAE Handbook - HVAC Applications American Society of Heating, Chapter 51 – Snow Melting and Freeze Protection*. Atlanta, GA, 51.1-51.20.

Barbagallo, D. (2013). “RPD 155 heated pavements,” *FAA ANG-E262 REDAC Committee Meeting*, March 19, 2013.

Cable, K.J. (2004). “Reassessing Two-Lift Paving”. National Concrete Pavement Technology Center, Iowa State University, Ames, Iowa.

Ceylan, H., Gopalakrishnan, K., and Kim, S. (2014). "Heated transportation infrastructure systems: existing and emerging technologies," *the Proceeding of 12th International Symposium on Concrete Roads*, Prague, Czech Republic, September 23-26, 2014.

Chang, L., Chen, Y., and Lee, S. (2004) “Using Precast Concrete Panels for Pavement Construction in Indiana,” Report No. FHWA/IN/JTRP-2003/26. Indiana Department of Transportation, Indianapolis, IN, 2004.

Chen, Y., Murrell, S., and Larrazabal, E., “Precast Concrete (PC) Pavement Test on Taxiway D-D at LaGuardia Airport,” In *In Airfield Pavements: Challenges and New Technologies,* pp. 447-483, 2003.

Federal Aviation Administration (FAA). (2016). “Airport Pavement Design and Evaluation,” Advisory Circular (AC) 150/5320-6F. Federal Aviation Administration, U.S. Department of Transportation, Washington, DC.

Federal Aviation Administration (FAA.) (2011). *Airside Use of Heated Pavement Systems*. FAA AC No. 150/5370-17. Washington, D.C.

Federal Aviation Administration (FAA.) (2008). *Airport Winter Safety and Operation*. FAA AC No. 150/5200-30C, Washington, D.C.

Harrington, D., and Fick, G. (2014). “Guide to Concrete Overlays: Sustainable Solutions for Resurfacing and Rehabilitating Existing Pavements (3rd edition),” National Concrete Pavement Technology Center, Ames, IA.

Harrington, D.S., and Riley, R.C. (2012). “Guide to Concrete Overlays of Asphalt Parking Lots,” National Concrete Pavement Technology Center, Ames, IA 2012.

Harrington, D., Degraaf, D., Riley, R., Rasmussen, R.O., Grove, J., and Mack, J. (2007) “Guide to Concrete Overlay Solutions,” National Concrete Pavement Technology Center, Ames, IA.

Joerger, M.D., and Martinez, F.C. (2006). “Electrical Heating of I-84 in Land Canyon, Oregon,” Report No. FHWA-OR-RD06-17. Oregon Department of Transportation, Salem, OR.

Kohler, E., Plessis, L., Smith, P.J., Harvery, J, and Pyle, T. (2004). “Precast concrete pavements and results of accelerated traffic load test,” *the Proceeding of the*

International Conference on Optimizing Paving Concrete Mixtures and Accelerated Concrete Pavement Construction and Rehabilitation, 263-281.

Kohn, D.S., Tayabji, S., Okamoto, P., Rollings, R., Detwiller, R., Perera, R., Barenberg, E., Anderson, J., Torres, M., Barzegar, H., Thompson, M., (2003) "Best Practices for Airport Portland Cement Concrete Pavement Construction (Rigid Airport Pavement)". ACPA Document No. JP007P, Innovative Pavement Research Foundation, Washington, DC.

McCartney, S. (2014). "The case for heated runways," *Wall Street Journal*, http://www.wsj.com/news/article_email/SB10001424052702304914204579392883809689994-lMyQjAxMTA0MDIwMDEyNDAyWj. (November 07, 2017).

Merritt, D.K., McCullough, B.F., Burns, N.H., and Rasmussen, R.O. (2004). *Construction of the California precast concrete pavement: demonstration project*. Report No.FHWA-IF-06-010, FHWA, U.S. DOT, Washington, D.C.

Minsk, L.D. (1999). *Heated Bridge Technology*. Report No. FHWA-RD-99-158, FHWA, U.S. DOT, Washington, D.C.

Priddy, L.P., Bly P.G., and Flintsch, G.W. (2013). "Review of precast portland cement concrete panel technologies for use in expedient portland cement concrete airfield pavement repairs," *Transportation Research Board 92th Annual Meeting Compendium of Papers*, No. 13-2956.

Sassani, A., Ceylan, H., Kim, S., Gopalakrishnan, K.' Arabzadeh, A., Taylor, C.P., (2017) "Influence of Mix Design Variables on Engineering Properties of Carbon Fiber-Modified Electrically Conductive Concrete". *Construction and Building Materials*, Vol. 1 152, pp. 168-181.

Xi, Y., and Olsgard, P. J. (2000). *Effect of De-icing Agents (Magnesium Chloride and Sodium Chloride) on Corrosion of Truck Components*. Final Report for Report No. CDOT-DTD-R-2000-10, Colorado Department of Transportation, Denver, CO.

Zenewitz, J.A. (1977). "Survey of Alternatives to the Use of Chlorides for Highway Deicing," Report No. FHWA-RD-77-52. Federal Highway Administration, U.S. Department of Transportation, Washington, DC.

Ziegler, W. (2013). "A Solar-Thermal Approach to Runway Ice Management," Binghamton University – State University of New York.

CHAPTER 7. CONCLUSION AND RECOMMENDATION FOR FUTURE WORK

7.1 Summary

The objective of this research study was to develop and demonstrate the feasibility of using heated pavement systems as an alternative promising technology for preventing ice/snow accumulation on paved surfaces to mitigate the use of conventional deicing methods. Such systems have the potential to keep airports accessible, safe, and sustainable during the winter season.

System requirements related to material selection, design, construction, and operational for an ECON-based HPS were identified. A small-scale prototype ECON slab was designed and constructed at the ISU Portland Cement Concrete Pavement and Materials Research Laboratory, then tested to determine its performance and efficiency. The ECON mix contained 6-mm-long carbon fibers, 0.75% by volume of the total concrete mix, and used methylcellulose as an agent to disperse the carbon fiber particles evenly and as a result improve electrical conductivity. The electrical resistivity value was 50 Ω-cm at room temperature (i.e., 20°C ambient temperature). Perforated steel bars with gaps larger than the maximum aggregate size was used for electrodes to ensure that conductive concrete can be bonded with an electrode to support electrical current flow within the ECON layer.

A series of experimental tests were conducted to evaluate ECON slab performance in terms of melting surface snow/ice and to calculate energy consumption and cost. The literature indicates that ECON performance provides the lowest energy consumption and cost in comparison to electrically-heated pavement systems. The better operational performance of the ECON heating slab in this study is attributed to higher conductivity in the newly

developed ECON mixture that allows the entire surface to heat uniformly and quickly melt snow and ice.

A developed 3-D finite element (FE) modeling approach could be used for designing and optimizing ECON parameters such as electrode spacing, power input, etc., to meet the design criteria for achieving the best heating performance. A 3-D FE model for an ECON slab was developed using COMSOL Multiphysics software and validated though comparison with experimental test results. Sensitivities of various ECON HPS design variables to heat generation and distribution performance were identified to identify the critical variables having the most influence on heating performance.

The design, construction, and performance of the world's first full-scale ECON-based HPS at a U.S. airport was demonstrated. Two ECON slabs were designed and constructed at the General Aviation (GA) apron at the Des Moines International Airport (DSM), Iowa, in 2016. The challenges and solutions of taking a prototype small-scale ECON heated concrete slab developed by ISU and implementing it at full scale in the airport were identified and addressed. Systematic design components were identified and construction procedures were developed and implemented for ECON-based HPS. Using sensor data, the performance of the constructed and remotely-operated ECON slabs was evaluated under real weather conditions at DSM during the 2016-2017 winter season, with results demonstrating that ECON-based HPS offer promising deicing and anti-icing capacities with respect to providing uniform heat distribution and preventing snow and ice accumulatios on the entire area of application under various winter weather conditions.

Advanced construction techniques and workflows using heated pavements with precast concrete (PC), two-lift paving, and concrete overlays were demonstrated through 3D

visualizations to provide design and construction guidance for large-scale heated airport pavement systems. A detailed review of advanced pavement construction techniques and practices, including precast concrete, two-lift paving, and concrete overlay, were addressed to evaluate their efficacy and applicability to construction of HPS at airports.

7.2 Conclusions

The major conclusions corresponding to each study objective are as follows:

7.2.1. A Prototype Small-Scale ECON Slab. This study identified ECON's system requirements and the use of ECON HPS as a cost-effective solution for preventing snow/ice accumulation on paved surface to eliminate related airport incidents and accidents. The results for the prototype ECON slab were evaluated and the following conclusions can be drawn:

- The energy consumption and energy cost of the prototype ECON heating slab was the lowest of the electric HPSs developed or reported in the literature to date. Such excellent operational performance is attributed to a recently-developed ECON mixture that provides higher conductivity (about 50 Ω-cm of electrical resistivity) to even out surface heating to melt snow and ice quickly.
- The prototype ECON heating slab is comprised of a thin ECON top layer on a conventional concrete bottom layer. This cost-effective two-layer approach can be implemented for large-scale ECON HPS using precast concrete, concrete overlay, and two-lift paving techniques.
- The design parameters to be determined for a large-scale ECON HPS include slab dimensions, inter-electrode distance, electrical resistance, and voltage. The design

flow developed in this study can be used to determine values of these parameters for given design criteria.

- Key construction materials required for a well-performing ECON HPS are low-resistivity (i.e., high-conductivity) ECON materials, electrodes that bond well with ECON, and cost-effective thermal insulation.
- ECON should be heated with AC to enable electrons to follow different paths through the conductive materials to distribute slab heat evenly.

7.2.2 Examination and Development of a 3-D Finite Element Model for Studying ECON HPS as an Alternative Design Approach to Optimize the ECON HPS Variables. A 3-D finite-element (FE) model of ECON HPS was developed for predicting heat performance under different input conditions (i.e., weather conditions, electrode spacing, ECON material properties, etc.) and it was validated through comparison with laboratory experimental test results. The major conclusions of this study are as follows:

- The developed 3-D FE model for ECON can predict heat generation and distribution changes over operational time. It can be utilized as a cost-effective evaluation tool for examining the effects of various design parameters on the time-dependent heating performance of optimized ECON HPS design.
- Given the assumed boundary conditions, the model shows that, during ECON operation, the temperature is initially highest in the central area of the ECON surface and then distributed across the entire slab.
- The temperature inside the conventional concrete layer increases with time because the insulation layer, and the slab boundaries reduce heat losses. This temperature becomes close to the temperature inside the ECON layer, indicating that thermal

stresses between surfaces will not be an issue because there are only small temperature differences between the ECON and conventional layers.

- The ECON electrical resistivity is one of the most influential parameters governing heating performance, and as the electrical resistivity increases, the time before achieving a temperature above the freezing point on the ECON surface increases. The 3-D FE model results indicates that electrical resistivity ranges of about 50 to 200 Ω·cm can provide sufficient heat for realistic ECON slab (4.6 m long × 4.6 m wide × 19 cm thick) dimensions representing an actual large-scale airport pavement slab.
- As the electrode spacing increases, the time to achieve a temperature above the freezing point on the ECON surface dramatically increases. Based on the 3-D FE model results, it is recommended that design electrode spacing should be designed such that more than two electrodes could be accommodated within an ECON slab to ensure that an ECON above-freezing surface temperature can be achieved.
- Voltage values and ambient temperatures can also affect the time before achieving above-freezing point temperatures on an ECON surface. As voltage increases, the ECON surface temperature reaches an above-freezing point temperature more quickly.
- Thirty minutes or less are required to increase surface temperatures from ambient (-5, -15, -25 ^{o}C) to above-freezing temperatures. Considering that the ambient temperature ranges selected for the study are representative of temperature conditions for a wide range of geographical locations in the US, ECON HPS employed in most geographical locations in the US should be able to achieve above-freezing point surface temperatures at those locations.

7.2.3. Design and Construction of the World's First Full-Scale ECON Heated Airport System. This study demonstrated the field implementation of ECON HPS in a real airport environment. The major conclusions of this study are as follows:

- The constructed ECON HPS demonstrated deicing and ant-icing capacities providing uniform heat distribution and preventing snow and ice accumulations on the entire area of application under various winter weather conditions, including extremely cold weather (i.e., arctic blast).
- The energy consumption of the ECON HSP for the deicing application ranged from 0.05 kW-h/ft^2 to 0.10 kW-h/ft^2 required to melt 0.5 to 1.5 in. of snow/ice accumulation under various winter weather conditions, except for an arctic blast event that required 0.59 kW-h/ft^2 to melt 1 in. of snow/ice accumulation. The energy consumption of the ECON HSP for the anti-icing application was estimated at 0.22 kW-h/ft^2 for preventing snow and ice accumulations for a 7-hr interval.
- The ECON HSP in DSM was constructed using a two-lift approach that placed a thin ECON layer (top layer) on a P-501 PCC layer (bottom layer). This approach can be effective not only in saving in the construction costs of a single thick ECON layer, but also in facilitating electrode installation and wire connections.
- The surface of the P-501 PCC layer (bottom layer) was screeded to create a rough surface that provided adequate bonding between the two layers.
- Because of its high corrosion resistance and so electrodes would not be reduced in efficiency, perforated stainless steel was used for the electrodes; the use of stainless steel also eliminated the cracking potential possible with steel or galvanized steel.

- Electrodes should be placed at least 1to 2 inches below the ECON surface so as not to interfere with a paver's vibrator, pan, and auger when slipform paving is used for large-scale construction.

7.3 Recommendations

The following recommendation are drawn from the studies presented in this dissertation.

7.3.1 Recommendation for ECON System Design and Full-Scale ECON HPS Construction

The recommendations for achieving successful long-term performance summarized below are based on lessons learned during the design and construction of the first full-scale of ECON HPS.

- Proper selection of materials for ECON HPS components, including ECON mixture and electrodes, can enhance the performance and increase the service life of ECON HPS. For example, galvanized steel is not recommended for use as electrodes because the coating material (i.e., zinc) protecting the steel from corrosion could eventually degrade and peel off when electrical power is applied.
- Steel fibers or shavings should be avoided in the ECON mix for airport application due to potential corrosion problems.
- A two-lift paving technique is the best approach for constructing ECON slabs; it is challenging to achieve wet-on-wet paving because electrode installation requires extra time for anchoring on the bottom lift, i.e., it should be allowed to stiffen to support the electrodes.
- For mass paving of ECON materials, slip-form or laser-screed paving would be the best option for enhancing the construction process.

7.3.2 Recommendation for Finite Element Model

The followings recommendations are suggested for use of the 3-D finite element (FE) model as an alternative tool for optimizing the ECON HPS parameters.

- The time required to heat the ECON surface above freezing point (i.e., 1~2 ^{o}C) is highly dependent on weather conditions such as ambient temperature, wind speed, etc., and it can be estimated either from data-driven models using historical experimental data, or through physics-based thermodynamic models such as finite-element (FE) model simulation.
- Avoid the use of a constant value of ECON electrical resistivity. Consider the electrical resistivity of the ECON sample as temperature-dependent when using the finite-element models to obtain more accurate analytical results.

7.3.2 Recommendations for Advanced Construction Techniques for HPS

To best automate and accelerate the construction work, the following recommendations are suggested for large-scale construction of heated pavement systems using PC, two-lift paving, and concrete overlay.

- Two-lift paving technique is the best approach for constructing ECON HPS.
- Contractors should be trained and educated in constructing ECON HPS using different techniques and should practice by constructing a small ECON area before paving larger areas.
- Provide a 3-D visualization of the ECON construction work so that contractors can easily understand and envision correct construction procedures.

- The surface of the bottom layer (regular concrete) should either be grooved or brooms/burlaps used to create a rough surface to achieve sufficient bonding between the two layers.
- Dowel baskets should be placed in the bottom layer (the PCC layer).
- Contraction/expansion joints should be used to isolate ECON slabs from PCC slabs to allow free movement during ECON heating operations.
- Electrodes should be positioned perpendicular to the traffic direction to reduce the likelihood of potential cracking from vehicle loads. Placing electrodes on a fresh concrete surface is challenging, so wet-on-wet procedures probably cannot be achieved.
- Electrodes should be placed at least 2 inches below the surface to avoid interference with a paver's vibrator, pan, and auger.
- Electrode material should be resistant to corrosion while applying voltage to electrodes. To address this issue, stainless steel 316-L is the recommended option for avoiding such corrosion problem.
- Reduce the electrical resistivity (i.e., the reciprocal of electrical conductivity) of the ECON mixture to provide better heat performance.

7.3.2 Recommendation for Future Research

The followings recommendations are proposed for future research:

- Investigate the long-term bonding between the ECON layer and the Portland cement concrete (PCC) layer and the expansion and contraction phenomena of both layers during ECON operation.

- Investigate the potential for developing more sustainable ECON mixes such as the use of recycled carbon fibers in ECON.
- Provide cost-effective guidance for ECON maintenance, including preservation, rehabilitation, and reconstruction. Investigate ECON heating performance when the ECON layer is cracked (i.e., small or large cracks).
- Develop a 3-D finite-element model for estimating dollar values of ECON operational costs for large-scale heated airport pavements and the energy required to warm the ECON surface for various pavement thicknesses.
- Investigate the curling and warping behavior of the ECON HPS during operation and the effect of the ECON temperature gradient.
- Investigate long-term ECON performance by measuring the effect of electrical resistivity on heating performance.
- Investigate the long-term ECON performance by measuring the electrical resistivity that has an effect on the heating performance.
- Assess the energy requirements and financial viability of installing a heated pavement system at an airport and its cost compared to that using conventional snow-removal strategies.
- Future studies can use the findings of this study to design and construct full-scale implementation of HPS using two-lift paving through field demonstration at actual airport environments. It would be beneficial to develop a mix design for the bottom lift to mitigate heat loss during HPS operation.

REFERENCES

Federal Aviation Administration (FAA.) (2011). *Airside Use of Heated Pavement Systems*. FAA AC No. 150/5370-17. Washington, D.C.

Gopalakrishnan, K., Ceylan, H., Kim, S., Yang, S., and Abdualla, H. (2015). "Electrically conductive mortar characterization for self-heating airfield concrete pavement mix design." *International Journal of Pavement Research and Technology* 8, No. 5, pp. 315-324.

Joerger, M.D., and Martinez, F.C. (2006). "Electrical Heating of I-84 in Land Canyon, Oregon," Report No. FHWA-OR-RD06-17. Oregon Department of Transportation, Salem, OR

Xi, Y., and Olsgard, P.J. (2000). *Effect of De-Icing Agents (Magnesium Chloride and Sodium Chloride) on Corrosion of Truck Components.* CDOT-DTDR-2000-10. Colorado Department of Transportation, Denver.

Zenewitz, J.A. (1977). "Survey of Alternatives to the Use of Chlorides for Highway Deicing," Report No. FHWA-RD-77-52. Federal Highway Administration, U.S. Department of Transportation, Washington, DC.

Abdualla, H., Ceylan, H., Kim, S., Gopalakrishnan, K., Taylor, P.C., and Turkan, Y. (2016). "System requirements for electrically conductive concrete heated pavements." *Transportation Research Record: Journal of the Transportation Research Board, No 2569,* Transportation Research Board of the National Academies, Washington, D.C., pp. 70-79.

ACI Committee 325. (2006). "Concrete Overlays for Pavement Rehabilitation," American Concrete Institute Publication ACI 325.13R-06. Farmington Hills, MI.

Arnott, M.R., Beaudoin, J.J., Myers, R. E., Pye, G.P., and Tumidajski, P.J. (2005). *Conductive concrete composition*. Patent no. EP1268360 B1, European Patent Office, Munich, Germany.

ASHRAE (2015). *ASHRAE Handbook - HVAC Applications American Society of Heating, Chapter 51 – Snow Melting and Freeze Protection.* American Society of Heating, Refrigeration and Air-Conditioning Engineer, Inc., Atlanta, GA, pp. 51.1 – 51.20.

Barbagallo, D. (2013). "RPD 155 heated pavements," *FAA ANG-E262 REDAC Committee Meeting*, March 19, 2013.

Barnard, E.H. (1965). *Electrically conductive cement and concrete*, Patent no. US3166518 A, U.S. Patent and Trademark Office, VA.

Bly, P.G., Priddy, L.P., Jackson, C.J., and Mason, Q.S. (2013). “Evaluation of Precast Panels for Airfield Pavement Repair Phase I: System Optimization and Test Section Construction,” Report No. ERDC/GSL TR 13-24. US Army Corps of Engineers Research and Development Center.

Brill, R.D. (2016). “Heated Pavement and Nanotechnology for Airport Pavements,” Presented at Summer Winter Integrated Field Technologies (SWIFT) Conference, Niagara Falls, ON L2G 3K7S, September 19-22, 2016.

Cable, J. (2004). “Reassessing Two-Lift Paving,” National Concrete Pavement Technology Center, September.

Cable, J.K., and Frentress, D.P. (2004). “Two-Lift Portland Cement Concrete Pavements to Meet Public Needs,” Report No. DTF61-01-X-00042 (Project 8). Center for Transportation Research and Education, Ames, IA.

Ceylan, H., Gopalakrishnan, K., and Kim, S. (2014). "Heated transportation infrastructure systems: existing and emerging technologies," *the Proceeding of 12th International Symposium on Concrete Roads,* Prague, Czech Republic, September 23-26, 2014.

Chang, L., Chen, Y., and Lee, S. (2004). “Using Precast Concrete Panels for Pavement Construction in Indiana,” Report No. FHWA/IN/JTRP-2003/26. Indiana Department of Transportation, Indianapolis, IN.

Chen, Y., Murrell, S., and Larrazabal, E. (2003). “Precast Concrete (PC) Pavement Test on Taxiway D-D at LaGuardia Airport,” In *In Airfield Pavements: Challenges and New Technologies,* pp. 447-483.

Dehdezi, P.K., Hall, M.R., and Dawson, A. (2011). “Thermophysical optimization of specialized concrete pavement materials for collection of surface heat energy and applications for shallow heat storage.” *Transportation Research Record: Journal of the Transportation Research Board,* No. 2240, 96–106.

Delatte, N.J. (2014). “Concrete Pavement Design, Construction, and Performance. CRC Press.

Federal Aviation Administration (FAA). (2016). “Airport Pavement Design and Evaluation,” Advisory Circular (AC) 150/5320-6F. Federal Aviation Administration, U.S. Department of Transportation, Washington, DC.

Federal Aviation Administration (FAA.) (2007). *Rapid Construction of Rigid (Portland Cement Concrete) Airfield Pavements*. FAA AC No. 150/5370-16. Washington, D.C.

Federal Aviation Administration (FAA.) (2011). *Airside Use of Heated Pavement Systems*. FAA AC No. 150/5370-17. Washington, D.C.

Freeman, A., and Hymers, W. (1976). *Electrically conductive concrete*, Patent no. US3962142 A, U.S. Patent and Trademark Office, VA.

Gerhardt, T. (2013). "Two-Lift Concrete Paving Workshop," Texas Department of Transportation, Austin, TX.

Gopalakrishnan, K., Ceylan, H., Kim, S., Yang, S., and Abdualla, H. (2015). "Electrically conductive mortar characterization for self-heating airfield concrete pavement mix design." *International Journal of Pavement Research and Technology* 8, No. 5, pp. 315-324.

Gopalakrishnan, K., Ceylan, H., Kim, S., Yang, S., and Abdualla, H. (2015). "Electrically conductive mortar characterization for self-heating airfield concrete pavement mix design." *International Journal of Pavement Research and Technology* 8, No. 5, pp. 315-324.

Harrington, D., Degraaf, D., Riley, R., Rasmussen, R.O., Grove, J., and Mack, J. (2007). "Guide to Concrete Overlay Solutions," National Concrete Pavement Technology Center, Ames, IA.

Heymsfield, E., Osweiler, A.B., Selvam, R.P., and Kuss, M. (2013). *Feasibility of anti-icing airfield pavements using conductive concrete and renewable solar energy*, Publication DOT/FAA/TC-13/8. FAA, U.S. Department of Transportation, NJ.

Hu, J., Fowler, D., Siddiqui, M.S., and Whitney, D. (2014). "Feasibility Study of Two-Lift Concrete Paving: Technical Report," Texas State University-San Marcos, and Center for Transportation Research, Austin, TX.

Jensen, D., and Hu, J. (2013). "Two-Lift Concrete Paving Workshop," Texas Department of Transportation, Austin, TX.

Joerger, M.D., and Martinez, F.C. (2006). "Electrical Heating of I-84 in Land Canyon, Oregon," Report No. FHWA-OR-RD06-17. Oregon Department of Transportation, Salem, OR.

Lai, Y., Liu, Y., and Ma, D. (2014). *"Automatically melting snow on airport cement concrete pavement with carbon fiber grille."* Cold Regions and Technology No. 103 (2014) 57-62

LoopCAD® *Snowmelt Design.* Alberta, Canada, 2016 Avenir Software Inc. http://www.avenir-online.com/AvenirWeb/LoopCAD/Pdfs/LoopCAD%20Features.pdf. Accessed April 09, 2017.

Lund, J.W. (2005). *Pavement Snow Melting*. Geo-Heat Center, Oregon Institute of Technology, Klamath Falls, OR.

Mallick, R.B., and El-Korchi, T. (2013). “Pavement Engineering: Principles and Practice,” CRC Press.

Merritt, D.K., McCullough, B.F., Burns, N.H., and Rasmussen, R.O. (2004). “Construction of the California Precast Concrete Pavement: Demonstration Project,” Report No.FHWA-IF-06-010. Federal Highway Administration, U.S. Department of Transportation, Washington, DC.

Minsk, L.D. (1999). “Heated Bridge Technology Report on ISTEA Sec. 6005 Program,” Report No. FHWA-RD-99-158, Federal Highway Administration.

Mowris, S. (1995). "Whitetopping Restores Air Traffic at Spirit of St. Louis." In Concrete Construction Vol. 40, Issue 6.

Priddy, L.P., Bly P.G., and Flintsch, G.W. (2013). “Review of Precast Portland Cement Concrete Panel Technologies for Use in Expedient Portland Cement Concrete Airfield Pavement Repairs,” In *Transportation Research Board 92th Annual Meeting Compendium of Papers*, No. 13-2956.

Ramme, B.W., Noegel, J.J., Setchell, R.H., and Bischke, R.F. (2012). *Electrically conductive concrete and controlled low-strength materials.* Patent no EP1260492 B1, European Patent Office, Munich, Germany.

Simon, T.K., and Vass, V. (2012). “The electrical resistivity of concrete.” *Concrete Structures*, Vol. 13, 61-64.

Spragg, R.P., Villani, C., Snyder, K., Bentz, D., Bullard, J.W., and Weiss, W.J. (2013). “Factors that influence electrical resistivity measurements in cementitious systems.” *Transportation Research Record: Journal of the Transportation Research Board, No. 2342*, 90-98.

Tayabji, S. (2010). “Precast Concrete Pavement Technology,” U.S. Department of Transportation,” Federal Highway Administration American Association of State Highway and Transportation Officials National Cooperative Highway Research Program, November.

Tayabji, S., Buch, N., and Kohler, E. (2009). “Precast Concrete Pavement for Intermittent Concrete Pavement Repair Applications,” In Proceedings of the National Conference of Preservation, Repair, and Rehabilitation of Concrete Pavements, St. Louis, MO.

Tayabji, S., Ye, D., and Buch, N. (2013). "SHRP 2 Report S2-R05-RR-1: Precast Concrete Pavement Technology," Transportation Research Board of the National Academies, Washington, DC.

Torres, H.N., Roesler, J., Rasmussen, R.O., and Harrington, D. (2012). “Guide to Concrete Overlays Using Existing Methodology,” Report No. DTFH61-09-H-00011 (Work

Plan 13), National Concrete Pavement Technology Center, and Institute for Transpiration, Iowa State University, Ames, IA.

Tuan, C.Y. (2008). *Implementation of conductive concrete for deicing (Roca Bridge)*, Final Report for Project No. SPR-PL-1(04) P565, University of Nebraska-Lincoln, NE.

Tuan, C.Y. (2004). *"Electrical resistance heating of conductive concrete containing steel fibers and shavings."* American Concrete Institute Materials Journal, 101(1), 65–71

Tuan, C.Y., Nguyen, L, and Chen, B. (2010). *Conductive concrete for heating and electrical safety.* Patent no. WO2010059169 A1, European Patent Office, Munich, Germany.

Viega. S-no-Ice Snow® Melting System Installation Manual. (2005). Wichita, KS. http://www.viega.us/xbcr/en-us/Viega_S-no-ice_Snow_Melting_System.pdf. Accessed July 15, 2015.

Whittington, H., McCarter, W., and Forde, M.C. (1981). "The conduction of electricity through concrete." *Magazine of Concrete Research*, Vol. 33, No. 114, 48-60.

Xie, P., Gu, P., and Beaudoin. J.J. (1996). "Electrical percolation phenomena in cement composites containing conductive fibers." *Journal of Materials Science*, Vol. 31, 4093-4097.

Yang, Z., Yang, T., Song, G., and Singla, M. *"Experimental Study on an Electrical Deicing Technology Utilizing Carbon Fiber Tape."* Alaska University Transportation Center, Fairbanks, AK 99775-5900 DTRT06-G-0011, 2012.

Yehia, S. and Tuan, C. (1998). *"Bridge Deck Deicing."* Transportation Conference Proceedings.

Yehia, S., Tuan, C.Y., Ferdon, D., and Chen, B. (2000). "Conductive concrete overlay for bridge deck deicing: mixture proportioning, optimization, and properties." *ACI Materials Journal*, Vol. 97, Issue 2, 172-181.

Zaleski, P. L., Derwin, D. J., and Flood, W. H. (2005). *Electrically conductive pavement mixture*. Patent no. US6971819 B2, U.S. Patent and Trademark Office, VA.

Zenewitz, J.A. (1977). "Survey of Alternatives to the Use of Chlorides for Highway Deicing," Report No. FHWA-RD-77-52. Federal Highway Administration, U.S. Department of Transportation, Washington, DC.

APPENDIX PERFORMANCE EVALUATION of ECON HPS at DSM

This appendix shows the detailed performance of the ECON HPS at DSM airport under different weather conditions for the first year (December 08, 2016 to March 13, 2017)

- First Performance Evaluation (12/08/2016):

Table 1 Weather condition

Date	December 08, 2016
Snow thickness	No snow event
Operation time	See the note below
Mean temperature	19°F (-7°C)
Minimum temperature	12°F (-11°C)
Maximum temperature	25°F (-3.8°C)
Wind speed	18 mph
Average relative humidity	61 %
Minimum relative humidity	55 %
Maximum relative humidity	67 %

Note: the ECON system was turned on at 6:00 am, however, the circuit breaker controlling electrodes in slab 1 was turned off and only slab 2 started at 6:00 am. Slab 1 operation started from 9:55 am to 5:00 pm. Slab 2 operation stated from 6:00 am to 5:00 pm

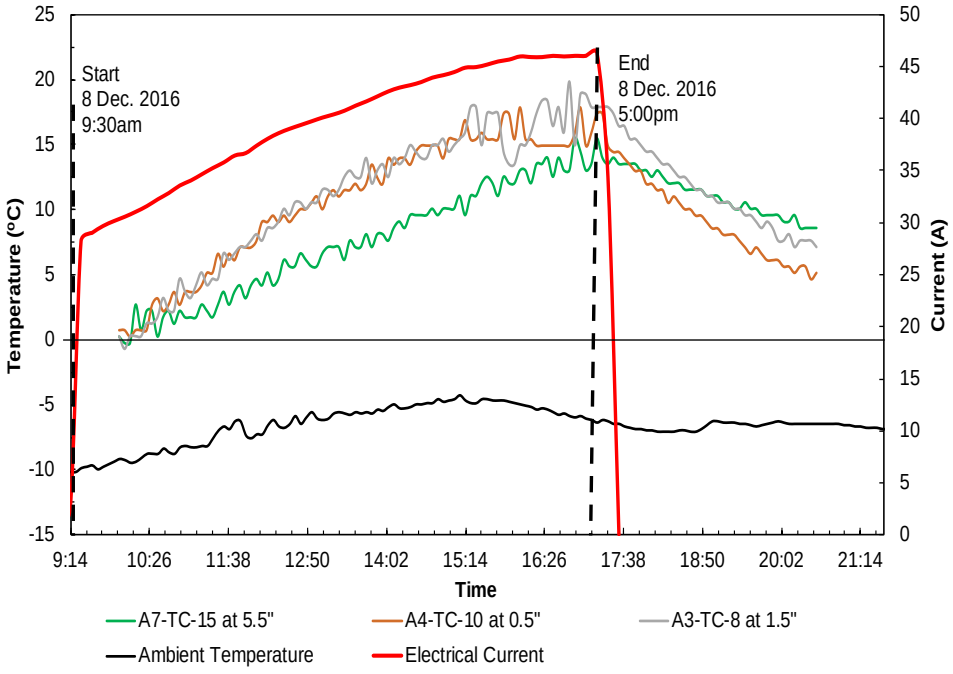

Figure 1 Slab 1 temperature and current measurements

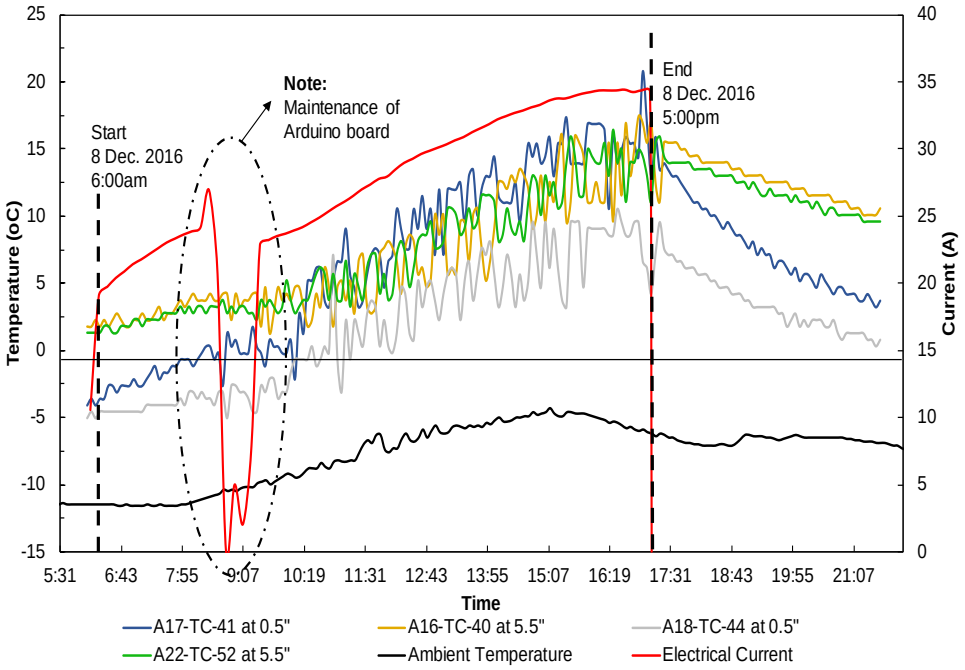

Figure 2 Slab 2 temperature and current measurements

- Second Performance Evaluation (12/10/2016):

Table 2 Weather condition

Date	December 10, 2016
Snow thickness	1.2 inch
Operation time	7 hours
Mean temperature	25°F (-3.8°C)
Minimum temperature	22°F (-5.5°C)
Maximum temperature	28°F (-2.2°C)
Wind speed	8 mph
Average relative humidity	77 %
Minimum relative humidity	65 %
Maximum relative humidity	87 %

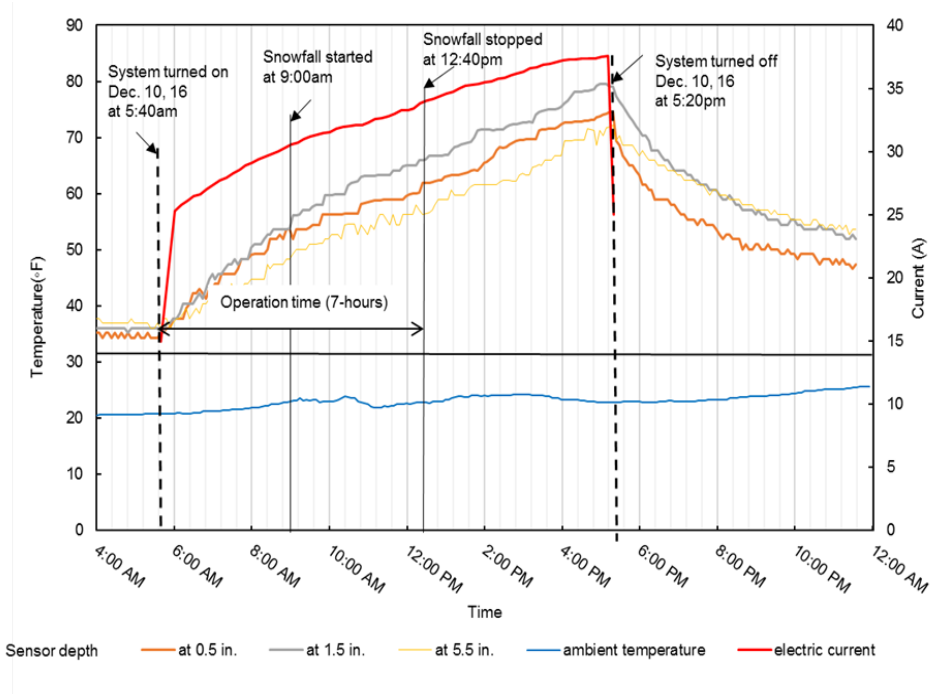

Figure 3 Slab 1 temperature and current measurements

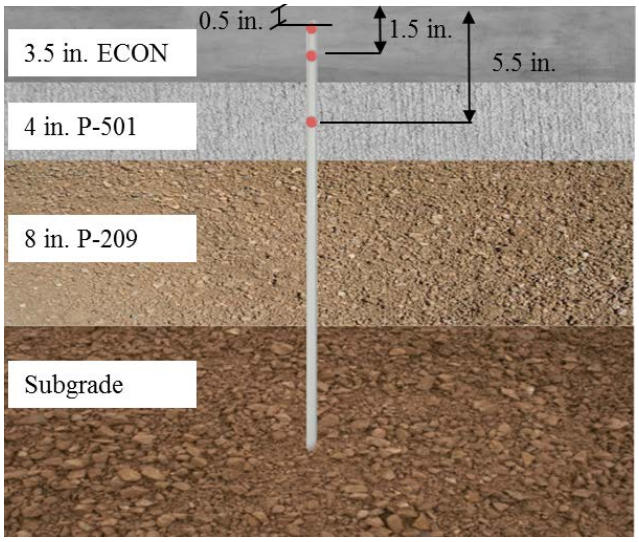

Figure 4 Slab 1 sensors location

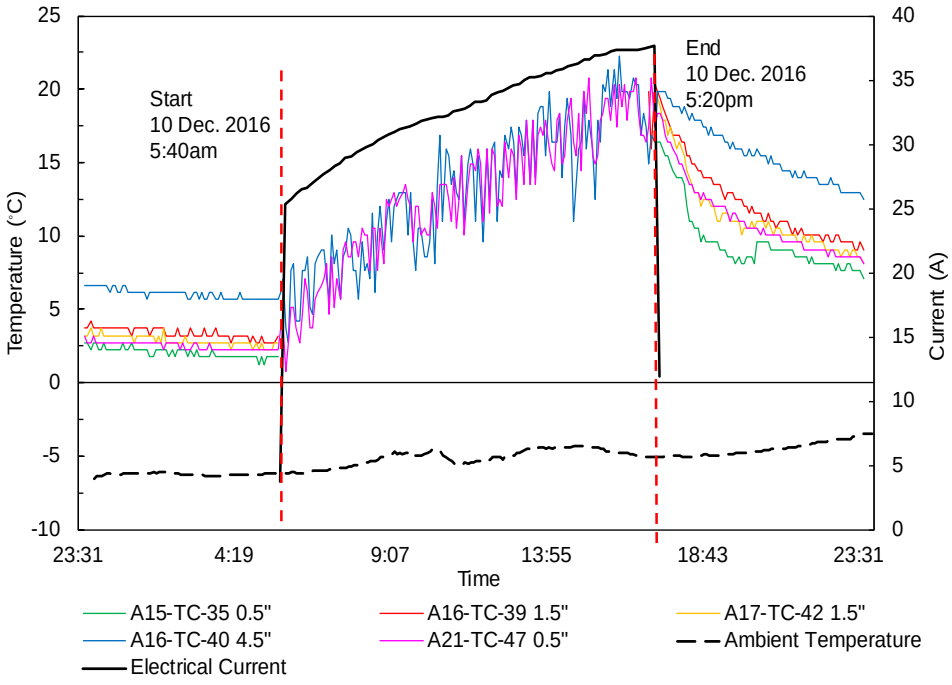

Figure 5 Slab 2 temperature and current measurements

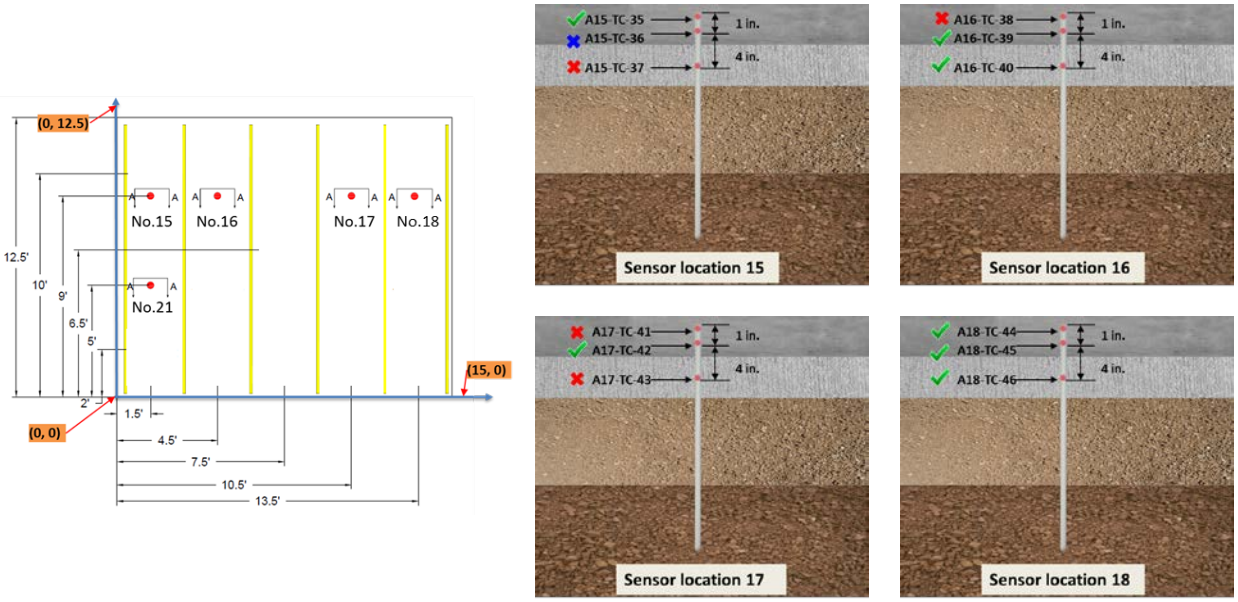

Figure 6 Slab 2 sensors location

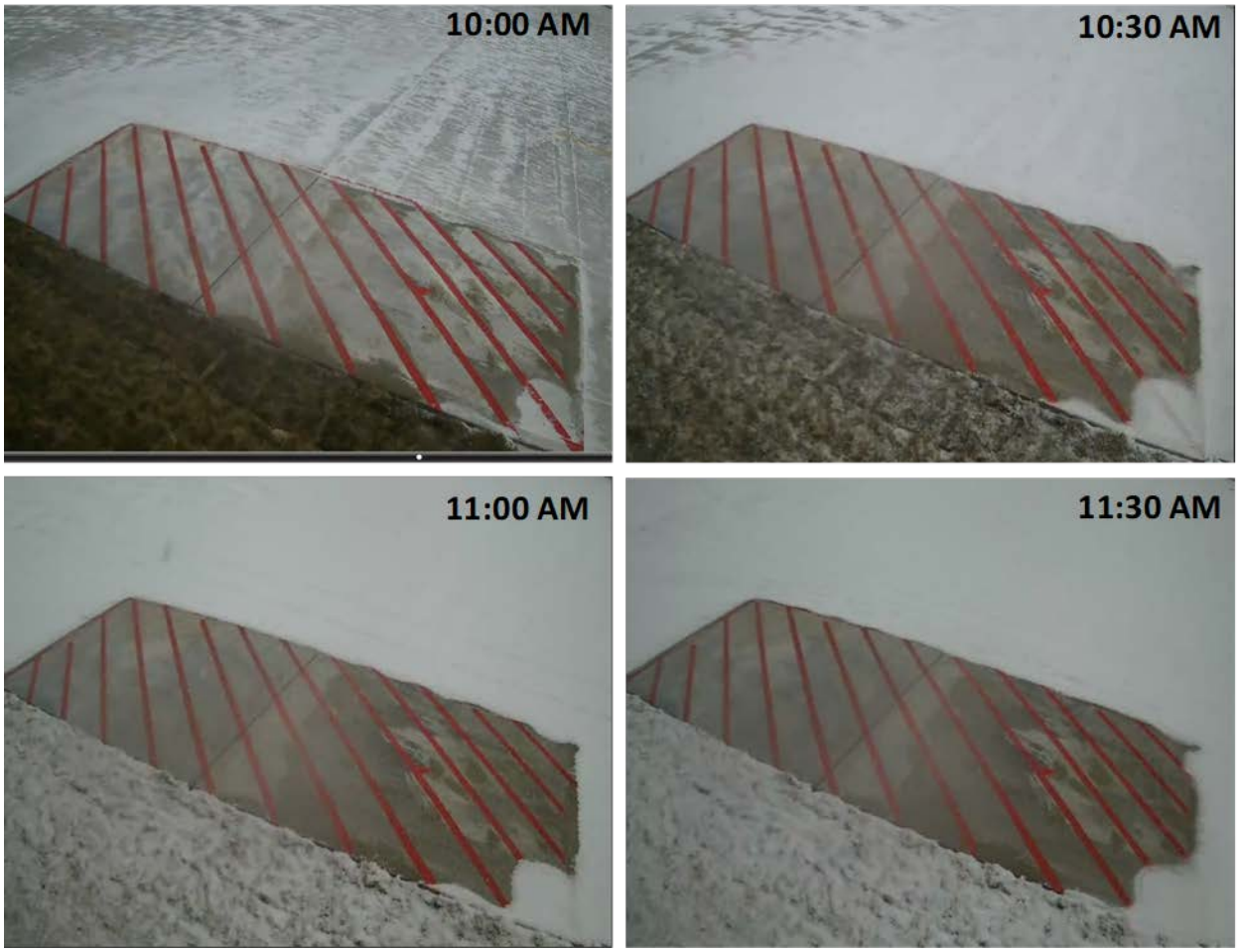

Figure 7 Performance of ECON HPS during snowfalls using surveillance cameras

Figure 8 shows the ECON slab 1 surface temperatures in comparison to the adjacent slab (a regular PCC slab) during operation time at 02:00 pm. The surface temperature on ECON slab 1 was about 12 ^{o}C (54 ^{o}F) and the temperature reading from the sensor located at 0.5-in from the ECON slab 1 was about 21 ^{o}C (70 ^{o}F). A temperature difference of about 9 ^{o}C was observed. However, a surface temperature of -8.5 ^{o}C (16 ^{o}F) in the regular PCC slab was much lower than the temperature readings observed in ECON slab 1.

Figure 8 Surface temperature reading at ECON slab 1 and adjacent slab during operation time

Figure 7 and figure 9 illustrates the performance of the ECON slab. There was no accumulation on the ECON slabs during the snowfall while the total snowfall accumulation was 1 inch. The performance of the ECON slab did not only prevent snow accumulation, but also completely made the ECON slab surface dry.

(a)

(b)

Figure Performance of the ECON HPS: (a) heavy snow remove machine verse ECON HPS and (b) snow removal truck verse ECON HPS

- Third Performance Evaluation (12/18-19/2016):

Table 3 Weather condition

Date	December 18-19, 2016
Snow thickness	0.5-1 inch (arctic blast weather)
Operation time	21 hours
Mean temperature	-4°F (-20°C)
Minimum temperature	-11°F (-24°C)
Maximum temperature	3°F (-16°C)
Wind speed	9 mph
Average relative humidity	67 %
Minimum relative humidity	60 %
Maximum relative humidity	75 %

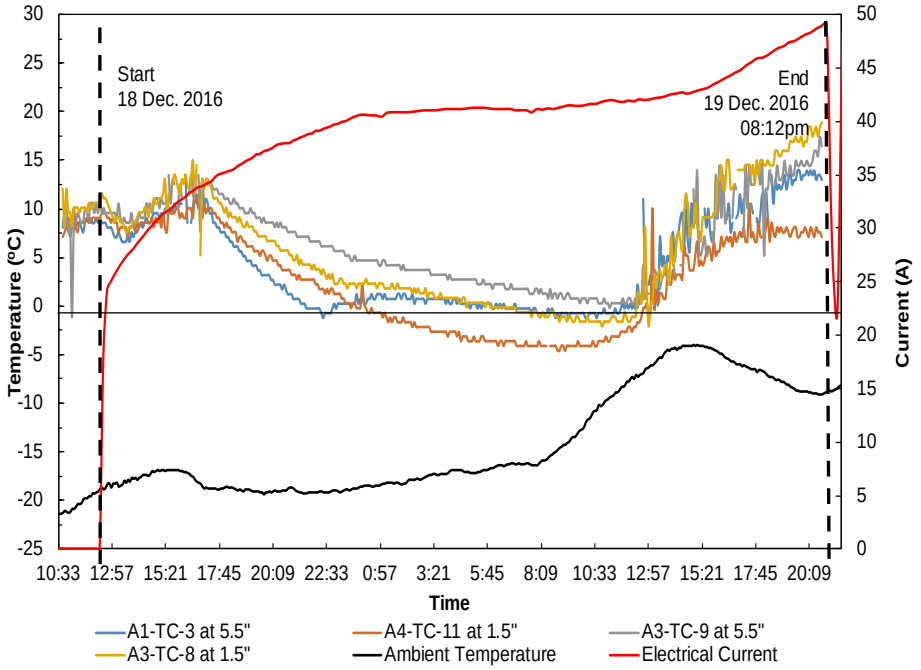

Figure 10 Slab 1 temperature and current measurements

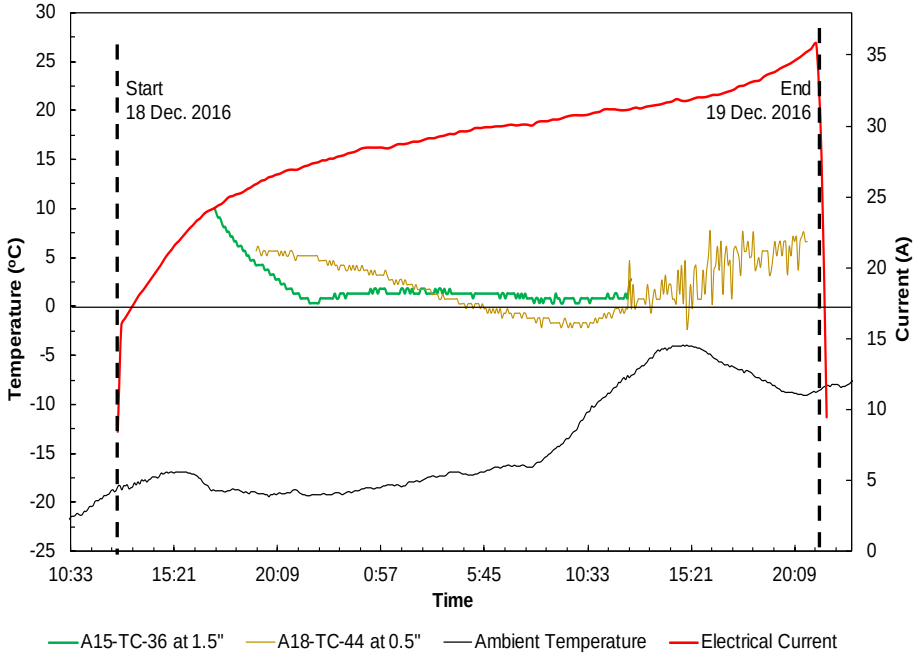

Figure 11 Slab 2 temperature and current measurements

(a)

(b)

Figure 12 Performance of the ECON HPS at DSM: (a) snow accumulation on slabs before turning the system on and (b) snow and ice free surface

- Forth Performance Evaluation (01/05/2017):

Table 4 Weather condition

Date	January 05, 2017
Snow thickness	No snow
Operation time	8 hours
Mean temperature	10°F (-12°C)
Minimum temperature	5°F (-15°C)
Maximum temperature	15°F (-9.5°C)
Wind speed	9 mph
Average relative humidity	67 %
Minimum relative humidity	60 %
Maximum relative humidity	75 %

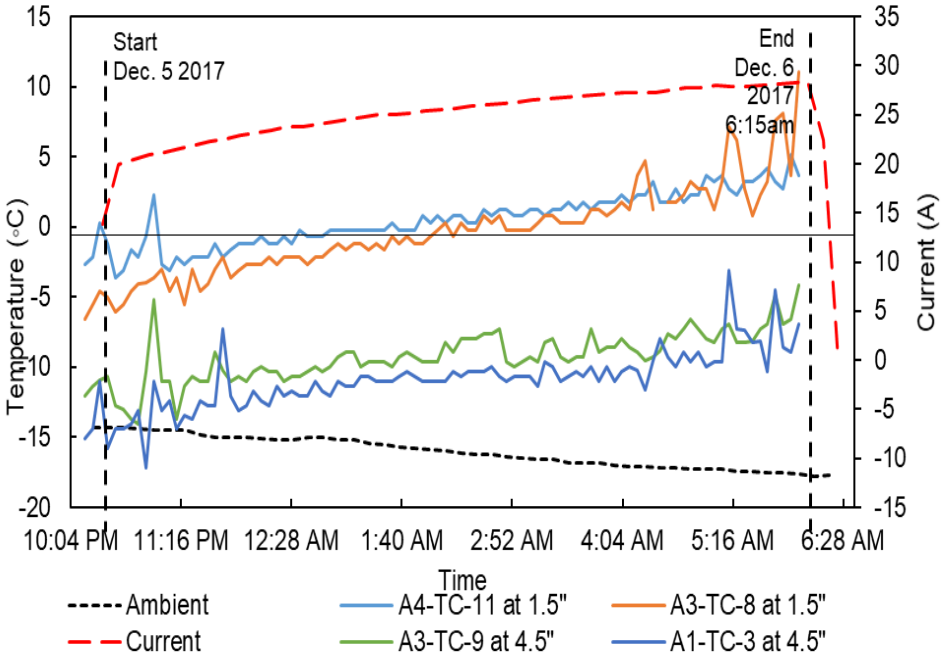

Figure 13 Slab 1 temperature and current measurements

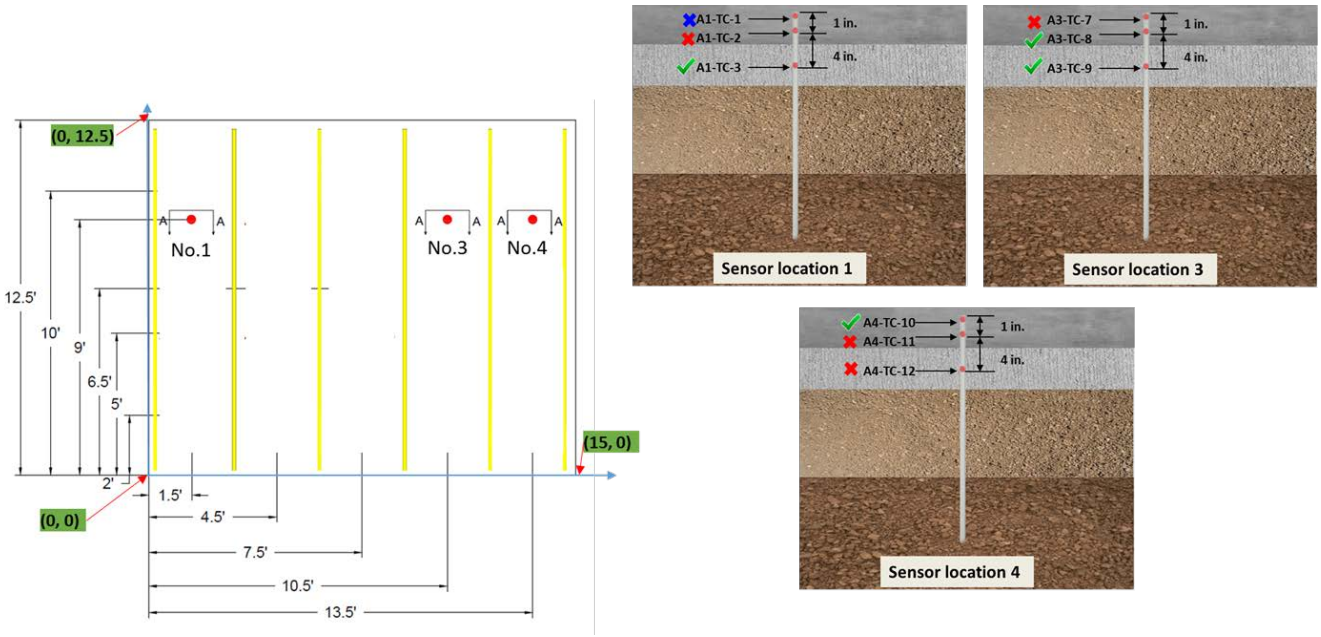

Figure 14 Slab 1 sensors location

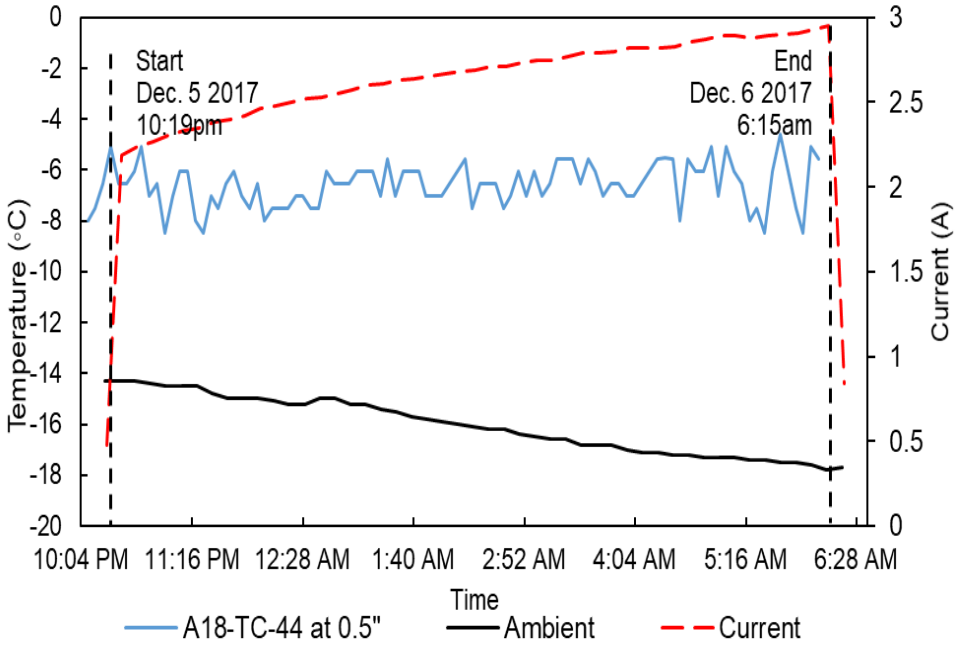

Figure 15 Slab 2 temperature and current measurements

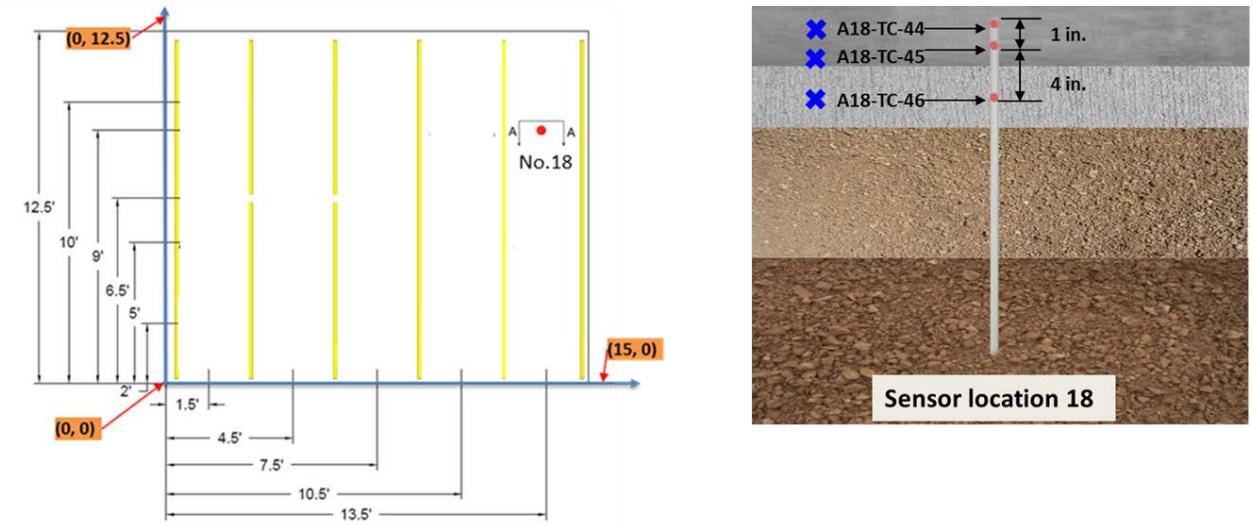

Figure 16 Slab 1 sensors lcation

- Fifth Performance Evaluation (01/20/2017):

Table 5 Weather condition

Date	January 20, 2017
Snow thickness	No snow
Operation time	2 hours
Mean temperature	22°F (-6.0°C)
Minimum temperature	15°F (-9.5°C)
Maximum temperature	30°F (-1.0°C)
Wind speed	6 mph
Average relative humidity	95 %
Minimum relative humidity	89 %
Maximum relative humidity	100 %

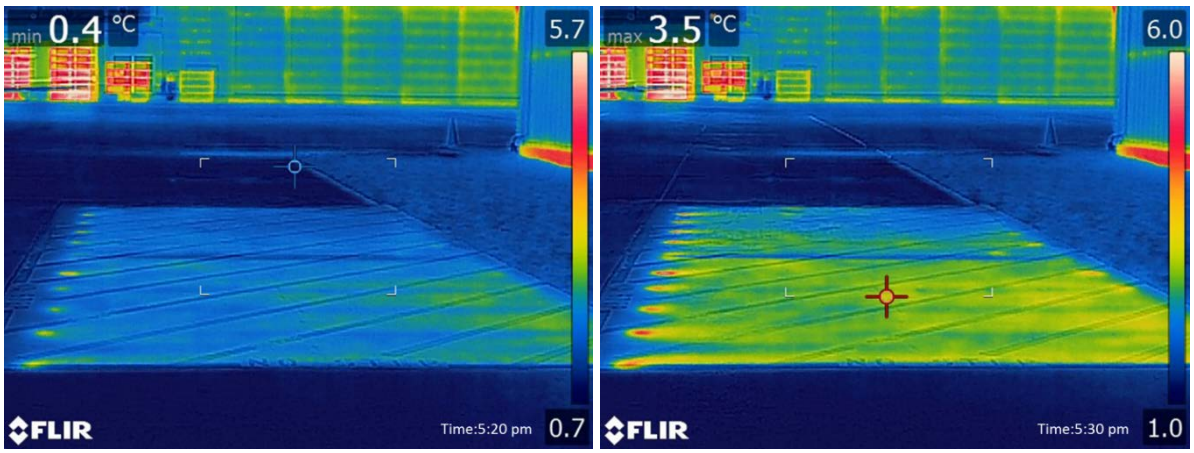

(a) (b)

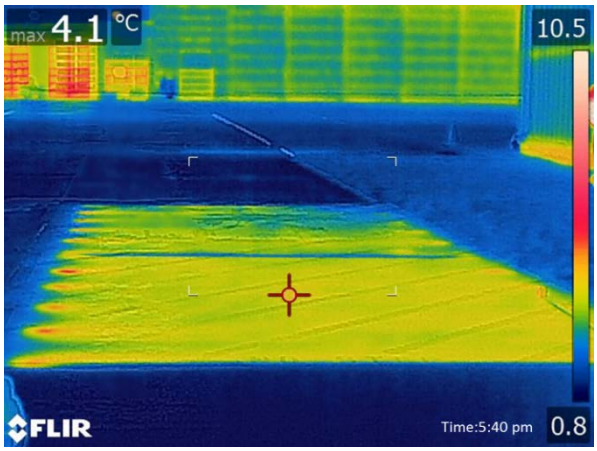

(c)

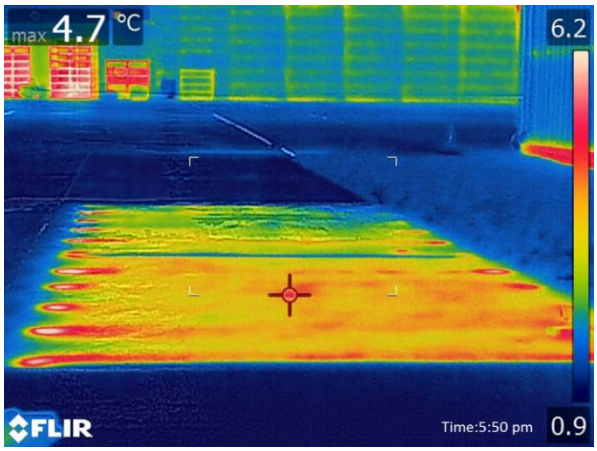

(d)

Figure 17 Performance of the ECON HPS: (a) thermal image after 20 minutes of operation, (b) 30 minutes of operation, (c) after 40 minutes of operation, and (d) after 50 minutes of operation

- Sixth Performance Evaluation (01/24/2017):

Table 6 Weather condition

Date	January 24, 2017
Snow thickness	No snow
Operation time	1 hour
Mean temperature	22°F (-6.0°C)
Minimum temperature	31°F (-0.5°C)
Maximum temperature	14°F (-10°C)
Wind speed	6 mph
Average relative humidity	95 %
Minimum relative humidity	89 %
Maximum relative humidity	100 %

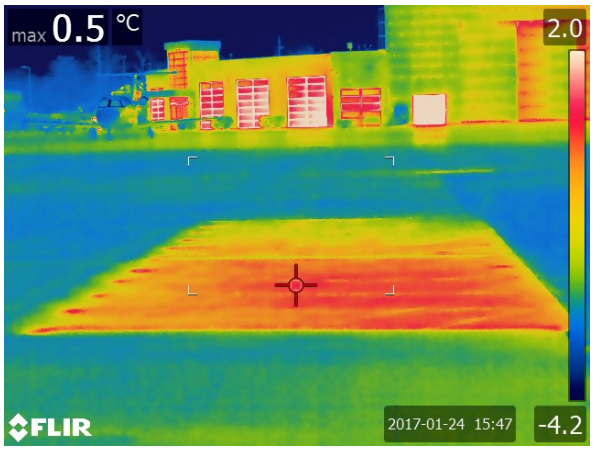

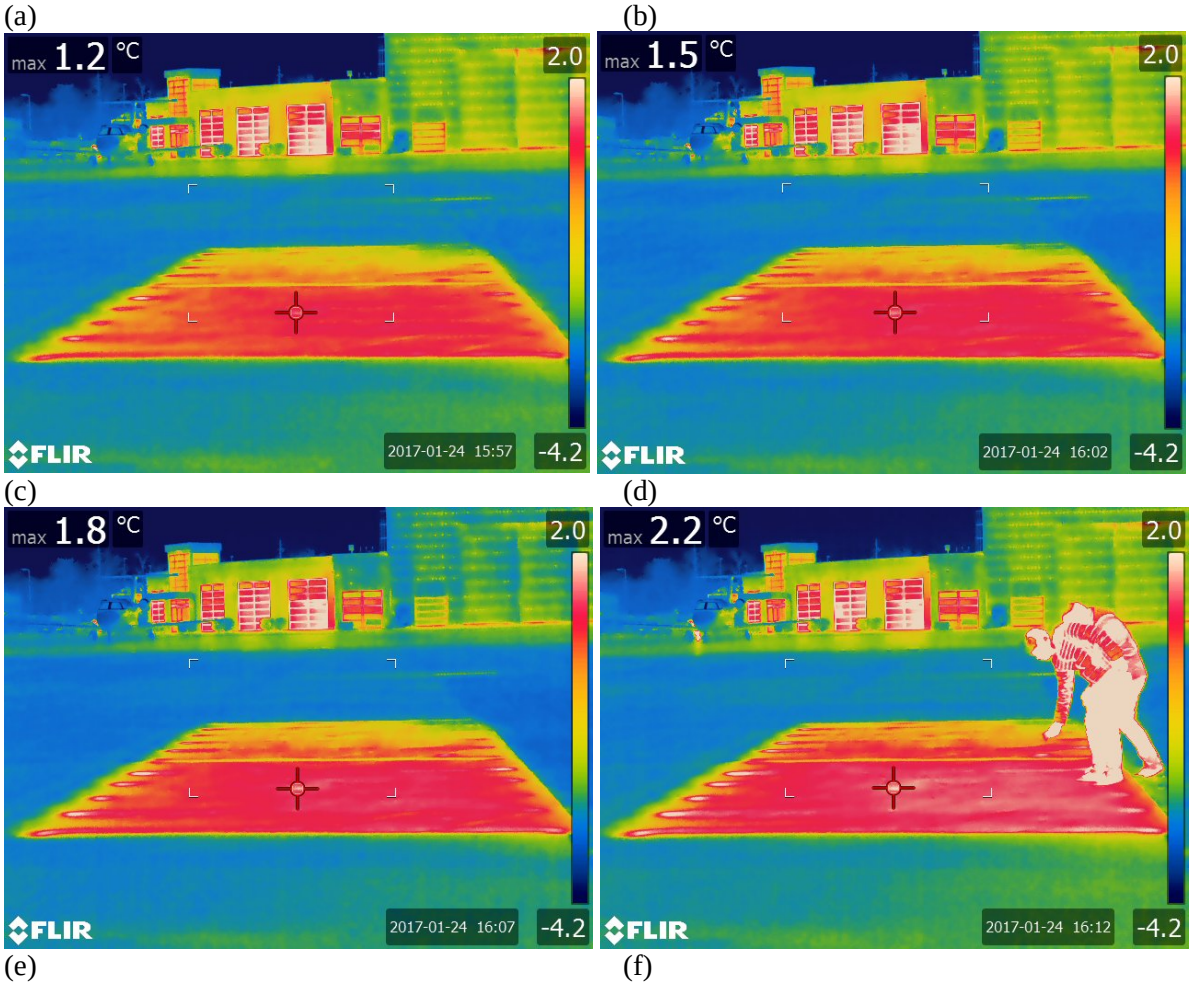

Figure 18 Infrared thermographic image of the ECON slabs: (a) at 0 minutes, (b) after 30 minutes, (c) after 40 minutes, (d) after 45 minutes, (e) after 50 minutes, and (f) after 55 minutes

- Seventh Performance Evaluation (01/25/2017):

Table 7 Weather condition

Date	January 25, 2017
Snow thickness	0.5 inch
Operation time	5 hours
Mean temperature	23°F (-5°C)
Minimum temperature	14°F (-10°C)
Maximum temperature	31°F (-0.5°C)
Wind speed	14 mph
Average relative humidity	93 %
Minimum relative humidity	85 %
Maximum relative humidity	100 %

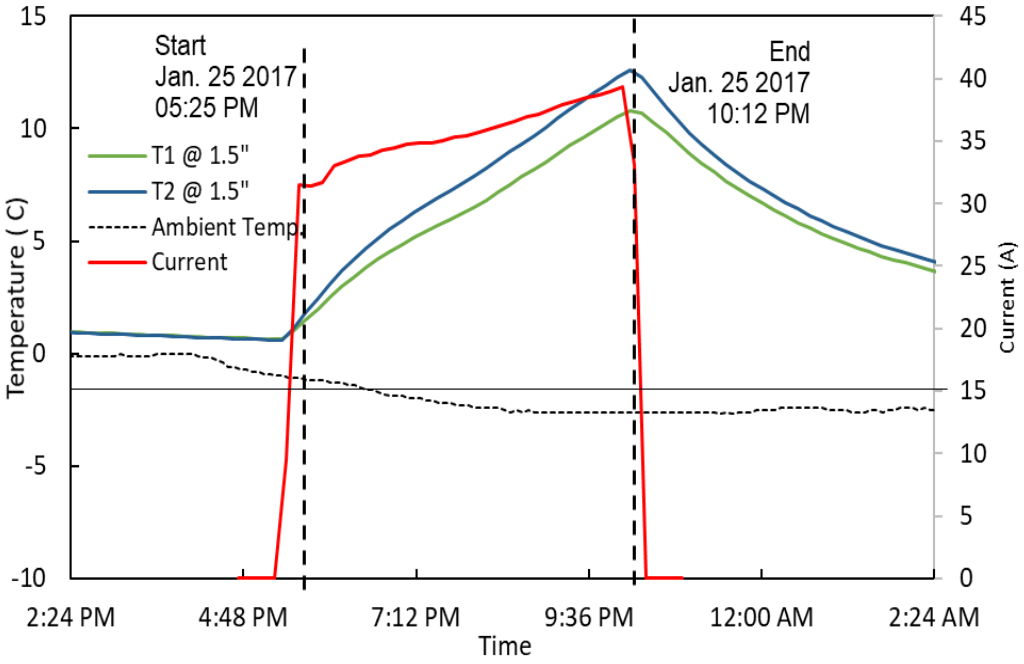

Figure 19 Slab 1 temperature and current measurements

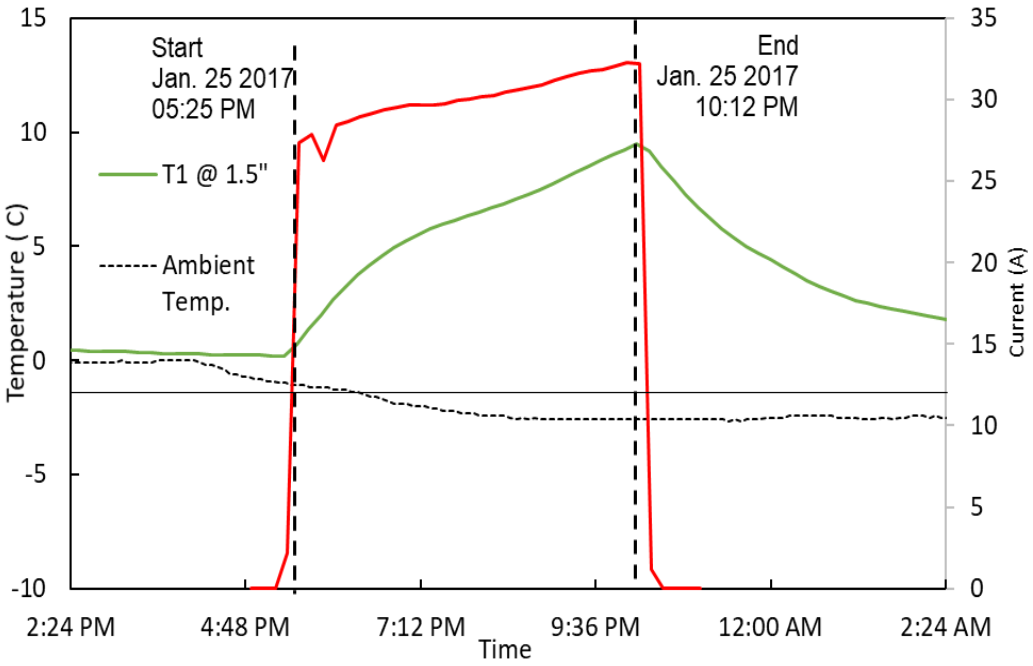

Figure 20 Slab 2 temperature and current measurements

(a) (b)

Figure 21 Surface temperature: (a) ECON surface temperature during Operation time and (b) adjacent PCC Slab

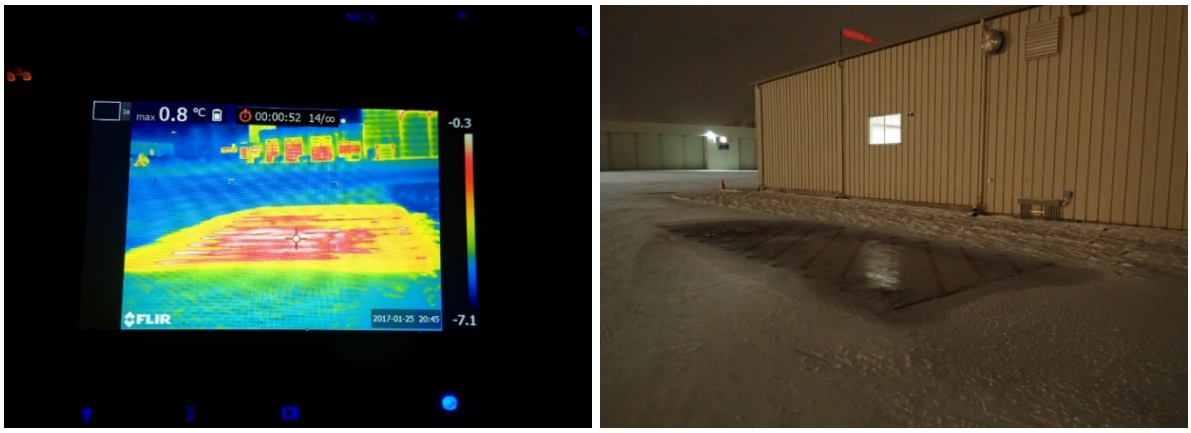

(a) (b)

Figure 22 Performance of the ECON HPS at 2 hours of operation: (a) thermal camera and (b) operation of melting snow and ice on ECON surface

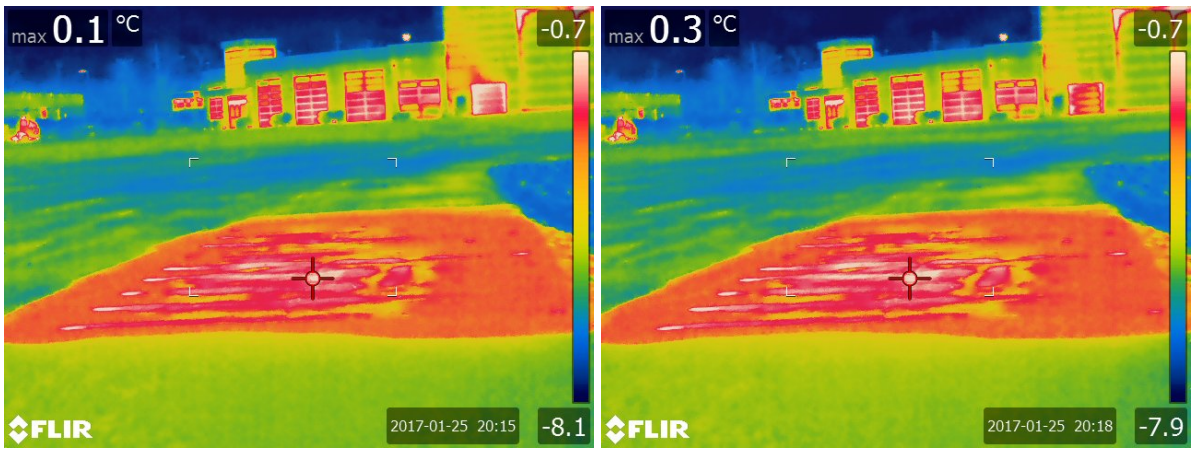

(a) (b)

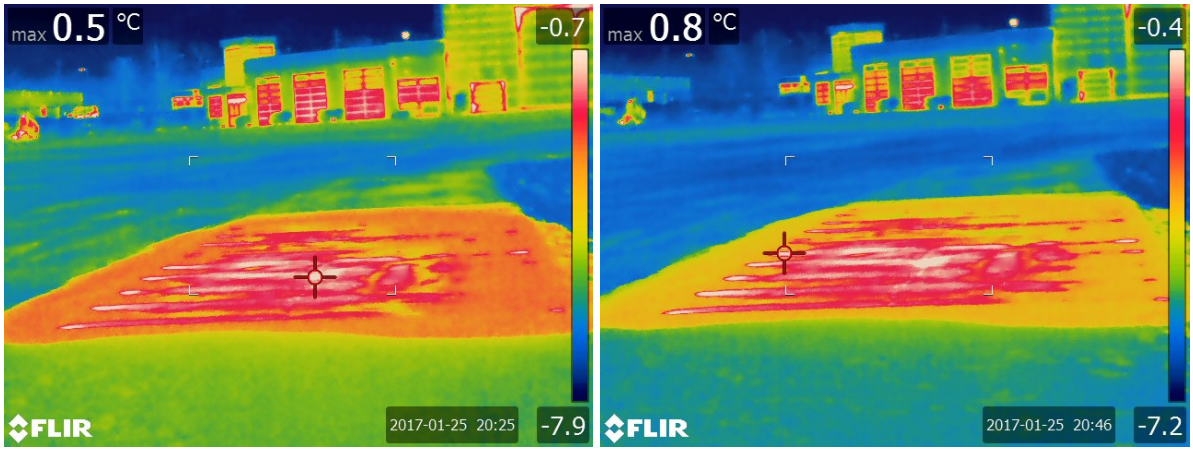

(c) (d)

Figure 23 Performance of the ECON HPS after snow completely melted when ISU team reached at DSM airport: (a) after 2 hours and 50 minutes of operation, (b) after 2 hours and 53 minutes of operation, (c) after 2 hours of operation, and (d) after 3 hours and 46 minutes of operation

- Eight Performance Evaluation (02/08/2017):

Table 8 Weather Condition

Date	February 08, 2017
Snow thickness	1.6 inch
Operation time	6 hours and 50 minutes
Mean temperature	19°F (-7°C)
Minimum temperature	14°F (-10°C)
Maximum temperature	23°F (-5°C)
Wind speed	13 mph
Average relative humidity	65 %
Minimum relative humidity	45 %
Maximum relative humidity	84 %

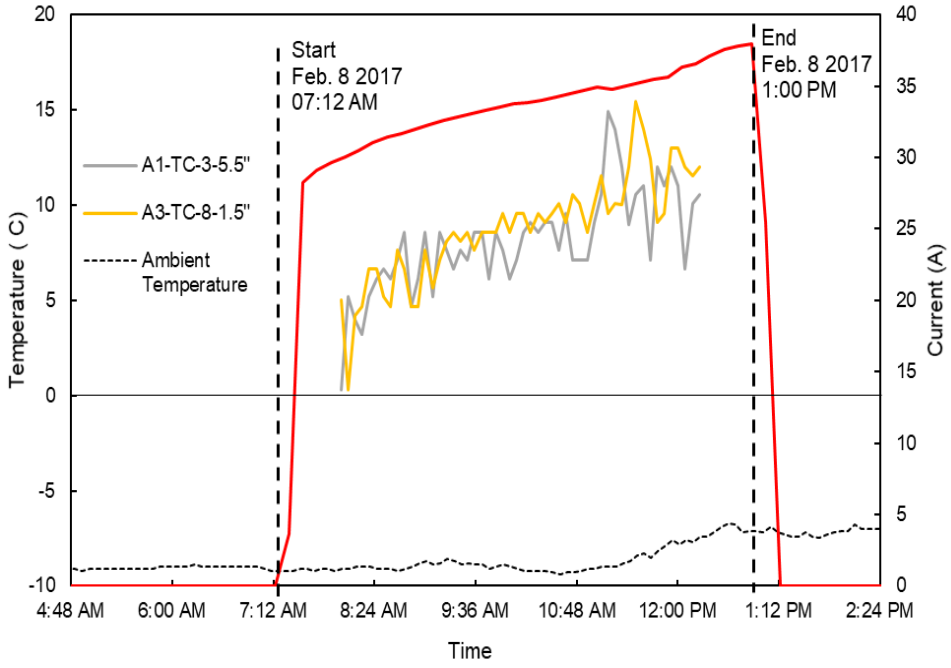

Figure 24 Slab 1 temperature and current measurements

(a)


Feb. 08, 2017, 10:57 AM
Wednesday, February 8, 2017 10:57 AM

(b)


Feb. 08, 2017, 11:24 AM

(c)

(d)

Figure 25 Performance of the ECON HPS at DSM, IA: (a) after 2 hours and 48 minutes of operation, (b) after 3 hours and 45 minutes of operation, (c) after 4 hours and 12 minutes of operation, and after 4 hours and 38 minutes of operation.

- Nine Performance Evaluation (02/24/2017):

Table 9 Weather condition

Date	February 24, 2017
Snow thickness	0.5~1 inch
Operation time	5 hours and 50 minutes
Mean temperature	31°F (-0.5°C)
Minimum temperature	22°F (-5.5°C)
Maximum temperature	40°F (4.4°C)
Wind speed	17 mph
Average relative humidity	81 %
Minimum relative humidity	68 %
Maximum relative humidity	93 %


Feb. 24, 2017, 5:50 PM
Friday, February 24, 2017 5:45 PM

(a)


Feb. 24, 2017, 7:10 PM
Friday, February 24, 2017 7:10 PM

(b)


Feb. 24, 2017, 7:37 PM
Friday, February 24, 2017 7:37 PM

(c)


Feb. 24, 2017, 8:03 PM
Friday, February 24, 2017 8:03 PM

(d)


Feb. 24, 2017, 8:29 PM
Friday, February 24, 2017 8:29 PM

(e)


Feb. 24, 2017, 8:41 PM
Friday, February 24, 2017 8:41 PM

(f)

(g)

Figure Performance of the ECON HPS at DSM, IA: (a) before turning on the HPS (b) after 1 hours and 20 minutes of operation, (c) after 1 hours and 37 minutes of operation, (d) after 2 hours and 13 minutes of operation, (e) after 2 hours and 39 minutes of operation, (f) after 2 hours and 41 minutes of operation, and (g) after 3 hours and 14 minutes of operation

- Tenth Performance Evaluation (03/13/2017):

Table 10 Weather condition

Date	March 13, 2017
Snow thickness	1.0~1.5 inch
Operation time	3 hours and 20 minutes
Mean temperature	26°F (-3.3°C)
Minimum temperature	21°F (-6.1°C)
Maximum temperature	30°F (-1.1°C)
Wind speed	13 mph
Average relative humidity	81 %
Minimum relative humidity	65 %
Maximum relative humidity	93 %

Figure 27 A 1.0~1.5 inch snow thickness

(a)


March 13, 2017, 10:25 AM
Monday, March 13, 2017 10:25 AM

(b)


March 13, 2017, 10:43 AM
Monday, March 13, 2017 10:43 AM

(c)

(d)

Figure 28 Performance of the ECON HPS at DSM, IA: (a) before turning on the HPS (b) after 1 hours and 5 minutes of operation, (c) after 1 hours and 23 minutes of operation, (d) after 1hours and 50 minutes of operation

Table 11 1st year Summary of ECON performance

Date	ECON slab	Air temp. (^{o}F)	Wind speed (mph)	Average snow thickness (in)	Average power density (W/ft^2)	Operation time minutes (hrs.)	Energy consumption (kWh/ft^2)	Unit cost (¢/ft^2)	Unit cost (¢/yd^2/ hour)
Dec. 10, 2016	Slab 1	25	8	1.2	38	420 (7)	0.27	2.15	2.77
	Slab 2	25	8	1.2	31	420 (7)	0.22	1.73	2.23
Dec. 18-19, 2016	Slab 1	-11	16	1	39	1286 (21.4)	0.84	6.70	2.80
	Slab 2	-11	16	1	27	1286 (21.4)	0.59	4.70	1.96
Jan. 25, 2017	Slab 1	14	14	0.5	38	90 (1.5)	0.06	0.45	2.66
	Slab 2	14	14	0.5	32	90 (1.5)	0.05	0.38	2.00
Feb. 08, 2017	Slab 1	14	13	1.5	35	210 (3.5)	0.12	0.98	2.57
	Slab 2	14	13	1.5	29	210 (3.5)	0.10	0.81	2.00
Feb. 24, 2017	Slab 1	22	17	0.8	37	150 (2.5)	0.09	0.75	2.80
	Slab 2	22	17	0.8	33	150 (2.5)	0.08	0.66	2.40
Mar. 13, 2017	Slab 1	21	13	1.3	33	120 (2)	0.07	0.53	2.50
	Slab 2	21	13	1.3	31	120 (2)	0.06	0.50	2.00

Second year evaluation of the ECON HPS at DSM airport under different weather conditions for the first year (December 24, 2017 to December 29, 2017)

- First Performance Evaluation (12/24/2017):

Table 12 Weather condition

Date	December 24, 2017
Snow thickness	1.0 inch
Operation time	5 hours and 30 minutes
Mean temperature	19°F (-7°C)
Minimum temperature	24°F (-4°C)
Maximum temperature	14°F (-10°C)
Wind speed	21 mph
Average relative humidity	79 %
Minimum relative humidity	93 %
Maximum relative humidity	57 %

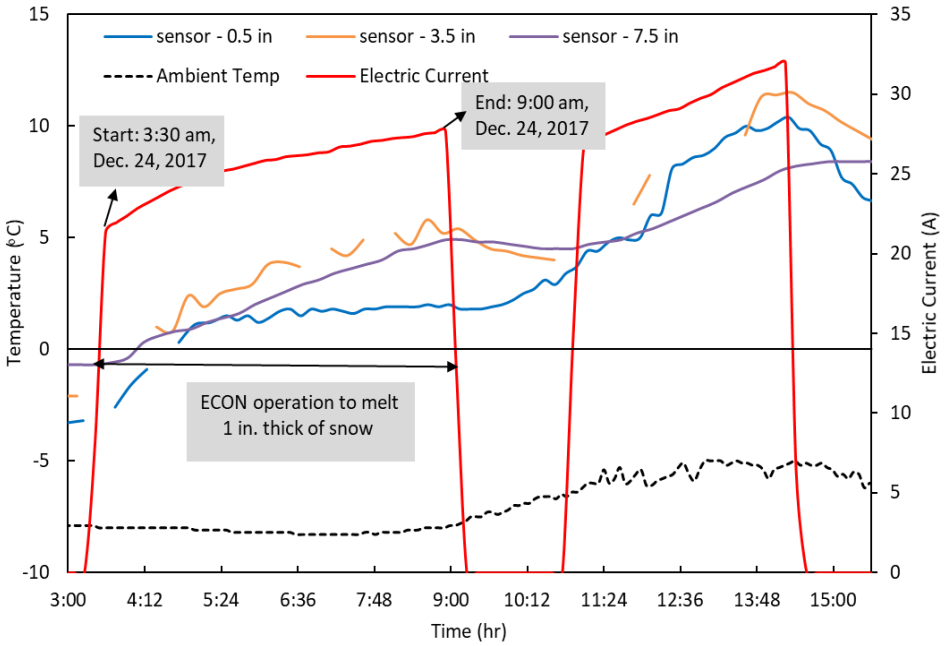

Figure 29 Slab 1 temperature and current measurements

(a)

(b)

(c)

(d)

(e)

(f)

(g)

(h)

Figure 30 Performance of the ECON HPS at DSM: (a) system turned on at 3:30 AM (b) after 1 hours of operation, (c) after 2 hours of operation, (d) after 4 hours operation, (e) after 4 hours and 55 minutes operation, (f) after 4 hours and 56 minutes of operation, (g) after 5 hours and 10 minutes of operation, and (h) after 5 hours and 20 minutes of operation

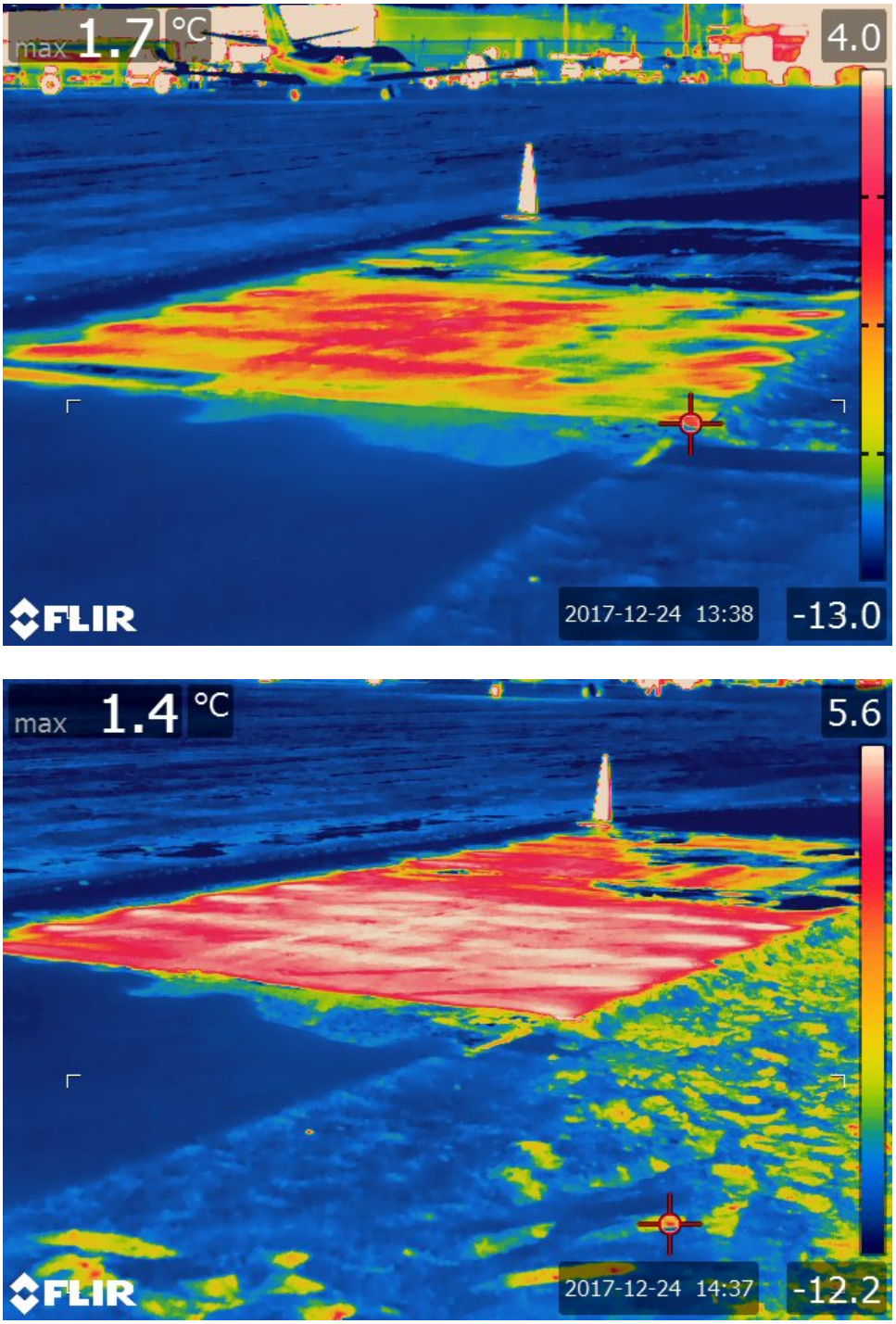

Figure 31 Infrared thermography of the ECON HPS at DSM

- Second Performance Evaluation (12/27/2017 to 12/28/2017):

Table 13 Weather condition

Date	December 27, 2017 to December 28, 2017
Snow thickness	1.1 inch
Operation time	10 hours and 55 minutes
Mean temperature	11°F (-11°C)
Minimum temperature	19°F (-7°C)
Maximum temperature	3°F (-16°C)
Wind speed	8 mph
Average relative humidity	77 %
Minimum relative humidity	86 %
Maximum relative humidity	67 %

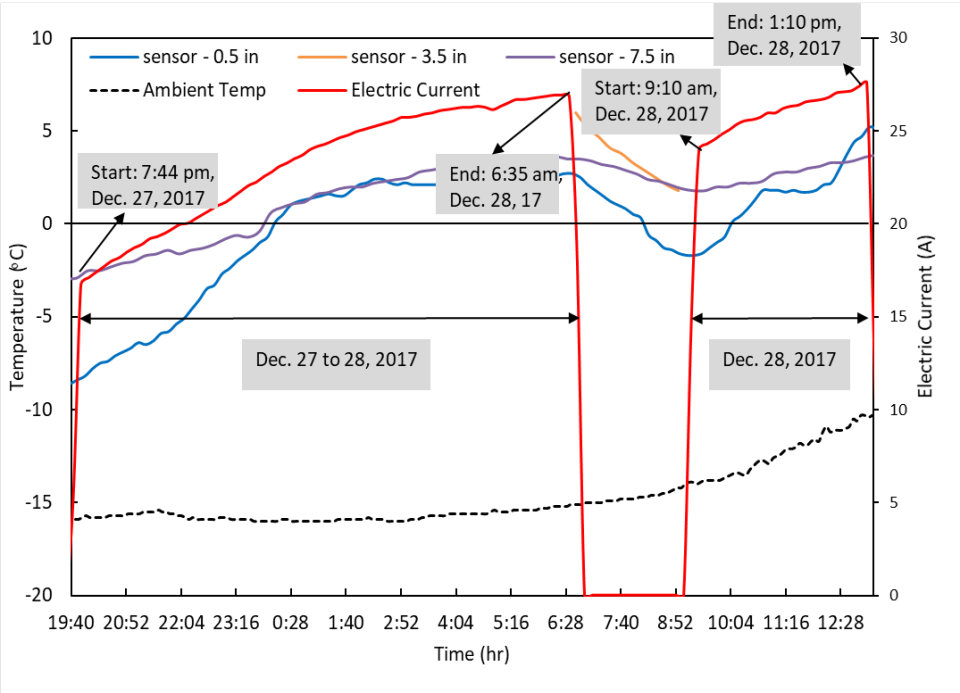

Figure 32 temperature and current measurements

(a)

(b)

(c)

(d)

(e)

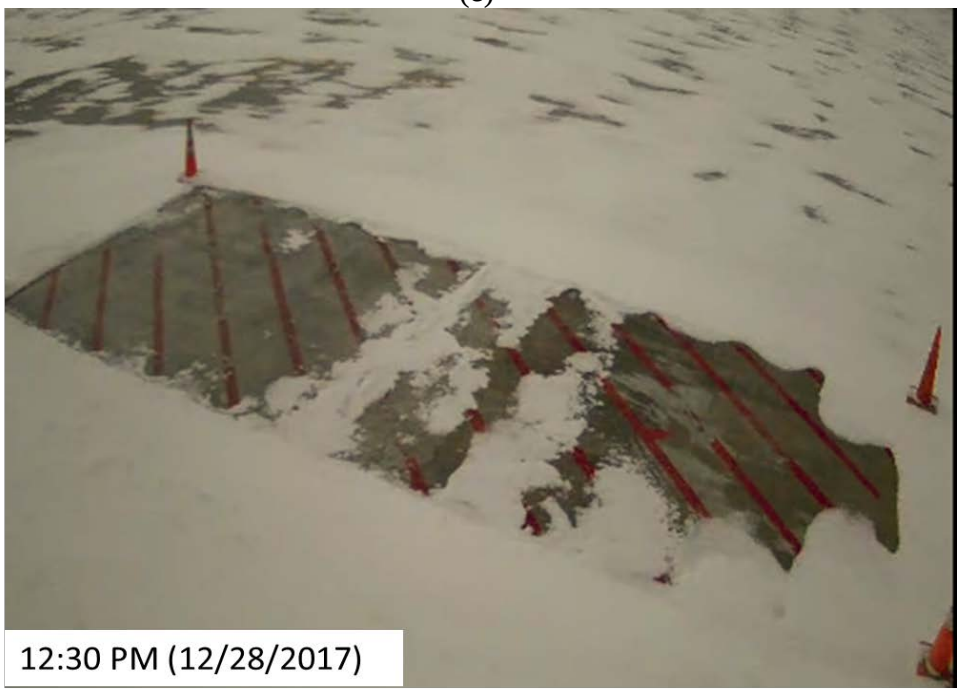

(f)

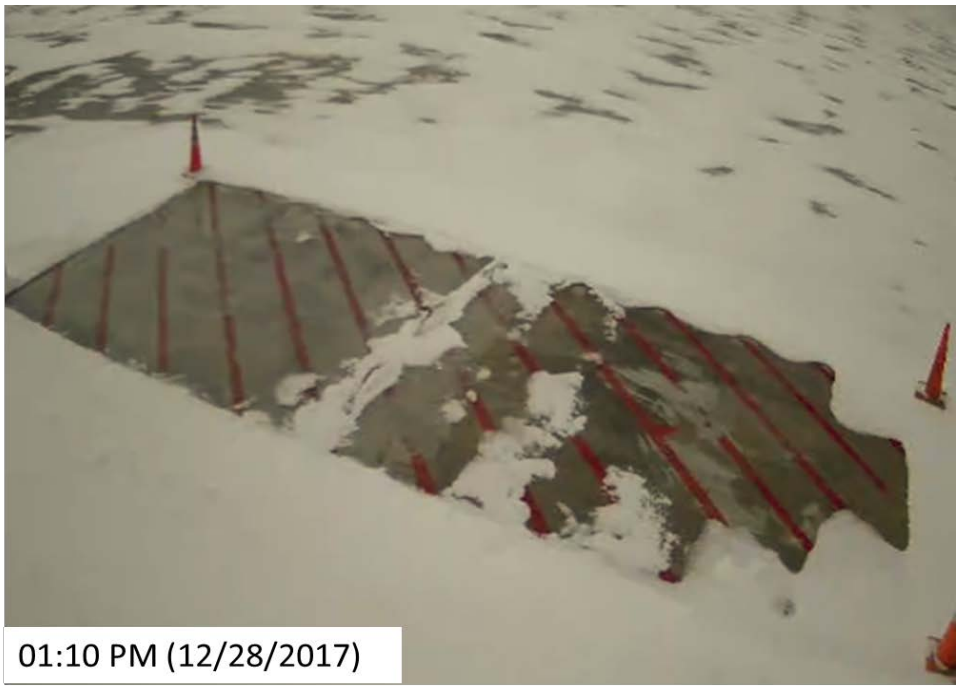

(g)

(h)

(i)

Figure 33 Performance of the ECON HPS at DSM: (a) system turned on at 9:10 AM (b) after 55 minutes of operation, (c) after 2 hours of operation, (d) after 2 hours and 15 minutes of operation, (e) after 2 hours and 55 minutes operation, (f) after 3 hours and 20 minutes of operation, (g) after 4 hours of operation, and (h) after 4 hours and 40 minutes of operation, (i) after 5 hours and 40 minutes

- Third Performance Evaluation (12/29/2017):

Table 14 Weather condition

Date	December 29, 2017
Snow thickness	2 inch
Operation time	See figure A-29
Mean temperature	10°F (-12°C)
Minimum temperature	16°F (-8°C)
Maximum temperature	5°F (-15°C)
Wind speed	6 mph
Average relative humidity	82 %
Minimum relative humidity	92 %
Maximum relative humidity	67 %

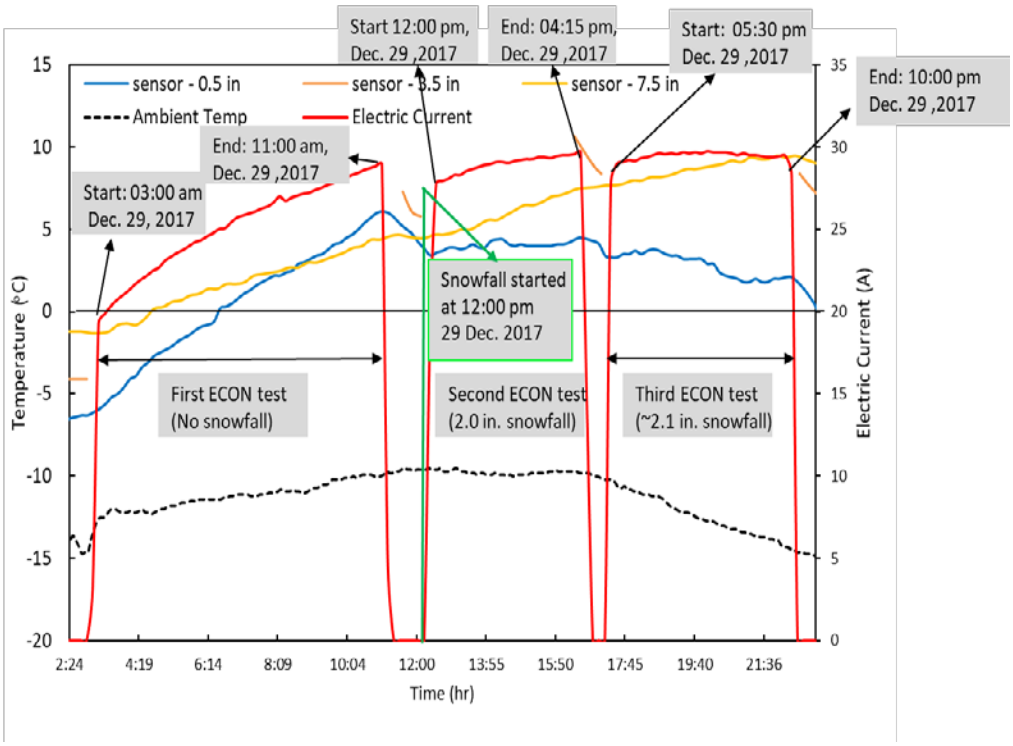

Figure 35 temperature and current measurements

(a)

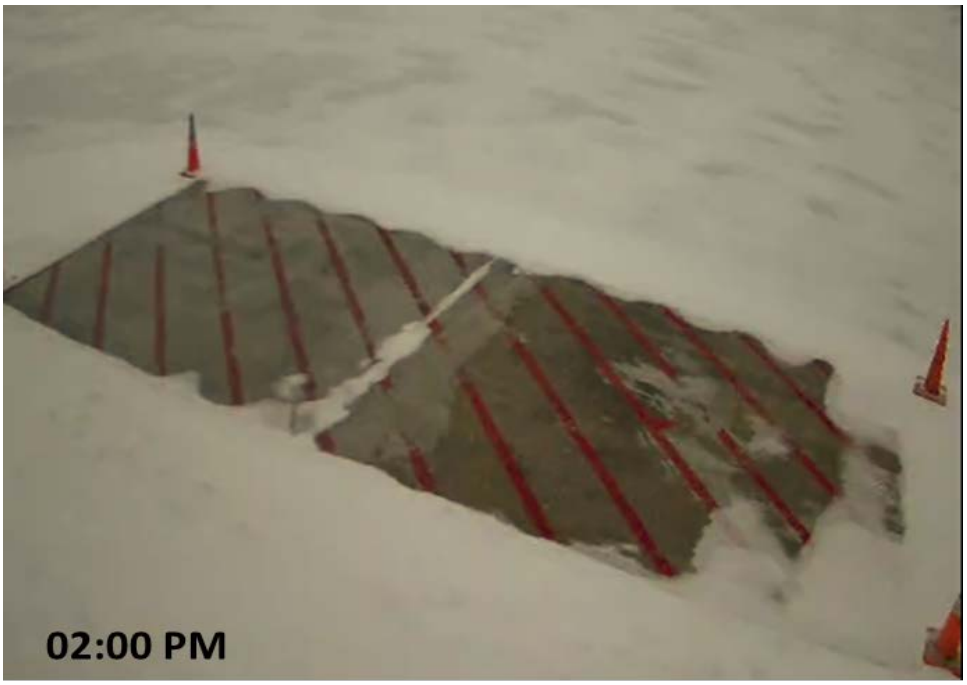

(b)

(c)

(d)

Figure 36 Performance of the ECON HPS at DSM: (a) system turned on at 12:10 PM (b) after 2 hours of operation, (c) after 3 hours of operation, and (d) after 4 hours and 20 minutes of operation

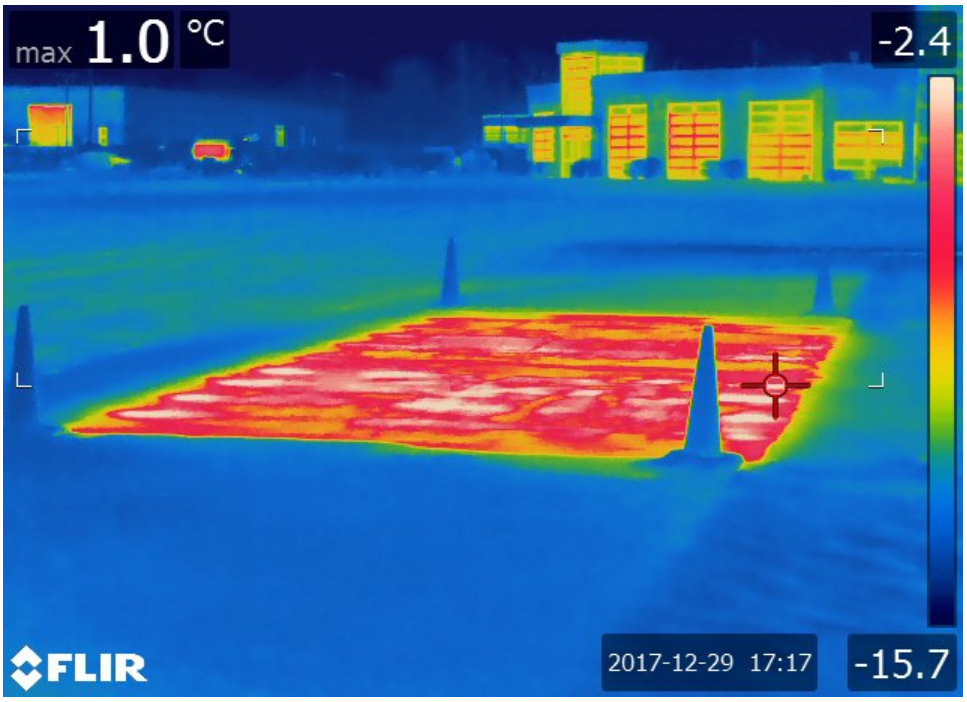

Figure 37 Infrared thermography of the ECON HPS at DSM

Table 15 2st year Summary of ECON performance

Date	Condition	Air temp. (°F)	Wind speed (mph)	Average snow thickness (in)	Average power density (W/ft^2)	Operation time minutes (hrs.)	Energy consumption (kWh/ft^2)	Unit cost (¢/ft^2)	Unit cost (¢/yd^2/ hour)
Dec. 24, 2017	Deicing	19.4	20.5	1.0	27	330 (5.5)	0.15	1.19	1.95
Dec. 27-28, 2017	Deicing	3.2	7.4	1.1	24	2,220 (37)	0.88	7.06	1.70
Dec. 27-28, 2017	Deicing	3.2	7.4	0.98	28	240 (4)	0.11	0.91	2.00
Dec. 29, 2017	Ant-icing	10.4	8.0	2.0	32	240 (4)	0.13	1.02	2.30

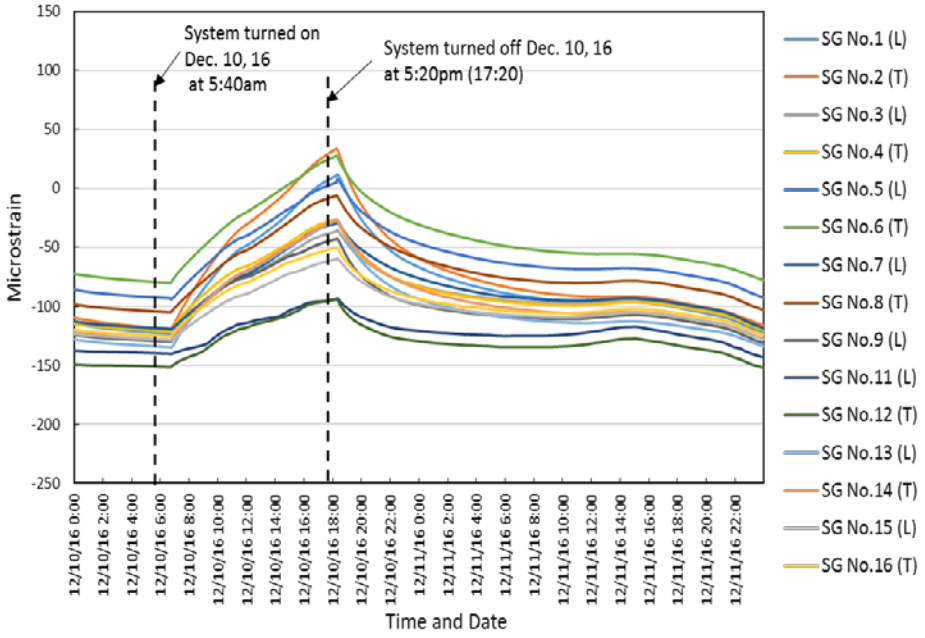

Figure 38 Strain changes during heating operation

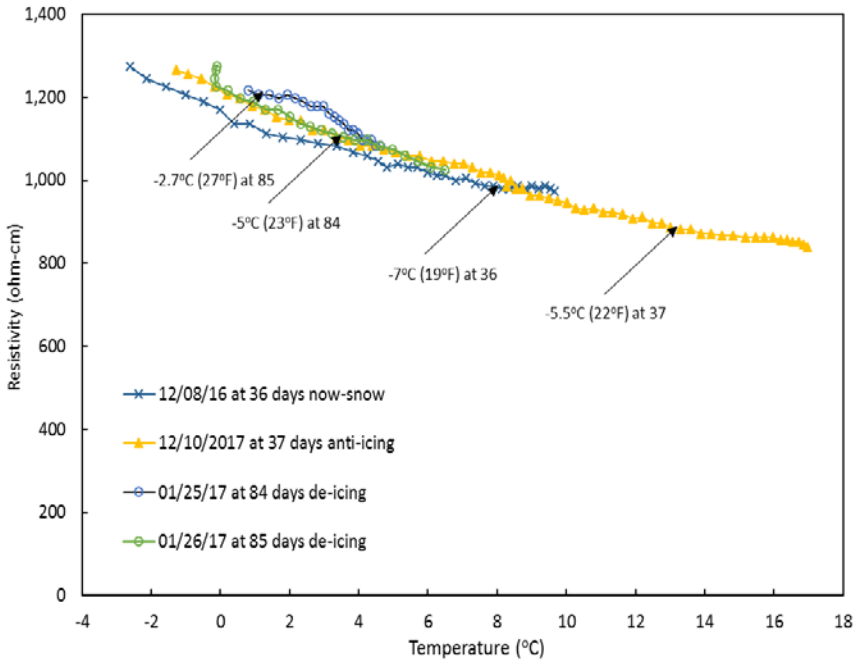

Figure 39 Measured field resistivity of the ECON slab for different weather conditions and operation tests

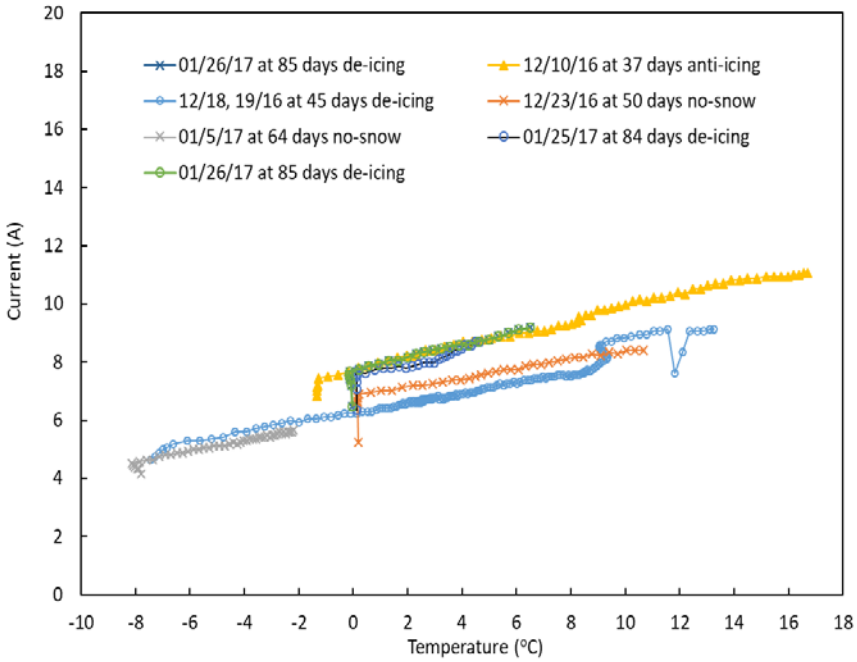

Figure 40 Temperature and current measurements

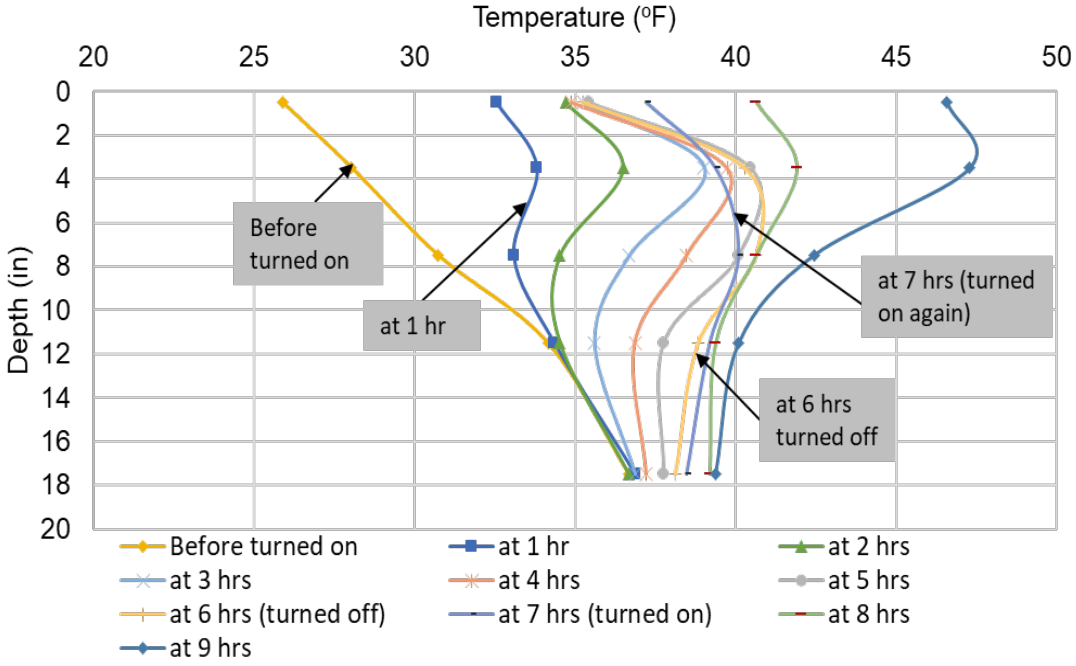
Temperature (°F)
20
25
30
35
40
45
50
Depth (in)
0
2
4
6
8
10
12
14
16
18
20
Before turned on
at 1 hr
at 7 hrs (turned on again)
at 6 hrs turned off
Before turned on
at 1 hr
at 2 hrs
at 3 hrs
at 4 hrs
at 5 hrs
at 6 hrs (turned off)
at 7 hrs (turned on)
at 8 hrs
at 9 hrs

(a)

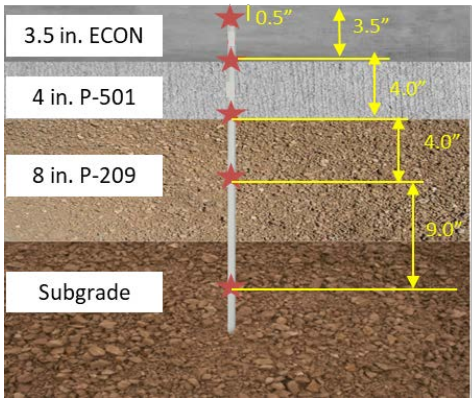
3.5 in. ECON
4 in. P-501
8 in. P-209
Subgrade
0.5"
3.5"
4.0"
4.0"
9.0"

(b)

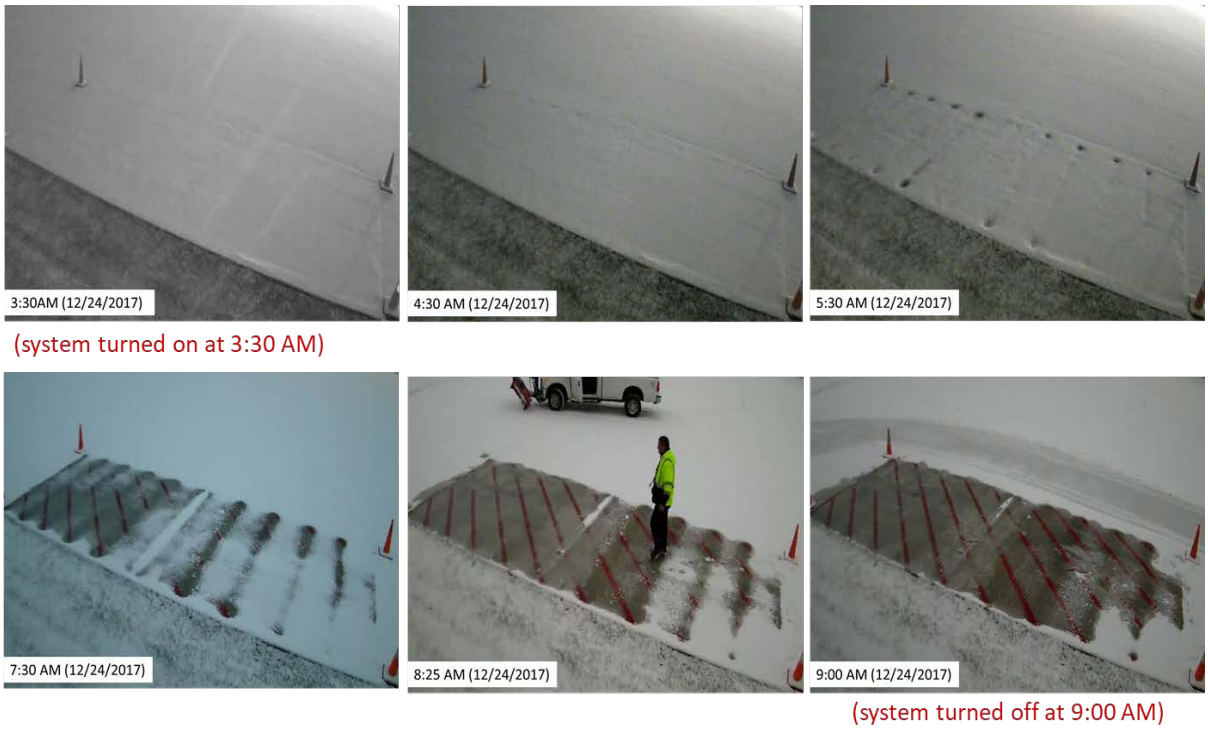

(c)

Figure 41 ECON performance: (a) Temperature variation across slab thickness on December 12, 2017, (b) sensors location, and (c) Deicing event on December 12, 2017